PREVENTION OF EXTREME ROLL MOTION THROUGH MEASUREMENTS OF SHIP'S MOTION RESPONSES

Hossein Enshaei

Submitted for the degree of Doctor of Philosophy

Supervisory committee:

Prof. Richard birmangham,
Prof. Ehsan Mesbahi,
Dr. Arun Dev

November 2013

School of Maine Science and Technology
Faculty of Science, Agriculture and Engineering
Newcastle University
Newcastle Upon Tyne, UK

Declaration

I hereby certify that this thesis, entitled as "Prevention of extreme roll motion through measurements of a ship's motion responses", which I now submit for assessment on the programme of study leading to the award of Doctor of Philosophy, is entirely my own work. The result of this study also includes a computer program which has been developed on the basis of novel ideas to identify some of the ocean wave's influential parameters. I have exercised all reasonable care to ensure that the work is original and to the best of my knowledge does not breach any law of copyright, and has not been taken from the work of others apart from that work that has been cited and acknowledged within the extent of my own work.

Signed:_____

Hossein Enshaei

Student No: S079067124

Date: Nov 2013

Acknowledgment

First and foremost I would like to acknowledge my supervisor, Professor Richard Birmingham, who has not only ably mentored me through the last 3 years but has also imparted an unrivalled array of experience and insight into academic publications. It has been an honour to work under his expert guidance.

I am most grateful to Professor Ehsan Mesbahi, who has far exceeded the usual role of supervisor. He gave me something to take home to think about besides homework. Thanks for taking such an interest, not only in the study but also in my life.

Sincere thanks to a third supervisor Dr Arun Dev who has provided ideas and valuable insight.

Throughout this process, my study has been made most enjoyable by the company of fellow PhD students, researchers and colleagues in the School of Marine Science and Technology. In particular I would like to thank Dr Kayvan Pazouki for sharing his views and past stories during lunch time, and John Garside who has provided valuable proof reading through his regular visits.

I would like to take this opportunity to express my deep respect to my parents for their continued support and encouragement during my life. The acknowledgments cannot end without my heartfelt thanks to my wife, Mehrangiz, our son, Parsa, and our daughter Diba for their never ending inspiration by sharing the joys and sorrows of this research period with me.

Abstract

Exploring the operational links between a sea state and a ship's heading and speed provides the opportunity to continuously monitor dynamic stability behaviour; and hence to avoid significant changes of stability in adverse weather. Significant changes of stability at sea can lead to dangerous transient situations and eventually stability failure. Despite its importance, the current intact stability (IS) criteria do not evaluate or consider the dynamics of the motion responses of a vessel in a wave environment.

In this thesis, the full six degrees of freedom motion responses of two models have been tested in irregular waves under intact vessel conditions. The general modelling approach for a mathematical model was based on numerical simulations at different speeds, sea conditions and angle of heading relative to the waves. In the second model, a physical model was tested in a towing tank under similar simulated environmental conditions to that employed for the first model. The investigation was limited to the effects of encountered frequency components and the associated magnitude of energy of the ship's motion responses. An analysis of heave, pitch and roll motion confirmed the vulnerability of the model to certain wave-excited frequency ranges. This particular range of frequency results in an adverse effect on the amplitude of the responses, and these were closely related to the natural mode frequencies and related coupling effects.

It was confirmed that the roll motion maintains its highest oscillation amplitude at around the natural frequency in all sea conditions regardless of ship heading angles. It was also observed that spectral analysis of the heave and pitch responses revealed the wave peak frequency. Roll is magnified when the peak frequency of the waves approaches the natural roll frequency, therefore keeping them sufficiently apart avoids potentially large motion responses. It was concluded that peak frequency and associated magnitude are the two important inherent characteristics of motion responses. Detection of the most influential parameters of encountered waves through measurements of heave and pitch responses could be utilised to provide a method to limit the large motion of a ship at sea.

The measurement of waves whilst a ship is underway is a major challenge, whereas ship motion, which is relatively easily measured, is a good indirect reflection of the encountered wave characteristics and which can be measured, stored and analysed using

on-board equipment. Motion responses are considered as continuous signals with a time-dependent spectral content, and signal processing is a suitable technique for detection, estimation and analysis of recorded time-varying signals. The method is fast enough to be considered as an on-board real-time monitoring of dynamic stability.

Signal processing techniques are used in the detection and estimation of the influential parameters of a wave environment through the analysis of motion responses. The variables of the system were detected by spectral analysis of the heave and pitch motions. These variables are the peak wave frequencies and associated magnitudes which can cause a large roll motion when reasonably close to the ship's natural roll frequency.

The instantaneous frequency (IF) present in the signal is revealed through spectral analysis of short-time Fourier transforms (STFT) in less than a minute. The IF is a parameter of practical importance which can be used in real-time on-board decision making processes to enable the vessel to take actions in order to avoid large roll motions.

Contents

List of Figures

List of Tables

Abbreviations

BEM	Boundary Element Method
CTs	Cross terms
DNV	Det Norske Veritas
DOF	Degree Of Freedom
DP	Dynamic positioning
FEM	Finite element method
FFT	Fast Fourier Transform
IF	Instantaneous Frequency
IMO	International Maritime Organization
IS	Intact Stability
ISC	Code on Intact Stability
ITTC	International Towing Tank Conference
MSC	Maritime Safety Committee
PLL	Phase locked loop
QTM	Qualisys Track Manager
RAO	Response Amplitude Operator
SESAM	DNV Software
SFV	Subcommittee on Safety of Fishing Vessels
SLF	Sub-Committee on Stability and Load lines and Fishing vessels safety
SOLAS	Safety Of Life At Sea
STFT	Short Time Fourier Transform
TFA	Time-Frequency Analysis
TFD	Time-frequency distribution
VLCC	Very large crude carrier
WVD	Wigner-Ville distribution

Nomenclatures

A_{44}	Roll hydrodynamic added moment
$A(t)$	Wave magnitude
A_W	Windage area
B	Breadth of ship
BM_0	Metacentric radius at the upright position
$B_\varphi M_\varphi$	Metacentric radius at the inclined position
C	Hydrostatic restoring coefficients
C_B	Block coefficient
C_e	Compression factor
e	Measure of dynamic stability
f	Probability density function of corresponding seaway
f	Frequency of spectrum
f_p	Peak frequency of spectrum

H	Moulded height
$\overline{H}$	Average wave height
h_H	Heeling arm
h_R	Righting arm, or GZ
H_W	Wave height
h_W	Apparent wave height
Hs	Significant wave height
g	Gravitational acceleration (metre per second squared m/s^2)
GM_0	Initial metacentric height
GM_L	Transverse metacentric height
GM_T	Longitudinal metacentric height
GM_φ	Metacentric height at any angle of heel
GZ	Static stability righting arm, or h_R
I_{WL}	Moment of inertia of water plane
L_W	Wave length
M	Metacentric height
M_H	Heeling moment
M_R	Righting moment
m_0	= Area under the response spectrum
m_2	= Second moments of area under the response spectrum
m_4	= Fourth moments of area under the response spectrum
M_W	Wind heeling moment
PSD	Power spectral density
Q_0	Total sea area
Q_S	Safe operational sea areas
Q_V	Selected sea area
r	Exceedance rate of corresponding seaway
T_c	Wave period
T_0	Modal period
T_P	Peak period
T_z	Mean zero up-crossing period
U	Wind velocity
V	Ship speed
∇	Submerged volume
W	Weight of ship
Y	Spatial domain of sea area
Z_W	Windage lever
φ	Angle of inclination
$\varphi_{d\ crit}$	Angle of dynamic capsizing
φ_{fd}	Angle of flooding
φ_m	Angle at which maximum righting moment occur
$\varphi_r(\omega)$	Response transfer function

φ_S	Angle of static heel
$\varphi(t)$	Phase of the wave
φ_v	Angle of vanishing stability
ζ	Instantaneous wave
ζ_a	Wave amplitude
$S_\zeta(\omega_w)$	Wave spectral ordinate
$S_r(\omega)$	Response spectrum,
χ_0	Original heading in action
Λ	Season domain of sea area
Δ	Mass of ship in tonnes
∇	Volumetric displacement
ρ	Water density
ω_w	Wave frequency
ω_e	Encountered wave frequency
λ	Shape parameter
θ_w	Wave direction
ε	Broadness parameter

Chapter 1

Introduction

1.1 Research Context

A good understanding of the dynamic behaviour of a ship at sea is the key to observing and meeting operational constraints. The inability to accurately model the nonlinear behaviour of ships in irregular waves is one of the major obstacles in the path to achieve safe operations in harsh marine environments.

A ship's motions in a seaway are directly influenced by the encountered wave heights and periods. It is also influenced by relationships between the encountered frequencies and the ship's natural frequencies. The largest ship motions occur when there is a synchronisation between the encountered frequency and natural frequency of the ship's respective motions. The encountered frequency depends on wave length, ship's speed and the ship's heading relative to the wave direction.

The primary effect of a ship's wave induced motion is on the stability of a ship, which can deteriorate as the motion becomes larger. Ship stability is regarded as a phenomenon which can be described by both physical and empirical relationships. However, ship stability in an overall question of safety is affected not only by engineering but also by management and operational factors, both of which are underpinned by human factors.

This view (Kuo, 2000) can be cross-related in the following reasons:

1) Safety cannot be numerically quantified; it is a quality which can only be relatively explained and must be improved by increasing knowledge and experience.
2) The perception of safety depends on actual circumstances and on the competence, experience and judgment of those who are directly involved in the situation.

3) The concept of safety is directly related to a number of independently-varying parameters; as such therefore, it has to be studied, analysed and assessed through a well-defined and systematic methodology.

The current Intact Stability Code (ISC), established by the IMO, has mandatory and recommendatory parts. It covers certain operational requirements which collectively have a significant impact on the safety level against capsizing. However, this code leaves the final operational decisions to the master, as quoted from ISC: "Compliance with the stability criteria does not ensure immunity against capsizing, regardless of the circumstances, or absolve the master from his responsibilities. Masters should therefore exercise prudence and good seamanship having regard to the season of the year, weather forecasts and the navigational zone, and should take the appropriate action as to speed and course warranted by the prevailing circumstances".

The navigation of a ship in rough seas demands comprehensive judgement from the navigator in order to assume full control of the ship's operation. This is normally practised by the master, and the limiting estimate (Hoffman, 1976) is usually exercised based on visual observation of the sea state and the prevailing meteorological conditions.

The key factor to ensuring safety is to maintain adequate ship stability at all times. It is vital for the master, who bears the ultimate responsibility for the protection of the lives on-board. The requirements of ISC are far from ideal (Rakhmanin, 1994) and cannot in themselves guarantee a defined level of safety. Therefore, the master's judgements play a decisive role for the ship's survival.

There is an inconsistency in maintaining the intended level of safety because of embedded misconceptions in the ways of approach that are taken by the regulators, operators and designers. The main differences (Cleary, 1975) are listed as follows:

1. The regulator assumes an experienced human will be there to take **correct** action in case of need.
2. The operator tests the marine craft to the limit with the support of craft being approved and certified.
3. The designer optimises the design specification in order to fulfil the minimum acceptable requirements.

These differences have been known to scientists for several decades, however there have not been any significant improvements so far.

The minimum requirements for ship stability that are enforced through the ISC are deterministic. This has been criticised because the real sea behaviour is non-linear and follows probabilistic laws (Kastner, 2003). Currently, the acceptability criteria for intact stability are based on the righting moment of the ship. It is often considered, or assumed, that this requirement is sufficient against the environmental forces and moments that may occur at sea.

Measuring the variation of stability behaviours in a seaway is a challenge. The variations can reduce the margin of safety that is implicitly required to maintain adequate stability. Additionally, there is always a level of uncertainty in the current static stability condition of a ship due to the potential for inaccuracy in various measurements.

Many analysts now argue that stability boundaries of the conventional vessel's concept form can probably be stretched (Belenky, 2008), but the extent of such remains undefined.

A serious weakness with this argument, however, is the effects of simplicity versus physical modelling (Francescutto, 2004) in the need to criticise current stability criteria. This argument relies on the fact that, based on the Resolution A.167[1] that the righting arm in calm water is to stay "sufficiently high" in a "sufficiently large range of angles", is not in itself a good and reliable indication of ship dynamic stability.

There is thus an inconsistency with this Resolution to compute static stability characteristics, because it expresses a correlation between observed ship losses in a particular class of ships sailing in a very restricted region. Francescutto's criticisms are mainly focused on the fact that ISC does not take the following parameters into account:

- Seakeeping ability
- Excitations due to marine environment
- Coupling between different motions
- Shifting of cargo due to large roll motions
- Any shortcomings in stability because of high index of reliability as long as the ship remains intact

[1] First international stability requirements for passenger and cargo ships under 100m in length adopted by Resolution A167(ES.IV), and for fishing vessels adopted by Resolution A168(ES.IV).

Rational stability is a new topic that is currently under discussion among many experts in order to consider the ship's status in a particular operational environment. Utilisation of measurements and computing techniques is one of the best options that are available to consider the chain of events to predict the probability of extreme motions. For such a prediction, the recording of information on wave heights and period of encounters is required.

1.2 Research Rationale

The application of empirical stability criteria has resulted in great improvements in the stability status of vessels, and fortunately the capsizing of an intact vessel is now rare among accidents with ships. However, many of these accidents are related to the development of large angles of **roll** that potentially lead to down flooding, cargo shift or loss, and a number of other dangerous and undesirable situations and their consequences.

The minimum requirements of the ISC, as illustrated by the GZ-curve, do not show the underlying assumptions on which the minimum set values were derived. This has a dangerous drawback (Kobilinski, 2000) when the ship encounters extremely severe environmental conditions at sea. Moreover, the deficiencies of deterministic single value GZ-curve when in extreme conditions require the master to take actions beyond the given standards.

Wave induced forces periodically change the transient stability of a ship and increase the probability of capsizing. The changes of stability are dangerous at large roll angles and also when stability reduces for a longer period of time. In a ship with a low reserve of stability this may result in a dangerously large increase of roll angle, particularly in a combined severe beam wind and waves situation. Accurate estimation of changes of stability in waves requires the employment of complicated mathematical techniques.

A ships' stability in waves changes in a nonlinear way, therefore application of a GZ curve in order to gauge a ship's stability is limited. Even the relatively recent approach by probabilistic characterisation (Kobylinski, 2003b) of the changes of stability could not be applied effectively in developing criteria for the loss of stability. Currently, there are six methods (Christopher, 2009) that are employed for the assessment of the Intact Stability

(IS) Code. These methods are mostly for use in the applicable form of criteria at the design stage rather than for the operational stages.

Significant progress has been achieved in predicting ship dynamics during the last two decades. This is mostly related to the development of numerical methods for nonlinear dynamics and its application to ships, to advanced model testing techniques, and to new computational methods. These new tools provide hope that some of the more adverse phenomena can be explained at a fundamental level and as a result can be more effectively predicted and prevented, either at the design stage or during the operational activities (Spyrou, 2000).

Operational stability is a topic which aims to address the ship stability issues specifically related to in-service operations. Basic stability is the capability of a ship to resist capsizing, whereas operational stability (Grochowalski, 1989) depends on the ship characteristics and on the ship operations, and these require to be optimised together. The most relevant researches (Molland, 2008) that are in line with this topic are as follows:

1. Continuous monitoring of automatic estimation of ship static stability
2. Measurements of a ship's motions behaviour
3. Numerical time domain simulation of dynamic ship behaviour
4. Forecast on adverse seakeeping behaviour
5. Management of stability and safety

It is convenient to use the term "operational stability" in order to specify the ability of a ship in service to prevent capsize and to reduce the potential for damage from rolling and roll accelerations. It is considered that continuous monitoring of the influential sea parameters can provide a warning if a dangerous situation, such as synchronous rolling, is developing. Influential parameters are defined as those parameters of waves which have a direct effect on the ship's motions. In this study, they refer to peak frequencies of the wave spectrum and their associated magnitudes.

A direct assessment based on analytical, numerical, experimental, or combined approaches is the key factor to improve the safety. Therefore, further development and application of the tools that are directly applicable in ensuring the operational stability of ships will contribute substantially to safer shipping in the near future.

1.3 Research Objectives and Scopes

1.3.1 Motivation

As an ex-master of a ship over a period of years, the author had the direct responsibility to maintain safety and seaworthiness of the vessel at all times and in every sea condition. It may not be difficult to handle a ship safely in a moderate sea, with the available navigational equipment and machineries which support the master's broad knowledge and years of experience. However, in a rough sea, the decisions are often made on the basis of intuitive assumptions of the probable best solution rather than entirely on acquired knowledge and experience. Figure 1.1 illustrates the complexity of making rational decisions in order to attempt to quantify the risk levels or safety margins of the ship's dynamics in certain operating conditions.

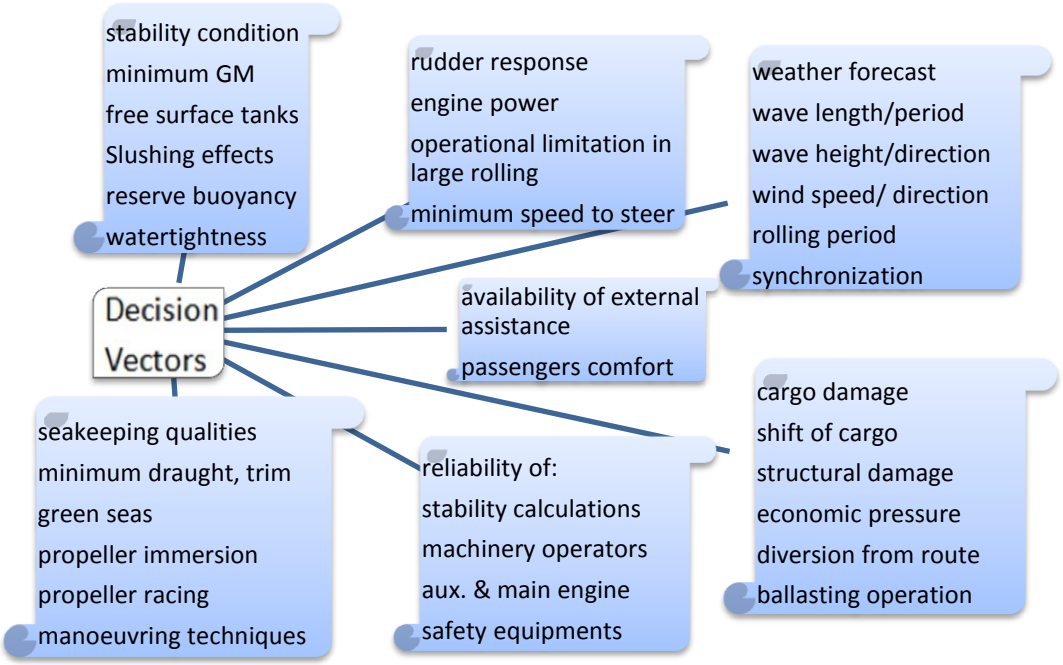

Figure 1.1 Factors influencing the master's decisions in the manoeuvring of a ship

In order to be able to achieve a greater degree of safety, an advisory real-time seakeeping tool is necessary. This tool should assess the behaviour of the ship for supporting decision-making on board.

The latest report by the World Casualty Statistics (Graham, 2013), as shown in Figure 1.2, indicates that there is a drastic increase in the frequency of the total number of losses of ships due to weather conditions; this is despite the fact that the overall number of ship losses has decreased from 84 to 53 from 2000 to 2012. Although this report does not list

the actual details of such accidents, loss of stability, shifting of cargo, green seas and flooding are typical consequences of extreme roll motions in bad weather.

Therefore, intelligent monitoring of the actual seaway that is being experienced is an ideal solution to ensure prevention of large roll motions from developing in critical weather conditions.

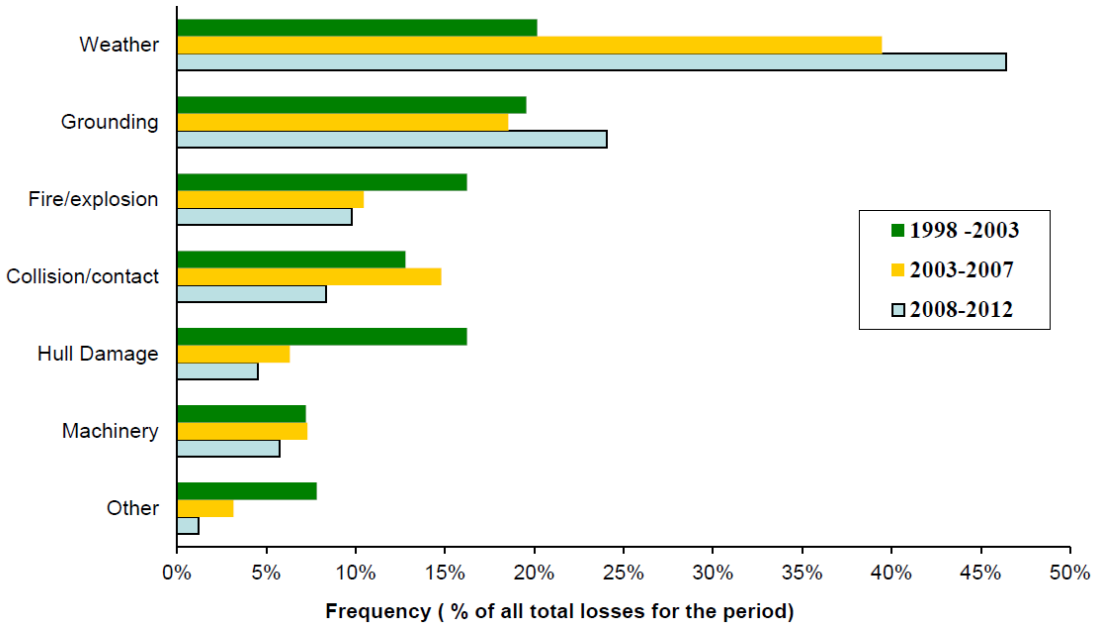

Figure 1.2 Total losses of vessels>500GT between 1998 – 2012 by the cause (Graham, 2013)

For effective ship handling in a rough sea, the master of the ship requires sufficient information of the ship's behaviour. That can lead to a change in the encountered period of the dominant waves by making an alteration in the ship's course and/or speed. Such information could be created by obtaining measurements of the waves, but waves are confused and irregular and are subject to constant changes. Additionally, it is a challenge for a ship to be able to measure the waves' influential parameters while itself underway and dynamically moving with the waves. The alternative approach is by the measurement and evaluation of the ship's motions because they are a good reflection of the dominant wave characteristics and can easily be captured.

The development of time-domain simulation is one of the more realistic and practical approaches to examining the link between a ship's wave-induced motions and of the non-linearity of the seaway environment (Francescutto, 1993). It facilitates and promotes an effective approach to many of the difficulties which lie in the understanding of a ship's dynamic behaviour.

1.3.2 Aims and Objectives

The aim of this research is to increase the level of ship safety by avoidance of extreme roll motions from developing. In order to achieve this aim, the research is focused on developing an understanding of how the ship motions can be utilised in the estimation of current sea conditions and to establish a causality link between the two.

There are certain parameters in the process that create a large roll angle of a ship, which are caused by the sea conditions, and they can be an examination of the ship's motions. These parameters particularly reflect the status of the current irregular waves through which the ship is sailing. The objectives of this thesis seek to:

- Consider the latest measurement techniques that have been implemented for the direct real-time estimation of sea conditions
- Investigate the most influential parameters through numerical analyses
- Conduct a series of experimental model-based tests in order to validate the numerical results
- Develop a tool for real-time detection of influential parameters and the prediction of the development of large angles of roll

Ship stability is clearly directly related to roll motion and deteriorates once the rolling angle increases. When a ship is underway, avoiding large roll motions as a consequence provides the opportunity for expanding the routine operations at sea.

This thesis has been formulated based on the idea of identifying the most influential parameters from the ship's motion responses. Hence, the probability of experiencing large roll motions can be prevented by sufficiently changing the encountered wave frequency through an alteration of course and/or speed.

The wave-induced ship motions are a time-varying phenomenon and can be measured and recorded by on-board sensors and equipment as discrete time signals. Subsequently, established signal-processing techniques can be employed as a tool in order to analyse such signals for data that is useful for operational purposes. The observer control system developed will enable an estimate to be made of the dynamic changes of the sea conditions, given the ship's heave and pitch motions as inputs and the predictions of the large roll angles as provided outputs.

Thus, the monitoring of the gradual effects of changes in a seaway and the consequent predicted impacts on the ships behaviour will provide valuable real-time information to the master in his decision-making.

1.3.3 Structure of the thesis

Chapter 1 starts with an introduction to the problem of operational stability and elaborates on the research question. The importance of decision-making has been discussed for a ship's master in a critically-developing sea environment. The expert views are reviewed and some of the possible routes to the solution of complex stability issues are mentioned. The motivation for starting this particular line of research is briefly noted and is followed by the aims and objectives to be achieved in this study.

Chapter 2 provides the historical background of seakeeping issues from both scientific and operational points of views. The development of Intact Stability and the changes that have been made in defining the standards covers a large portion of this chapter. The study focuses specifically on the development of operational stability over the last two decades. These developments are explored in sequence in order to illustrate a broader picture of the progress that has been made over the time period. The current IMO operational guidelines are presented as a consequence of those studies. The simplification of the IMO guidelines is discussed and their effectiveness in ensuring operational safety is reviewed.

Chapter 3 discusses the analytical approaches that can be used to model the sea conditions as well as the wave-induced ship's motions in the context of seakeeping, and it explores the current methods that are applicable in this field. Wave spectrum estimation is the base of the study in this research, hence the directional wave spectrum is reviewed in detail. The estimated outputs are demonstrated by the results obtained in two recent studies. The approaches of this kind have been successful in the estimation of the seaway, however there are significant limitations that need to be considered. This method of approach provides the foundation of the study that has been undertaken and given in this thesis.

Chapter 4 describes the methodologies that are employed in Chapter 5, 6 & 7 with special reference to spectral analysis. The types of irregular waves to be generated in towing tank experiments are explained, and the procedures to identify the waves' parameters are

schematically illustrated. The boundary element method (BEM) is selected for assessing the wave-induced loads and motions on large volume structures. BEM is introduced as being a suitable numerical approach on the basis of incorporating potential theory. This chapter also presents the mathematical derivation of the principle of signal processing and describes the advantages of the Short Time Fourier Transform (STFT). The relative influences of certain parameters on the accuracy of the presented data are emphasised at the end of the chapter.

Chapter 5 presents the comprehensive numerical experiments, using the boundary element method (BEM) that was undertaken. The numerical experiments are demonstrated, using the DNV SESAM (SESAM, 2010) nonlinear BEM, in order to investigate the wave-influential parameters through examination of the ship's motion responses. The general modelling approach in this environment includes running the analyses with different ship speeds. It uses flat panel based elementary Rankine sources that are distributed over both the mean wetted surface of the hull and the mean water-free surface. A rigorous modelling approach is thus developed which includes both the influence of various geometric and wave-loading conditions; it provides adequate recognition of factors which affect the motion responses.

The findings of this chapter are subsequently utilised in developing an operational guidance methodology. However, the analytical results are required to be validated by experimental tests, which are supported by the next chapter.

Chapter 6 describes the conducting of a series of physical experiments by employing a scaled ship model which was tested in a towing tank. The main objectives were the identification of the influential wave parameters through coupling effects of heave and pitch motions and the corresponding rigid body natural frequencies. This was achieved by spectral analyses of the measured responses of a selected generic mono-hull. The findings are discussed for three degrees of motion at different sea conditions and headings. The detected parameters are utilised in the decision-making process in order to avoid large roll motions. The time intervals in the identification and detection of selected parameters were found to be crucial for online monitoring, which is addressed in the next chapter.

Chapter 7 develops a computer program on the basis of the signal-processing technique that is discussed in Chapter 4. This approach utilises the results of Chapter 6 in order to

detect the influential parameters within a fraction of a minute. The methodology was tested by the numerical and experimental data that was obtained from the simulations and the model tests. The effects of window technique and sampling size on the quality of detection are finally discussed. The results suggest that this tool is unique in the fast identification of the influential parameters. It presents and identifies the dynamic changes of the ship's behaviour in a seaway. This tool can be used effectively in predicting the relatively immediate future roll motions of the ship in sufficient time for avoidance actions to be taken.

Chapter 8 provides the overall conclusions from the study and recommends areas for future research efforts.

Chapter 2

Historical Background

2.1 Introduction

For hundreds of years the potential risk of losing life and property has been one of the major considerations of the seafarer. To this has now been added the need to avoid pollution.

“Looking back at the history of seafaring, one may find that in old times perils of the sea were well recognised, and great risks to which ships were subjected at sea were in a way accepted. In fact, even in the nineteenth century, people risking a sea voyage considered themselves to be very fortunate if they arrived safely at the port of destination. The reflection of this situation could be found easily in the literature, art and tales of seamen but also in the reports on casualties” (Kobylinski, 2003b).

Earliest records indicate that shipbuilders were fully aware that ships must be stable when at sea in order to be safe and to have good seakeeping characteristics. Historically, stability calculations for ships relied on rule-of-thumb which was based entirely on experience that had been gained over a long time and subsequently passed on. Master shipbuilders in the past used a system of adaptive and variant designs. Successful ships were often essentially copied from one generation to the next with only minor changes being made and, by doing so, serious problems were not often experienced. Ships today by and large still use the process of adaptation and variation with hull shape families being scaled and tested.

With the industrial revolution of the nineteenth century and the associated rapid expansion of sea transportation, seafaring and growth in shipbuilding caused the issue of marine safety to become more important. From one perspective, in view of the growing

numbers of ships at sea, the very high risk involved in seafaring could not continue to be accepted. On the other hand, progress in marine technology provided realistic possibilities of ways to improve safety against capsizing or foundering (Kobylinski, 2003b). The concept of insuring both vessels and their cargoes also evolved, and so on.

2.2 Seakeeping: Scientific Improvement

One of the real problems soon recognised, with the demise of sail and the advent of steam as becoming the prime motive power, was in seakeeping. For the first time, ships could steam directly into the wind and sea and with consequent increases of pitch and heave motions. Steam ships were found to roll heavily and the various consequences of relatively high speed in rough weather were not fully understood.

The first systematic study was carried out by William Froude through a series of experiments in towing tank to investigate ways of reducing the rolling motions of ships.

Some progress was made through the serious discussions and various analyses of seakeeping that emerged during the 1949 period, with Ursell's theory (Ursell, 1949a; Ursell, 1949b) for predicting the characteristics of the flow around a circular cylinder that was oscillating in a free water surface. In another approach, St Denies and Pierson (St Denies, 1953) showed how the ship motions experienced in the random waves of the ocean could be calculated using the techniques of spectral analysis.

Since that time seakeeping has remained an active field of research, however developments have largely been in the nature of progressive refinements rather than by significant advances. Techniques such as designing roll stabilisers, criteria determination, prediction of long-term motion statistics and operational effectiveness are among those that have been considered in seakeeping performance prediction (Lloyd, 1998).

A ship's complex motion in a seaway is a mixture of surge, heave, sway, roll, pitch and yaw, which is the full six degrees of freedom motions. It includes any coupling effects developing between them in response to the action of the waves. The sideways drift is superimposed on to the progressing vessel's surge motion due to the action of wind. The three motions of heave, pitch and roll provide the balance between the forces of weight and of buoyancy. These actions create restoring forces or moments proportional to the changes of displacement of the ship from its still-water equilibrium position. These

motions result in stability variations and inadequate stability could lead to the capsizing of the vessel and the loss of the crew. Stability is one of the most important safety features of all ships, therefore it is essential to maintain adequate stability and reserves at all times. The research studies to date have tended to focus on adequate static stability either at the design stage or during loading operations. However, far too little attention has been paid to the stability of ships at sea and exposed to waves.

At the same time computational fluid dynamics, ship model testing and a better overall understanding of fluid and ship motion interactions has allowed for much more in-depth analyses of seakeeping performance. Although applications progress has been slow, many changes have occurred on the scientific level. For example great improvements are evident in the capability for mathematically simulating complex phenomena in the time domain.

2.3 Seakeeping: Operational Analysis

The main cause of the ship stability-related casualties (about 80%) are operational factors (Kobylinski, 2008) and those are generally related to human factors.

The handling of a ship effectively in heavy weather depends on the type, size and capabilities of the particular ship on the one hand, and on the other hand, her handling qualities in the wind and sea, the manoeuvring room available and other circumstances as mentioned in Figure 1-1. It is not advisable to set down precise instructions to help the master in the process of operations decision-making. Therefore, any attempt to improve a ship's handling should be in the form of an advisory tool. Cases are on record to show that while the handling of a particular ship in a certain way has proved to be successful in one instance, yet in another similar instance such handling has apparently led to a ship's foundering (MOD, 1983).

It would not be easy to develop a comprehensive range of potentially unstable ship scenarios with different options for a master to consider. The activity of ship-handling is essentially one of trial and error (Hoffman, 1976). Wave directions, available propulsive power, and the ability to control and steer the ship at reduced speeds are all factors which can affect the decision. A prudent master always studies carefully the reactions of a ship in heavy weather in order to better understand her seakeeping qualities.

Conventionally, navigators record the important information of their ship's behaviour on particular occasions, including in heavy weather, as well as any other useful advice based on these experiences. Such information will be invaluable to succeeding navigators when they join the ship.

An important effect of wave-induced motions on a ship is the partial loss of stability that may occur as the ship rides over the crest of a wave. Therefore, in order to preserve safety, it is essential to take early steps to improve the stability of a ship in sufficient time before the weather deteriorates. This lies in the fact that dynamic stability cannot be sensed, measured and monitored accurately in heavy weather. Improvement of the stability provides an additional degree of safety in many cases, especially for ships with a low reserve of stability, but it may equally penalise other ships if it is generalised.

The condition becomes worse in a ship that has a low reserve of stability, and which may result in a dangerously increased roll, particularly in a beam wind and waves situation. The resulting large ship motions will have a serious effect by reducing efficiency and causing a slowdown of general operations.

2.4 Development of the Intact Stability Criteria

In the second half of the eighteen century Lloyd's Register of Shipping was concerned initially with the insurance against loss of cargo. They issued the first recommendation on the magnitude of the minimum freeboard for a vessel; it required 2-3 inches per foot of the depth of freight in the hold and was subsequently amended. However, the Liverpool Underwriters Society had issued more detailed freeboard recommendations much earlier (Cowley, 1988).

The British Government was a pioneer in the development of freeboard standards by forming the Marine Department of the Board of Trade. The development of freeboard rules under the Load-Line Convention covered, however, only one aspect of ship stability. Consequently, stability standards were slowly developed in the early 20th century on the basis of several recommendations in order to respond to international needs, and it gave a boost to a more scientific approach to the subject.

The initial requirements for a stability standard at the international level were originated at the SOLAS 1948 Convention and, at that time, did not directly refer to intact stability.

They included provisions concerning stability information to be provided to the master of a vessel, the understanding of an inclining experiment, and on specific requirements on the carriage of bulk grain.

2.4.1 Stability Criteria

Probably the oldest stability criterion that is related to the physical properties of the ship was the criterion that was proposed by Denny (Kobylinski, 2003b) who established standard curves of minimal righting arms which were related to the minimal metacentric height, GM_0 = 0.244. However, the metacentric height alone was considered to be a sufficient measure to be used to evaluate the stability of ships until the late nineteenth century. By that time, minimum metacentric height values and some other parameters were proposed as initial criteria. The idea of replacing static stability by dynamic stability was initiated at first by Benjamin, but it was not well received for quite a number of years.

Stability standards, using the method of the balance of heeling and restoring moments, were first introduced by Blagoveshchensky. In his static approach, he assumed heeling moments to be the sum of the moments caused by the wind, the crowding of passengers to one side, and vessel turning. Were these to combine in an adverse moment they should be balanced by the hydrostatic righting moments. He also suggested taking into account the amplitude of rolling by adding it to the heeling angle. His simplified formula is:

$$M_W = 0.001C.U^2.A_W.Z_W \qquad (2.1)$$

Where, M_W is the heeling moment, C is a coefficient, U is the wind velocity, A_W is the windage area and Z_W is the lever.

Rahola (Rahola, 1939) completed previous tasks by his valuable contribution on the analysis of 14 Baltic ships that encountered stability failure between “1870 – 1938”. This comparison was based on a dynamic approach to the stability parameters of those ships that were considered to be safe in operation. He developed a set of criteria that formed as a foundation of the ISC, depicted in Figure 2.1.

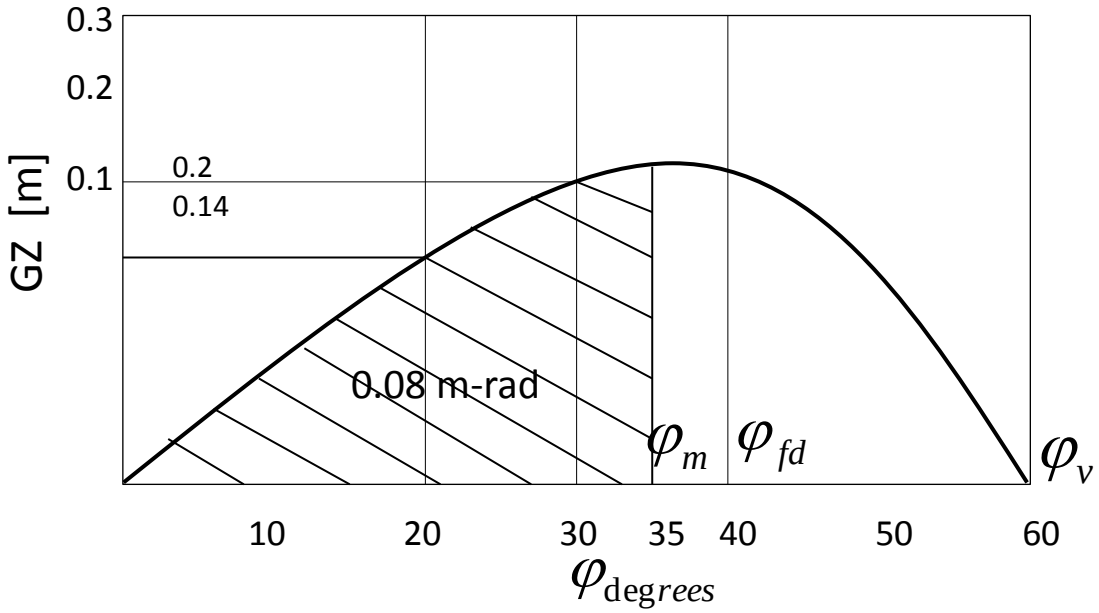

Figure 2.1 Limiting curve of righting arms according to Rahola, [1939]

2.4.2 Stability Standards

The development of stability criteria by the IMO was the outcome of several studies that can be categorised into three main approaches (see Figure 2.2). These three approaches are:

- Stability standard based on GM, proposed by Anderson, Posdyunin and Niedermair. However whereas this method is simple, it cannot ensure safety at large angles of heel.
- Stability standard based on GZ curve, proposed by Denny, Benjamin and Skinner. In this method, the physical parameters of the ship are taken into consideration but the action of heeling moments is ignored.
- Stability standard based on dynamic stability with consideration of heeling moments proposed by Blagoveshchensky, Pierrottet, Rahola and Norrby. In this method, due consideration is given to various physical phenomena.

2.4.3 Stability Failures

In response to the potential risk of stability failures, the 48th session of the SLF Sub-Committee of the IMO identified various phenomena in seaways which may cause large roll angles and/or accelerations. The identifications are for those ships that are considered to be more at risk of encountering critical stability situations in large waves.

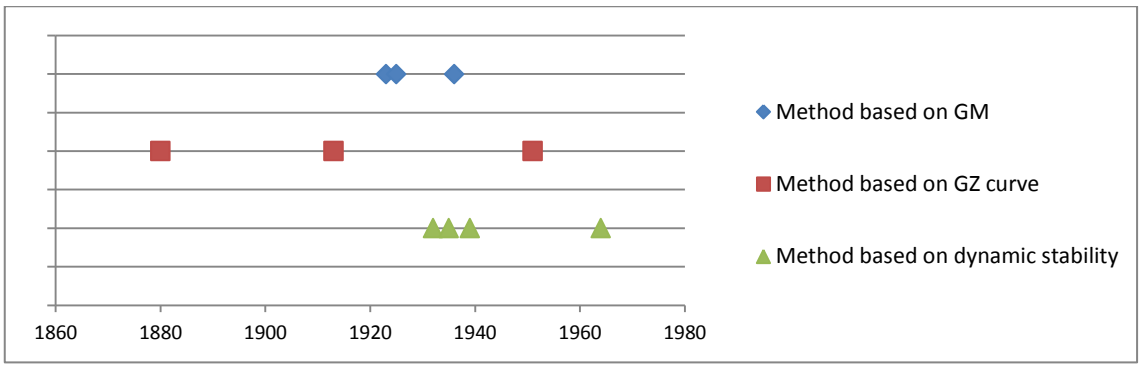

Figure 2.2 Approaches by various methods of for the development of stability standards

Three distinct physical phenomena considered to be responsible for stability failures have been identified (IMO, 2006). These are:

- Righting lever variation
- Resonant roll in the dead-ship condition (SOLAS II-1/3)
- Broaching and other manoeuvring-related phenomena

In order to ensure a uniform level of safety, the physical mechanisms of these phenomena are expected to be modelled within performance-based criteria.

2.4.4 Performance-Based Approach

In 2002 the IMO decided to revise the IS Code due to the occurrence of several serious accidents caused by head-seas parametric roll, as well as from design difficulties with large passenger ships and roll-on/roll-off- passenger (RoPax) ferries. In line with this revision, one of the major outcomes from the SLF subcommittee was an initial discussion for the development of performance-based or dynamics-based stability criteria.

Finally the 51st session of the SLF subcommittee of the IMO instructed the working group to consider:

1. The dynamic stability and performance-based criteria.
2. The Intact Stability of the dead ship condition under the effects of wind and waves, which needs to be assessed.
3. Phenomena for which criteria should be developed, defined as:
    - phenomena in beam sea waves
    - phenomena linked to stability alterations and stability loss in waves

- phenomena linked to manoeuvrability (e.g. large heeling angles in full speed turning, broaching, etc.)
- Phenomena related to wind action

4. New generation criteria applied to certain ship types that possibly could be more susceptible to hazards as assessed by way of “vulnerability criteria”.

The development of performance-based criteria is basically the development of methods for the prediction of conditions that lead to stability failure. This might be technically challenging for total stability failure because of the extreme nonlinearity of this problem. However, depending on the kind of mathematical model that is used, the performance-based criterion could be either probabilistic or deterministic.

The evidence of the probabilistic nature of the problem can be clearly seen in the case of some parameters that are chosen to serve as a measure, and which could be dependent on the stochastic nature of the environment. For example, the value of GM is commonly used as being the most basic parameter of initial stability. The GM could be calculated for the actual instantaneous waterline in irregular waves, similar to the study that Shin et al. (2004) carried out on regular waves as summarised by Kobylinski (2003b). In this case, GM becomes a stochastic process, and the theory of probability could be used to formulate a criterion for loss of stability. Such a criterion would be both parametric and probabilistic. Studies of GM being as a random quantity have been carried out by several researchers (Vassalos, 2000); Dunwoody (1989a, 1989b), Palmquist (Palmquist, 1994), Roberts (1982), Bulian and Francescutto (2006).

Summarizing the aforementioned considerations, four types of method could be defined for establishing stability criteria, namely: probabilistic performance-based criterion, deterministic performance-based criterion, probabilistic parametric criterion, and deterministic parametric criterion (Belenky, 2008).

2.5 Guidelines for Avoiding Dangerous Situations

Both operational practice and extensive experience have always been obvious ways to judge the validity of current stability criteria. Therefore, an operational guideline would be a great help to the ship operators in recognising and avoiding dangerous situations.

For example, some combinations of wave lengths and wave heights under certain operational conditions may lead to dangerous situations even for ships that are complying with the ISC (IMO, 2007b). There are also rare situations where relying on the minimum required stability is not sufficient (Kastner, 2003), and danger of high roll motions is imminent. In this situation a quick reaction by the master is clearly needed, however decisions that are made under pressure with an urgency and lack of time can cause human errors with severe consequences.

The MSC in 1995 approved the annex “Guidance to the master for avoiding dangerous situations in following and quartering seas”, with a view of providing masters with a basis for decision making on ship-handling in following and quartering seas, so assisting them to avoid dangerous phenomena that they may encounter in such circumstances (IMO, 1995). (Diagrams are given in Section 2.7).

The idea of simplifying the initial Guidance, based on a qualitative nature which is to be ship-independent, was predominantly the view of delegates at the time who believed in the value of a guideline with worked-out examples. This method of approach, however, exposed the guidance to different interpretations and consequently diminished its effectiveness.

The application of this guidance is not employed by seafarers so far for the following reasons:

- Lack of familiarity of navigating officers with hydrodynamic approaches
- Missing out rare and dangerous phenomena due to such not being part of routine checks
- Uncertainty in the methods of approach to measure or otherwise quantify wave length and wave period, particularly at night

When sailing in adverse weather conditions, a ship is likely to encounter various kinds and combinations of dangerous phenomena. The situation may eventually lead to capsizing or to severe roll motions with the latter causing damage to cargo, equipment and persons on board. The sensitivity of an individual ship to dangerous phenomena will depend on the actual stability parameters, the hull geometry, and both the ship size and ship speed. This implies that the probability of occurrence in a particular sea state may differ for each

ship in terms of degree of vulnerability in responding to dangerous situations and capsizing (IMO, 2007b).

Employment of the IMO recommendations can certainly promote the enhanced safety of a ship in a seaway. However a reliable method with ease of application is essential in order to alleviate the dangers of a following and a quartering sea, and should be designed in such a way as to avoid any reliance on manual computations. The results derived from such calculations should only be regarded as being a supporting tool during the decision-making process.

2.6 Developed Operational Guidance

A number of studies have attempted to develop operational guidance for the ship stability in order to address the capsizing hypotheses (Belenky, 2008). The research approaches can be categorised into those based on the classic definition of stability and those based on escape from, or avoidance of, the stability range.

Kastner (Kastner, 1986) defined a safety margin for operational stability to cope with extreme situations as depicted in Figure 2.3. His work was undertaken in response to major criticisms of the danger of relying on the mandatory minimum stability criteria when more stability is actually needed.

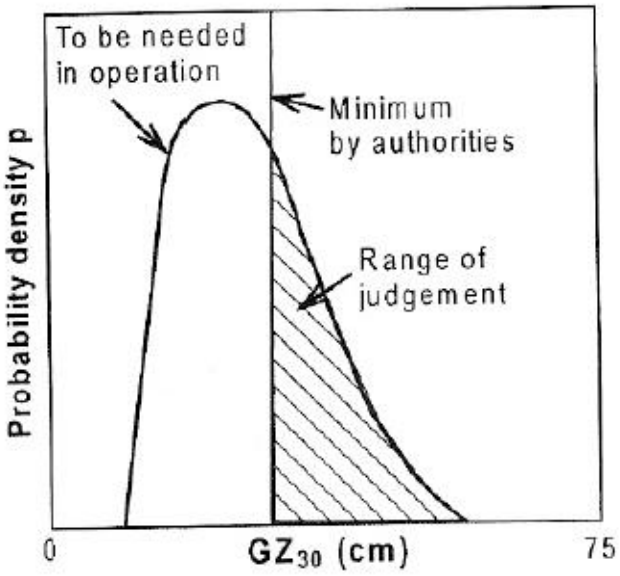

Figure 2.3 Master's range of judgement in operational ship stability (Kastner, 1986)

A ship's operations in the area marked as "range of judgement" requires the master to act particularly responsibly in severe seas, rather than relying on mandatory minimum standards. Kastner expressed his views on operating in extreme conditions by requiring thoughtful navigation of the master, and advising him to avoid severe situations at all times. That can be achieved by ship's routeing, anticipating changing ballast in advance, and by changing speed and heading as the sea conditions develop, and so on.

However, approaches of this kind carry with them various known limitations. Ballasting of a ship in advance improves stability situations, but there might be restrictions or limitations in ballasting operations in extreme conditions. Two of those known limitations are free surface effects and severe sloshing. Difficulties also arise in using ship's routeing due to availability and additional expenses.

An alteration of speed may have a considerable effect on the pitching of a ship but it does not necessarily reduce it to acceptable levels. After a reduction of speed it sometimes becomes more uncomfortable and the shipping of water on deck may increase. Alterations of speed are unlikely to have a significant effect on the rolling. Thus the decision for any changes of course and/or speed is a difficult judgement to make, and if the outcome has been misjudged then the ship may sustain serious damages.

The appropriate actions that are necessary in order to avoid potential danger not only require greater than a minimal level of knowledge and experience, but also need adequate real-time information about prevailing sea conditions. These are the minimum requirements that are necessary for a master to be able to take a decision on encountering adverse heavy weather conditions, or with the likelihood of encountering such.

In order to improve operational quality, numerous studies have developed various guidance charts and diagrams by defining the relationships between safety and either course and speed, or with wave characteristics.

Hoffman (Hoffman, 1976) identified a number of motion criteria that are relevant to dynamic stability, such as slamming, deck wetness, vertical bending moment at the mid-section, vertical and lateral accelerations, as well as rolling amplitude, in order to design an operational diagram. The diagrams in Figures 2.4 inclusive show the safety-

operational region for a typical container ship at various speeds and heading angles in high Beaufort wind scales.

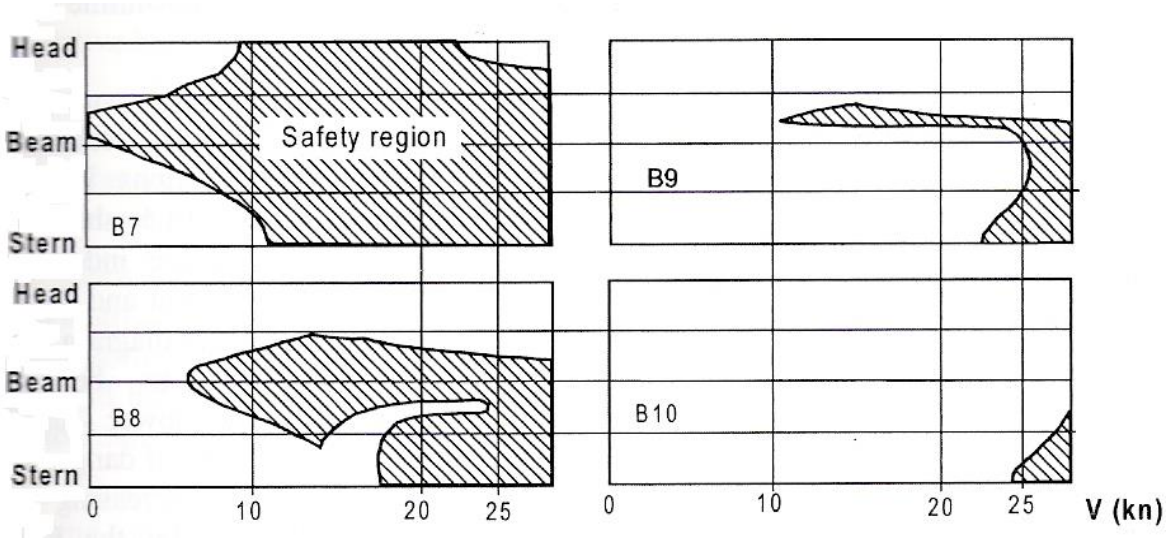

Figure 2.4 Safety region of container ship (Hoffman, 1976), showing the influence of increasing wind strength

This type of diagram can only be used as providing advice to the master of a ship. One criticism of the use of such a diagram in heavy weather relates to its effectiveness.

On the base of available statistical data, Hutchinson (Hutchinson, 1986) developed a diagram to show the operability domain of a ship. He considered three distinct criteria to be employed to define hatched regions in Figure 2.5. These are,

- Deck inclination (A)
- Local acceleration (B)
- Critical motion transverse displacement (C)

The probability of each region is shown in the Figure 2.5 which is based on the contiguous probability of the significant wave height and mean period. The probability of response, e.g. expected high roll motions in the spatial domain of a particular sea area and during a particular season, is derived from the following linear probabilistic formula:

$$P(H_s, T_m, V, \chi \,|\, Y, \Lambda) = P(V, \chi \,|\, H_s, T_m, \chi_0).P(H_s, T_m, V, \chi_0 \,|\, Y, \Lambda)d\chi_0) \qquad (2.2)$$

where,

χ_0	Original heading in action,	Y	Spatial domain of sea area
Λ	Season domain of sea area,	V	Ship speed

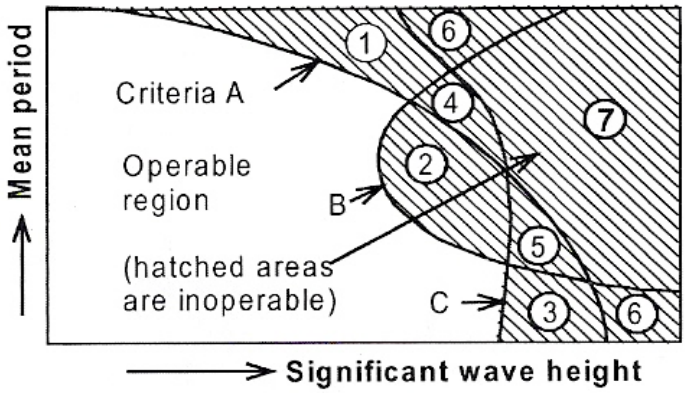

Figure 2.5 Operability domain showing downtime region (Hutchinson, 1986), numbers 1 to 7 show combination of criteria, 1 is due to A and not B or C, 7 is due to A and B and C

This method does not, however, include the region of nonlinear extreme ship motions and obviously does not identify the capsize threshold.

Mathematical models could be implemented in numerical simulation procedures in order to explain the relationships between various physical parameters. De kat and Thomas (De kat, 1994) used simulation techniques to calculate the extreme ship motions, including capsize, by use of the minimum metacentric height values. Figure 2.6 shows the results in the form of a capsizing index verses heading angles and the ship's speed. The most dangerous conditions are shown to be in quartering seas and when the speed increases. It has an advantage of being simple to use without the understanding of any physical modelling considerations, while seakeeping parameters are involved.

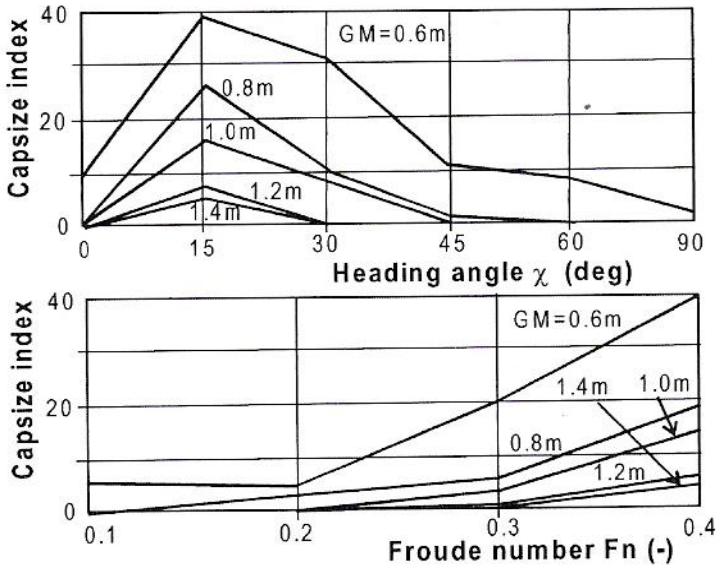

Figure 2.6 Calculated capsize index for GM, heading angle and speed (De kat, 1994)

The most important limitation of this method lies in the fact that the consideration of only one stability parameter is not sufficient to judge the capsizing of a ship. The key problem in using dynamic analysis to gauge the operational stability is in the large number of parameters that can be involved.

The threshold concept is becoming an increasingly important area in ship stability assessment, and there are several studies that are attempting to define this idea further in one form or another. Rainey and Thompson (Rainey, 1990) studied the links between wave characteristics and ship's length and heading in order to propose the transient capsize diagram that is shown in Figure 2.7. It shows the wave height above which a ship can potentially capsize. In the development of this diagram, groups of regular waves are used instead of assuming irregular seas. They also suggest using equivalent regular wave conditions when reaching some critical wave height so to reduce the number of simulations. The authors suggest "using the transient capsize diagram as the basis for stability regulation which includes the ship dynamics as well as an operational aid".
One question that needs to be asked, however, is the conclusion that follows from Figure 2.7 that beam seas are more dangerous than are quartering seas, which is in contradiction to the study depicted earlier in Figure 2.6.

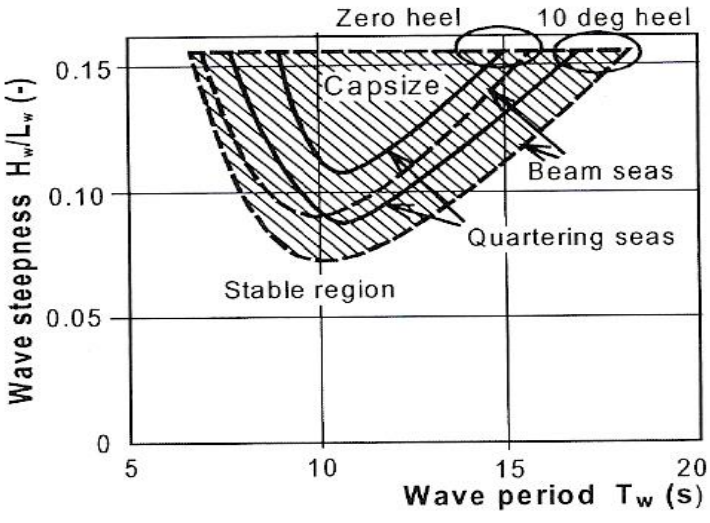

Figure 2.7 Typical transient capsize diagram (Rainey, 1990)

The decisive role of the "human factor" is obvious in operational stability, and technical proof of a captain's actions depends on the level of technology that is used on-board. The Russian Maritime Register of Shipping developed a system on the basis of the possibility

of assigning restrictions. These restrictions apply to ships that are not satisfying navigation conditions of an unrestricted region, through an index method that is related to ship seaworthiness (Kuteynikov, 2000). The factors that influence the calculation of these indices are individual ship parameters, the loading condition (including draught and stability), the sea region and the season of navigation. It is considered to be used as a supporting tool for operational decision-making on the basis of two control parameters: permissible distance from a place of refuge or between places of refuge, and on maximum allowable waves heights in different regions.

In order to support stability management, an applicable software (SAFESEA) was developed to provide a polar diagram acceptable to indicate, for a specific ship, the safe and the dangerous zones where the calculations have been maintained by the measurements.

Kuteynikov and Lipis (Kuteynikov, 2000) determined a common factor to aid in the possibility to choose safe ship navigation modes on the basis of the ratio $W = \frac{Q_S}{Q_0}$.

where Q_S is defined to be all safe operational areas and Q_0 is the total area of concern ($Q_0 = \pi V_0^2$, V_0 is the speed in still water).

Index W is defined as: $W = W_S \cdot W_V$ (refer to Figure 2.8)

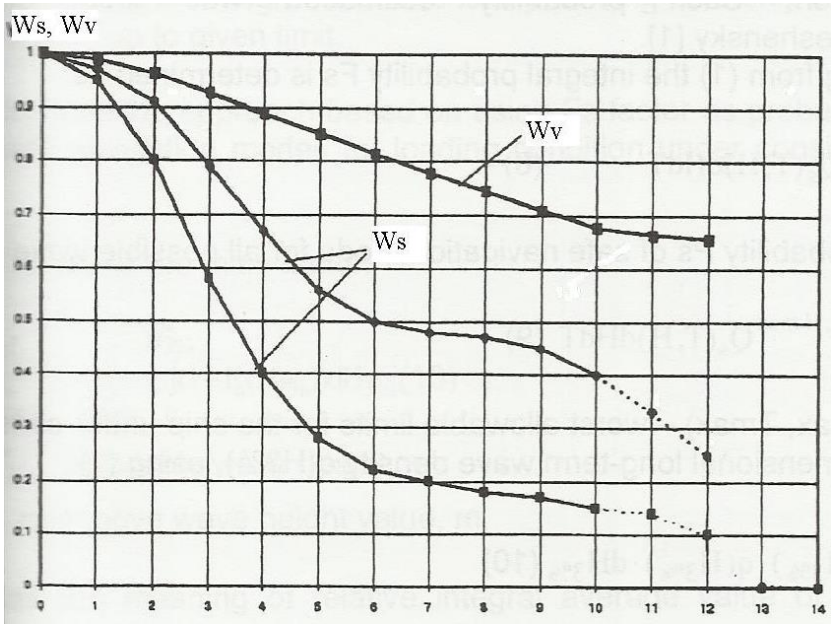

Figure 2.8 W_S and W_V verses wave celerity (kn) accounts for safety mode of cargo ship in two different loading conditions (GM = 0.27m and GM = 2.68m) and two different trims (Kuteynikov, 2000)

Where $W_S = Q_S / Q_V$ and $W_V = Q_V / Q_0$, Q_V is the selected area.

A seakeeping information booklet can be prepared to serve as guidance of a specific ship for avoiding dangerous situations in extreme weather conditions.

Papanikolaou, et al (Papanikolao u, 2000) studied the behaviour of bulk carriers at different heading angles for a range of speeds. It was observed that small changes of speed and/or heading can cause large differences in the wave excited ship motions, particularly in the heave, pitch and roll motion responses. The study focused on the seakeeping behaviour (wave induced motions and loads) of the four standardised bulk carriers and where results were found to be tremendously different.

In a systematic study they demonstrated that stern quartering seas are the most dangerous of situations. It is depicted in Figure 2.9 that the roll response becomes significant when the speed increases and thus stability of the ship can be drastically reduced as a consequence of speed and heading combinations.

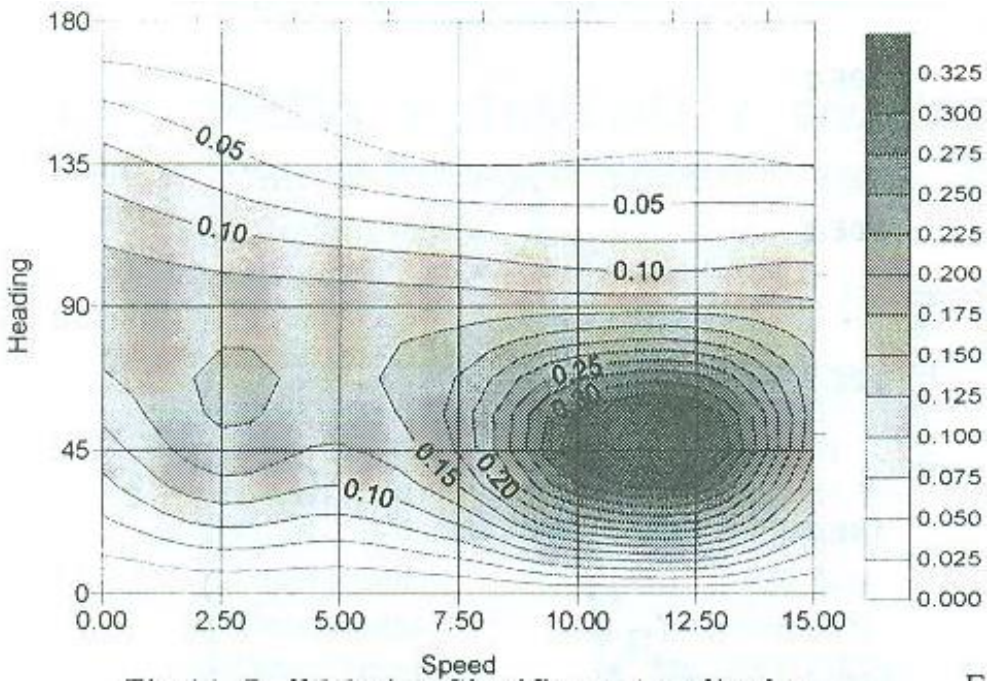

Figure 2.9 Roll motion significant amplitudes – (the contours are in radians) (Vassalos, 2000)

This study was proposed to the IMO in 1998 as providing guidance for avoiding dangerous situations in extreme weather conditions.

The various developments that have taken place in this field have led to an interest in real time motions monitoring. Such a monitoring can be used in providing seakeeping predictions for supporting real-time operational guidance on-board a ship. A prototype

system was developed which includes a mathematical model of the ship for direct hydrostatic and hydrodynamic analysis of arbitrary operating conditions (Huss, 1994). The actual sea state that is experienced is not directly measured but is evaluated through measurements of the ships motions. Criteria for providing warnings of undesirable events can therefore be initiated on board, and could be set to raise the alarm when defined risk levels are being exceeded.

Response spectra, in principle, can be calculated from transfer functions and utilisation of a known wave spectrum relevant to sea area. Consequently, if a response spectrum is measured and the transfer function is known through earlier theoretical calculations, then the wave spectrum $S_\zeta(\omega)$ can be evaluated by the following formula:

$$S_\zeta(\omega) = \frac{S_r(\omega)}{\varphi_r(\omega)^2} \qquad (2.3)$$

However Huss and Olander (Huss, 1994) highlighted number of difficulties in this otherwise practical application:

- The response transfer function $\varphi_r(\omega)$, must be calculated on the basis of a known relative wave heading.
- The waves are assumed to be long crested, or to be short crested and taken to have a known directional spreading.
- The response spectrum $S_r(\omega)$, is measured over the encountering wave frequency, in irregular waves.
- The wave energy at frequencies with low response levels cannot be evaluated with sufficient accuracy

To date, various methods have been developed and introduced in order to measure the wave spectrum, and each has its own advantages and drawbacks. Two of these studies have employed a similar methodology but in more detail, and which are explored in Chapter 3.

Several questions have been raised about the reliability of the IS code to be able to deliver sufficient answers to some of the dynamics of ship stability. Some well-known examples are large containerships being susceptible to parametric rolling and pure loss of stability, whereas ferries and cruise ships are generally suffering from very short roll periods and high related accelerations.

The formulated guidance can be presented in the form of diagrams (Cramer, 2003) as shown in Figure 2.10. It is given as a typical example of a polar plot presenting the condensed results from numerous simulations. It is designed on the basis of different speeds and encounter angles in short crested seas with a significant wave length of the order of the ship's length.

The colour-intensity graph illustrates the wave heights that the vessel can consider to be safe to operate in according to a certain criterion.

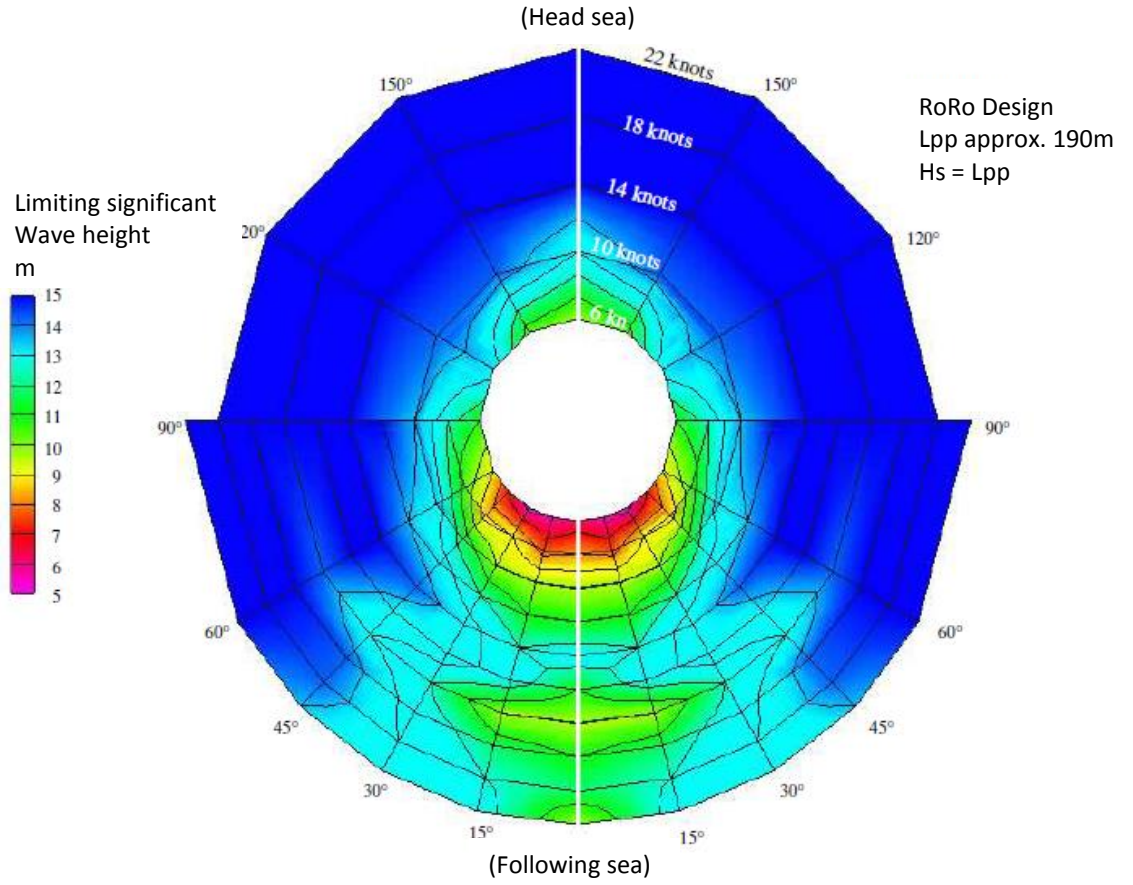

Figure 2.10 Example for a polar plot showing limiting significant wave heights for a RoRo-Design (Cramer, 2003)

These types of diagrams can be used to identify potentially dangerous operating conditions. This method of approach allows for investigation and illustration of the physical background potentially causing the stability problem and possible solutions for a better performance.

It was found to be convenient by Shigunov (Shigunov, 2009) to use probabilistic measures to develop operational guidance for container vessels. Operational guidance should be

able to differentiate which combinations of operational parameters are acceptable for any given loading and sea conditions. Therefore, initially, two criteria were defined, namely short-term and long-term.

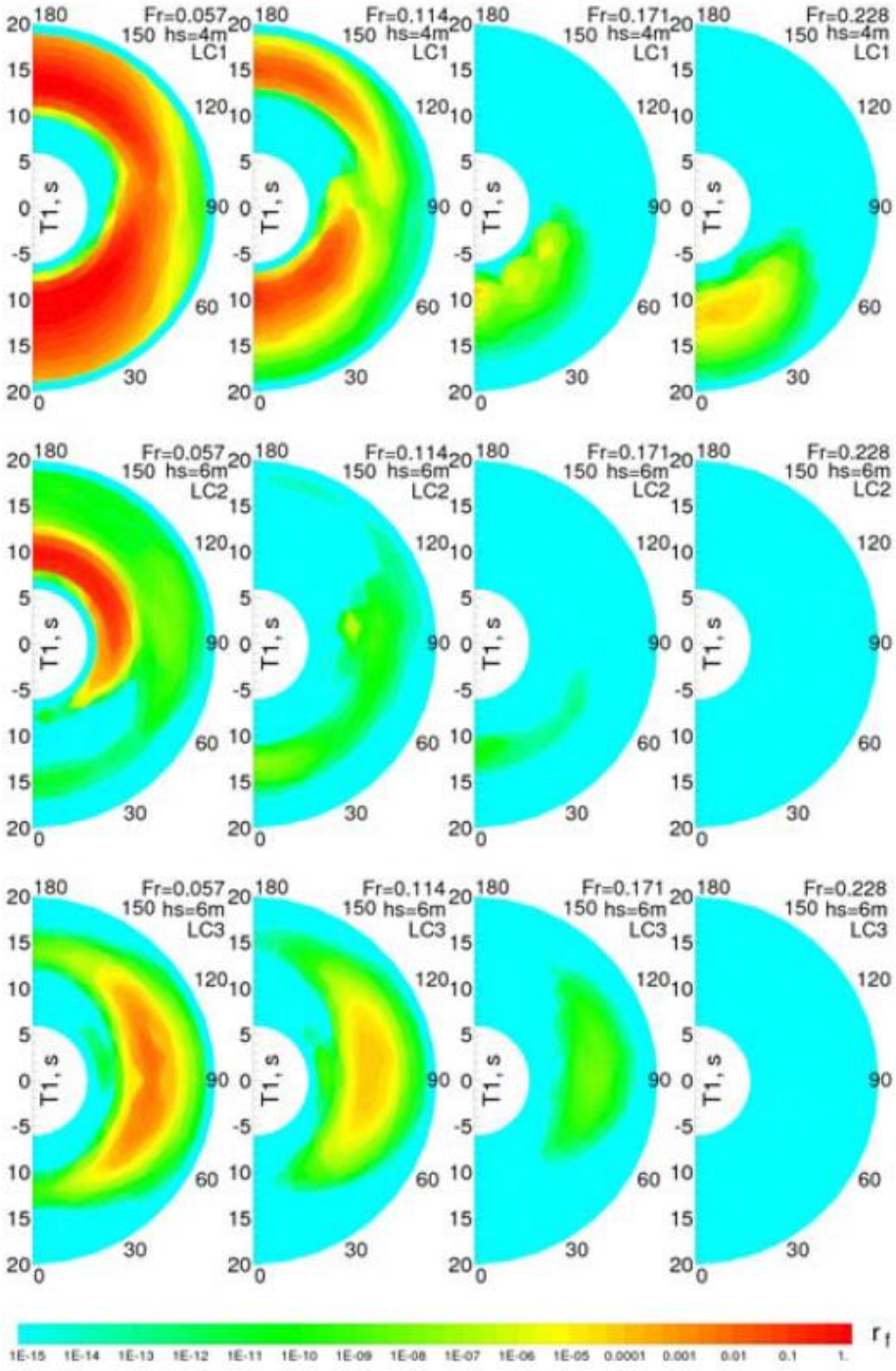

Figure 2.11 Polar plots of $\ln(r_f)$ vs. mean wave direction (μ) and mean wave period (T) for different ship speeds (Fr) and loading conditions (LC) (Shigunov, 2009)

Short-term criteria should ensure, on average, the necessary level of safety that is expected, and the long-term measures of safety are to be defined by the average over a large number of ships, loading conditions, routes, seaways and operational parameters.

The exceedance rate is defined as the basis of the short-term criteria, because it is independent of the chosen time intervals. It was argued that exceedance probability depends exponentially on the exceedance rate, which makes criteria more sensitive based on rate.

Short-term criteria is the product of $r_f = r \cdot f$

Where, r is the exceedance rate and f is probability density function of corresponding seaway. An example of colour polar plots of r_f, based on the exceedance rate of the maximum allowable lateral acceleration of 0.5*g*, is shown in figure 2.11.

On the basis of previous research findings Ovegard et al (Ovegard, 2012) categorised different possible approaches for ship-specific operational guidance into three options:

- Pre-computed polar plots based on extensive time-domain simulations for all sea states, loading conditions, etc.
- Real-time, on-board time-domain simulations based on actual measured sea states and loading conditions
- Simplified methods that are able to identify stability boundaries instead of providing quantitative roll angle predictions

The main limitations with the first approach are the difficulties of simulation models to adapt to the actual conditions with complex wave spectra. It becomes more complicated with non-linear phenomena, which require a multi-dimensional grid.

The second approach seems to be probably the ultimate goal to be achieved but which still requires further development. However, the third approach uses simplified models for actual conditions to identify risk boundaries (Ovegard, 2012) instead of predicting the consequences.

In the latest attempt to apply the third approach, a simplified method was used in the assessment of pure loss of stability and parametric rolling. The metacentric height (GM) variation in irregular waves was considered as being a linear stationary Gaussian stochastic process. The result is presented by GM variation spectra as shown in figure 2.12.

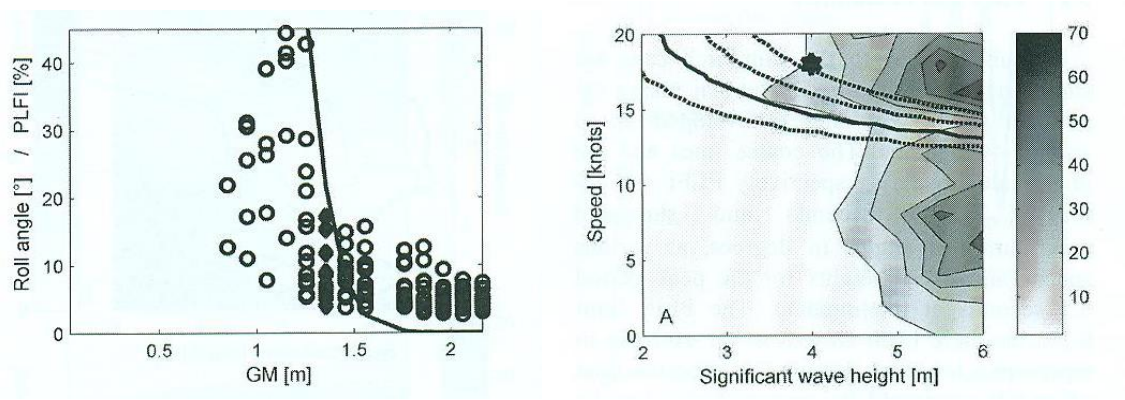

Figure 2.12 (Left) Maximum roll angles at each realization with different GM and the PLFI in percentage. (Longuet Higgins)

The grey areas shown in Figure 2.12 are a simulated overall maximum roll angle for each speed – sea state combinations. The lines are GM_{Crit} (Ovegard, 2012)

2.7 Current IMO Views over Operational Stability

A lack of operational guidance in the statutory regulations and the importance of decision-making when operating in adverse weather were the initial reasons which lead to this document being prepared with international consensus. The first document (IMO, 2007b) was produced in 1995 and amended later in 2007.

The purpose of this document, as the title implies is providing "guidance to the master for avoiding dangerous situations in adverse weather and sea conditions".

A number of stability-related phenomena are defined in the document and some cautious advice is given. A diagram is provided to show the relationship between the wave period and encountered wave period when considering a ship's speed and heading angle (see Figure 2.13).

Two more diagrams are provided, one for avoiding "surf-riding and broaching-to" and the other for "successive high-wave attack" (see Figures 2.14 & 2.15).

The most significant limitation with the use of various graphs and tables lies in the fact that this method of approach might be counterproductive (Kuo, 2000) in adverse weather conditions. The deficiencies in applicability of this form of guidance are discussed in detail in Section 2.5 of this chapter.

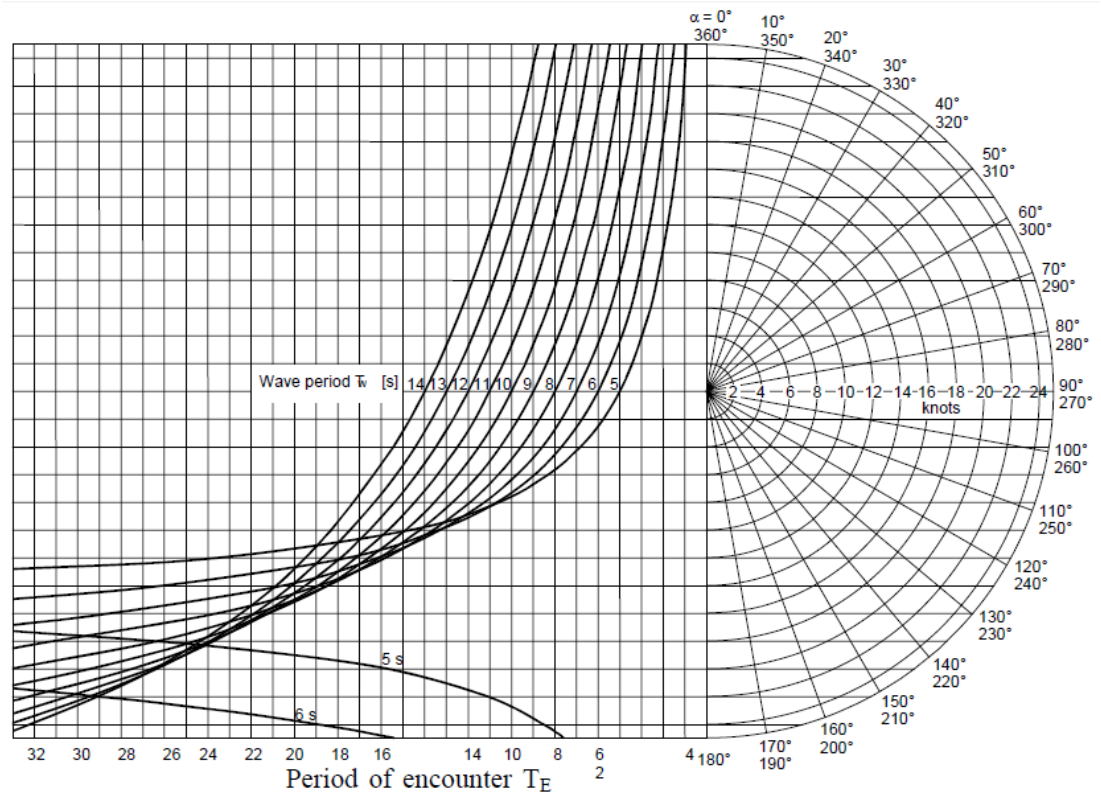

Figure 2.13 Determination of the period of wave encounter (IMO, 2007b)

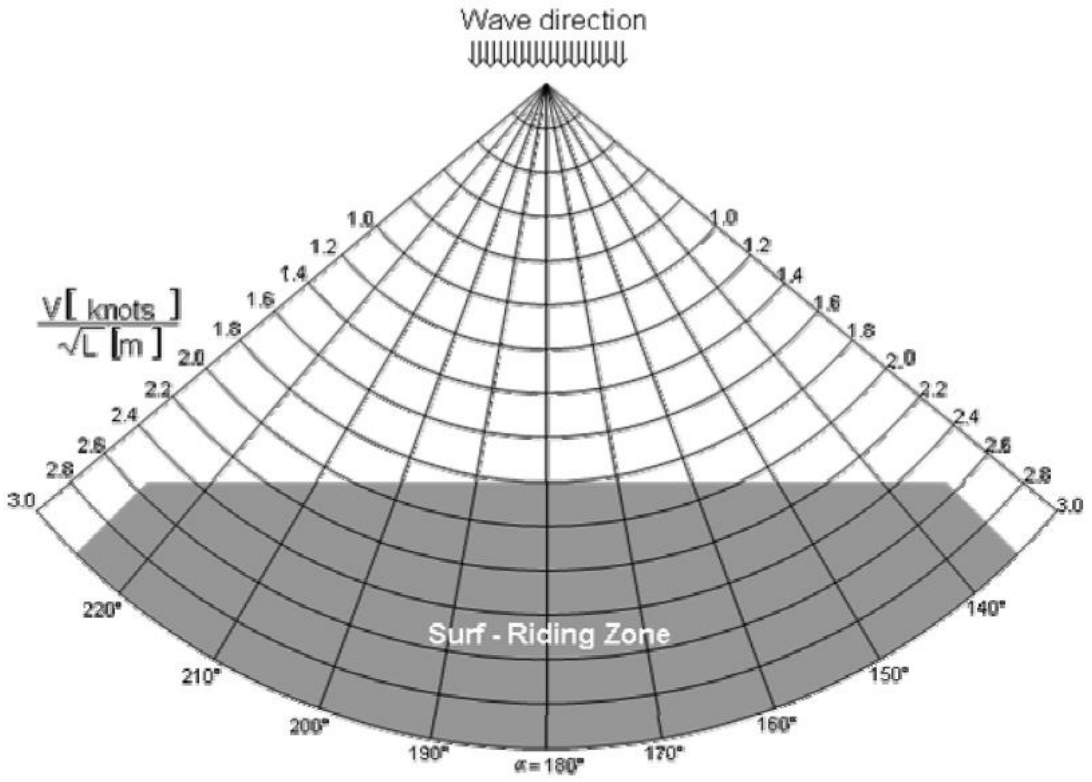

Figure 2.14 Risk of surf-riding in following or quartering seas (IMO, 2007b)

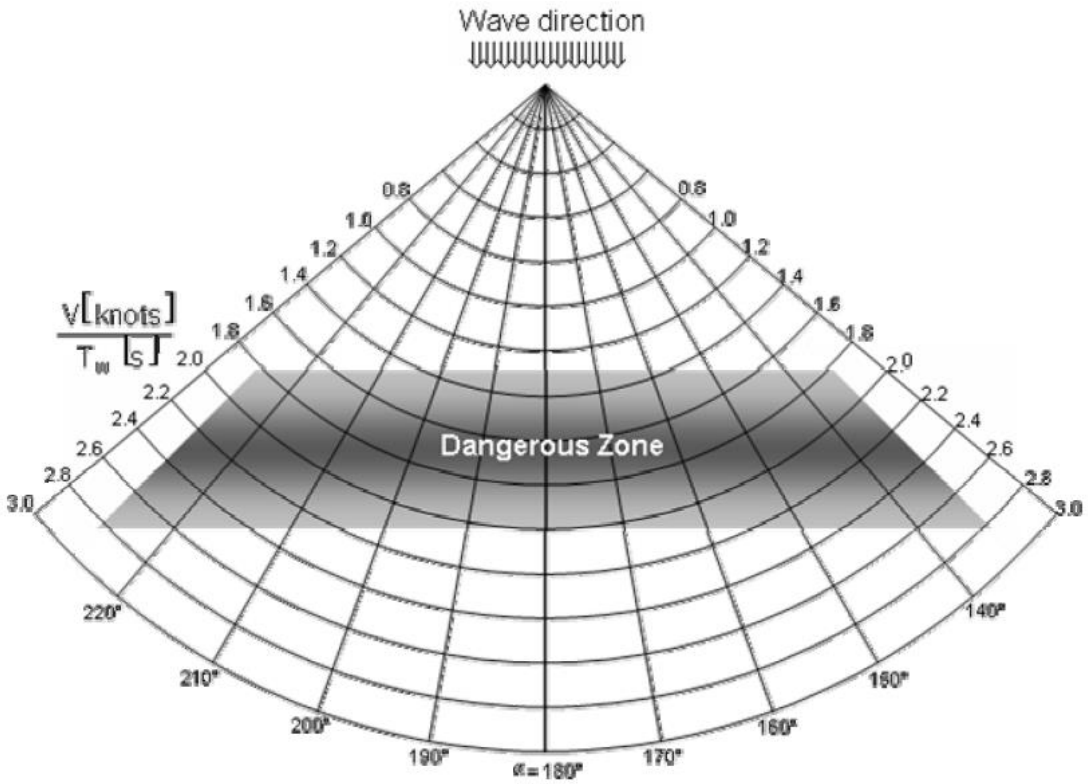

Figure 2.15 Risk of successive high-wave attack in following and quartering seas (IMO, 2007b)

2.7.1 Decision Support System Using IMO Guidelines

Rodrigues (Rodrigues, 2012) published a paper in which he discussed the application of the IMO Guidelines. He designed a program to function as a software component of an on-board decision to support the operation of fishing vessels in waves, in order to improve the vessels' safety. The main objective of the proposed system is to predict the motions and the acceleration of the vessel at given locations, for comparison with operational criteria. The study suggests the criteria for operability and seasickness that has been proposed by Faltinsen (Faltinsen, 1990) and in O'Halon and McCauley (O'Hanlon, 1974) for this evaluation.

The data flow of the implemented algorithm to monitor the dynamic behaviour is shown in Figure 2.16. The vessel motion is measured through several sensors such as accelerometer, angular rate sensor, inclinometer and wave height measurement.

The system is based on the real-time computation of the predicted responses of a ship, taking into consideration the local sea state. The prediction of the motions is estimated through the construction of the directional JONSWAP spectrum and then applies the

respective motion transfer function (details of this computation are given in the next Chapter).

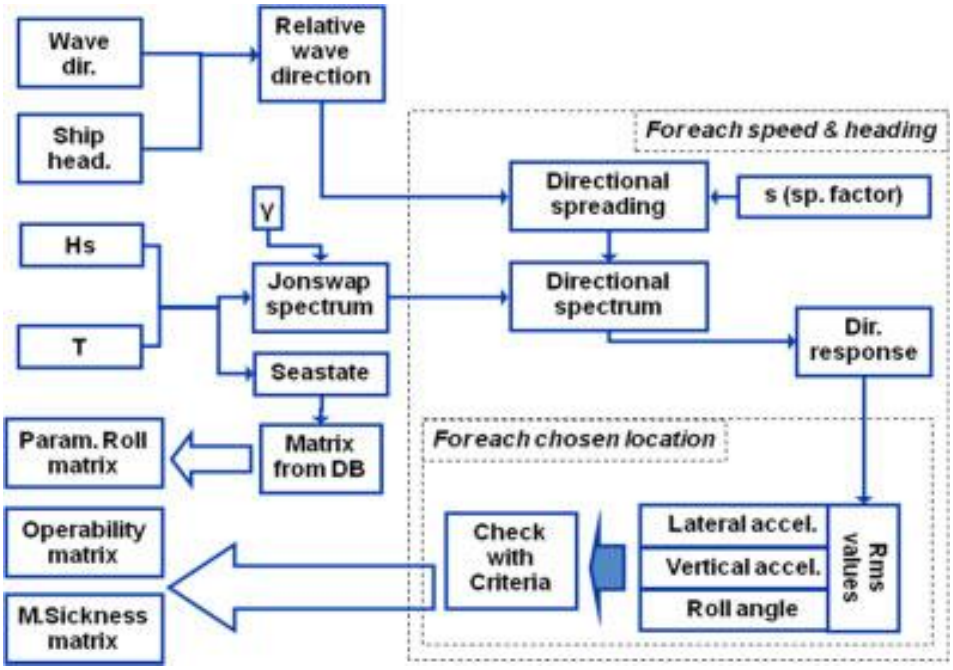

Figure 2.16 The data flow of the module that monitors the dynamic behaviour of a fishing vessel and provides supporting information to the master

The main wave characteristics required for the construction of the spectrum are significant wave height, wave modal period and wave direction. These characteristics are estimated from the wave frequency motions of a vessel at zero or low advance speed. The development and full description of the wave frequency motions can be found in Pascoal et al. (Pascoal, 2007).

A simplified analysis is finally conducted on the basis of procedures advised by the IMO (IMO, 2007b) guidance. When the calculations for a given speed and course result in a high probability of dangerous phenomena which may occur, the corresponding speed/course combinations are identified and mapped into a polar plot.

However, these methods of analysis have a number of limitations. The first concept has been developed on the basis of linear spectral analysis, and tends to overlook the nonlinearity of the motions in a severe sea condition. Therefore, the study might be useful for a ship operating in a less harsh environment. The advice to a master of a ship on the basis of the second concept relies on over-simplified formulae and several assumptions which add to the uncertainty of the results. However, the authors expect an

opportunity to proceed to ship installation and trials, with regard to validation and troubleshooting.

2.8 Summary and Conclusions

This chapter begins by laying out the theoretical and practical dimensions of the current research area, and looks at the major ship stability problems and the improvements that have been made over the years. Recent developments in ship stability have heightened the necessity to provide guidance specifically for ship operations. The idea is supported by the considerable experiences from ship operation. The safety of a vessel and its crew depends strongly on the ability of the navigator to judge the vessel's dynamic behaviour and to recognise its limitations. Therefore, it is not only necessary to appreciate and have a good understanding of a ship's dynamics in the design process but also by providing support for in-service decision making to avoid dangerous situations from developing.

Numerical simulations could be one of the solutions that could be developed to provide a better insight into the physical phenomena involved. An advanced programming approach is required to monitor real-time intact stability and seakeeping characteristics in order to cover the entire range of operations in adverse environmental conditions.

This chapter has briefly investigated the development of shipboard guidance for the operation of a ship in rough seas. The main focus of this research was to provide adequate information for the task of handling ships in adverse weather conditions. It was apparent that a number of parameters are to be considered in monitoring dynamic stability, and it becomes complicated with a greater number of parameters. These parameters are ship's type, size, loading conditions, speed, sea conditions and so on. The effects of non-linearity compounds considerably increase the problem.

The two fundamental discussions that need to be taken forward are sea conditions and the behaviour of the ships among the waves. Therefore the next chapter explains the modelling of irregular waves as well as the modelling of the process for determining the ship's motion responses, and provides a review of two recent studies that have utilised these techniques.

Chapter 3

Mathematical Modelling of the Sea Conditions and Ship Motions

3.1 Introduction

Over the last century there has been an increasing interest in the study of both ship motions and the nature of regular waves and, to a considerable extent, these have become a central issue. There are a number of important differences between regular waves and actual natural seas, as the normal free surface is not sinusoidally corrugated and the wave pattern is rather complex, confused and extremely irregular.

More recently among the various traditional approaches of pattern recognition, the addition of artificial neural network (ANN) techniques theory has been receiving significant attention. The pattern recognition is critical in most human decision-making tasks because if the more relevant patterns are available, the better decisions will be taken (Basu, 2010). Automatic recognition of ocean wave patterns through ship motion responses can be utilised to identify the influential parameter so avoiding synchronisation and hence extreme roll motion. There are however some limitations in the applications of ANN.

Neural networks are trained with complete data sets consisting of input and output data. When the network has learned the complete data sets, then an independent collection of complete data sets is taken to test the generalisation capability of the network. Both collections of complete data sets must be large enough and properly distributed within the range of possible data (Mielke, 2011). The system needs several training cycles to obtain an optimal structure of the network. Designing a network with the input data from

the ship motions which would be under continuous variation is time consuming, and does not suggest the suitability of ANN for this study.

A variety of developed mathematical methods can be used to model the irregularity and variety of the seaway, and the most acceptable approach is the statistical model. These mathematical models can predict how often various wave heights and periods may occur over a certain period of time for a particular regional sea surface.

The obvious characteristic of irregular waves is in the changes of the surface at any time and at any place. The initial disturbance of the surface is directly proportional to the wind speed and duration, and is classified in the Beaufort table. The observation of the wind condition is considered to be the simplest way for making a visual estimation of the current seaway.

For an irregular seaway, the disturbance of the sea surface at any given point as a function of time is shown in the Figure 3.1. These properties are constantly changing from time to time, whereas in the case of sinusoidal waves they are assumed to remain constant.

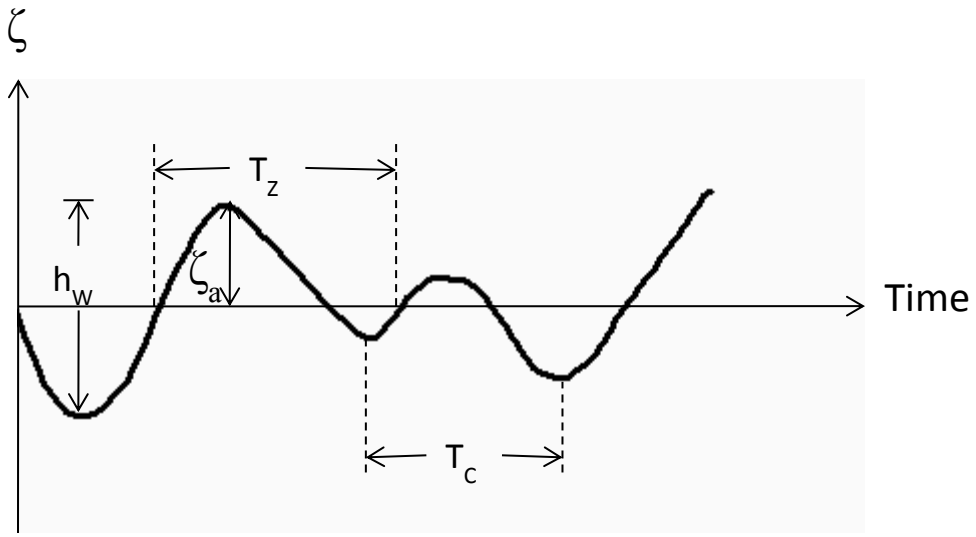

Figure 3.1 Irregular seaway generated in towing tank plotted to the base of time at a given point

The average wave height in an irregular seaway is the arithmetic mean of the heights of all of the waves for a given set of continuous observations. The longer the period of the set of observations, the more accurate will be the value that is determined for the average wave height.

3.2 Modelling of the Seaway

The waves which are of the most concern for the modelling of a seaway are those which are formed in the open sea by the action of the natural wind. A steady wind blowing over a calm surface of water gradually creates ripples that travel across the surface in relatively the same direction as the wind. The waves gradually grow over time, through the blending of ripples. Therefore the observed waves at any particular place and time consist of a superposition of all the components of heights and periods of a variety of regular waves. However, wind-generated wave systems may be confused by swells generated elsewhere by other winds probably blowing in different directions, and so on.

3.2.1 Statistical Concepts

Over the last few decades the irregularity of a seaway could be represented with the help of a histogram. The frequency function of the individual wave characteristics within a seaway configures the shape of the histogram at a given moment in time or in a given geographical place. Experiences confirm that distribution of wave elevations takes the shape of a Gaussian or normal function. The histogram can also be produced in the form of wave periods rather than wave elevations. In that case the location of the "centre of gravity" of the histogram with reference to the y-axis defines the average wave period T, and is found through the following formula:

$$T = \frac{\int p \cdot T_Z \cdot dT_Z}{\int p \cdot dT_Z} \tag{3.1}$$

where p is the percentage of occurrence and T_Z are the zero crossing periods.

Accumulated experience suggests that an irregular seaway will produce a low, wider histogram (Ochi, 1998) and one which can be mathematically modelled by the theoretical Rayleigh function (see Figure 3.2). The Rayleigh distribution function is expressed by the following equation:

$$P(H_i) = \frac{2H_i}{\overline{H}^2} e^{-H_i^2 / \overline{H}^2} \tag{3.2}$$

The term $\overline{H}^2$ is understood to mean the average height of the entire number of all experienced wave heights squared, and is defined by:

$$\overline{H}^2 = \frac{\sum\left[(H_i)^2 \times f(H_i)\right]}{\sum\left[f(H_i)\right]} \tag{3.3}$$

where $f(H_i)$ is the number of occurrences of H_i in a given period of time.

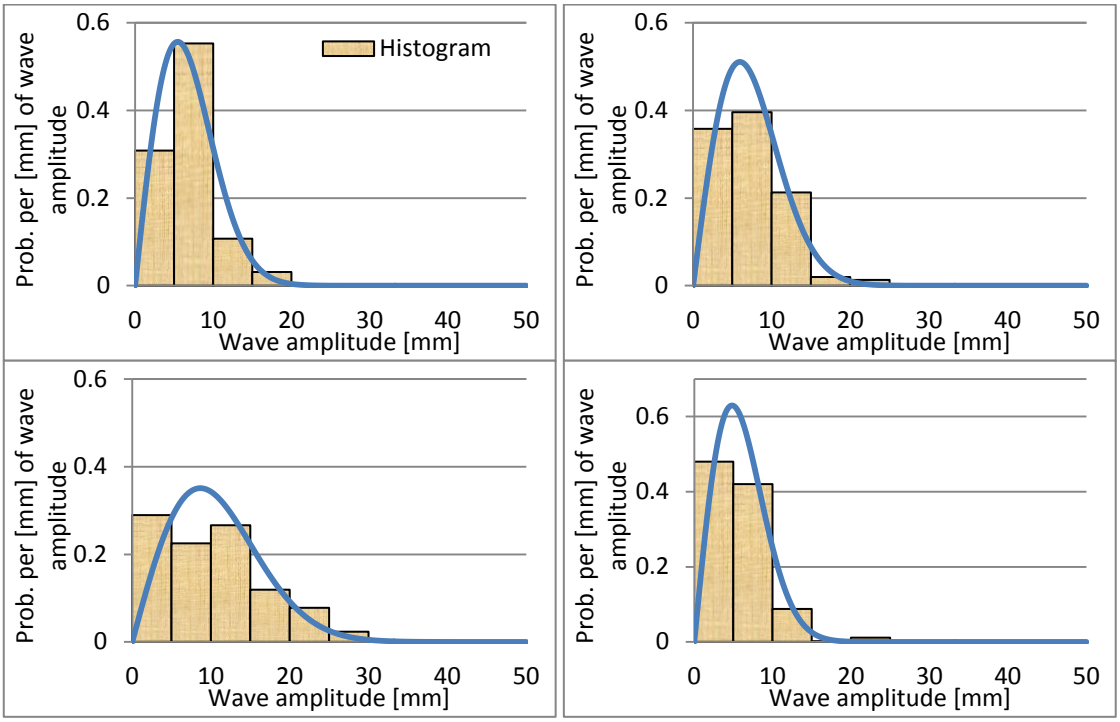

Figure 3.2 Probability density function of the up-crossing wave elevation for particular peak freq. and H_S. In row from top left a) 1.022Hz, 0.024m, b) 1.022Hz, 0.048m, c) 1.022Hz, 0.072m, a) 1.579Hz, 0.072m

Figure 3.2 presents the same experimental data from waves that have been generated by the mechanical wave maker in a towing tank. These irregular waves follow the Rayleigh distribution function with reasonable accuracy.

However, approaches of this kind carry with them various well-known limitations. The histograms can define only one single characteristic measure of the irregular seaway which can be the period, the height or the amplitude.

The broad use of the term $\overline{H}$ is sometimes equated with that which it closely represents, and is the average energy of the sea state, that is

$$\frac{\rho g \overline{H}^2}{8} = \frac{\rho g}{8}\left(h_{w1}^2 + h_{w2}^2 + \cdots\right) = Energy \tag{3.4}$$

Or $E_T = \frac{1}{2}\rho g\left(\zeta_{a1}^2 + \zeta_{a2}^2 + \cdots + \zeta_{an}^2\right)$ in terms of wave amplitude ζ_a.

Once the area under the histogram curve has been computed then $\overline{H}$ can be directly related to the Rayleigh distribution formula in order to determine the probability of occurrence of the different wave heights within the sea state. Thus the probability that $h > H_i$ is given by

$$p\{h > H_i\} = 1 - \int_0^{H_i} \frac{2H_i}{\overline{H}^2} e^{-H_i^2/\overline{H}^2} = e^{-H_i^2/\overline{H}^2} \tag{3.5}$$

From the proposed model it becomes possible to find the average wave height or the average height of the one-third highest waves and so on.

The average wave height is $(H)_0 = 0.89\left(\overline{H}^2\right)^{1/2}$

The average height of the one-third highest waves is $(H)_{1/3} = 1.41\left(\overline{H}^2\right)^{1/2}$

The average height of the one-tenth highest waves is $(H)_{1/10} = 1.80\left(\overline{H}^2\right)^{1/2}$

One major drawback of this approach is that the above-mentioned method is considered to be one dimensional e.g. it cannot represent highly-confused seas of say, waves and swells from different directions, and so on. There are also limits as to how far the Rayleigh distribution concept for predicting the high waves can be taken. We may obtain the prediction of a very high wave within a defined period if the wave records are also made for a very long period of time. However, the confidence in the probability of occurrence for the extremely high wave is very low. Nevertheless, it will be important for design purposes, and so on.

An alternative approach is to employ the wave energy spectrum which takes into account both the frequencies and the wave amplitudes in describing a seaway. The following factors determine the shape of the spectrum:

a. Wind speed (the most significant parameter)
b. Wind duration (assuming direction does not change)
c. Fetch
d. Location of other storm areas from which the local swell may have travelled

Several numerical methods apply the Rayleigh distribution approach for mathematical modelling of the sea conditions. The SESAM computer program is among these, and this has been used for numerical analyses undertaken in Chapter 5. For the stochastic method, the SESAM program estimates a linearization matrix that is based on the most probable largest motion response that is obtained by assuming a Rayleigh distribution. Prior to this estimation process, the wave spectrum has to be defined, and subsequently both applied forces and motions damping will be updated according to this matrix.

3.2.2 Wave Spectrum Concept

One of the key concepts in the evaluation of seakeeping is in the analysis of the wave spectra, and the principle of super-positioning is one of the most widely used techniques that is employed to create an extremely irregular seaway. In this method many sinusoidal waves of various amplitudes and periods are employed to illustrate the complex pattern of the seaway, which does not itself repeat at regular intervals of time.

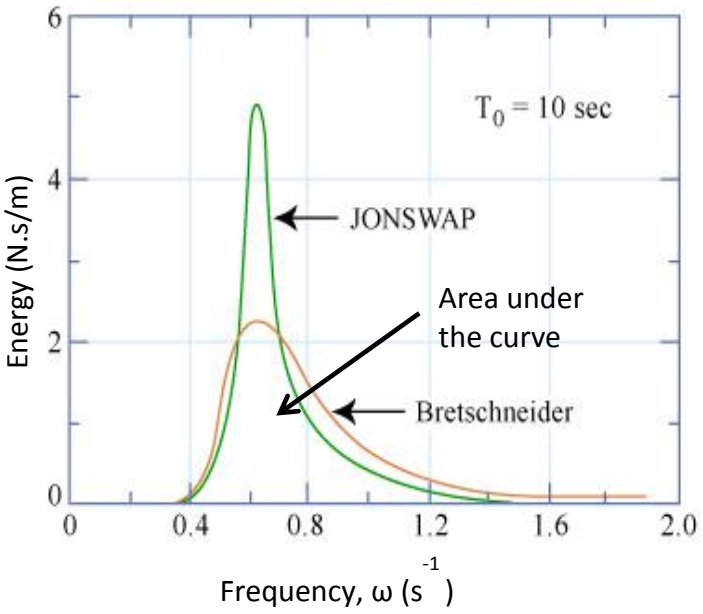

Figure 3.3 Two different wave energy spectra generated with H_S of 4 m and modal period of 10 s (MIT, 2012)

In Figure 3.3 the areas under the curve represent the energy of the seaway which is measured in N/m. Since the abscissa has the dimension of s^{-1}, then the ordinates represent N.s/m.

The energy spectrum depicted in Figure 3.3 is a continuous curve, and assumed to be comprised of an infinite number of regular waves, having different wavelengths and

different wave heights. Since a real sea is made up of all frequencies, the area under the curve thus illustrates the total combined energy of all of the wave components. It is noticeable from the graph that there is a steep decline in the energy content as ω_w approaches infinity. However, the total amount of energy available in the seaway remains the same.

One of the most significant observations is the fact that the waves that are evolving are doing so by absorbing energy from the wind, and for a given wind's speed the waves that are initially generated are small. The rate of energy absorption is balanced by the rate of energy dissipation and eventually a fully-developed sea is produced, as shown in figure 3.4. The developed waves gradually decay if the wind ceases to blow as the energy in the waves is dissipated. Therefore, the energy spectrum changes continuously until a fully-developed sea is formed.

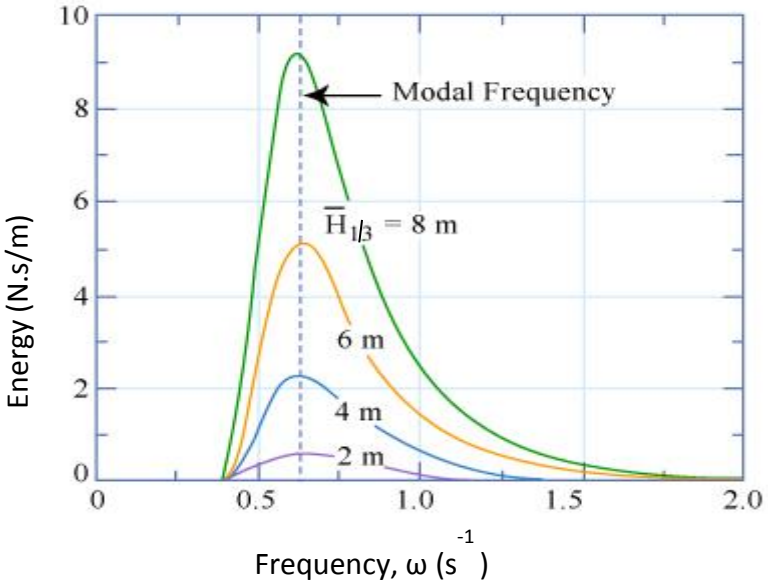

Figure 3.4 Energy spectra of fully developed seas for various wind speeds (MIT, 2012)

Longer waves are developed during the sea state's growth, and the energy spectrum tends to shift towards the lower frequency values as illustrated in Figure 3.5. Therefore, a continuous blow of wind over a period of time is the main reason for development of the longer wavelengths. It is to be noted that at certain geographical locations, for example, large seas and oceans, the fast-moving long waves can travel several thousands of miles and emerge as a swell.

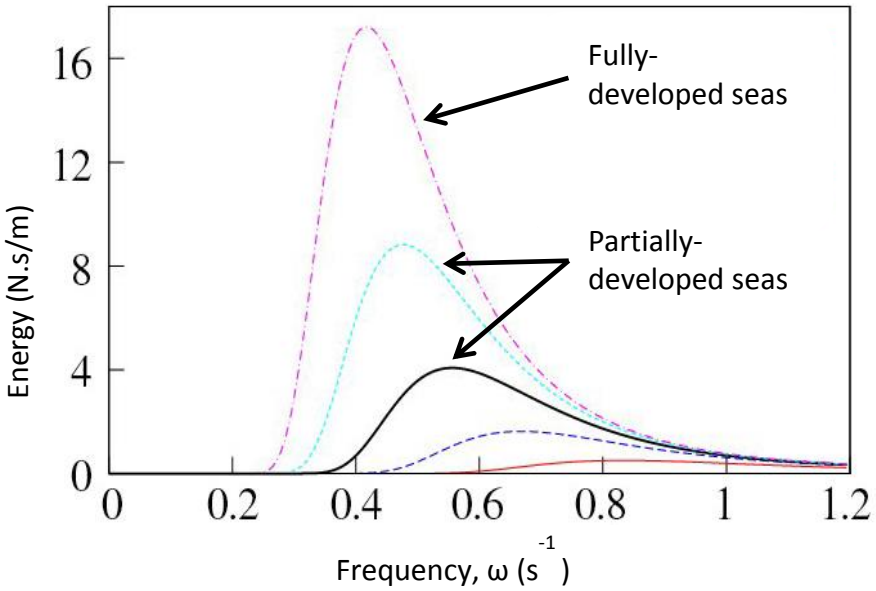

Figure 3.5 Energy build-up of partially and fully developed seas (Frechot, 2006)

The energy spectrum presented in Figures 3.3, 3.4 and 3.5 can be drawn in a different ways by modifying Equation 3.4 in which the ordinates represent

$$\frac{1}{2}\left(\zeta_{a1}^2+\zeta_{a2}^2+\cdots+\zeta_{an}^2\right) \tag{3.6}$$

In the modified diagram, the area under the curve remains the same but the ordinate unit changes. The area under the curve is generally denoted as m_0, a measure of the statistical variance of the distribution, because it represents the mean of the deviations squared from the zero line, hence $\sqrt{m_0}$ = root mean square (rms) of wave. The Y-axis unit changes to be [m^2.s] as the ρg is divided out which has a unit of [N/m^3]. The new curves shown in Figure 3.6 are called the wave spectrum, and the ordinates are represented by the spectral density of the wave energy, $S_\zeta(\omega_w)$.

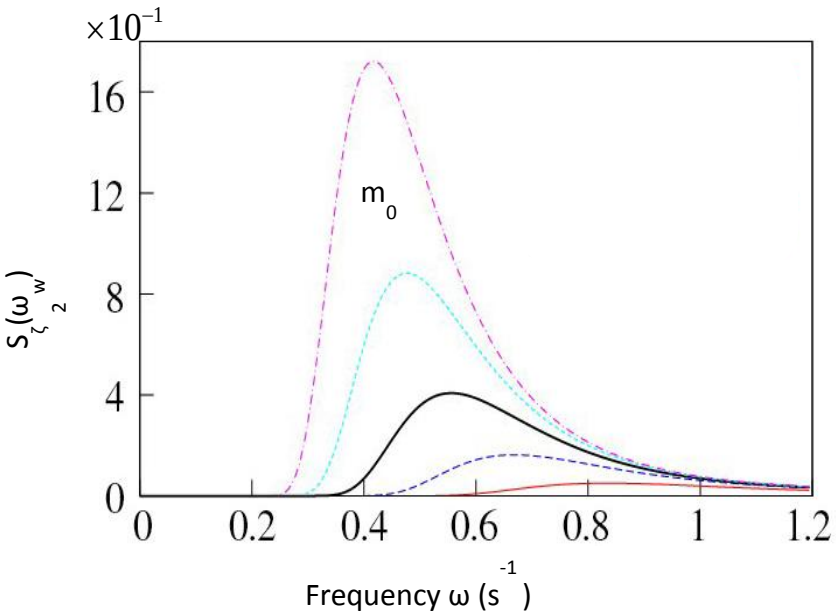

Figure 3.6 Wave spectrum of different developing seas (Frechot, 2006)

The ordinates of the wave spectrum for each of the curves are obtained by dividing the individual ½(amplitude)^2 values by the bandwidth $\Delta\omega_w$. For the determination of the wave spectrum, a record of 1000 waves is often considered to be sufficiently representative for design purposes (Bhattacharyya, 1978).

3.3 Prediction of an Irregular Seaway

Accurately-measured sample records of wave heights and frequencies, for specific sea areas, are needed to define a seaway in order to measure the wave energy. A specific wave pattern is never exactly repeated, but we expect that the wave spectrum remains the same. Therefore with the advantage of statistical analysis the wave energy can be obtained.

In order to draw a spectral density curve for a particular sea area, it is customary to take samples of wave records over a period of time to obtain the average wave characteristics. It can also be approximated by an analytical expression based on the probability theory described in previous sections. It shall be noted that energy spectrum does not appear in a Gaussian form (Bhattacharyya, 1978), however it can have any functional format. It is the range of wave heights which can then be estimated by assuming Rayleigh distribution. It is thus of prime importance to quantify the wave spectrum for further study and which can also be achieved through different formulas. In conclusion, the spectral density can

be related to the square of the amplitude of the waves, since the energy of the component waves in the sea state is directly related to the square of their amplitudes. Moreover, from a given known wave spectrum, the relationship between the area under the curve and significant heights can be obtained from Table 3.1.

Table 3.1 Various average values of waves

	Amplitude	Height
Average wave	$1.25\sqrt{m_0}$	$2.5\sqrt{m_0}$
Average of one-third highest waves	$2.0\sqrt{m_0}$	$4.0\sqrt{m_0}$
Average of one-tenth highest waves	$2.55\sqrt{m_0}$	$5.09\sqrt{m_0}$
Average of one-hundredth highest waves	$3.34\sqrt{m_0}$	$6.67\sqrt{m_0}$

where $\sqrt{m_0}$ is the root mean square (rms) value of the wave elevations in an irregular seaway. It is measured from the zero (still water) line at a constant interval of time Δt, in order to present the mean of the deviations i.e., $m_0 = \frac{1}{n}\sum \zeta_n^2$ where n is the number of measurements (see Figure 3.7).

To get reasonably accurate results, n should be large and Δt should be less than half the minimum time between successive crests.

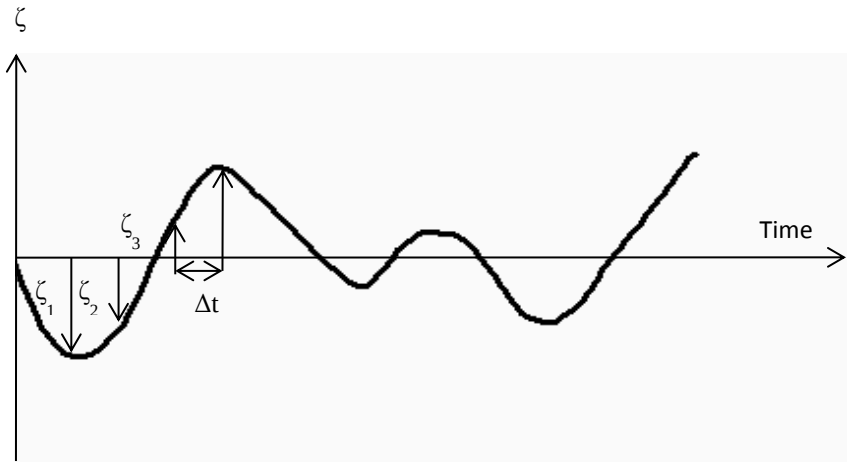

Figure 3.7 Surface elevation of an irregular wave at equal intervals of times

The continuous wave spectrum curve can be defined by the following mathematical expression:

$$area = m_0 = \int_0^{\infty} S_{\zeta}(\omega_w) \cdot d\omega_w \tag{3.7}$$

and for a small value of the bandwidth $\delta\omega_w$, we have

$$S_{\zeta}(\omega_w) \cdot \delta\omega_w = \frac{1}{2}\left(\zeta_{a1}^2 + \zeta_{a2}^2 + \cdots\right) \tag{3.8}$$

The advantage of using a statistical approach in an analysis of the wave spectrum is to obtain various average values of the wave environment as well as the extreme values.

The following useful information can be derived from a wave spectrum (Bhattacharyya, 1978):

a. The range of frequencies that is important for their contribution of the energy in the seaway
b. The frequency at which the maximum energy is supplied
c. The energy content at different frequency bands
d. The existence of a swell at low frequencies

It is worth mentioning that the derivation of the formulae in Table 3.1 is on the basis of a Rayleigh distribution of the wave heights which covers a narrow frequency; therefore a correction factor CF (Longuet-Higgins, 1952) is introduced to increase the level of accuracy. The Equation 3.9 is thus used to take into account the broadness of the spectrum:

$$CF = \left(1 - \varepsilon^2\right)^{1/2} \qquad 0 < \varepsilon < 1 \tag{3.9}$$

where the broadness parameter is

$$\varepsilon^2 = \frac{m_0 m_4 - m_2^2}{m_0 m_4} \tag{3.10}$$

$m_0 =$ Area under the response spectrum

$m_2 =$ Second moments of area under the response spectrum

$m_4 =$ Fourth moments of area under the response spectrum

The CF is more applicable to wide-band spectra where high frequencies are important. The CF can be used suitably, as the wave height distribution of a wind-generated wave system approaches the Gaussian law. In the case of any effects of swells in the spectrum,

the high frequencies are not dominant and the height distribution thus approaches the theoretical Rayleigh law.

The moment of the area under the spectrum is calculated using the equation below

$$m_n = \int_0^\infty \omega_w^n \cdot S_\zeta(\omega_w) \cdot d\omega_w \qquad (3.11)$$

where m_n is the nth moment of the area under the spectrum and n is any integer.

One of the most widely-used applications of the spectral moment is to find the important characteristics of an irregular seaway, such as the average zero up-crossing period T_Z, the crest to crest period T_C, and the average wavelength L_W, and each of which are defined as follows:

$$T_Z = 2\pi\sqrt{\frac{m_0}{m_2}} \quad , \quad T_C = 2\pi\sqrt{\frac{m_2}{m_4}} \quad , \quad L_W = 2\pi g\sqrt{\frac{m_0}{m_4}} \qquad (3.12)$$

T_Z is considered to be more closely related to visual estimates than is T_C because it does not include the small superimposed ripples which do not cross the zero line.

3.3.1 Standard Wave Spectrum

It is often useful to define inclusive wave spectra which broadly represent the characteristics of real 'local' wave-energy spectra. Some of the widely applicable spectra are described below:

The Breschneider or ITTC two-parameter spectrum, which is generally used when the wave spectrum of a particular sea area is not available, and it is calculated using the equation below

$$S(\omega_w) = \frac{A}{\omega_w^5} e^{-B/\omega_w^4} \qquad (3.13)$$

where ω_w is the circular frequency in radians per second

$$A = 172.75\frac{\overline{H}_{char}^2}{\overline{T}^4} \quad , \quad B = \frac{691}{\overline{T}^4}$$

In theory, the ITTC is classed as a broad-band spectrum and contains all wave frequencies. The average period between adjacent peaks is zero, since there will be infinitesimally small ripples with adjacent peaks. However in practice the spectrum is effectively

considered to be narrow banded, since the high-frequency ripples are neglected. Therefore

$$\overline{H}_{Char} \approx H_{1/3} = 4\sqrt{m_0} \qquad (3.14)$$

The maximum period of the wave energy within the spectrum is known as the modal period which is found through differentiation and is equal to

$T_0 = 1.296\overline{T}$ where $T_Z = 0.92\overline{T}$

If the above information is not available then the one-parameter Bretschneider spectrum can be assumed and which is defined in terms of wave height.

Table 3.2 Significant wave height vs. wind speed – ITTC standard wave spectrum

Wind speed [knots]	Significant wave height [m]
20	3.0
30	5.2
40	8.1
50	11.2
60	14.6

The significant wave height is also estimated from the wind speed as given in Table 3.2. The wind speed is taken to be sensed by personnel on board ship.

To avoid any complication, it is assumed by the ITTC that the wave height histogram follows the Rayleigh distribution and CF is taken to be 1.0.

The JONSWAP spectrum is based on the ITTC spectrum and is used to describe the sea states in coastal waters, where the fetch is relatively limited. In fact, both spectra do not contain the same energy for H_S or the characteristic period; JONSWAP has a taller “spike” than does the ITTC spectrum.

The Pierson Moskowitz method is used to define a wave spectrum by reference to the value of a nominal wind speed in m/s measured at a height of 19.5m above the sea surface.

The DNV Spectrum is a more generalised formulation of JONSWAP and Bretschneider spectrum and can be differentiated by it having a further peak-factor enhancement.

3.4 Motion Response in an Irregular Seaway

A considerable amount of literature has been published on the observation that the response of a ship in an irregular seaway follows the same statistical laws as do the waves themselves. In this concept, actual records of ship responses show patterns similar to those of wave records. By analogy, one can produce a graph of the square of the motions (e.g. heaving, pitching and rolling) amplitudes as a function of the frequency that a particular wave component of that amplitude and frequency would produce (Bhattacharyya, 1978). The spectrum created in this way is known as the response spectrum, and we can obtain statistical properties that are similar to those of the seaway. The theoretical Rayleigh approximation can define the percentage of times $P(x_i)$ that any particular double amplitude of motion x_i will appear

$$P(x_i) = \frac{2x_i}{\bar{x}^2} e^{-x_i^2 / \bar{x}^2} \tag{3.15}$$

where $\bar{x}$ is the rms of the double amplitude of motion.

The Equation 3.7 can also be used for representing the continuous motion spectrum and to be presented as

$$m_0 = \int_0^\infty S(\omega_e) \cdot d\omega_e \tag{3.16}$$

where $S(\omega_e)$ is the spectral density of the motion at frequency of encounter ω_e.

3.4.1 Method of Prediction

In order to obtain the motion characteristics of a vessel in an irregular seaway, it is essential to develop the motion-amplitude spectrum. Hence a similar procedure to that which was used for the statistical analysis of the wave system can be applied to the area under the motion spectrum.

The development of the motion spectrum is largely based on several steps that are discussed in a considerable amount of literature. These steps are as follows:

a. The selection should be made of a suitable spectrum for a particular seaway from which to generate the wave spectrum.
b. The wave spectrum should be corrected for the frequency of encounter, in order to take into account the angle of attack and the relative speed. It adds no variation to the area under the curve since the total energy is unchanged.

c. The motion spectrum is then developed by plotting the motion amplitude versus the encounter frequency distribution. Generally, regular waves are utilised to produce such a plot and could be obtained either analytically or by experiment.
d. The explicit part of this process is to develop a diagram with the two spectra obtained in parts (b) and (c). The ordinates of motion spectrum are replaced with the ratio of the square of the motion amplitude to the square of the wave amplitude. This diagram is known as the response amplitude operator (RAO). The RAOs are obtained from the simultaneous recordings of both motions and wave amplitudes. Figure 3.8 shows sampled RAO for all 6 degrees of freedom of a bulkcarrier.
e. Finally, the ordinates of the transformed wave spectrum should be multiplied by the ordinates of the RAO to obtain the motion amplitude spectrum.

This method of analysis has a number of limitations for representing ship responses in an irregular seaway. It is valid if the responses are linearly proportional to wave excitation and moreover the sum of the responses of a ship to a number of simple sine waves is equal to the response of the ship to the sum of the waves. It is assumed that although the ship's response to regular waves is a deterministic process, in summing these responses the stochastic nature of the seaway should be taken into account.

The results and observations from several experiments confirm the nonlinear behaviour of ship responses; however, the nonlinearities can be ignored up to a certain level. The results of previous investigations show that the fundamental assumption of linearity is reasonable if the seaway is moderate, and that only moderate responses are expected (Bhattacharyya, 1978). Therefore, whereas linear theory might be an appropriate technique for seakeeping design purposes it should certainly be questioned from the operational point of view.

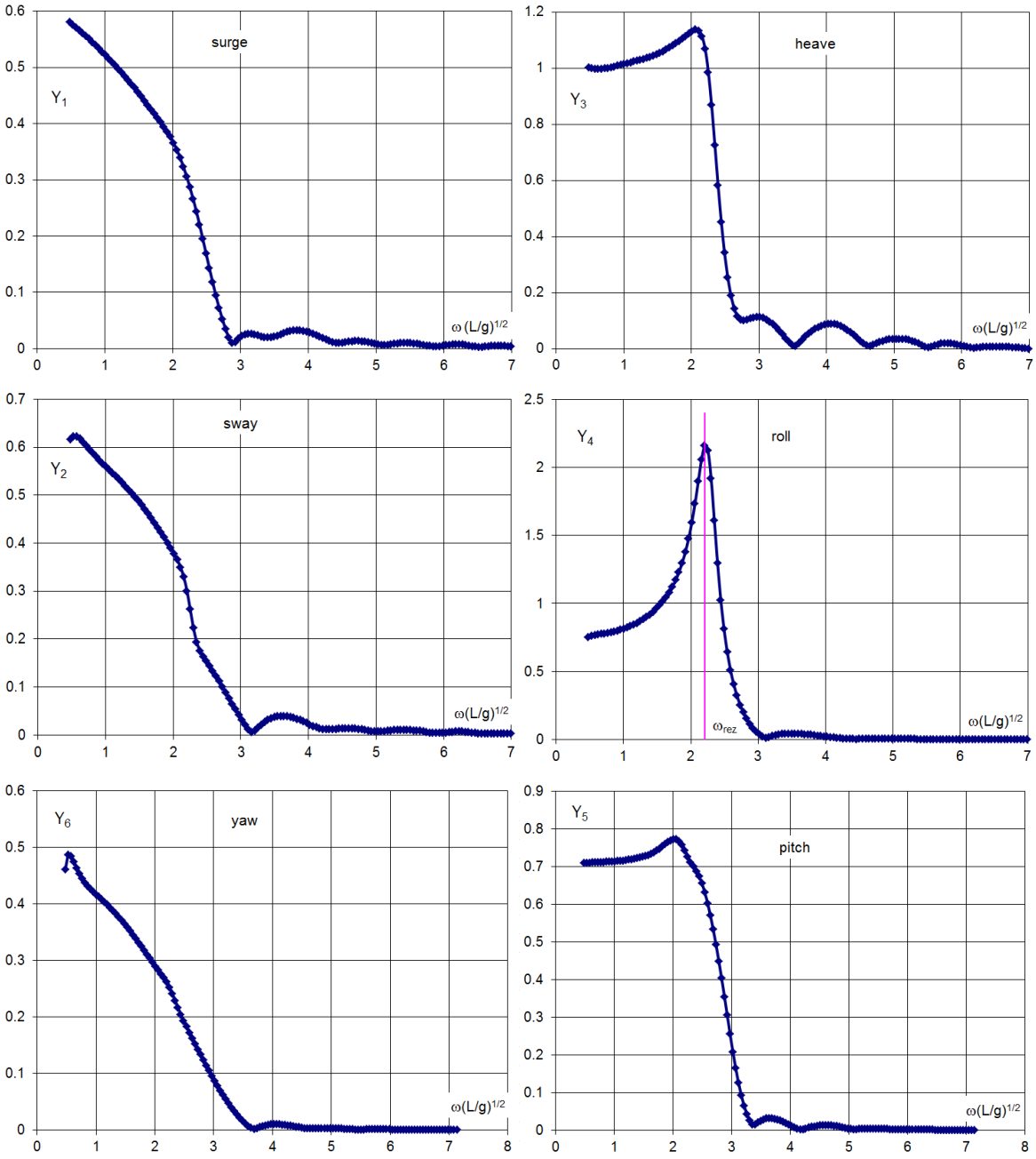

Figure 3.8 Amplitude characteristics for a bulkcarrier (β=135°, Fn=0.106) (Pawlowski, 2013)

It should be pointed out that in the case of a head sea condition the energy is spread out over a wider band of higher frequencies than it is for a stationary point spectrum. Whereas for a following sea at moderate negative velocities, the energy tends to be concentrated in narrower bands and at low frequencies; also the spectral density becomes infinite at the frequency of encounter

$$\omega_{e\max} = -\frac{1}{4}\frac{g}{V} \qquad \text{for} \qquad V < 0, \quad so \quad \omega_{e\max} > 0 \tag{3.17}$$

These conditions are depicted in Figure 3.9 and Figure 3.10.

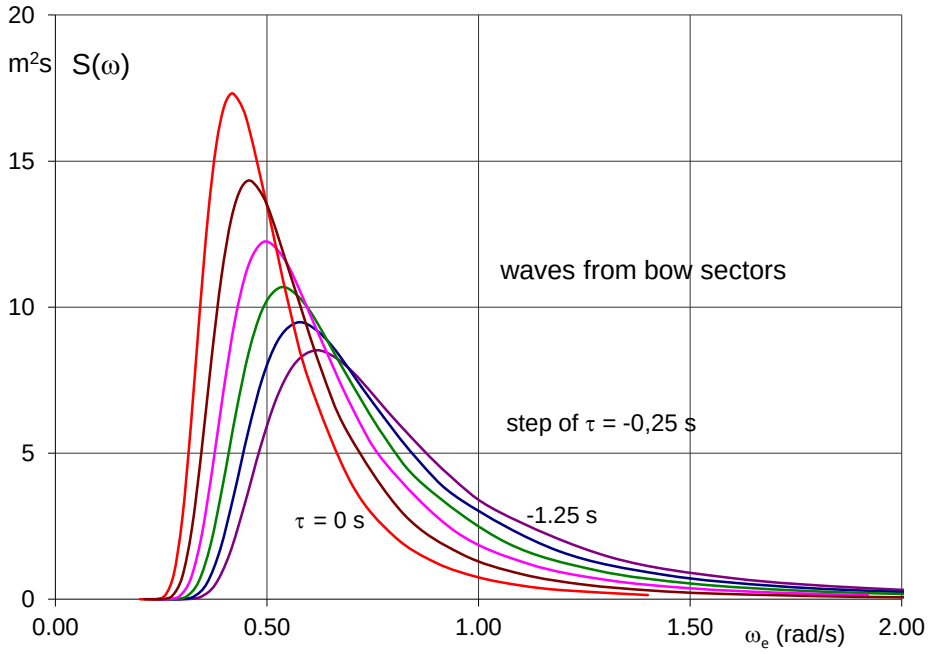

Figure 3.9 Wave spectra in moving system on waves from bow sectors (Pawlowski, 2013)

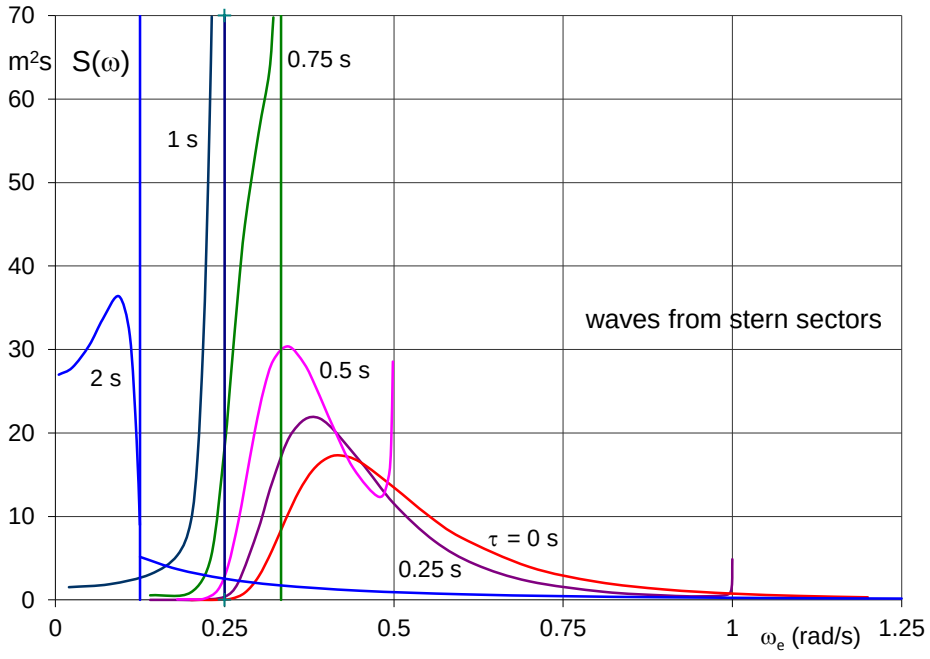

Figure 3.10 Wave spectra in moving system on waves from stern sectors (Pawlowski, 2013)

To obtain the RAOs for every ship speeds of interest, the tests need to be carried out for a wide range of wave frequencies and directions. Therefore the RAOs are different for different kinds of motions (refer to section 3.4.2)

3.4.2 Ship Responses

The linear superposition method is the leading technique that is used for the calculations of ship response in an irregular seaway. A major problem with this kind of approach is that it is based on two fundamental assumptions:

1. The response of the ship follows a simple harmonic motion with a frequency equal to the frequency of encounter. The response of a vessel to any individual regular wave component is a linear function of the amplitude of this component.
2. The coupling effect is ignored, in other words, the response of a vessel to any individual wave component is independent of its response to any other wave component.

With the above statements we can assume that the response of a vessel to the seaway is the sum of its responses to the individual wave components that are selected to model the seaway.

The linear response to wave amplitude can be mathematically expressed as

$$B = AH(\omega_i) \tag{3.18}$$

where $B = b_i \sin(\omega_i t + \varepsilon_i)$ is the response, $A = a_i \sin \omega_i t$ is the wave and $H(\omega_i)$ is the frequency response function.

The spectral density function of a mode of ship response (e.g. heave, pitch and roll) is equal to the product of the spectral density function of the waves and the response-amplitude operator, defined as below:

In the case of heaving motion

$$S_z(\omega_e) = S_\zeta(\omega_e) \cdot |H(\omega_e)|^2 \tag{3.19}$$

where $S_\zeta(\omega_e)$ is the density function of the wave spectrum [m^2-s]

$S_z(\omega_e)$ is the density function of the ship response for heaving [m^2-s]

$|H(\omega_e)|^2$ is the response amplitude operator, i.e. $RAO = \left|\frac{z_a{}^2}{\zeta_a{}^2}\right| \left[\frac{m^2}{m^2}\right]$

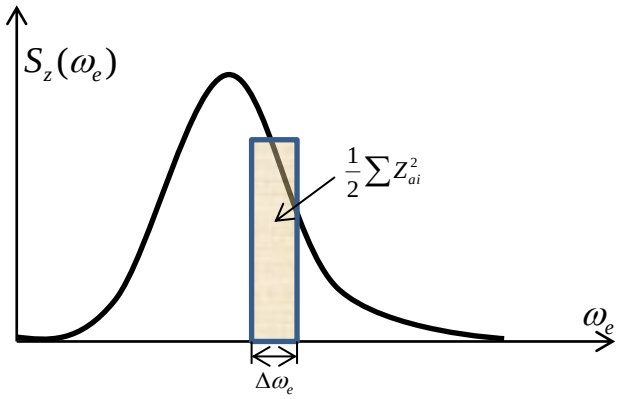

Figure 3.11 Response spectrum for heaving motion

Every elemental division of the area in Figure 3.11 represents half of the squared heaving amplitudes $\frac{1}{2}\sum Z_{ai}^2$ within $\pm\Delta\omega_e/2$ of the encountering frequency bandwidth. The total area under the spectrum represents the mean square value of the heaving deviations from the zero line.

Each term of the Equation 3.19 can be computed if the other two quantities are known. The application of this equation is very significant from two points of view:

- Predicting the ship motion response from the design point of view
- Severity of the seaway from the operational point of view

It is clearly a challenge to measure the actual wave heights being experienced in order to predict the severity of the seaway while the ship is underway. Under this condition, the response spectrum is produced for each motion and the spectral density of the sea can then be calculated with application of the RAO.

The RAO is obtained by conducting model tests in different sea conditions. In each test, the wave and the corresponding motion spectra are measured and RAO is computed. If the response is linear, then a similar RAO is generated for each individual test at each frequency component. The final response is considered to be the sum of the individual responses to a range of various frequencies. This method can be utilised to check the principle of superposition and the linearity of the whole process.

A serious weakness with this argument is in the application of Equation 3.19, which applies only to a one-dimensional irregular seaway. It is due to the fact that no spreading of the seaway components in other directions takes place.

It is to be noted that phase information is not detected in the calculation of an energy spectrum. Phase information can provide the instantaneous relationship between ship position and wave surface profile. Phase data is of little importance however in calculating motion behaviour, but it is essential for it to be considered for measurement of some of the ship's dynamic responses, such as deck wetness, bow emergence and slamming, and so on.

The motion response spectrum shall be modified with the correction factor by analogy to earlier argument in Section 3.3. In the case of roll motion, the spectrum is rather narrow and the correction factor is close to 1.

3.5 Motion in a Three-Dimensional Irregular Seaway

In the case of a two-dimensional irregular seaway, the wave heights are plotted against wave frequency ω_w, and the waves are considered to approach from one direction only. In this method wave crests remain steady and it is known as being a long-crested seaway. A real sea however is composed of waves travelling in slightly different directions. Therefore, the variations in directions of approach are to be considered along with the wave heights and frequencies, and which collectively make the seaway to be three-dimensional. Thus, the spectral density $S_\zeta(\omega_w, \theta_w)$ that is achieved is a function of frequency ω_w, and directions of the component waves, relative to the dominant wave direction θ_w. It is known as being a short-crested seaway and the spectrum is referred to as a cross-spectral density in order to indicate directional dependence.

In this approach the wave spectrum is obtained by summing the squares of the component wave amplitudes. Both frequency intervals and directional intervals are considered as defined below:

$$S_\zeta(\omega_w, \theta_w) = \frac{1}{2}\left[(\zeta_{a1})^2 + (\zeta_{a2})^2 + \cdots + (\zeta_{an})^2\right] \tag{3.20}$$

It is necessary to note that at any one point, the total energy is approximately constant, and it is regardless of the wave direction that the energy is coming from.

As a consequence of taking the wave direction into account, the area under the wave spectrum becomes a double integral (Bhattacharyya, 1978) and is defined as below:

$$m_{0\zeta} = \int_0^{\infty}\int_{-\pi/2}^{\pi/2} S_\zeta(\omega_w,\theta_w)d\theta_w d\omega_w$$
$$= \int_0^{\infty}\int_{-\pi/2}^{\pi/2} S_\zeta(\omega_w)\times f(\theta_w)d\theta_w d\omega_w \quad (3.21)$$

Since it is assumed that

$$S_\zeta(\omega_w,\theta_w) \approx S_\zeta(\omega_w)\times f(\theta_w) \quad (3.22)$$

where θ_w is the spreading function to account for any directionality in the component waves.

3.5.1 Frequency Dependent Spreading Function

It is extremely difficult to obtain a two-dimensional spectrum that represents a seaway. However, in the light of having same energy for both one-dimensional and two-dimensional spectra, then the integral value of the spreading function (Frechot, 2006) should remain as 1, thus Equation 3.21 can be written as

$$\int_0^{\infty}\int_{-\pi/2}^{\pi/2} S_\zeta(\omega_w,\theta_w)d\theta_w d\omega_w = \int_0^{\infty} S_\zeta(\omega_w)d\omega_w \quad (3.23)$$

where $f(\theta_w)$ is taken to be one of the two options (ITTC, 1966) that are given below

$$f(\theta_w) = \begin{cases} \frac{2}{\pi}\cos^2\theta_w \\ \frac{8}{3\pi}\cos^4\theta_w \end{cases}, \quad |\theta_w| \le \frac{\pi}{2} \quad (3.24)$$

and $$\int_{-\pi/2}^{\pi/2} f(\theta_w) = 1.0 \quad (3.25)$$

A two-dimensional wave spectrum is shown in Figure 3.12. Each curve is a function of both frequency ω_w and direction of the wave components θ_w, obtained from Equations 3.21 & 3.24.

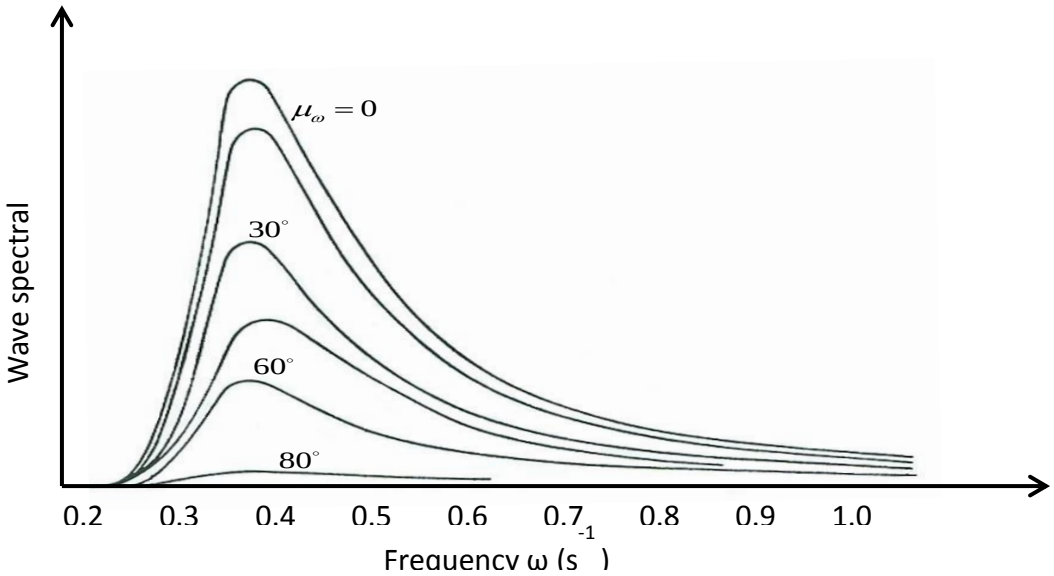

Figure 3.12 Two-dimensional wave spectrum presenting angular wave components.

Reference can be made to a number of studies (Longuet Higgins, 1963; Mitsuyasu, 1975; Goda, 2000) suggests that the spreading function varies with wave frequency.

3.5.2 Motions in a Short-Crested Seaway

The method of processing that is used to develop a mathematical model of a three-dimensional seaway is similarly applicable to describing ship motions. The spectral densities so obtained are functions of the encountering wave spectra and the RAOs.

For example, the ratios of the pitch angle to the wave slope can be obtained in head seas as well as can the ratios of the roll angle to the wave slope in beam seas. These motion responses can also be achieved for other encountering wave directions.

The cross spectra $S_{ij}(\omega_e)$ is a function of encounter frequency ω_e and can be obtained through a time-series analysis of a given set of measured ship responses. By assuming linearity between waves and ship responses, the relationship is defined by means of the following integral (Bhattacharyya, 1978)

$$S_{ij}(\omega_e) = \int_{-\pi}^{\pi} RAO_i(\omega_e,\theta)\cdot RAO_j(\omega_e,\theta)\cdot S_\zeta(\omega_e,\theta)d\theta \qquad (3.26)$$

where the transfer function RAO, is the theoretical relationship between the ith and jth components of the cross spectra and $S_\zeta(\omega_e,\theta)$ is the Directional Wave Spectrum (DWS) at an incident direction θ. The cross spectra $S_{ij}(\omega_e)$ is real when $i = j$ and is a complex value otherwise.

The power spectrum $S(\omega)$ is obtained from the directional spectrum in order to describe energy-frequency distribution of either the wave or the ship response, and can be expressed by

$$S(\omega) = \int_{-\pi}^{\pi} S(\omega, \theta) d\theta \qquad (3.27)$$

3.6 Directional Wave Spectrum (DWS)

In recent years, researchers have shown an increasing interest in approaches to estimate the experienced wave spectrum from simultaneously-measured ship motions responses. Ship responses can be measured through combinations of relevant sensors fixed at specific locations on board the ship.

Obviously ship responses can also be generated theoretically from a known wave spectrum as discussed in previous sections. Hence, the underlying wave spectrum can be estimated by the comparison of an assumed theoretically-computed spectrum with the measured-spectrum that actually being experienced. As the result of a good estimation, the same procedure could be applied to predict the response spectra from measured motion responses (see Figure 3.13).

There are two distinct concepts for motion-response prediction which are fundamentally quite similar, and are defined as:

1. Parametric modelling
2. Non - parametric modelling

Both concepts have been developed on the basis of linear spectral analysis, which relates the measured ship responses with the complex valued transfer functions that are needed in order to estimate the wave spectrum.

Numerous studies have attempted to explain the parametric modelling concept, for example (Hua, 1994; Aschehoug, 2003; Tannuri, 2003), whereas several studies have been undertaken investigating non-parametric modelling e.g. (Isobe, 1984; Iseki, 1999; Iseki, 2002; Waals, 2002). The mode of processing is shown in Figure 3.13 where a feedback system minimises the least-squared error of the measured and calculated response spectra, where the underlying wave spectrum is estimated.

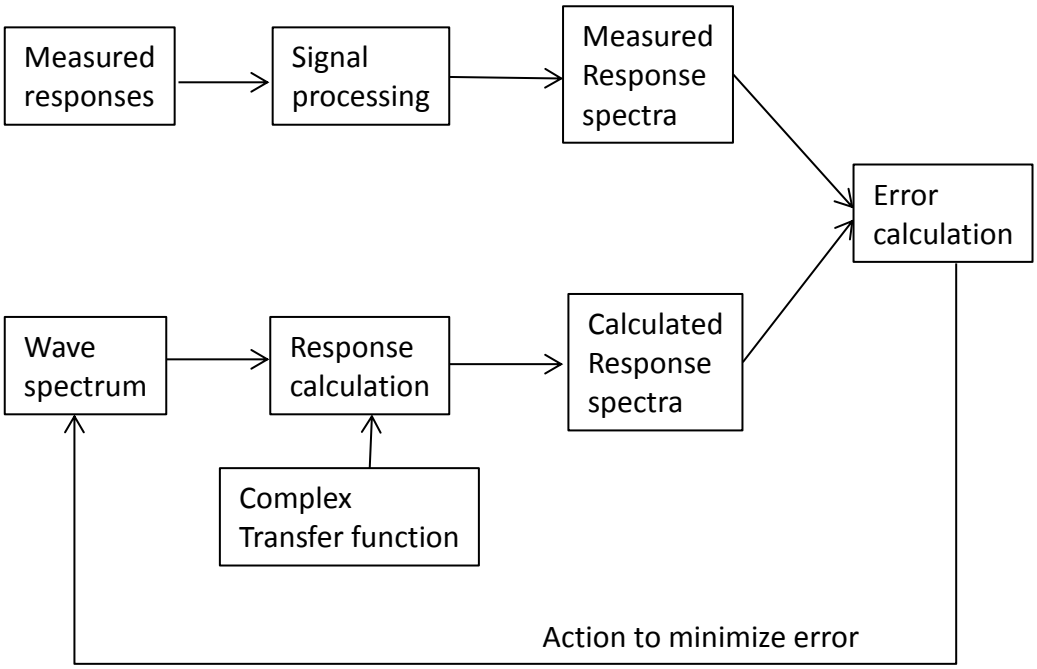

Figure 3.13 The fundamental idea in the estimation of the wave spectra based on measured ship responses (Aschehoug, 2003).

3.7 Estimation of Directional Wave Spectrum

The seaway is considered to be made up of an infinite sum of component regular waves from 360° directions, with a range of heights and frequencies. The local instantaneous height of the sea surface $h(t)$ above a fixed horizontal plane is defined (Iseki, 1999) using the directional wave spectra $S_\zeta(\omega,\theta)$

$$h(t) = \int_{-\pi}^{\pi}\int_{0}^{\infty} \cos(\omega t + \varepsilon)\sqrt{2S_\zeta(\omega,\theta)}\,d\omega\,d\theta \tag{3.28}$$

If the vector-valued time series, such as a ship motions, is taken to be a linear response to the incident waves, then the cross spectrum of these time series and the directional wave spectra are related by the frequency response functions through the relationship expressed by Equation 3.26.

In order to perform numerical computations, the integration progress of Equation 3.26 is first transformed into a discrete format. By assuming the integrand to remain constant for each interval $\Delta\theta$, it can introduce M interested points of the wave frequency and K, the specified encounter angles, as shown in Figure 3.14. Hence, the discrete expression is derived to be (Tannuri, 2003)

$$S_{ij}(\omega_m) = \Delta\theta \sum_{k=1}^{K} RAO_{ik}(\omega_m) \cdot RAO_{jk}(\omega_m) \cdot S_{\zeta k}(\omega_m) \tag{3.29}$$

with ω_m as $m = 0,1,\ldots,M-1$, $\Delta\theta = 2\pi/K$, $S_{\zeta k}(\omega_m) = S_{\zeta}(\omega_m, \theta_k)$

$RAO_{ik}(\omega_m) = RAO_i(\omega_m, \theta_k)$, $RAO_{jk}(\omega_m) = RAO_j(\omega_m, \theta_k)$

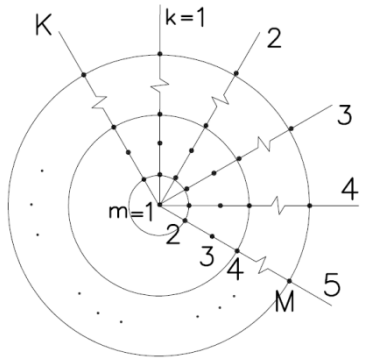

Figure 3.14 Discretisation of wave frequencies and encounter angles (Nielsen, 2005).

By using Equation 3.29, for a given sea state spectrum, the values of $S_{ij}(\omega_m)$ can be calculated. If $\bar{S}_{ij}(\omega_m)$ represents the measured values of the ship motions spectrum, then the potential quadratic error can be expressed by the following equation (refer to Figure 3.13):

$$E(x) = \sqrt{\sum_{i,j} \sum_{m=0}^{M-1} \left[S_{ij}(\omega_m) - \bar{S}_{ij}(\omega_m) \right]^2} \tag{3.30}$$

For the purpose of minimizing the error $E(x)$, it is crucial that Equation 3.30 converges. Such estimation is described by the angular spread of wave spectra.

3.7.1 Triple Value Function Problem

In the estimation of directional wave spectrum (DWS), one major theoretical issue exists, and which is known as the triple-value function problem. It occurs when the right-hand side of the Equation 3.26 is transformed into a true wave frequency ω_0. What is known about this particular problem is depicted in Figure 3.15 and it is based on the relationship between the true and the encountered wave frequencies in deep water

$$\omega_e = \omega_0 \left| 1 - \omega_0 \tau \right| \quad , \quad \tau = \frac{V}{g} \cos\theta \tag{3.31}$$

where V is the ship speed and θ is the angle of heading.

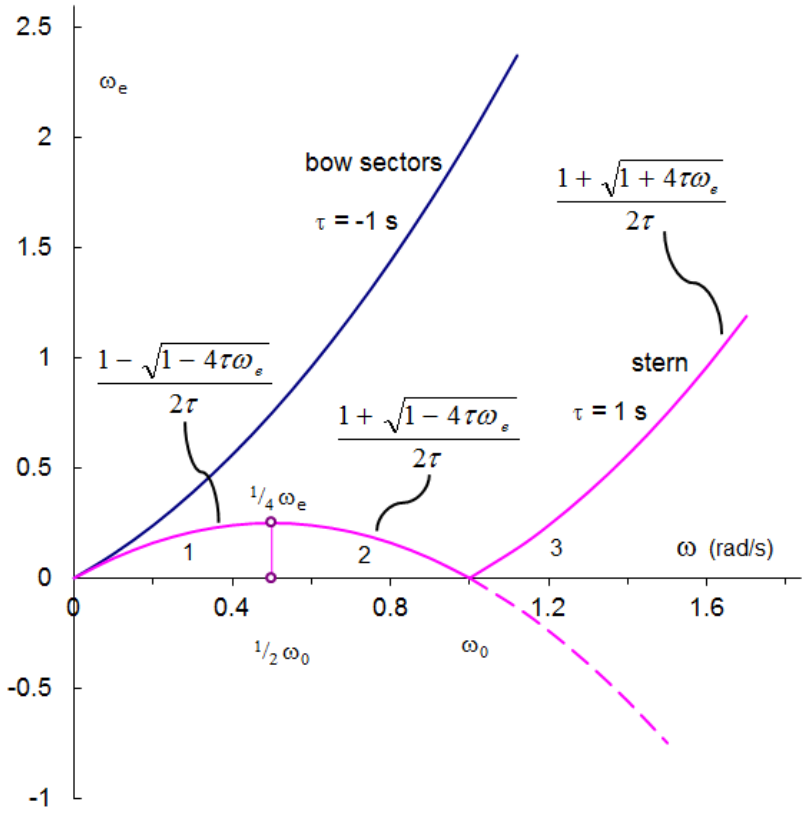

Figure 3.15 The relationship between true and encountered wave frequencies (Pawlowski, 2013)

There exist three relationships between encountered frequency and wave frequency in following seas (Iseki, 1999) so that $\theta \in \left[-\frac{\pi}{2}, \frac{\pi}{2}\right]$. However, there is no prior knowledge to determine which of the frequencies is true, therefore with $\omega_e < \frac{1}{4\tau}$ the frequencies are denoted by ω_{0i} , $i = 1 \sim 3$,

$$\omega_{01} = \frac{1-\sqrt{1-4\tau\omega_e}}{2\tau} \quad , \quad \left|\frac{d\omega_{01}}{d\omega_e}\right| = \frac{1}{\sqrt{1-4\tau\omega_e}}$$

$$\omega_{02} = \frac{1+\sqrt{1-4\tau\omega_e}}{2\tau} \quad , \quad \left|\frac{d\omega_{02}}{d\omega_e}\right| = \frac{1}{\sqrt{1-4\tau\omega_e}} \qquad (3.32)$$

$$\omega_{03} = \frac{1+\sqrt{1+4\tau\omega_e}}{2\tau} \quad , \quad \left|\frac{d\omega_{03}}{d\omega_e}\right| = \frac{1}{\sqrt{1+4\tau\omega_e}}$$

Hence, the transformation of Equation 3.26 is modified as follows:

$$
\begin{aligned}
S_{ij}(\omega_e) = & \int_{\frac{\pi}{2}}^{\pi} RAO_i(\omega_{01},\theta)\cdot RAO_j(\omega_{01},\theta)\cdot S_\zeta(\omega_{01},\theta)\cdot\left|\frac{d\omega_{01}}{d\omega_e}\right| d\theta \\
& + \int_{-\frac{\pi}{2}}^{\frac{\pi}{2}} RAO_i(\omega_{01},\theta)\cdot RAO_j(\omega_{01},\theta)\cdot S_\zeta(\omega_{01},\theta)\cdot\left|\frac{d\omega_{01}}{d\omega_e}\right| d\theta \ (\omega_e < 1/4\tau) \\
& + \int_{-\frac{\pi}{2}}^{\frac{\pi}{2}} RAO_i(\omega_{02},\theta)\cdot RAO_j(\omega_{02},\theta)\cdot S_\zeta(\omega_{02},\theta)\cdot\left|\frac{d\omega_{02}}{d\omega_e}\right| d\theta \ (\omega_e < 1/4\tau) \\
& + \int_{-\frac{\pi}{2}}^{\frac{\pi}{2}} RAO_i(\omega_{03},\theta)\cdot RAO_j(\omega_{03},\theta)\cdot S_\zeta(\omega_{03},\theta)\cdot\left|\frac{d\omega_{03}}{d\omega_e}\right| d\theta \\
& + \int_{-\pi}^{-\frac{\pi}{2}} RAO_i(\omega_{01},\theta)\cdot RAO_j(\omega_{01},\theta)\cdot S_\zeta(\omega_{01},\theta)\cdot\left|\frac{d\omega_{01}}{d\omega_e}\right| d\theta
\end{aligned}
\tag{3.33}
$$

In this new format, the Equation 3.33 is a generalised form and the components in lines two and three are added to cover only the following seas occurrence.

3.7.2 Computation of Directional Wave Spectrum

Iseki (Iseki, 1999) showed that cross spectra of the components can be expressed in matrix form

$$
\begin{aligned}
\mathbf{S}(\omega) = & RAO(\omega_{01})\cdot S_\zeta(\omega_{01})\cdot RAO(\omega_{01})^{*T} + RAO(\omega_{02})\cdot S_\zeta(\omega_{02})\cdot RAO(\omega_{02})^{*T} \\
& + RAO(\omega_{03})\cdot S_\zeta(\omega_{03})\cdot RAO(\omega_{03})^{*T}
\end{aligned}
\tag{3.34}
$$

For example, if more than one data, such as heave, pitch and roll motions, are measured then the sizes of matrices would be as follows:

with $S(\omega)$, $RAO(\omega_{01})$ and $S_\zeta(\omega_{01})$ being square matrix (3×3), rectangular matrix $(3\times K)$ and square matrix $(K\times K)$ respectively. It should be noted that $S(\omega)$ is a Hermitian matrix, and the upper triangle values only are used.

Equation 3-33 can then be transformed into a multivariate regressive model expressed by

$$\mathbf{B} = \mathbf{A}\mathbf{F}(\mathbf{x}) + \mathbf{W} \tag{3.35}$$

$\mathbf{B}$ represents the cross-spectrum vector which is a Hermitian matrix composed of both real and imaginary parts, $\mathbf{A}$ represents the coefficient matrix composed of the products of the response functions, $\mathbf{F}(\mathbf{x})$ represents the unknown discretised directional wave spectrum and $\mathbf{W}$ is a Gaussian white noise sequence vector that is introduced for stochastic treatment. Without the introduction of the white noise, virtually no

assumption is made initially on the potential error between the measured and the calculated response spectra.

Several studies have been undertaken investigating the estimation of the directional wave spectrum through numerical analyses based on Equation 3.35, where details of such studies can be found in references (Iseki, 1999; Tannuri, 2003; Nielsen, 2005).

3.8 Parametric Modelling

A parameterised spectrum is a concept that is commonly used to describe the frequency variation of ocean waves (Goda, 2000). It is based on the summation of a number of generalised JONSWAP spectra used to estimate wave spectrum. The Parametric method is conceptually simple and considers several parameters to model the bimodal spectrum. The parametric derivation (Hogben, 1986) is proposed by using the following formulae:

$$S(\omega,\theta)=\frac{1}{4}\sum_{i=1}^{2}\frac{\left(\frac{4\lambda_i+1}{4}\omega_{mi}^4\right)^{\lambda_i}}{\Gamma(\lambda_i)}\frac{Hs_i^2}{\omega^{4\lambda_i+1}}A(s_i)\cdot\cos^{2s_i}\left(\frac{\theta-\theta_{mean\ i}}{2}\right)\exp\left[-\frac{4\lambda_i+1}{4}\left(\frac{\omega_{mi}}{\omega}\right)^4\right] \tag{3.36}$$

where Hs is the significant wave height, λ is the shape parameter, θ_{mean} is the mean wave direction, ω_m is the modal frequency, s represents the spreading parameter (about the mean direction) and $A(s)$ is a normalization factor for the area under a $\cos^{2s_i}$ curve and which is defined as

$$A(s)=\frac{2^{2s-1}\Gamma^2(s+1)}{\pi\,\Gamma(2s+1)} \tag{3.37}$$

where Γ is the Gamma function.

Since this formulation considers two separated wave components, namely $i=1 and\ 2$, it is possible in theory to model most ocean wave spectra.

The Parametric method is based on the minimization of the quadratic error of the ship motions, between measured values and ones predicted using the estimated spectrum. The optimal wave spectrum, estimated by the parametric method, is found from the optimization of the following parameters:

$$x=\left[\omega_{m1}\ \ Hs_1\ \ s_1\ \ \theta_{mean1}\ \lambda_1\ \ \ \omega_{m2}\ \ Hs_2\ \ s_2\ \ \theta_{mean2}\ \lambda_2\right] \tag{3.38}$$

Alternatively, Nielson (Nielsen, 2005) derived a method which has many similarities to the idea that was introduced by Hua (Hua, 1994), and where the wave spectrum is composed of the summation of N shape functions $f_n^s(\omega)$, defined as follows:

$$S(\omega)=\sum_{n=1}^{N} a_n \cdot f_n^s(\omega) \tag{3.39}$$

To avoid any manual input parameters that have been obtained by assumption, this method (Nielsen, 2005) estimates the parameters through optimisation of the JONSWAP spectrum. The process considers four shape functions with $Hs=1\text{m}$ and ignores the phase lags between the individual responses. With regard to a spreading parameter, reference is made to an investigation of frequency dependency (Goda, 2000). It is assumed that s takes a maximum value around the spectral peak frequency and decreases on either side of it. The model is thus presented to be as follows

$$s=\begin{cases}\left(\dfrac{\omega}{\omega_p}\right)^{5} s_{\max} & , \quad \omega \le \omega_p \\ \left(\dfrac{\omega}{\omega_p}\right)^{-2.5} s_{\max} & , \quad \omega > \omega_p \end{cases} \tag{3.40}$$

where $s_{\max}$ is the peak value and represents the principal parameter. For practical applications, the following values are suggested (Goda, 2000):

$$s_{\max}=\begin{cases}10 & , \quad wind\ waves \\ 25 & , \quad swell\ with\ short\ decay\ distance \\ 75 & , \quad swell\ with\ long\ decay\ distance \end{cases} \tag{3.41}$$

3.8.1 Case Studies

Tannuri et al (Tannuri, 2003) considered the relatively weak influence of the parameter λ_i on the wave-induced loads and ship motions, and sets its value to be fixed at $\lambda_i=1$ in the Equation 3.36. By this correction, the parametric wave spectrum is reduced to a Pierson Moskowitz spectrum. Tannuri showed in his work that the relevant parameters are well estimated after this initial simplification. In conclusion, the parametric approach is able to estimate the bimodal spectra through an estimation of eight component vector x. For unimodal seas, one of the two estimated significant heights H_{S1} or H_{S2} is ignored.

For estimation of the wave spectrum, the parametric estimation method (Tannuri, 2003) was applied to a moored VLCC. It was known that the ship responses were strongly dependent on the RAOs, since service information about ships' response to incident waves was available. Due to the extreme sensitivity of the motions, it was decided to use the sway motions instead of the roll motions, with the assumption of preserving the directional information implicitly contained.

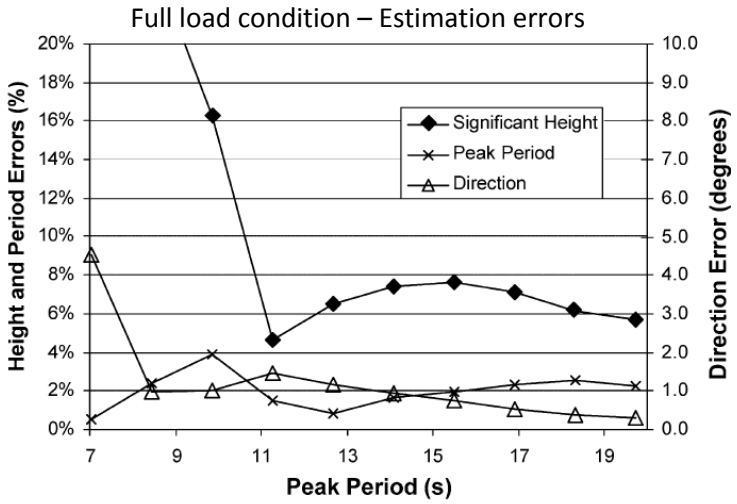

Figure 3.16 Estimation of errors for unimodal waves with $Hs = 1\text{m}$ and $Tp = 7s$ to $20s$ (Tannuri, 2003)

Finally, in the study, the parametric method was then applied to sway, heave and pitch motions in three different directions. Figure 3.16 presents the maximum estimated error for the ship in a loaded condition.

The purpose of this study was to predict the required response from a dynamic positioning (DP) system for counteracting the estimated environmental forces. The accurate estimation of mean drift forces and moments plays an important role in maintaining the vessel's position. The result of such estimation is shown in Figure 3.17 which presents the maximum error for surge, sway forces and yaw moment drift.

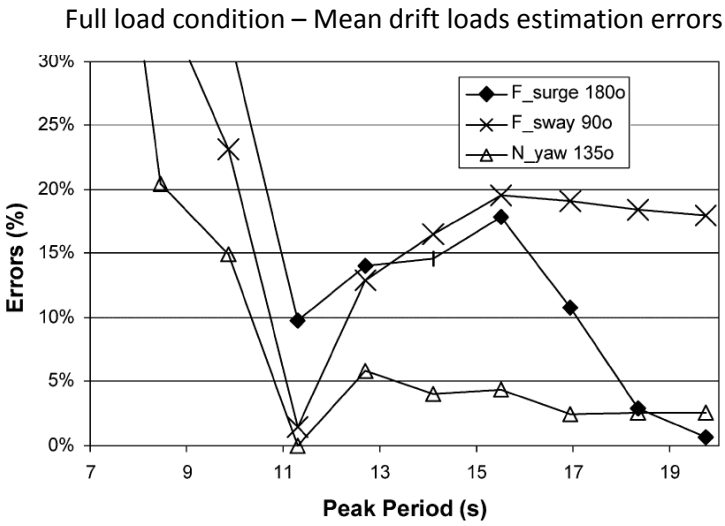

Figure 3.17 Estimation of errors for mean drift forces with $Hs = 1\text{m}$ and $Tp = 5s$ to $20s$ (Tannuri, 2003)

In an alternative approach, the numerical analysis that was performed to estimate the wave parameters was by the Bayesian method (discussed in following section), and the results that were obtained were considered to be not satisfactory owing to higher errors being found.

Nielsen (Nielsen, 2005) used full-scale measured vessel motions data for subsequent estimation of the wave spectra on the basis of a parametric estimation analysis. Three types of data were recorded for this study and compared to see the relative sensitivity and quality of the responses. The estimated spectra, using data from strain gauges, accelerometers and relative motion sensors, are shown in Figure 3.18. The estimation seems to be reasonable, since both sea and swell were present at the time of the measurements, and the tendency towards a double-peaked spectrum is obvious.

The recorded significant wave heights and wave zero up-crossing periods are given in the Table 3.3 for the three terms of waves, swell and combined conditions. The corresponding estimated values are tabulated in Table 3.4, and were computed on the basis of two methods of employing shape functions and optimisation. The significant wave heights and the peak periods are the recorded time series of actual ship responses that were obtained through using different sensing mechanisms. The two tables can be thus used to compare the recorded and computed quantities.

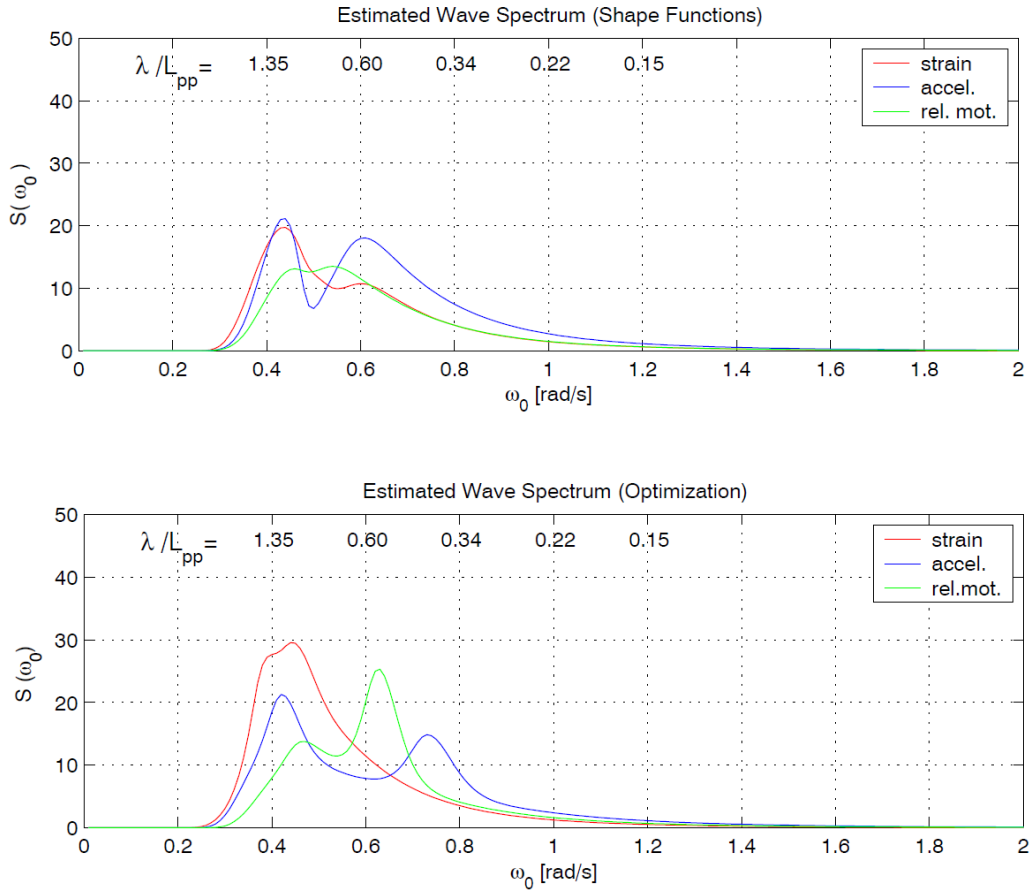

Figure 3.18 Estimated wave spectra by use of shape functions and by optimisation (Nielsen, 2005). The analysis of data is based on time series of strain, acceleration and relative motion measured on board.

Table 3.3 Recorded wave heights and periods.

	Wave	Swell	Combined
Hs	7.8m	4.2m	8.9m
Tp	11.2s	15.3s	---

Table 3.4 Estimated significant wave height and peak periods for seas and swell by two diferent methods (shape functions / optimisation) based on recorded timeseries of ship responses.

	Strain	Acceleration	Relative motion
Hs [m]	9.7 /11.3	11.1 / 10.8	9.1 / 10.1
Tp swell [s]	14.6 / 15.5	14.6 / 15.6	14.4 / 13.7
Tp wave [s]	10.5 / ---	10.5 / 8.7	12.1 / 10.1

The shape function method is the faster in computation time, but the number of parameters, such as T_Z, γ and θ, should be defined in the first place. One major drawback of this approach is in the fact that it sometimes produces a negative value spectrum.

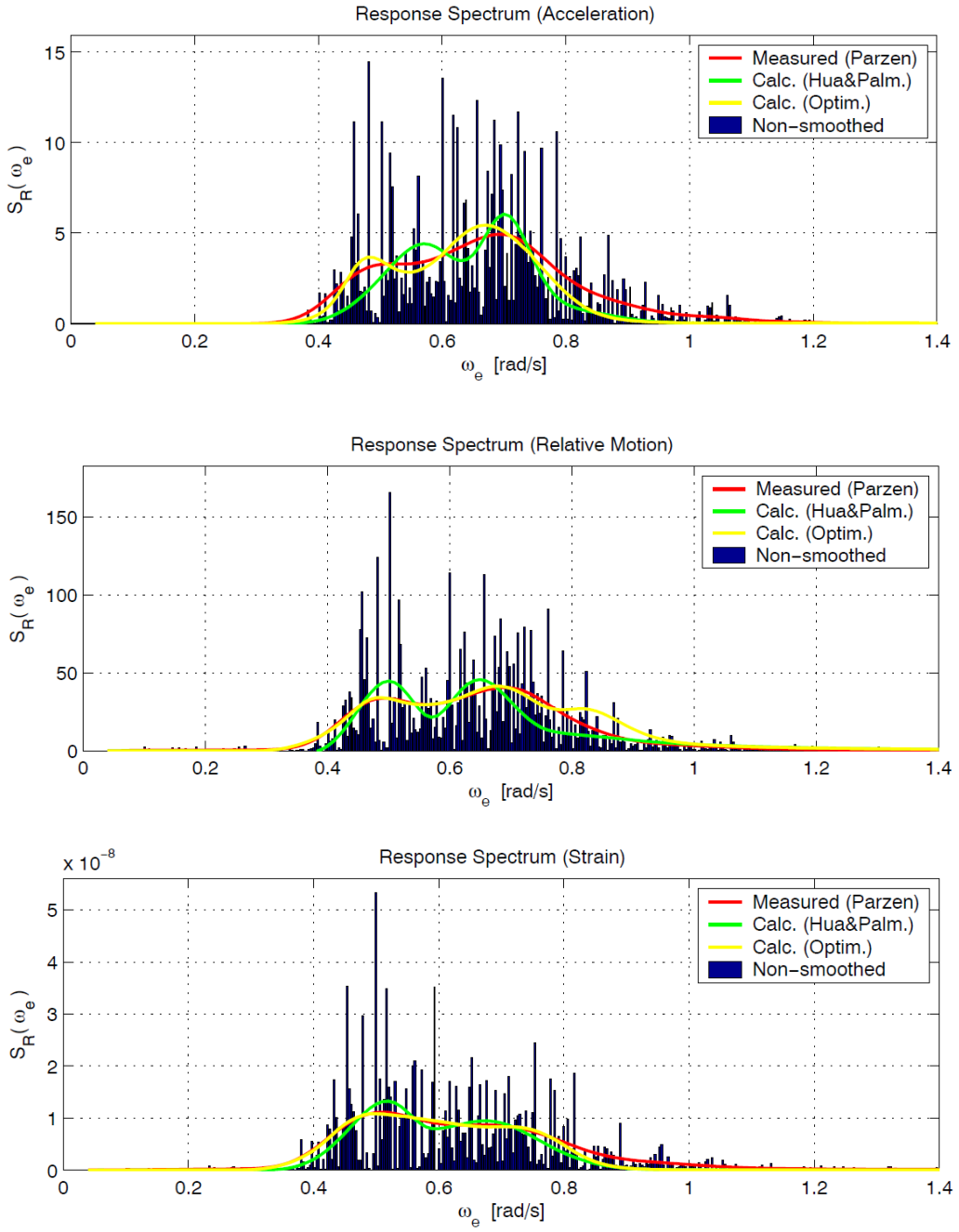

Figure 3.19 Measured and calculated response spectra based on time series of strains, accelerations and relative motions (Nielsen, 2005).

On the contrary, the optimisation method is slower because it leads to a non-linear process. However, it does not require the input wave parameters except for an initial guess.

Figure 3.19 shows the response spectra computed with FFT aligned with the smoothed spectrum by a different method.

3.9 Non-Parametric Modelling (Bayesian Method)

This method considers a number of discretised frequency-directional points in the wave field in order to estimate the directional wave spectrum. The Bayesian modelling procedure was proposed by Akaike (Akaike, 1980) and later on it was developed by Iseki (Iseki, 1999; Iseki, 2002), with the view of capturing the overall wave parameters and the wave direction with reasonable accuracy.

The Bayesian statistic is defined by the following expression

$$p(\theta|X) = \frac{p(X|\theta)\,p(\theta)}{p(X)} \tag{3.42}$$

Where posterior probability $p(\theta|X)$ is the conditional distribution of the parameter θ given the data X. Here $X = (x_1, x_{2,\ldots}, x_n)^T$ is a set of observations, and the likelihood function $p(X|\theta)$ is the probability distribution of the parameters X conditioned to the K parameters of $\theta = (\theta_1, \theta_2, \cdots, \theta_K)^T$. The probability density function $p(\theta)$ could be considered as the prior assumption.

If the following conclusion can be derived from the Equation 3.42,

$$\underset{(posterior)}{p(\theta|X)} \propto \underset{(Likelihood)}{p(X|\theta)}\,\underset{(prior)}{p(\theta)} \tag{3.43}$$

then, for a given data set X, $p(X|\theta)$ may be regarded as a function (Fisher, 1922) of θ and not of X. Therefore, $p(X|\theta)$ is called the likelihood function of θ given the X and is written as $L(\theta|X)$. The Bayes formula may then be written as

$$p(\theta|X) \propto L(\theta|x)\,p(\theta) \tag{3.44}$$

For the model obtained in Equation 3.35, if a set of N encountered frequencies is taken into account at the same time, then $\omega_{ei}(i=1,2,3)$ could be expanded into a range of discrete wave frequencies. In that case the likelihood function of the cross spectra of data is given by the multivariate Gaussian distribution (Iseki, 2002)

$$L(X|\sigma^2)=\left(\frac{1}{2\pi\sigma^2}\right)^{9N/2}\exp\left[-\frac{1}{2\pi}\|\mathbf{AF}(\mathbf{x})-\mathbf{B}\|^2\right] \tag{3.45}$$

where it is assumed that $\mathbf{W}$ in Equation 3.35 has a zero mean with a variance σ^2. The $\|a\|$ term symbolises the norm of a vector a.

Two types of prior distribution, (Iseki, 2002) $p(\theta)$, are taken into account for the calculation of the right-hand side of Equation 3.43. The first prior distribution is the Gaussian smoothness, which minimises the sum of the squared differences of the unknown coefficients, in order to make the changes of the parameters to be smooth. The second prior distribution minimises the squared sum of the differences between the power spectra and the defined initial value in order to avoid excessive estimation.

The smoothness prior $p(x)$, is written as

$$P(x)=\left(\frac{u^2}{2\pi\sigma^2}\right)^{3MN/2}\exp\left[-\frac{u^2}{2\sigma^2}\sum_{i=1}^{3}\sum_{m=1}^{M}\sum_{n=1}^{N}\varepsilon_{imn}^2\right] \tag{3.46}$$

where M and N are the numbers of the discrete wave frequencies and the discrete encountered angles respectively, ε is a smoothness parameter and u^2 is hyper-parameter that controls the trade-off between the good fit to the data and the smoothness of the parameter change in the model.

Akaike (Akaike, 1980) proposed a criterion to be employed to determine the optimum hyper-parameter and its variance. It can be achieved by minimisation of the Akaike Bayesian Information Criterion (ABIC) which is expressed as follows:

$$ABIC=-2\log\int L(x|\sigma^2)p(x)dx \tag{3.47}$$

The results of these derivations suggest that the Bayesian modelling method uses a stochastic approach for the estimation of the directional wave spectra by the introduction of likelihood functions and prior distributions.

In order to verify the Bayesian estimation method, Nielson (Nielsen, 2005) utilised numerical simulation as well as a set of full scale data. He finally compared the wave parameters of the estimated spectra with the parameters of the visual observations. In one of the experiments a set of four data was considered, one at a time, and each piece of data consisted of three measured ship responses: the pitch motions, the roll motions and the vertical acceleration.

The results of the study indicated that the mean wave period that was estimated was fairly accurate relative to the wave observation. However, the significant wave heights were only estimated at the values of about 60% of the visual observations for all of the data set.

One major drawback of this approach for the estimation of the wave spectrum lies in the fact that visual observations of wave heights and periods themselves contain a certain amount of uncertainty.

The appropriate transfer functions can be assumed by employing a wave spectrum which has been obtained through estimated wave parameters. Eventually, transfer functions are utilised in order to relate the responses with the wave spectrum. Table 3.5 and Figure 3.20 show the actual differences between the measured and the estimated response spectra for the analysed full-scale data.

It is to be noted that with only a small sample size, caution must be taken, as the findings may not be transferable. The results should also be questioned in the case of rough seas, where non-linearity may play an important role.

The Bayesian method can also suffer from some similar limitations, since linearity is the underlying principal in development of this method. The results may also be significantly influenced in certain conditions.

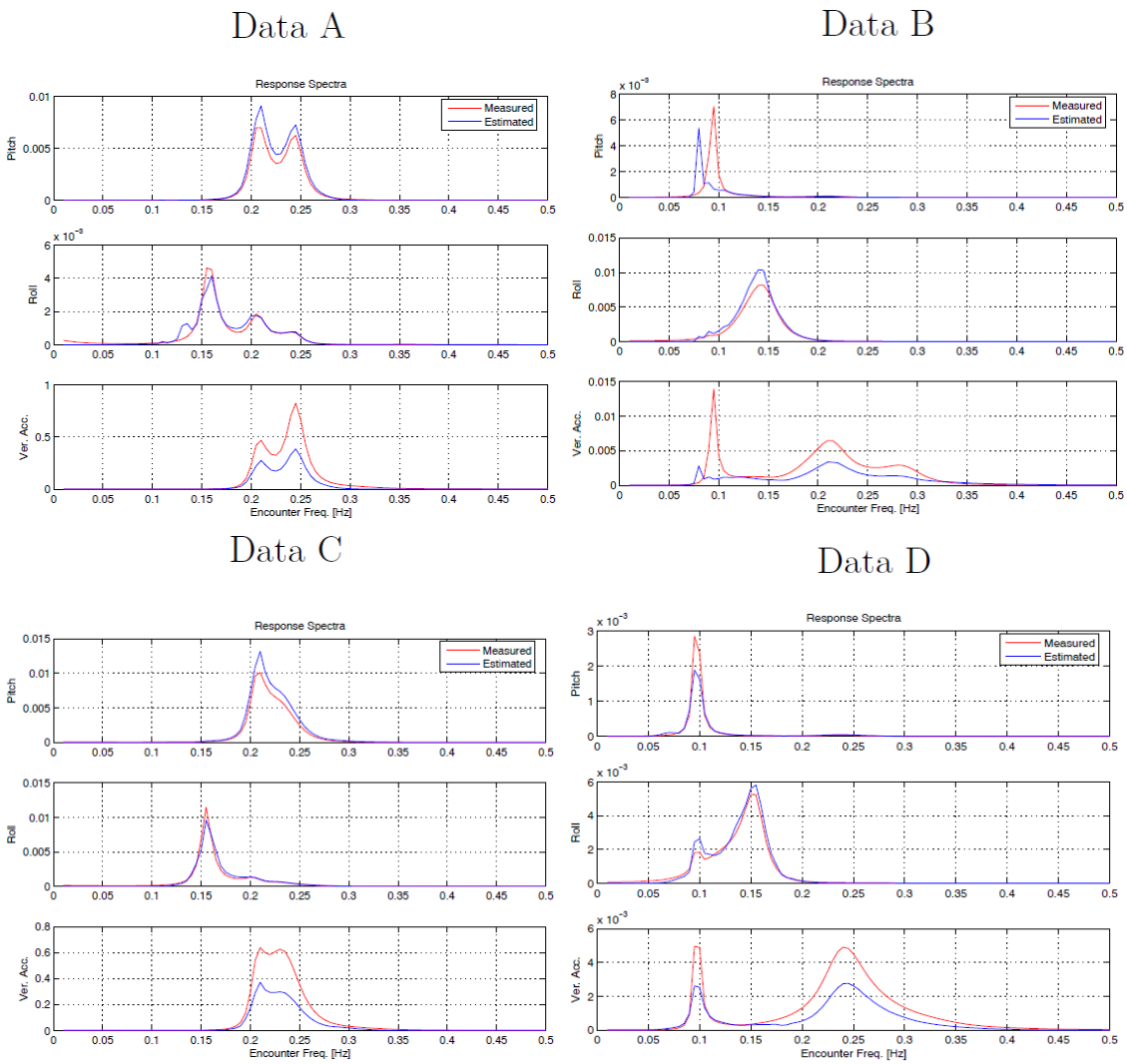

Figure 3.20 Comparison of measured and estimated response for the four data sets illustrated as function of the encountered frequency (Nielsen, 2005). Scales are: Pitch [rad^2-s], Roll [rad^2-s], Ver. Acc. [m^2/s^3].

Table 3.1 Absolute variances and deviations for the estimated and measured response spectra.

	Pitch		Roll		Ver. Acc.	
Data	Dev.	Var. [rad^2]	Dev.	Var. [rad^2]	Dev.	Var. [(m/s^2)^2]
A	20%	$35 \cdot 10^{-5}$	2%	$1.9 \cdot 10^{-4}$	-51%	$350 \cdot 10^{-4}$
B	-38%	$9.6 \cdot 10^{-5}$	16%	$3.8 \cdot 10^{-4}$	-48%	$7.5 \cdot 10^{-4}$
C	23%	$42 \cdot 10^{-5}$	-3%	$2.9 \cdot 10^{-4}$	-49%	$370 \cdot 10^{-4}$
D	-15%	$4.3 \cdot 10^{-5}$	7%	$2.5 \cdot 10^{-4}$	-43%	$4.8 \cdot 10^{-4}$

3.10 Summary and Conclusions

This chapter sets out the aim of assessing the importance of spectral application in the prediction of motions responses. The application of linear superposition is discussed with regard to the energy spectrum method. In this approach, the validity for an analysis of ship motion responses in an irregular seaway is reviewed on the basis of RAOs that have been obtained in relatively moderate regular waves.

It was shown that, with the assumption of the Rayleigh probability distribution to model the amplitudes of motions, even severe responses can be predicted with a reasonable accuracy. Such a prediction can be useful for design purposes after application of a correction factor.

The results of this chapter equally suggest that statistical analysis is a reasonable way for the prediction of ship motion characteristics, and that a time series of the motion response may not necessarily need to be used. It was also concluded that linear theory has certain limitations for it to be valid for extreme sea conditions.

It should also be emphasized that statistical analysis is a valuable tool for use in predicting motion responses but that while the significant values obtained are most useful for design criteria, there are fundamental shortcomings, such as it being two-dimensional, which makes this approach doubtful for operational purposes.

The feasibility of the estimation of the directional wave spectrum was analysed on the basis of both a stationary ship and of a moving ship's motion measurements. The ship itself is considered as being effectively a wave sensor, where its dynamics must be well known in advance in order to perform good estimates of future wave spectra. The estimation methods depend on previous knowledge of the response of the ship when subjected to waves, expressed in the form of RAOs.

The influence of different parameters and conditions on the estimations of the wave spectra was investigated. It was also shown how the weighting needs to be considered in the estimation of responses and of the so-called hyperparameter.

One serious weakness with this approach is in the practical limitations that need to be considered, mainly due to non-linear effects and variations in loading conditions. It was discussed that this method of approach is not effective for high-frequency wave spectra, since they do not induce significant ship motions.

The next chapter defines the specific methodologies that are to be used in this thesis, and which is on the basis of the implication of wave spectrum estimation. The estimation is obtained through measured ship response spectra. The new method of approach implies the wave influential parameters, rather than to assume responses computed by RAOs. Signal processing techniques will be utilised for detection of these parameters in order to improve the applicability of the system for real time on-line monitoring purposes for the provision of operational guidance.

Chapter 4

Methodologies

4.1 Introduction

Waves are physical disturbances of water, and contain and transmit vast amounts of energy. Wave energy is the major source of environmentally-caused ship motions, therefore an understanding of the behaviour of waves and their associated characteristics is essential. The forces on a floating structure that are generated by waves can pose a significant threat during a sea passage, and can deteriorate the stability of a ship beyond any acceptable criteria.

Simple cyclic waves are readily analysed in respect to their perfect regularity, but they do not accurately depict the great and complex variability of ocean waves. The sea surface is generally composed of many waves of varying heights and periods and is constantly moving in different directions. When the wind is continuously blowing and the waves are growing in direct response, the sea tends to be confused, that is, there is no clearly discernible pattern, and a wide range of different heights and periods is observed. Swell is of a more regular geometric nature, but it is still fundamentally irregular in nature, with some variability in heights and periods.

Conventionally, sea state measurements were and are carried out mainly by employing moored directional buoys. Such devices provide good estimates of the local wave spectrum, since their own dynamics are known and their wave-induced motions can be accurately measured by installed accelerometers and tilt sensors (Ewans, 1999). The measured motions, such as heave, pitch and roll, are considered to have the same heights and slopes as of the passing incident waves if the moored buoy dynamics are neglected. Perhaps a similar analogy can be applied if the ship is considered as the equivalent to an un-moored buoy in encountering the waves.

Accuracy, availability and delays in obtaining data for the mathematical analysis of a time series are the main constraints to implementing the buoy's intrinsic technology for the real-time monitoring of ship responses, not to mention the practical aspect of calibration and maintenance.

A ship's motion is of a complex, time-varying nature, and it can be measured by the means of suitably-positioned various types of sensors, and recorded as a continuous time signal. Hence, signal processing techniques, either on-line or off-line, can be employed as a tool to analyse the composition of such a signal for subsequent operational decision-making purposes.

Ships' motions are good direct reflections of the current local sea conditions and are probably one of the more practical of means for estimating the wave spectrum in a real-time. It can be demonstrated that some influential parameters of encountered waves can be detected through the monitoring of heave and pitch motions. Because of a strong coupling nature, these motions are in tune with irregular wave patterns and therefore actively monitoring their responses can be regarded as providing applicable tools for the detection and estimation of the influential wave parameters.

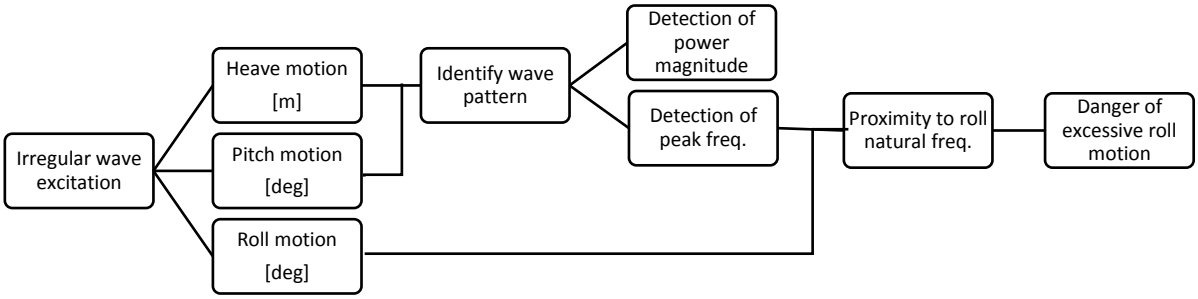

Figure 4.1 Fundamental concept to the prediction of large roll motions.

This method of approach can be effective in providing data so that decisions can be made to avoid large roll angles and thus excessive reductions of stability (Enshaei, 2012a), which may occur over longer periods of time in a complex sea, hence reducing the probability of capsize. Detection of the peak frequency of a ship's motion and its corresponding magnitude in real-time is a practical solution. These can be utilised in the monitoring of the potential vulnerability of particular ships for specific loading conditions in different seas and operating conditions. By this method, the encountered peak frequency of irregular waves can be detected by the spectral analysis of the heave and

pitch motions over a period of time. Figure 4.1 shows how the sensitivity of the ship-to-roll response is monitored, while the encountered peak frequencies may be close to the natural roll frequency and thus alerting the crew to a serious developing situation.

Following the fundamental idea shown in block diagram form in Figure 4.1, three distinct methods illustrated within it are applied in this study in order to investigate the rationality and practicality of this approach. The two elements of the methods involving numerical and experimental analyses are discussed in detail in the following sections, and subsequently employed individually in the next two chapters. The objective is to investigate whether the two methods give the same measurement results in different sea condition scenarios. This is achieved through the use of spectral analysis techniques as explained later. The most appropriate method found to be able to provide the sufficient information in real-time as the third method is then sought from a signal processing technique, which is discussed at the end of this chapter and then employed in Chapter 7.

4.2 Analytical Methods to Predict Wave-Influential Parameters

Model testing has always been a time-consuming and an expensive process, but it is considered to be important in reaching an understanding of the nature of ship hydrodynamics. However, as an alternative potentially more flexible solution, the application of numerical methods has been gaining in popularity in the study of a ship's dynamic behaviour. Numerical methods and associated algorithms are used to solve and analyse problems that involve complex fluid flows around solid bodies. Computers are used to perform the very large number of calculations that are required in order to simulate the interaction of liquids with surfaces that are defined by boundary conditions. This approach has led to development of fully three-dimensional boundary integral element methods.

The fundamental bases of almost all numerical methods are the Navier-Stokes equations, which define any single-phase fluid flow behaviour. These equations can be simplified by removing the terms describing viscous actions in order to yield the Euler equations. Further simplification, by removing terms describing vortices, yields the full potential

equations. Finally, these equations can then be linearized to yield the linearized potential equations.

The method that is used for complex three-dimensional models is to discretise the surface of the geometry with a mesh of elementary flat panels, giving rise to a class of programs called Panel Methods. A number of three-dimensional codes have been developed, leading to numerous commercial packages. The fineness of the mesh, with the increased number of panels, can improve the quality of the flow. In all of these approaches the same basic procedure is followed:

1. Pre-processing stage:
    - The surface geometry of the problem is defined and it is represented by a complete fully-connecting set of general quadrilateral flat panels.
    - The volume of fluid is divided into discrete cells known as mesh.
    - The equations of motions for physical modelling of the flow at all points are defined.
    - The various boundary conditions are defined. This involves specifying the fluid behaviour and properties at the boundaries of the problem. For transient problems, the initial conditions are also defined.
2. Simulation stage: The complete set of equations is solved iteratively as either a steady-state or a transient dynamic problem.
3. Post-processing stage: Results of the analysis and graphical display of the results.

The application of the boundary element method has dominated much research effort in recent years, and numerous studies have successfully applied the method to the investigation of the dynamic behaviour of ships in various sea conditions. However, other approaches of discretisation methods are also available to be used but are not discussed here. These are:

- Finite volume method
- Finite element method
- Finite difference method
- Spectral element method
- High-resolution discretisation schemes

One of the practical theories for the calculation of the wave induced motions of a ship is strip theory. It is generally applied to the wide range of mono-hull slender body types in the early design stage of a ship.

The strip theory is based upon linearity that incorporates potential theory. This means that the ship motions are considered to be small relative to the cross sectional dimensions of the ship. Only hydrodynamic effects of the hull below the still water level are accounted for (Journee, 1992), therefore when parts of the ship emerge or immerse into the water, inaccuracies are expected.

In this method, viscous effects are neglected, which increases uncertainty when predicting roll motions at resonance frequencies. Therefore, results for large ship motions in extreme sea states can be less accurate. Therefore, this method is not used for further application in this study.

Whilst numerical analysis is now considered to be useful for this study, simplified methods are also highly relevant in order to provide a suitably accurate, computationally efficient prediction of a ship's motions. Therefore, Chapter 5 uses comprehensive numerical experiments, by the Rankine panel method, to investigate the behaviour of a conventional mono-hulled ship in different sea conditions, for a range of speeds and heading directions.

4.2.1 Rankine Panel Method

This method, known as a panel method, discretises boundaries of the fluid into elements with associated singularity strength and imposes appropriate boundary conditions. It uses linear potential flow theory to attempt to numerically reproduce the flow past the ship. A class of such methods, which has produced especially promising results, employs the Rankine source as the elementary singularity. It is very flexible in the free surface conditions that it enforces. The method can even be extended to include non-linear effects when combined with a time-domain approach.

Boundary integral element methods form the basis of the majority of the computational algorithms for the numerical solution. The computation is to solve the forces and wave patterns of bodies travelling near the boundary between two fluids. The Rankine panel method is in a class of such methods which use the Rankine source as their elementary

singularity (Gadd, 1976 and Dawson, 1977). The singularities are distributed on the discretised free surface as well as on the body, and solve for their unknown strengths.

The Rankine panel method discretises the hull surface and a portion of the $z = 0$ plane, representing the free surface. Each of the unknowns (velocity potential, the wave elevation and the normal velocity) is approximated independently by a set of bi-quadratic spline functions that provide continuity of value and the first derivative across the panels. The advantage of such methods is the freedom to impose a wide range of free surface boundary conditions. This leads to a flexibility of linearization about a basis flow or even extension to the fully non-linear problem.

4.2.2 Equations of Motion

The equation of motion for a ship is defined according to Newton's law

$$M\ddot{\vec{\xi}}(t) = \vec{F}_D\left(\ddot{\vec{\xi}}, \dot{\vec{\xi}}, \vec{\xi}, t\right) - C\vec{\xi}(t) \qquad (4.1)$$

where M is the inertial matrix for the body and C is the matrix of hydrostatic restoring coefficients.

The body performs time-dependent motions about the reference frame (x, y, z) in the six degrees of freedom. The displacement $\vec{\delta}$, at position $\vec{x} = (x, y, z)$, may then be written as

$$\vec{\delta}(\vec{x}, t) = \vec{\xi}_T(t) + \vec{\xi}_R(t) \times \vec{x} \qquad (4.2)$$

where $\vec{\xi}_T = (\xi_1, \xi_2, \xi_3)$ is the rigid body translation and $\vec{\xi}_R = (\xi_4, \xi_5, \xi_6)$ is the rigid body rotation.

In order to obtain the hydrodynamic forces F_D, a potential flow boundary-value problem is solved.

4.2.3 Boundary-Value Problem

It is assumed that inertia and gravity forces will dominate wave propagation and therefore the flow within the fluid domain is inviscid, irrotational and incompressible. Under this assumption, the flow is governed by a total disturbance velocity potential $\Phi(\vec{x}, t)$, which satisfies the Laplace equation in the fluid domain, and is subject to the kinematic and dynamic free surface conditions

$$\left[\frac{\partial}{\partial t}+\left(\nabla\Phi-\vec{W}\right)\cdot\nabla\right]\left[z-\zeta\right]=0 \qquad (4.3)$$

$$\left(\frac{\partial}{\partial t}-\vec{W}\cdot\nabla\right)\Phi+g\zeta+\frac{1}{2}\nabla\Phi\cdot\nabla\Phi=0 \qquad (4.4)$$

which is imposed at the instantaneous position of the free surface, $\zeta(x,y,t)$. Here the free surface has been assumed to be single-valued, thereby neglecting non-linear effects. $\vec{W}$ is the mean forward speed.

The no-flux body boundary conditions are on the wetted surface of the hull and are given by

$$\frac{\partial\Phi}{\partial n}=\left(\vec{W}+\frac{\partial\vec{\delta}}{\partial t}\right)\cdot\vec{n} \qquad (4.5)$$

Therefore, initial conditions should be defined for $\frac{\partial}{\partial t}\Phi(\vec{x},t)$, $\Phi(\vec{x},t)$, body displacement and velocity. The gradients of the disturbance potential are also required to vanish at a sufficiently large distance from the vessel at any given finite time.

Two linearizations are applied to the three-dimensional problem. The Neumann-Kelvin linearization, proposed by Gadd (1976) and Dawson (1977), where a uniform stream is taken as the basis flow and the best results for the hull forms, is obtained by linearizing about a double-body flow.

The panel method is used to solve the double-body flow by distributing sources on the body boundary S_B, and its mirror image S_{B*} about the $z=0$ plane. Then using the boundary condition (Equation 4.5) to derive an integral equation for their unknown strengths, $\sigma(\vec{x})$.

$$\iint_{S_B\cup S_{B*}}\sigma(\vec{x}')\frac{\partial G(\vec{x}';\vec{x})}{\partial n}dx'=\vec{W}\cdot\vec{n} \qquad (4.6)$$

where $G(\vec{x}';\vec{x})=\frac{1}{|x'-\vec{x}'|}$ is the Rankine source potential and $\vec{x}\in S_B$

A more detailed discussion of the formulation, numerical method and applications can be found in the work of Mantzaris, 1998.

4.3 Experimental Methods to Predict Wave-Influential Parameters

Ships indeed must cope with rough sea conditions influencing both safety and reasonable levels of comfort on board the vessel during service operations. Provisions must also be made for many other environmentally-related factors, e.g. winds, green seas, icing and so on. Much can be done in the design phase to predict and improve a ship's performance in waves, but cannot fully guarantee the safe operations at sea while underway. An alternative way to determine the ship's likely real life sea-going behaviour is to test a model in a towing tank. These tests are made analogous to the various situations that may occur when ship is operating at sea with varying wave heights and frequencies and so on. Well-conducted tests with scale models under realistic conditions remain invaluable as an accurate and objective way to quantify and demonstrate the dynamic behaviour of a ship.

There are different mathematical models that can be employed to represent an irregular sea, and they can normally be generated in a towing tank under a controlled environment. However, one limitation of a towing tank with a wave-maker facility is that a considerable degree of directionality is imposed on the waves, thus with a reduced 'spreading' function implied.

One of the popular wave spectrum models is the Pierson Moskowitz model, and one which is used, and discussed, elsewhere in this study. The results of measurements made during such tests are numerically analysed with various tools. A popular and well- known mathematical tool that is used in a frequency domain is spectral analysis, which is also used and discussed in detail in this study.

4.3.1 Spectral Analysis

Spectral analysis could be utilised in dealing with the recorded time series of ship responses. It is a powerful and popular approach available for treating complex waves. In application of this technique, it is assumed that the sea state is a combination of a large number of regular sinusoidal wave components. This is a very useful assumption in wave analysis since sea states are in fact composed of waves from a number of different sources, each with its own characteristic heights, periods, and directions of travel.

Mathematically, spectral analysis is based on the Fourier Transform of the sea surface. The Fourier Transform allows any continuous, zero-mean signal, to be transformed into a summation of simple harmonic waves, like a time series record of the sea surface elevation. These harmonic waves are the components of the sea state, each with a distinct height, frequency, and direction. In other words, the spectral analysis method determines the distribution of wave energy and average statistics for each wave frequency. It is performed by converting the time series of the wave record into a wave spectrum. This is essentially a transformation from the time-domain to the frequency-domain, and is accomplished most conveniently using a mathematical tool known as Fast Fourier Transform (FFT).

The spectral approach indicates which frequencies have significant energy content. It can readily be plotted in a frequency vs. energy density graph, which can provide important information about a wave sample and the corresponding ocean conditions.

The valuable information produced by the spectral analysis is based on time-series of sea surface elevations. The recorded data are analysed over short periods from about 20 minutes to several hours, which wouldn't be sufficiently fast for the application of real-time monitoring. Without a proper technique to record and analyse the time signal experienced by the ship, the results obtained can only be unreliable visual estimates of the sea state.

Chapters 5 and 6 use spectral analysis to investigate the influential parameters of the encountered waves by a series of model testings. The main objective of these experiments is to estimate the wave spectrum through motion responses.

4.3.2 Pierson Moskowitz Spectrum

There are a number of mathematical models which can model a wave spectrum. Some of the more popular of these, which could be used in this study, were discussed in Chapter 3. To generate irregular waves in a towing tank, the Pierson Moskowitz spectrum was utilised. It is a spectrum for a fully-developed sea over a long period of time (see figure 4.2). This semi-empirical equation of a stable sea state is naturally scalable, therefore a single parameter of significant wave height, Hs, is required to fully specify it. It also requires the characteristic period or frequency of the wave to be defined. Giving the equation (Rogers, 1997) in terms of the frequency, the power spectra is defined as

$$PM(f) = \frac{\alpha g^2}{(2\pi)^4 f'^5} \exp\left[-\frac{5}{4}\left(\frac{f_p}{f'}\right)^4\right] \quad (4.7)$$

where

$$f' = \frac{f_e}{\frac{f_p / f - \tau}{C_e} + \tau} \quad (4.8)$$

f Frequency of spectrum

f_p Peak frequency of spectrum

C_e Compression factor

$\tau = 0.857222$

$f_e = f_p / 0.857222$, frequency for which amplitude is calculated

$\alpha = 8.1E-3$ Phillips empirical constant used universally to govern the overall amplitude of the wave.

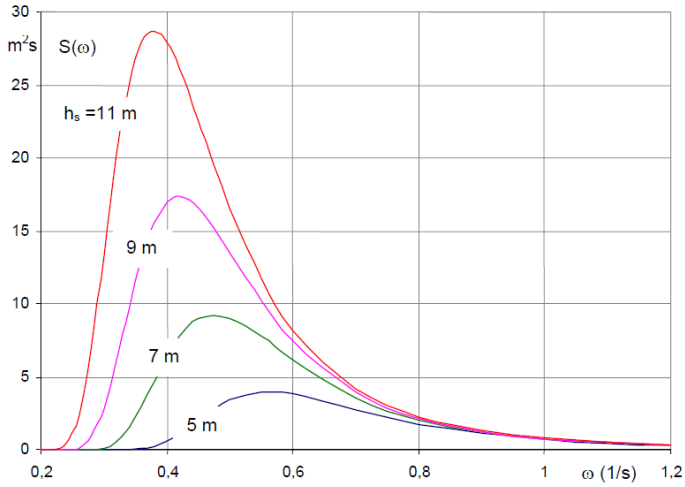

Figure 4.2 Pierson–Moskowitz spectra as a function of significant wave height h_S (Pawłowski, 2009).

4.4 Signal Processing Methods to Predict Wave-Influential Parameters

For the master of a ship, it is vital to make a correct decision in a short time. Therefore, providing sufficient and clear information to him in real-time would provide an invaluable

support to him in critical sea conditions. The influential parameters can be detected in the shortest possible time through signal processing methods, which can portray the changes and trends of the current sea state. The techniques that are employed need to consider both the time and frequency, as well as being simple to use with maximum clarity between the components of the signals.

4.4.1 Signal Processing Methodology

The introduction of time-frequency (TF) signal processing has led to the representation and characterisation of a time-varying signal using a time-frequency distribution (TFD) (Boashash, 2003). TFD is a two-dimensional function which simultaneously provides time and spectral information. The distribution of signal energy over the TF plane shows information not available in the time or frequency domain alone. This includes a number of components present in the signal, such as time duration, frequency bands, relative amplitudes, phase information and instantaneous frequency (Munif, 2006) in the TF plane (Shafi, 2009).

The typical aim of signal processing is to find a representation in which certain attributes of the signal are made explicit. However, the representations of a signal are not unique, therefore the central issues of signal processing are concerned with how to construct a set of the elementary functions $\{\psi_n\}_{n\in Z}$ and how to compute the corresponding dual functions $\{\hat{\psi}_n\}_{n\in Z}$. Either of these can then be used for analysis functions to compute the expansion coefficients or to transform. By the expansion, we can represent a given signal in an infinite number of ways. For good measurements, the set of analysis functions should be selected to give the less computational and reasonably accurate measurements.

The motion responses of a ship are a time-varying signal, and signal processing techniques could be an effective way to detect wave influential parameters. Therefore Chapter 7 explores the application of different methods in analysing of the results from Chapter 6.

The detailed discussion of characterising the time duration and frequency bandwidth to find the relationship in terms of joint time-frequency analysis is given in the next section.

4.4.2 Application of Instantaneous Frequency

The most important relationship in terms of joint time-frequency analysis is the relationship between a signal time duration and the frequency bandwidth. Time duration and frequency bandwidth can be defined in several different ways, and different parameters lead to different interpretations. One of the most common definitions is the standard deviation, the concept used in the probability theorem to characterize the time duration and frequency bandwidth. The following mathematical derivations model such relationships:

The convolution theorem for the two time signals of $s(t)$ and $h(t)$ is defined as

$$(s*h)(t) = \int s(\tau)h(t-\tau)d\tau \qquad (4.9)$$

where the horizontal axis is τ for s and h, and t for $s*h$. The convolution can be written in the form of the inverse Fourier transform

$$\int s(\tau)h(t-\tau)d\tau = \frac{1}{2\pi}\int S(\omega)H(\omega)e^{j\omega t}d\omega \qquad (4.10)$$

where $S(\omega)$ and $H(\omega)$ is the Fourier transform of the signal $s(t)$ and $h(t)$ respectively. Setting $t=0$ in the equation 4.10 and considering $h(-t)$ to be the conjugate form of $s(t)$, then $H(\omega)$ would be the conjugate form of $S(\omega)$. By substituting these terms, the equation 4.10 can be modified as

$$\int |s(t)|^2 dt = \frac{1}{2\pi}\int |S(\omega)|^2 d\omega = E \qquad (4.11)$$

which is known as the Parseval formula, and which indicates that the Fourier transformation is energy-conserved.

The normalized functions $|s(t)|^2/E$ and $|S(\omega)|^2/2\pi E$ can be thought of as signal energy density functions in the time and frequency domains respectively. Given that idea, the signal behaviour can be quantitatively characterized on the basis of probability theory, therefore the mean time and mean frequency computed from the first moment is:

$$\bar{t} = \frac{1}{E}\int t|s(t)|^2 dt \qquad \text{and} \qquad \bar{\omega} = \frac{1}{2\pi E}\int \omega|S(\omega)|^2 d\omega \qquad (4.12)$$

An alternative method to compute the mean frequency of equation 4.12 is the application of the time-derivative property of the Fourier transform

$$F\left[\frac{d^n}{dt^n}s(t)\right] = (j\omega)^n S(j\omega) \tag{4. 13}$$

This method simplifies the computations involved and assists to understand the relation between time and frequency behaviour as explained by Qian (Qian, 1996a). We define a new function, $H(\omega) = \omega\, S(\omega)$, which can be converted into time derivative $h(t)$,

$$h(t) = -j\frac{d}{dt}s(t) \tag{4. 14}$$

By substituting $H(\omega)$ into equation 4.12 and then applying the Parseval formula by considering the time derivative , $h(t)$ the followings are obtained:

$$\begin{aligned}\overline{\omega} &= \frac{1}{2\pi E}\int H(\omega)S^*(\omega)d\omega \\ &= \frac{1}{E}\int -j\frac{d}{dt}s(t)s^*(t)dt\end{aligned} \tag{4. 15}$$

the general form of time signal $s(t) = A(t)\,e^{j\varphi(t)}$, where $A(t)$ and $\varphi(t)$ are magnitude and phase respectively, and both are real.

After substituting the time signal in equation 4.15 we have:

$$\begin{aligned}\overline{\omega} &= \frac{1}{E}\int -j\left(A'(t)e^{j\varphi t} + A(t)\,j\varphi'(t)e^{j\varphi t}\right)s^*(t)dt \\ &= \frac{1}{E}\int -j\left(A'(t) + A(t)\,j\varphi'(t)\right)A(t)dt \\ &= \frac{1}{E}\int \varphi'(t)[A(t)]^2\,dt - \frac{j}{E}\int A'(t)A(t)dt\end{aligned} \tag{4. 16}$$

The mean frequency $\overline{\omega}$ is real, therefore equation 4.16 reduces to

$$\overline{\omega} = \int \varphi'(t)\frac{|s(t)|^2}{E}dt \tag{4. 17}$$

Equation 4.17 defines the relationship between time and frequency where $\varphi'(t)$ is known as the mean instantaneous frequency (Munif, 2006) and acts as weighted average.

Boashash (Boashash, 1992) makes clear that apart from differentiation of the phase and smoothing thereof, there are many well-established methods for estimating the IF, for example, adaptive frequency estimation techniques such as the phase locked loop (PLL), and extraction of the peak frequency from time-varying spectral representations.

Processing the frequencies of the spectral peaks reveals unambiguous and accurate information about the IFs present in the signals (Shafi, 2009), which makes the IF a

parameter of practical importance in situations such as a ship's motion applications. Similarly, the concept of variance can be used to measure the signal energy spreading in time and frequency domains. If $2\Delta t$ and $2\Delta\omega$ are defined for the time duration and frequency bandwidth, then:

$$\Delta t^2 = \frac{1}{E}\int (t-\bar{t})^2 |s(t)|^2 dt = \int t^2 \frac{|s(t)|^2}{E} dt - \bar{t}^2 \qquad (4.18)$$

and

$$\Delta\omega^2 = \frac{1}{2\pi}\int (\omega-\bar{\omega})^2 \frac{|s(\omega)|^2}{E} d\omega = \frac{1}{2\pi}\int \omega^2 \frac{|s(\omega)|^2}{E} d\omega - \omega^2 \qquad (4.19)$$

Equations 4.18 and 4.19 are the standard definitions of variance, and specify the signal spreading with respect to mean time and mean frequency.

Frequency variance can also be expressed as a function of time (Qian, 1996b), similar to mean frequency as discussed earlier,

$$\Delta\omega^2 = \frac{1}{2\pi}\int (\varphi'(t)-\bar{\omega})^2 A^2(t) dt + \frac{1}{E}\int (A'(t))^2 dt \qquad (4.20)$$

Equation 4.20 indicates that the frequency bandwidth can be determined from $\varphi'(t)$ and the magnitude variation $A'(t)$. Therefore, to obtain a narrow band signal, either the magnitude or phase could be smoothed.

4.4.3 Alternative Approaches in Signal Processing

The main focus of this research is to determine a distribution that represents the signal energy concentration simultaneously in time and frequency. The energy distribution needs to be without blur and cross terms (CTs) in order that closely-spaced components can be easily distinguished.

The spectrogram is the most widely-used tool for the analysis of time-varying spectra and is expressed mathematically as the magnitude-square of the STFT. Another approach is a tool which was developed upon the concept of scale rather than frequency (Daubechies, 1990), and is the squared modulus of the wavelet transform. The scaling function filters the lowest level of the transform and ensures the entire spectrum is covered. The key to successful design of TFD lies in the selection of the decomposition algorithm. The components obtained from a decomposition algorithm depend largely on the type of basis functions used. In both analyses, the basis functions are localised in frequency,

making mathematical tools such as power spectra and Scaleogram (equivalent of a spectrogram for wavelets) useful for identifying frequencies and calculating power distributions.

For STFT-based signal decomposition, virtually any function can be used as the window function, whereas one main issue for wavelet analysis is how to generate a desired mother wavelet. Thus wavelet analysis provides immediate access to information that can be obscured by other time-frequency methods such as STFT. However to apply wavelet analysis, a certain level of mathematical preparation is required for windowing technique with variable size.

The Wigner-Ville distribution (WVD) is a form of TFD formulated by a multiplicative comparison of a signal with itself (Stankovic, 1995), expanded in different directions about each point in time. It is qualitatively different from a spectrogram, and produces the energy concentration along the IF for linear frequency modulation. However, the use of the WVD in practical applications is limited (Shafi, 2009) by the presence of CTs resulting from interactions between signal components. These CTs may lead to an incorrect visual interpretation of the signal's TF structure, and are also an interference to pattern recognition. Moreover, if the IF variations are nonlinear, then the WVD cannot produce the ideal concentration.

These methods are known as quadratic TFDs because the signal representation is in quadratic form. None can be effectively used in all possible applications because all suffer from one or more problems. However, STFT and its variations are simple and easy to manipulate and are still the primary and most commonly-used methods for analysis of a time-varying signal. Therefore, in this study STFT is chosen as a suitable technique to analyse motion responses, and the detailed procedure for computing STFT is in the next section.

4.4.4 The Short Time Fourier Transform (STFT) Approach

STFT approach can be utilised to provide both time and spectral information simultaneously which cannot be achieved with the Fourier transform alone. STFT compares the signal with elementary functions (Qian, 1996b) that are localized in time and frequency domains and presented mathematically as

$$STFT(t,\omega) = \int s(\tau)\gamma_{t,\omega}(\tau)d\tau = \int s(\tau)\gamma_{t,\omega}(\tau - t)e^{-j\omega\tau}d\tau \qquad (4.\ 21)$$

Equation 4.21 is called the STFT, or windowed Fourier transform, which is a regular inner product where $s(t)$ is the signal and $\gamma(\tau - t)e^{-j\omega t}$ the elementary function. The function $\gamma(t)$ usually has short time duration and therefore it is named the window function.

The procedure for computing the STFT can be interpreted in two different ways. As shown in Figure 4.3, the function $\gamma(t)$ is multiplied with signal $s(t)$ before the Fourier transform is computed from their product $s(t)\gamma(t-\tau)$. Because the window function $\gamma(t)$ has short time duration, the Fourier transform of $s(t)\gamma(t-\tau)$ reflects the signal local frequency properties. By moving $\gamma(t)$ and repeating the same process, an approximation of how the signal frequency contents evolve over time can be obtained.

For a more accurate measurement of a signal at a particular time and frequency (t,ω), the time duration and frequency bandwidth, Δt and $\Delta\omega$ should be as narrow as possible. Due to the dependency of Δt and $\Delta\omega$ via the Fourier transform, if $\gamma(t)$ is chosen to have good time (smaller Δt) resolution, then its frequency resolution must be decreased (larger $\Delta\omega$), or vice versa.

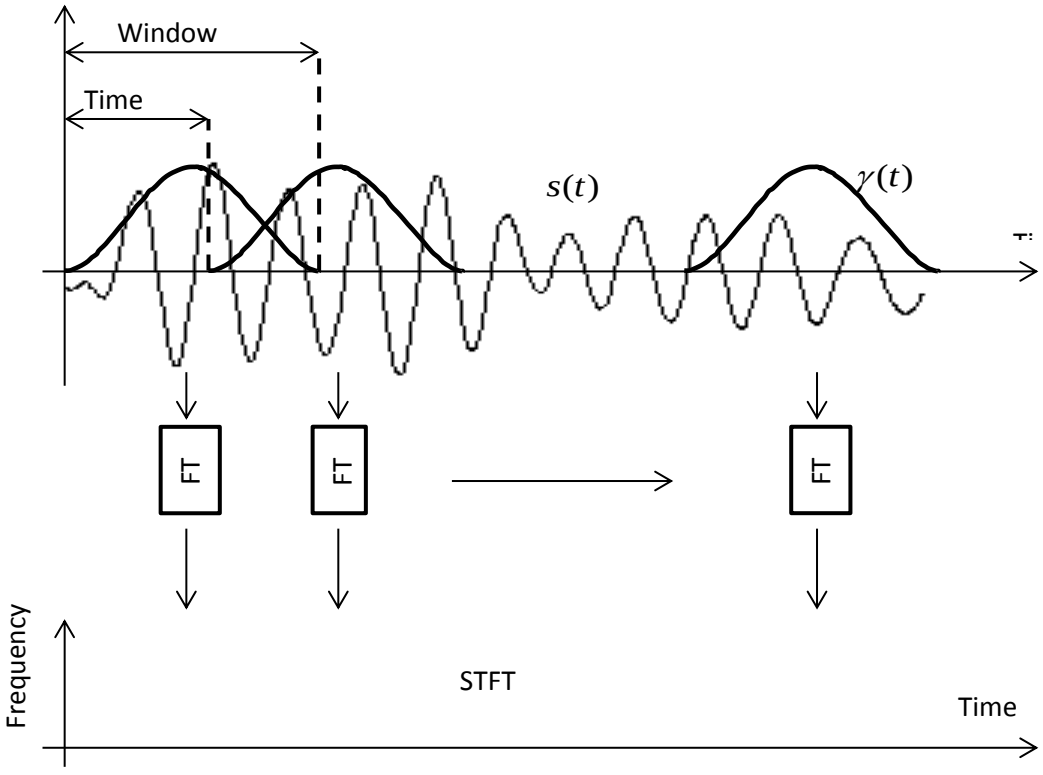

Figure 4.3 Procedure to compute the STFT

The latter approach has been chosen in this study to compute the STFT of a signal. Although the concepts of exploring a time-varying signal are quite similar (performing inner-product operations), the different ways of building elementary functions lead to very different outcomes. All linear transformations are achieved by comparing the analysed signal with a set of prudently-selected elementary functions.

4.4.5 Windowing Technique

A window function is a mathematical function that is zero-valued outside of a chosen interval. The window function (Harris, 1978) uses non-negative smooth "bell-shaped" curves, however, rectangle and triangle functions and other functions are sometimes used. The Fourier transform is applied to the product of the waveform and a window function, however different window types affect the spectral estimate computed by this method.

Critical analysis. A serious weakness with the window method is the spectral leakage. Windowing develops non-zero values at frequencies other than ω which tend to be highest near the ω. The leakage from the larger component can obscure the weaker frequencies.

The rectangular window has excellent resolution (low-dynamic-range) characteristics for signals of comparable strength, whereas low resolution (high-dynamic-range) windows such as Blackman-Harris and Flat top are often justified in wideband applications, where the spectrum being analysed is expected to contain many different signals of various amplitudes.

The sensitivity is the key issue with low resolution windows where the response to noise will be higher. In other words, the ability to find weak sinusoids among the noise is diminished by a high-dynamic-range window.

In between the extremes are moderate windows, such as Hamming and Hanning. They can be used in narrowband applications, such as the spectrum of a seaway.

Taken together, these results suggest that the spectral analyses involve a trade-off between resolving comparable strength signals with similar frequencies, and resolving disparate strength signals with dissimilar frequencies, when the window function is chosen.

In 1978 Harris published a paper in which he described these windows to be in the general form of

$$\omega(n) = \sum_{k=0}^{K} a_k \cos\left(\frac{2\pi kn}{N}\right) \qquad (4.\ 22)$$

where

N represents the width in the samples of a discrete-time window function

n is an integer with the values of $0 \le n \le N-1$

$\omega(n)$ is frequency sequence and the maximum value occurs at $\omega(0)$.

In equation 4.22 there is only $2K+1$ non-zero DFT coefficient, which makes them good choices for applications that require windowing by convolution in the frequency domain.

Window types

The rectangular window is the simplest window and is defined by $\omega(n) = 1$ shown in figure 4.4.

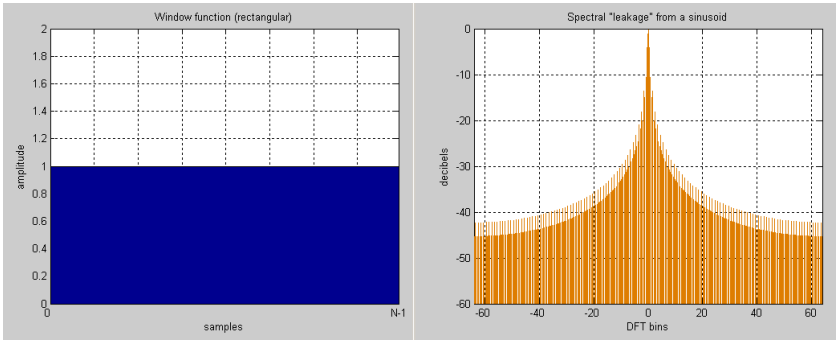

Figure 4.4 Rectangular window function and its spectral analyses (Website1, 2012)

Figure 4.5 shows a Hanning window where the end of the cosine just touches zero and the mathematical model is represented as follows:

$$\omega(n) = 0.5\left(1 - \cos\left(\frac{2\pi n}{N-1}\right)\right) \qquad (4.\ 23)$$

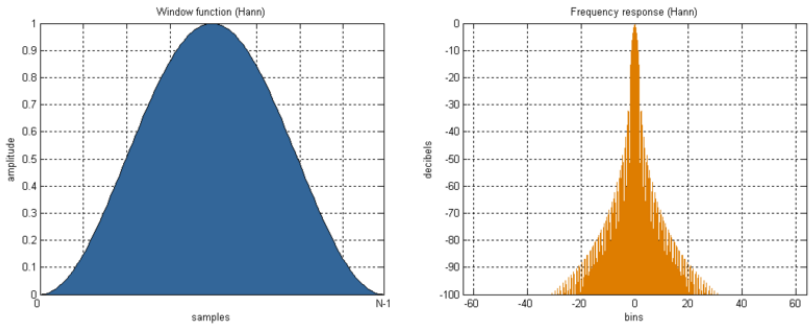

Figure 4.5 Hanning window functions and its spectral analyses (Website1, 2012)

The Hamming window is optimised to minimise the maximum side lobe, giving it a height of about one-fifth that of the Hanning window (see Figure 4.6). The mathematical presentation is as follows,

$$\omega(n) = 0.54 - 0.46\cos\left(\frac{2\pi n}{N-1}\right) \qquad (4.\ 24)$$

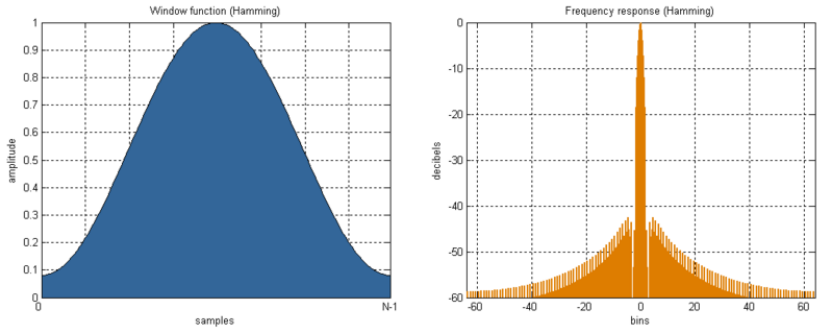

Figure 4.6 Hamming window functions (Website1, 2012)

The Blackman-Harris window shown in Figure 4.7 is a generalisation of the Hamming window which is produced by adding more shifted sinc functions to minimise the side lobes. The mathematical presentation is as follows:

$$\omega(n) = a_0 - a_1\cos\left(\frac{2\pi n}{N-1}\right) + a_2\cos\left(\frac{4\pi n}{N-1}\right) - a_3\cos\left(\frac{6\pi n}{N-1}\right) \qquad (4.\ 25)$$

$$a_0 = 0.35875, \quad a_1 = 0.48829, \quad a_2 = 0.14128, \quad a_3 = 0.01168$$

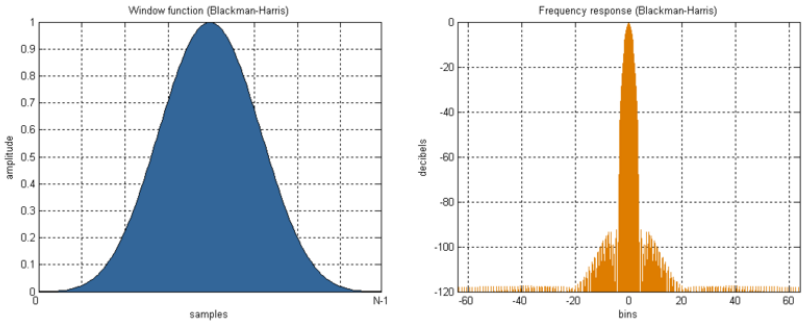

Figure 4.7 Blackman-Harris window functions (Website1, 2012)

The flat-top window shown in Figure 4.8 is presented mathematically by the following formulas:

$$\omega(n) = a_0 - a_1\cos\left(\frac{2\pi n}{N-1}\right) + a_2\cos\left(\frac{4\pi n}{N-1}\right) - a_3\cos\left(\frac{6\pi n}{N-1}\right) + a_4\cos\left(\frac{8\pi n}{N-1}\right) \qquad (4.\ 26)$$

$$a_0 = 1, \quad a_1 = 1.93, \quad a_2 = 1.29, \quad a_3 = 0.388, \quad a_4 = 0.032$$

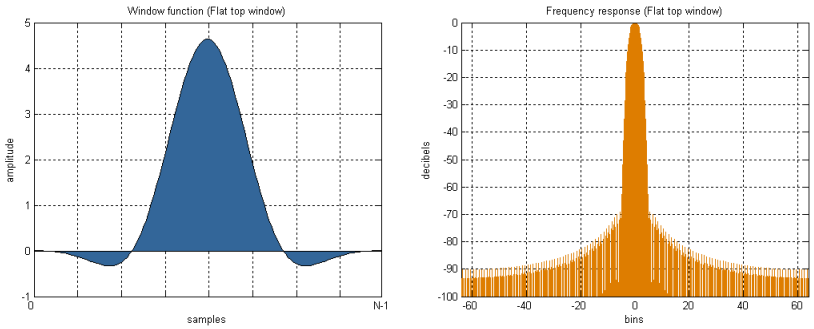

Figure 4.8 Flat-top window functions (Website1, 2012)

The window is a raised cosine with simpler coefficients and optimized to minimize the maximum (nearest) side lobe, giving it a height of about one fifth of that of the Hann window.

4.4.6 Accuracy of the Presented Data

The theoretical properties and application fields for the large number of time-frequency energy distributions methods have now been well determined and are widespread (Hlawatsch, 1992). Although many quadratic TFDs have been proposed, none can be effectively used in all possible applications.

An important feature of TFD methods is readability, and an ideal TFD function requires the following four properties (Shafi, 2009):

- High clarity which makes it easier to be analyzed. This requires high concentration and good resolution of the individual components for multi-component signals.
- Cross terms elimination which avoids confusion between noise and real components in a TFD for nonlinear TF structures and multi-component signals.
- Good mathematical properties which benefit its application. This requires that a TFD should satisfy the total energy constraint, univariate marginal distributions in time and frequency and positivity issue not to be negative elsewhere.
- Low computational complexity means the time needed to represent a signal on a TF plane. Weak signal mitigation may increase computation complexity in some cases.

A spectrogram is expressed mathematically as the magnitude-square of the STFT of a signal, and is given by:

$$S(t,\omega) = \left| \int x(\tau) h(t-\tau) e^{-i\omega\tau} d\tau \right|^2 \quad (4.\ 27)$$

where x(t) is a signal and h(t) is a window function.

However, STFT method of analysis suffers from a number of limitations (Altes, 1980):

- Time and frequency representations are related by the Fourier transformation, so that signal behaviour in the time domain and frequency domain are not independent. Therefore, the signal time-duration and frequency bandwidth cannot be made arbitrarily small simultaneously.
- Presentation of data by a spectrogram provides bias estimation of the signal IF and should be taken into consideration when used as a measuring tool.
- All real measurements are disturbed by noise (i.e. wind, wave, hull and engine vibrations, variations of temperature, variations of humidity, etc).

4.5 Summary

This chapter maps the selected methodologies that are to be employed in this research in order to study the dynamic behaviour of a ship at sea. It was decided that the best strategy to adopt for this investigation was to perform a series of numerical and experimental tests with the aim to identify the links between a prevailing sea condition and a ship's corresponding motions. These tests are conducted on the basis of the eventual identification of the influential irregular wave's parameters through an analysis of the wave-induced ship's motions. The general idea is presented by a block diagram to demonstrate the overall method of approach.

Spectral analysis is introduced as the main technique that is to be employed in the analyses of data that have been recorded from ship's motion responses. Spectral analysis is very effective as being a powerful mathematical technique for treating complex waves that have been recorded as a time series.

The Pierson Moskowitz (PM) spectrum is reviewed in detail because it has been chosen as one of the most practical of ways in generating irregular waves. A physical model was tested in a towing tank under the various sea models generated according to the PM spectrum. The details of these tests are given in Chapter 7.

For the numerical analysis, the boundary element method (BEM) is selected to be applied to assess the wave-induced loads and wave-induced motions of a mathematical model. The results of these simulations are presented and discussed in Chapter 6. The BEM has been introduced as being a suitable numerical approach on the basis of incorporating potential theory which is considered to have a number of attractive features that are discussed in this chapter.

The analysing procedure reviewed in this chapter has also yielded some important insights with relevance to the STFT mechanism. The main focus is to determine a distribution that represents the signal energy concentration simultaneously in both time and frequency. This technique is suitable for detecting the peak frequencies and associated magnitudes of a recorded signal, and its application is subsequently discussed in detail in Chapter 8. The spectrogram technique is also introduced as being the most widely-used tool for the analyses of time-varying spectra, and which is expressed mathematically as the magnitude-square of the STFT. The important features and limitations of TFD methods were discussed at the end of this chapter.

Chapter 5

Numerical experiments

5.1 Introduction

Numerical analysis approaches are particularly important due to the limited availability of costly experimental data, and they provide a reasonable and readily-obtained understanding of a ship's behaviour in various sea states. This chapter presents a review of comprehensive numerical experiments, using the established boundary element method (BEM), investigating the characteristics of a ship's motions in different sea conditions. The boundary element method is a well-known numerical approach to efficiently model potential flow where the velocity potential in the fluid domain is represented by a distribution of sources over the mean wetted body surface. The numerical experiments are demonstrated, using the SESAM (SESAM, 2010) nonlinear BEM software, to investigate the waves' influential parameters through a ship's motion responses.

BEM is increasingly being used for assessing the wave-induced loads on large complex three-dimensional volume structures on the basis of potential theory. In this method the source function satisfies the free surface condition, therefore satisfying the boundary condition on the full body surface gives an integral equation for determining the source strength.

The general modelling approach in this environment allows for the vessel travelling at different speeds, and uses elementary Rankine sources distributed over both the mean wetted body surface and the mean still water-free surface; A Rankine source method is preferred for forward speed problems (DNV, 2011).

A rigorous modelling approach is developed which includes the influence of geometric and deadweight loading conditions and provides an adequate recognition of the various factors that affect the motion responses, including:

- Wave spectrum
- Significant wave heights and peak periods
- Water density, kinematic viscosity and depth
- Wave angle of attack
- Mesh sizes and radius of water local region
- Number of panels on hull-wetted surface
- Speed of vessel through the water
- Duration and time steps for integration/iteration processes

A key objective is to reduce the uncertainties that are inherent in appropriately modelling these factors, thus discounting those which are found to make a relatively minimal difference to the motion behaviour, whilst ensuring that the methods properly take into account those that do influence the outcome. This is therefore a form of 'sensitivity' study.

The findings of the ships' motions study, as described in the latter part of this chapter, are important to consider therefore when developing an operational guidance procedure. Consequently, the studies detailed below not only generate raw data to quantify the ship's motion responses but also provide a case study for identifying the influential wave parameters within a model ship, and how these are to be presented within an BEM analysis. The detail of the model used in this study is given in Table 5.1.

5.2 Coordinate Systems

To represent a quadrilateral flat panel as an integral part replicating the hull surface of a ship's structure, the boundary conditions of the BEM model needs to adequately reflect the local support and load scenarios. The panel element local coordinate system is defined by a right-handed Cartesian coordinate system where the z-axis points upwards. The input and the results refer to coordinates in the body, such as the centre of gravity, the centre of buoyancy, the centre of free surface and so on, and are based on the

coordinate system shown in Figure 5.1. However, in order to define lightweight and deadweight loading conditions, the global coordinate system is defined, which affects trim, heel and draught. In this coordinate system, the model is transformed by first performing the rotations (Euler angles with the order RY-RX, trim-heel) and subsequently changing the draught.

The approach that is proposed in the present work is based on the application of the Wasim program, which is as an integrated part of the SESAM suite of programs. Wasim uses three different coordinate systems:

- The User system, which is utilised for the geometry input and other input coordinates.
- The Global system where the xy-plane is the mean still water-free surface and x=0 at midship. Here, midship is defined as the mean between the two perpendiculars given on the geometry file. The transformation sequence from the Global system to the User system is first to translate and then to rotate.
- The Body-fixed system, which is an internal coordinate system fixed in the vessel. At the starting point of the time simulations the Body-fixed and Global systems coincide.

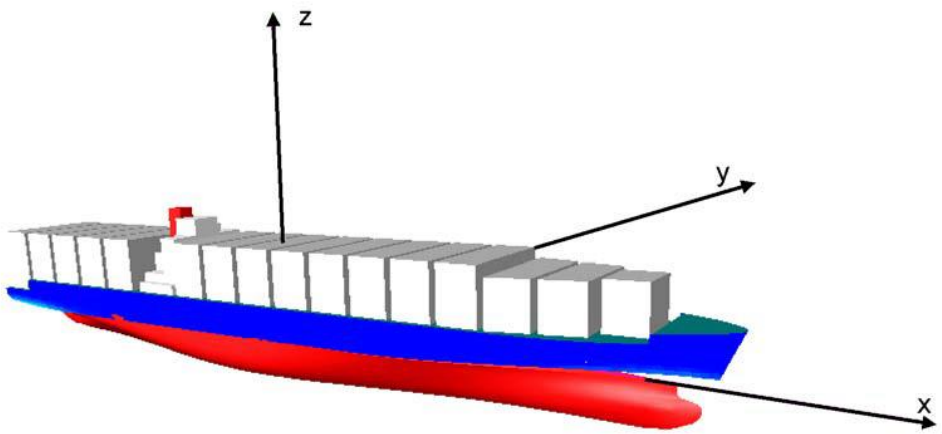

Figure 5.1 Eample ship used for numerical analyses, showing Wasim user coordinate system

Care should be taken in the transformation of the coordinate systems when the angle between the xy-plane and the mean free surface plane is becoming large. This condition will occur if, for example, the vessel is very badly trimmed for any reason, e.g. poor deadweight loading, accidental flooding and so on.

5.3 Wave Loading Program: Wasim

Wasim is a program for computing global responses and local loading on vessels moving at any forward speed. The simulations are carried out in the time domain, but results can be transformed to the frequency domain by using the Fourier transform. The analyses capabilities of Wasim are quite diverse but this study focuses only on the outcome of the hull rigid body motions.

Wasim solves the fully 3-dimensional radiation/diffraction problem by a Rankine panel method, therefore panels are required to fully cover both on the hull and on the water-free surface (for more details refer to Chapter 4).

The radiation/diffraction problems are solved on the mean free surface and mean wetted surface panels, having both linear and nonlinear options. In the nonlinear mode of operation the following terms are included (DNV, 2011):

- Integration of Froude-Krylov and hydrostatic pressures over the exact wetted surface
- Quadratic terms in the Bernoulli equation
- Exact treatment of rotation angles in both inertia and gravity terms
- Quadratic roll damping

5.3.1 Wasim Program Theory of Operations

The wave input to Wasim is given as a sum of the component harmonic waves of the form given by Equation 5.1.

$$\eta(x, y, t) = A\cos[(k\cos\beta)x + (k\sin\beta)y - \omega t + \gamma] \quad (5.1)$$

k is the wave number and which in an infinite depth of water is given as: $k = \omega^2/g$

For each of the wave components the following parameters must be specified:

A wave amplitude

T wave period $= 2\pi/\omega$

β wave direction

γ phase angle

Therefore, it is possible to define different representations of a given sea state by defining both the wave amplitudes and the phase angles. From the Environment folder of Data Organisation in Wasim it is possible to select from any of three different wave spectra

that have been pre-defined. A more detailed discussion of the formulations, numerical methods and range of applications can be found in the Wasim manual (DNV, 2011).

5.3.2 Modelling Conditions

The modelling techniques in SESAM are utilised to construct the complete ship's hull envelope, and the practical FEM modelling techniques provide the justification for employing the approach. They also summarise the knowledge that has been gained through the present work in effectively developing FEM models for rigorous analyses.

The available robust modelling methodology, thus used for development, enables an efficient generation of the full hull model including all relevant internal geometric and mass distribution aspects.

The geometry of the hull is supplied by the user to the program externally and the defining external surface mesh is generated by an inbuilt program. As a consequence, the Wasim Manager will create the full panel model and the relevant coordinate data from the uploaded geometry input.

The Wasim computer program consists of several different executable elements, and in these experimental simulations the following must be among those that are taken into account:

- Wasim_Mass, computes the overall body mass matrix and the various sectional mass matrices from a given comprehensive mass model
- Wasim_Setup**,** sets up and inverts the influence matrix for the radiation/diffraction problem, and solves for the basis flow (i.e. the solution in calm water)
- Wasim_Solve, performs the time domain simulation

All of the modules in the system, except for the pre-processor, require significant execution time, however Wasim_Solve is by far the most demanding. The computational time that is required depends heavily on the number of panels defining the hull envelope, user-specified number of time steps, the number of wave directions, and so on.

If the panel model and other data are symmetric about the centreline xz-plane, it is possible to model only one half of the hull panel model. This will reduce calculation time and memory requirements. The model must then be defined on the positive side of the

symmetry plane shown in Figure 5.2. However, the Geometry File, the FEM model and the Mass model must all be in the same frame of reference.

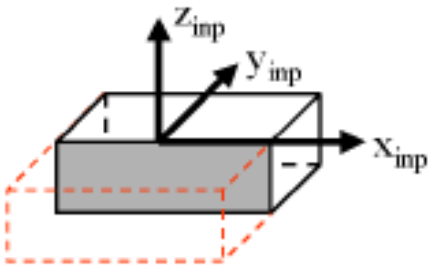

Figure 5.2 Symmetry of an object generated in SESAM program

The solution method in Wasim_Solve is a Rankine Panel method and the elementary solution in the Rankine method does not satisfy the free surface boundary condition. Therefore, the integral equations have unknowns on both the hull and the water-free surface panels that are to be solved; this causes the equation system to become larger. On the other hand, the computation of the matrices in this equation system is easier than with the full Green's function, since the elementary solution is much simpler to compute (DNV, 2011). Other benefits with the Rankine panel method are:

- Since the free surface condition is not automatically satisfied, then different free surface conditions can be handled.
- There are no irregular frequencies.

A mesh is created on both the hull surface and the water-free surface since the equation system is required to be solved simultaneously on both surfaces. An example of a free surface grid is shown in Figure 5.3 (complete grid), and a close-up view to highlight the panel details of the vessel is shown in Figure 5.4. Grids on both the hull and the free surface are created in HydroD from the geometry input file.

The extension of the grid depends on the encountered wave frequency, which shall not be less than the equivalent of one wavelength of the longest radiated or scattered wave. In infinite water depth, the wave length of the radiated and scattered waves is given by

$$\lambda = \frac{2\pi g}{\omega_e^2} \tag{5.2}$$

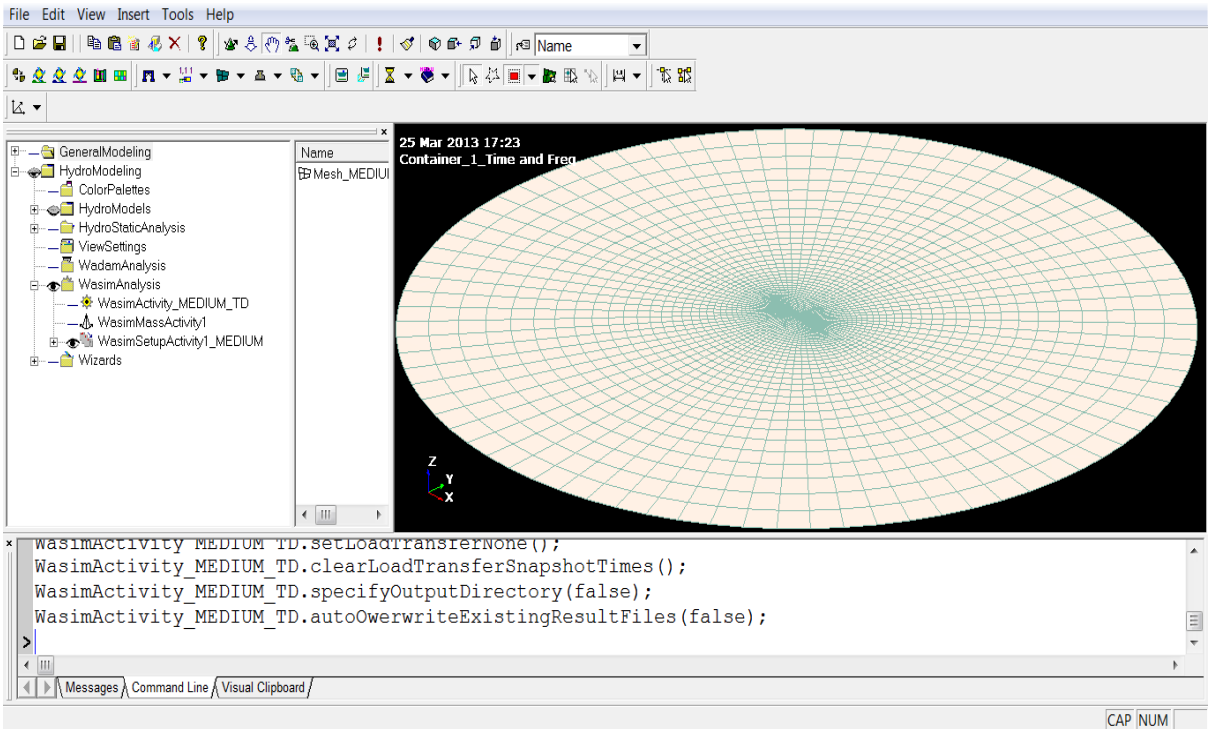

Figure 5.3 A typical water-free surface grid generated in HydroD

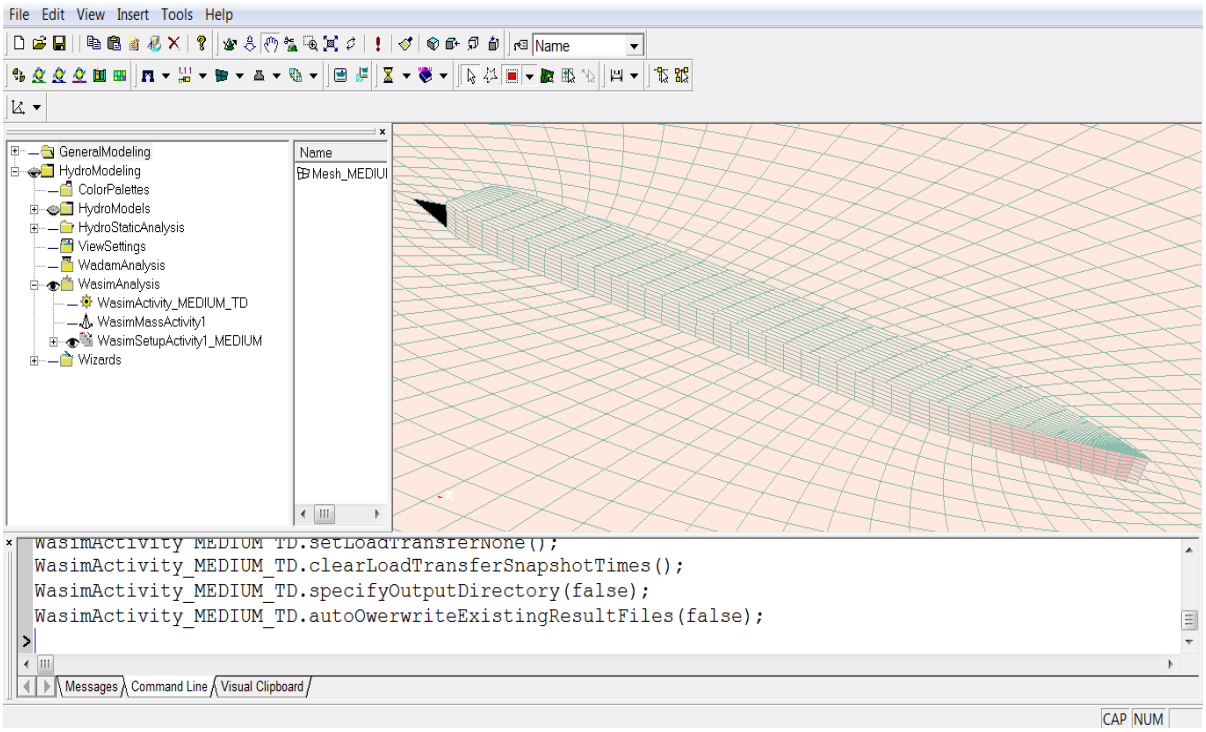

Figure 5.4 A typical hull and free surface grid generated in HydroD, hence it is for a view point that is above the free surface

5.4 Time-Domain Simulation

Time-domain analysis methods are usually used for the prediction of extreme load effects. Some hydrodynamic load effects can be adequately linearized and included in a frequency-domain approach, however others are highly nonlinear and can only be handled in the time domain.

An advantage of a time-domain analysis, as used in running these simulations, is to capture higher-order load effects which are essential due to the potential coupling effects of the responses. In addition, a time-domain analysis generates the response statistics without making assumptions regarding the response distribution. This type of analysis involves numerical integration of the equations of motions, and should be used when nonlinear effects are important.

In this chapter, the solution of the ship-wave interaction problem is computed in the time domain by the module, Wasim_Solve. This module requires discretisation in both space and time in order to take into account the accuracy and stability of the solution process. Therefore, determining the appropriate length of the time step is crucial in order to obtain acceptable results.

Solution accuracy tends to be the most important consideration in the low to moderate speed cases, whereas stability of the process is the dominating issue in high-speed cases. The solution process becomes unstable if the time step is too large, whereas it remains neutrally stable if the time step is sufficiently small. The precise value of the limiting time step depends largely on the shape and orientation of the many individual panels in the mesh. An operational curve is provided in the Wasim manual to provide time-step advice on dissimilar cases.

5.5 Some Facts about Testing in Irregular Waves

The results from tests that have been undertaken in irregular waves generally include simple statistics (for example, mean, standard deviation, maximum, minimum, Skewness and Kurtosis), and spectra and spectral parameters. Analyses of the acquired wave-induced motions data, including heave and pitch responses, typically indicate positive Skewness, whereas the distribution of the roll response results is generally too narrow and with a good indication of positive Kurtosis (see Ch.6). One of the main outcomes of

motion response statistics is the peak distribution plots, and which are helpful in identifying the various more influential parameters.

For linear processes, the behaviour of the extremes is well known (DNV, 2007), and is generally based on the standard deviation of the process, whilst for nonlinear processes it is essential to use and interpret the measured extremes in a proper and consistent way. Therefore, in this study, multiple sea state idealisations have been run for better estimates of extremes.

In order to obtain acceptable estimates, a large number of different conditions were run to overcome the statistical variability problem. Strongly nonlinear processes exhibit a larger statistical scatter (DNV, 2007) than do weak nonlinear processes, and the multiple approach is often recommended.

5.6 Frequency Setup for Simulations

An understanding of the response characteristics of a system is clearly important for undertaking a correct treatment and inclusion of all relevant load effects. The form of response itself may also be important for the resulting induced loads, for example coupled effects.

The largest wave forces on structures take place at the same frequencies as the waves themselves, causing wave frequency (WF) motions of the structure. To avoid large resonant effects, floating offshore structures and their mooring systems are often designed in such a way that the resonant frequencies are shifted well outside the dominant wave frequency range in a particular sea region. For a freely floating structure the same principle is also applicable in order to avoid large resonant conditions. However, it is challenging to achieve this goal at the design stage, as the ship is subject to different sea conditions and hence every wave frequency.

Due to nonlinear load effects, some wave-induced responses always appear at the hull rigid body natural frequencies. It is worth mentioning that, out of the six degrees of freedom, the roll behaviour is the most dangerous motion from an operational point of view. Therefore, any simulation should be set to run for a range of wave frequencies that sweep across the roll natural frequency, allowing for a range of deadweight conditions if and where appropriate and so on.

There are several empirical formulae that can be used to calculate the natural periods of uncoupled restorative motions of a freely floating body, as follows:

Heave motion: $T_3 = 2\pi\left(\frac{M + A_{33}}{\rho g S}\right)^{\frac{1}{2}}$ (5.3)

where M is the mass of the ship, A_{33} is the heave hydrodynamic added mass and S is the waterplane area.

Pitch motion: $T_5 = 2\pi\left(\frac{Mr_{55}^2 + A_{55}}{\rho g V\, GM_L}\right)^{\frac{1}{2}}$ (5.4)

where r_{55} is the pitch radius of gyration, A_{55} is the pitch hydrodynamic added moment, V is submerged volume and GM_L is the longitudinal metacentric height.

Roll motion: $T_4 = 2\pi\left(\frac{Mr_{44}^2 + A_{44}}{\rho g V\, GM_T}\right)^{\frac{1}{2}}$ (5.5)

where r_{44} is the roll radius of gyration, A_{44} is the roll hydrodynamic added moment and GM_T is the transverse metacentric height.

In general, the behaviour of a ship is studied when the structure is assumed to be exposed to the regular incident waves, and which is referred to as being a frequency-domain analysis. The general understanding, when assuming a steady state condition, with all transient effects being neglected, is that the loads and the dynamic response of the structure are oscillating harmonically with the same frequency as the incident waves. However, it is modified with the frequency of encounter in the case of the vessel having forward speed.

The real sea is very irregular by its general nature, and the dynamic responses of a ship constantly change before it reaches steady state conditions. Therefore, we do not generally expect to get harmonic oscillations in a ship's motions through the effects of irregular wave loads. However, it is quite essential to explore the links between incident wave frequencies and a ship's motions responses for the real-time monitoring of a sea state. Hence, a series of simulation experiments were scheduled in order to test a model in different sea conditions and through a range of frequencies.

5.7 Reference Ship

The hull lines model of a typical containership is shown in Figure 5.5 and which is used to investigate the influence of the sea state on the dynamics responses in irregular seas.

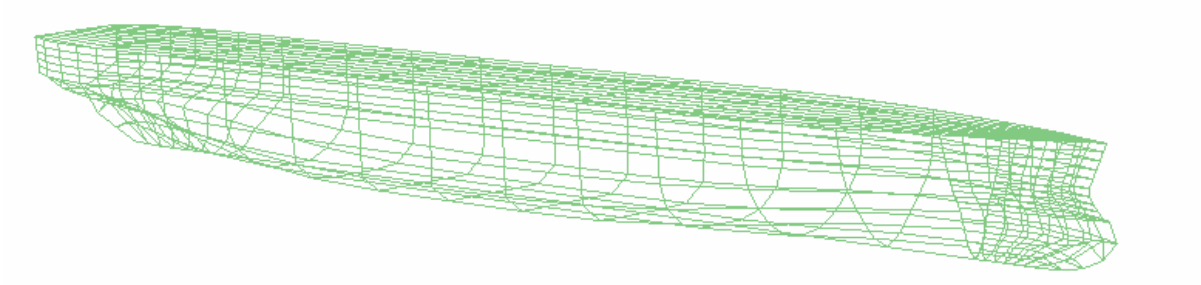

Figure 5.5 Containership model lines generated by Genei-SESAM

The Majority of the cargo compartments and ballast tanks of the vessel were taken to be loaded and ballasted on the presumption of the present-day loading style. Containerships are frequently scheduled to call at several ports in a round voyage, and typically engage with several loading and discharging operations. This situation raises the possibility of ships being partially loaded for most of the time.

Table 5.1 Parameters of the Containership model

Particulars	**Values**	**Particulars**	**Values**
Length	278 m	Mass	94917254 kg
Breadth	33.48 m	Vol. of displacement	92602 m^3
Depth	23.08	COG from App	122.98 m
Draught	15 m	Cargo density	900 kg/m3
Heel	0 deg	Light Cargo density	450 kg/m3
Trim	Even keel	Ballast Water density	1000 kg/m3
VCG	11.92 m	Sea Water density	1025 kg/m3
KM	15.17 m	Heave radius of gyration	11.92 m
KG	11.92 m	Pitch radius of gyration	2.28 m
GMt	3.25 m	Roll radius of gyration	18.97 m
NOs of nodes	4816	Roll added moment	20%
NOs of plates/shell	4298	NOs of wave components	106

A trial run of the simulation revealed the general particulars of this model, and details of the generated data are given in Appendix III. Some of these are presented in Table 5.1. The main focus in this study is on the impact of the waves on the roll motions. Therefore, the roll period needs to be known in order to identify the particular range of the wave spectrum to be examined. Thus prior to commencing the simulation processes, the roll natural period is estimated numerically by employing Equation 5.5. This equation has been evaluated in several text books and understood to provide a reasonable estimation. The computation is based on the parameters given in Table 5.1, where the natural period of roll is found to be 23s or 0.043Hz. The details of the wave spectrum and the setting of relevant values are discussed in detail in the following sections.

5.8 Data Analysis of the Results

A sample of the simulation results of the motion responses and the incoming waves is shown in Figure 5.6, which were generated by the Wasin program and then recorded. The recorded files are formatted in such a way that they can be read by the time- domain post processor, Postresp_time. The file contains several data columns for each time step and all columns are on the same line. The first three columns that are shown in Figure 5.6 are the ship's three selected motion amplitudes at the specified motion reference point, and the last column is the time trace of the incoming wave amplitudes at the origin of the Global system. For a nonlinear run, this origin follows the translations of the vessel.

1	Time	Heave - WasimActivity	Roll - WasimActivity	Pitch - WasimActivity	Incoming wave - WasimActivity
2	0	0	0	0	0
3	0.25	8.77267E-05	-1.28847E-06	9.19803E-05	2.60377E-05
4	0.5	0.000293537	-4.3921E-06	0.000315733	4.09467E-05
5	0.75	0.000591442	-9.07154E-06	0.000657524	-4.88835E-05
6	1	0.000946132	-1.49825E-05	0.00109727	-0.000335127
7	1.25	0.00132698	-2.16649E-05	0.00160775	-0.000909003

Figure 5.6 A sample of discrete time-varying simulation results from the Wasim program

The recorded data was analysed, using power from a spectral density (PSD) facility that is provided in the LabVIEW software (National Instruments, 2011), and which illustrates how the power of a signal or time series is distributed with frequency; the time-domain window selected was the Hanning type. The details of the spectral analyses are discussed in Chapter 4.

The time duration of each simulation can vary from one hour to several hours depending on the significant wave height and the forward speed; the discrete time steps are adjusted accordingly to expedite the process.

5.8.1 Simulation Conditions

The model was tested in three different simulated conditions, namely with the vessel stationary, and then with two different forward speeds. The total number of recorded runs was 135, which comprised of three peak periods, with three significant wave heights and five heading angles. The heading angles were 0°, 45°, 90°, 135° and 180° corresponding to following, quartering, beam, bow and head seas respectively. Table 5.2 lists the intended spectrum characteristic applied to run the simulations to generate irregular waves. The wave spectrum chosen was the Pierson Moskowitz, which is a spectrum for a fully-developed sea over a long period of time (for more detail refers to Chapter 4).

Table 5.2 Sea spectrum setting parameters

Peak period s	Sea state	Significant wave Height H_s (m)	Forward speed m/s
10	High	3 (Small)	Zero
15	Medium	6 (Medium)	5
20	Low	9 (Large)	10

The wave conditions stated above were selected in order to maximise the scope of the possible test runs over a wide range of frequencies.

In the presentation of the results, some of the graphs are not provided with the related units in Section 5.9. Where the unit is not mentioned it is considered to be as follows:

The y-axis presents the PSD and the unit is measured as $S(\omega)[m^2 s/rad]$ for the wave and heave motions, whilst it is $S(\omega)[\deg^2 s/rad]$ for the pitch and roll motions. To include all responses in the same plot, a secondary vertical axis is added in Section 5.9. The left axis gauges the wave and heave magnitudes and the right axis is allocated for gauging the pitch and roll magnitudes. The magnitude scales are adjusted for each graph for presentation purposes because those tested with lower Hs have comparably much lower values.

5.8.2 Linear vs Nonlinear Results

The Wasim program can operate in either linear or nonlinear modes. The primary difference between these two simulations is in the time required for computations. Despite a short duration being required for the linear mode, the operation in a nonlinear mode is significantly longer. This is because in the nonlinear mode the simulation time is drastically amplified when the significant wave height is increased.

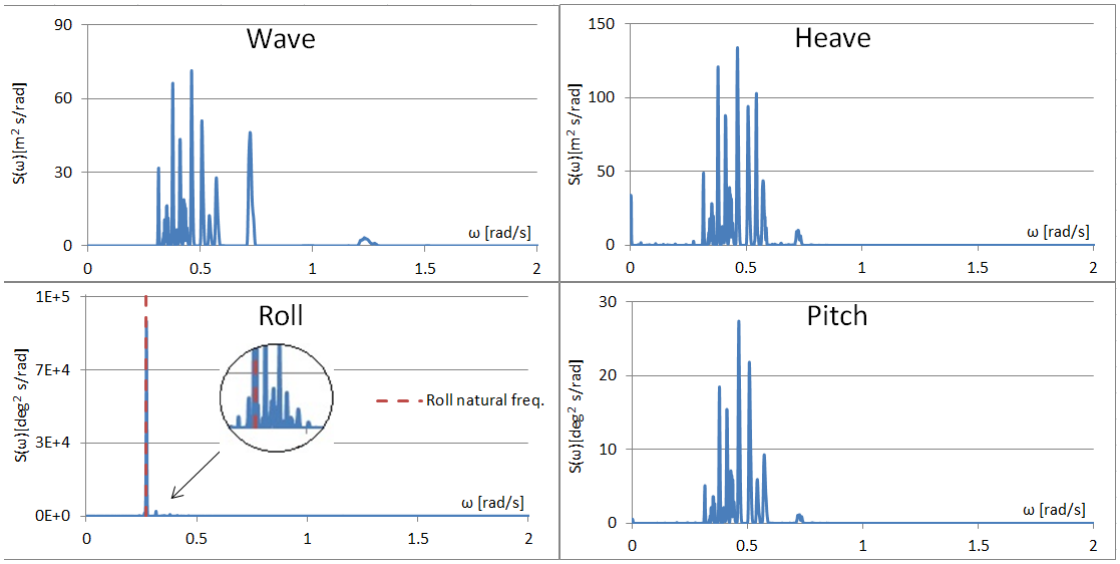

Figure 5.7 The nonlinear results of incident wave and motion responses in the frequency domain. The simulation is conducted at a quartering sea, at zero speed with Hs of 3m and a peak period of 15s.

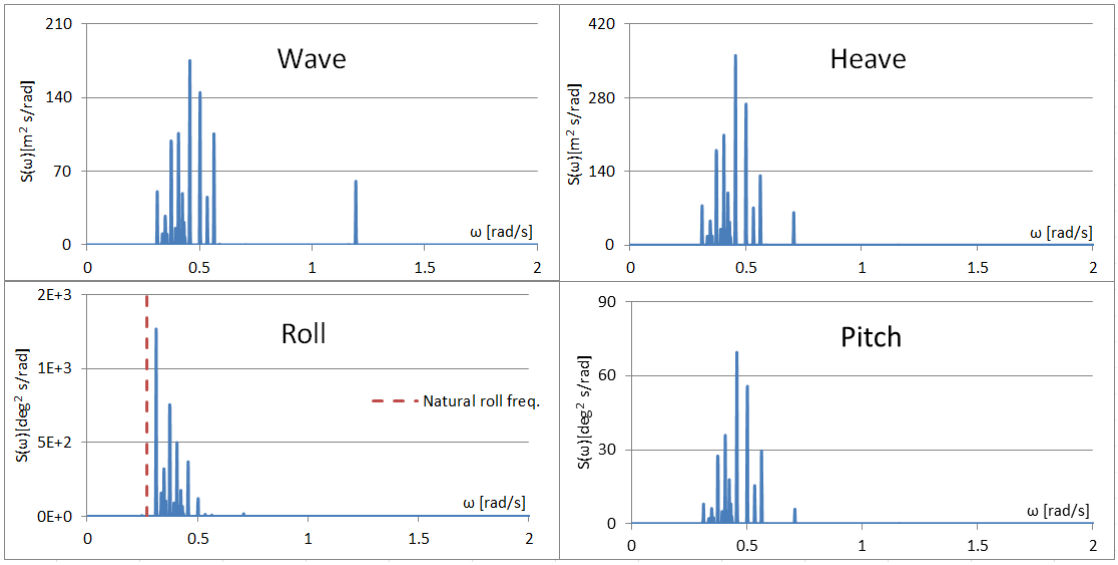

Figure 5.8 Linear results of incident wave and motion responses in frequency domain. The simulation is conducted at a quartering sea, at zero speed with Hs of 3m and a peak period of 15s.

This condition deteriorates further when the model is tested at a forward speed; the simulation time could be over 100 hours. Therefore, all the tests were carried out in the linear mode and analysed accordingly. However, several checks were made by comparing many of these simulations with one that was tested in the nonlinear mode.

The two results of an identical sampled simulation in linear and nonlinear modes in a quartering sea are shown in Figures 5.7 & 5.8. The patterns and frequencies detected are similar, but the magnitude has been amplified considerably in the linear mode. However, there are some oscillations close to the roll natural frequency in the linear mode, which have been reduced in the nonlinear mode because of changes in scale (see Figure 5.7).

5.8.3 The Effect of Changing Parameters

Setting up the various parameters to be used in running a simulation might have a detrimental effect on the interpretation and efficiency of the final outcome. To investigate the effects of different parameters on the results of the simulation, the numbers of panels changed from 6 to 40, and the step sizes for the numerical calculations modified from 0.5s to 0.1s.

In comparison, the results that are illustrated in Figure 5.9 & 5.10 do not indicate any significant changes. There is a slight change in the magnitudes of the motion responses whereas the distributions in heave and pitch remain identical. For the roll motion, the energy distribution is more scattered around the natural frequency in Figure 5.10, which justifies the reduction of the maximum magnitude for the equal amount of energy. It seems that roll in Figure 5.10 is a better representative as it has been computed more accurately, however the simulation time was 5 times larger.

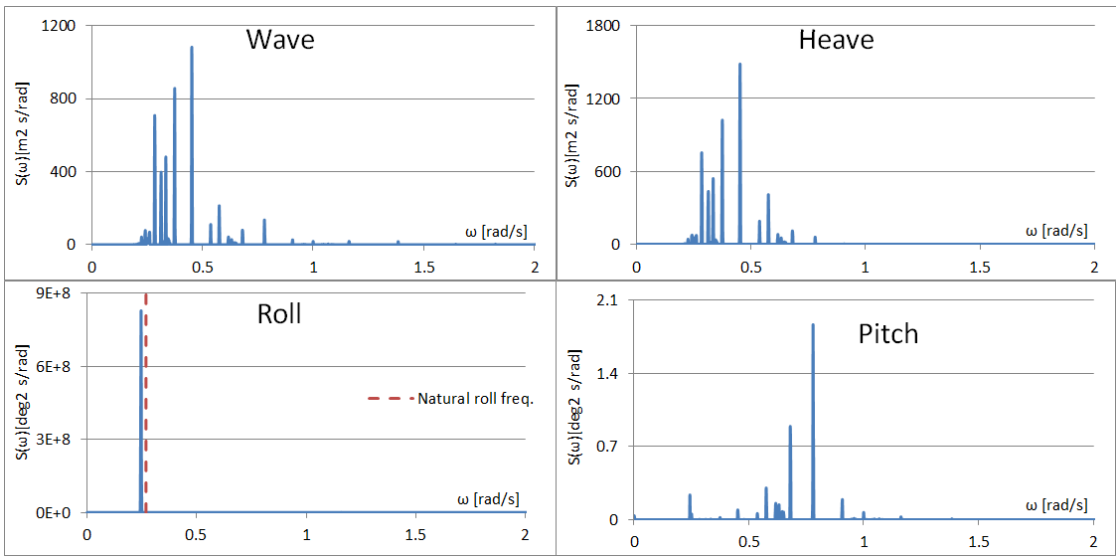

Figure 5.9 Linear results of incident wave and motion responses in the frequency domain. The simulation is conducted in beam seas, at zero speed with Hs of 6m and a peak period of 20s. The number of panels is 6 with a time step of 0.5s.

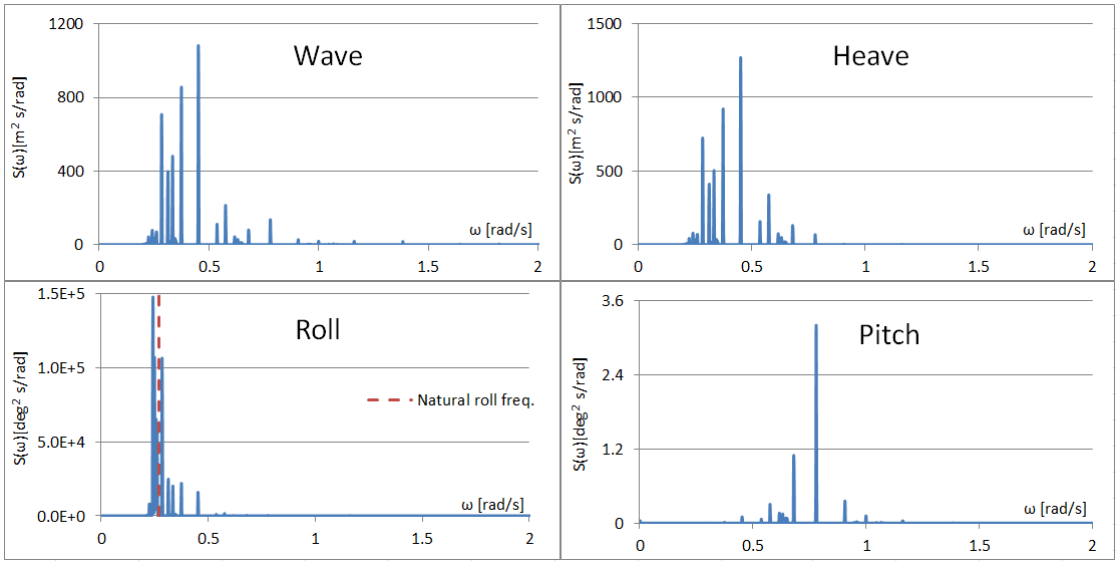

Figure 5.10 Linear results of incident wave and motion responses in frequency domain. The simulation is conducted in a beam sea, at zero speed with Hs of 6m and a peak period of 20s. The number of panels is 40 with a time step of 0.1s.

5.9 Presentation of the Results

Each of the figures in this section is in two parts: the right-hand side demonstrates the peak frequencies of the three motions responses (heave, pitch and roll) as well as the incident waves in the three different sea conditions of high, medium and low. The sea conditions are related to the wave-frequency of propagation. The simulations are carried

out in triplicate according to the significant wave height (Hs) being small, medium or large.

The left-hand side of the figures demonstrates the magnitudes of the peak power computed by the power spectral density (PSD) in the same sea conditions as described above for the right-hand side. Two different vertical axes are given for the different units employed, which are explained in "simulation conditions" Section 5.8.1.

In order to compare the distributions of identified peak powers of every ship's motions and the wave, the dot plots are used along with every set of simulation results. In this type of plot, Minitab (Minitab, 2012) displays a dot for each observation of peak power that was recorded during the simulation. Where synchronous rolling occurs in any sea condition then the roll magnitude suddenly magnifies and the peak power increases. Therefore, the intervals between the dots in this form of diagram are a good indication of where the peak frequency of the wave spectrum gets closer to the roll natural frequency and thus a large roll is to be expected.

For a better comparison, a dot plot was chosen in groups and thus the attention was brought on the distribution rather than on the identified values. The intention here is to illustrate where synchronous rolling occurs. However, care should be taken to read these diagrams along with the corresponding graphs, showing the quantitative magnitude values.

5.9.1 Following Seas

At a stationary condition in following seas, the peak frequency of both heave and pitch motions track the wave peak frequency, whereas roll oscillates around its natural frequency as depicted in Figure 5.11. Roll is less sensitive to high frequency waves, and hence its magnitude as evaluated by the power peak appears to be very low. However, when the wave peak frequency is getting close to the roll natural frequency, the power peak becomes extremely high, which is an indication of synchronous rolling. The power peak of the roll at the low frequency is on average 27 times as large as a medium sea condition.

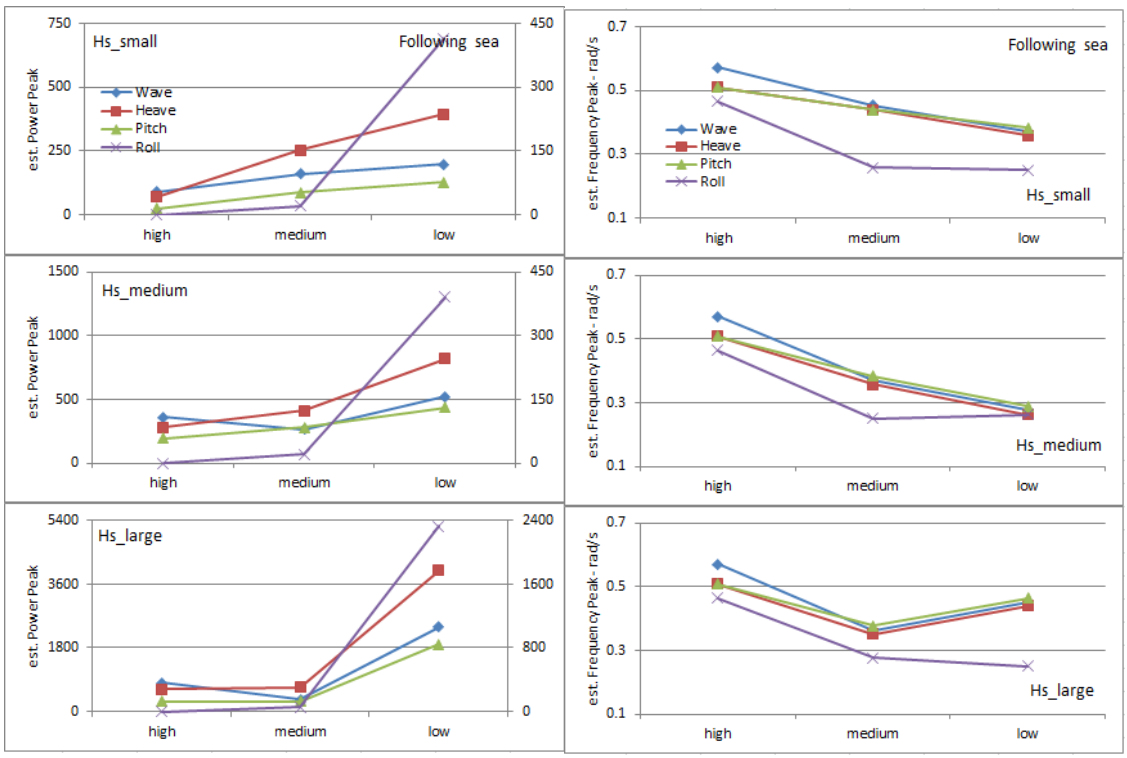

Figure 5.11 Identified Peak magnitudes and peak frequencies of incoming waves and motions responses at zero speed in following seas; tested at different sea conditions and a range of Hs.

There is seen to be a considerable increase in the roll magnitude as the significant wave height gets larger (left-hand of figure 5.11), but the significant wave height does not have a great influence on the peak frequencies.

This simulation test can also reasonably represent a condition where the following seas wave celerity is the same as ship's speed, where we may expect broaching to possibly occur.

A dot plot of the peak magnitudes of the wave and motion responses is shown in Figure 5.12. The dots on the left are at the high frequency level and shift towards the right through medium then to low frequencies. The intervals between dots of the terms of each category demonstrate if the motion response is linear with regard to the incident wave. The sudden increase in the interval between the roll-motion dots from medium to low frequency is an indication of synchronous rolling, which occurs as the wave frequency approaches natural roll frequency. This condition is maintained while the sea condition changes from small to medium and then to large Hs values.

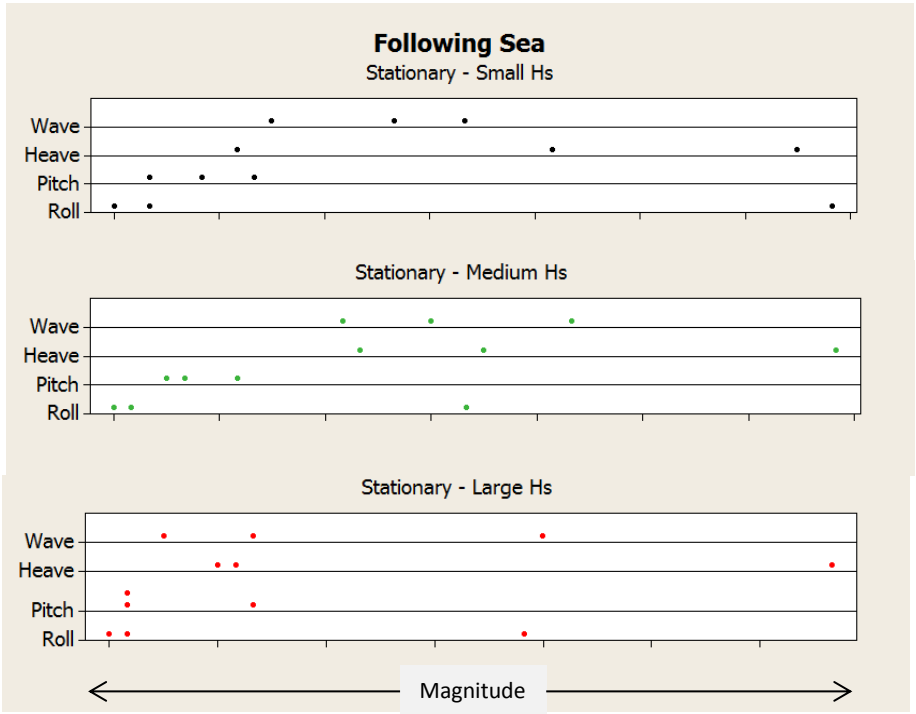

Figure 5.12 Dot plots of peak magnitudes of the wave and motion responses in the following sea at a stationary vessel condition.

The roll motion remains less sensitive to response in the high sea conditions as depicted in Figure 5.13, which is tested at forward speed of 5m/s. The results for the power peak at every Hs value, depicted in the left-hand figures, clearly confirm the insignificance of the roll motion contribution at a higher frequency level. This is the kind of response expected for the roll motion in the following seas under these conditions.

However, the roll power peaks increase considerably at low frequency levels whilst being closer to the incident wave frequency. Both of the heave motion and the pitch motion peak frequencies are shown to track the encountered wave peak frequency as shown in Figure 5.13. The corresponding estimated power peaks of the heave and the pitch increase through high and then to low sea conditions, and from a small to large Hs value.

The results of the dot plots shown in Figure 5.14 are for the simulation tests at a forward speed of 5m/s. The intervals between the dots for the wave, the heave and the pitch remain fairly uniform, whereas for the roll magnitude dots there is a significant jump through a medium and then a high sea condition which is due to the synchronous rolling.

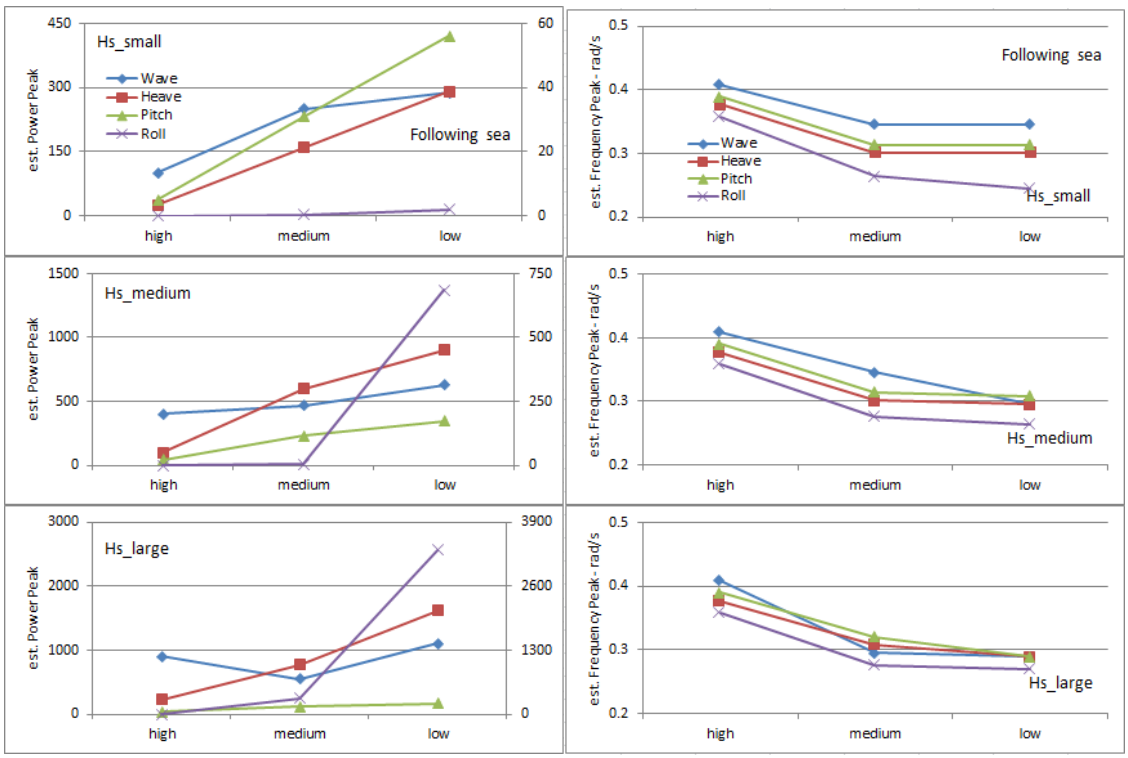

Figure 5.13 Identified Peak magnitudes and peak frequencies of incoming waves and motions responses at forward speed of 5m/s in following seas; tested at different sea conditions and range of Hs.

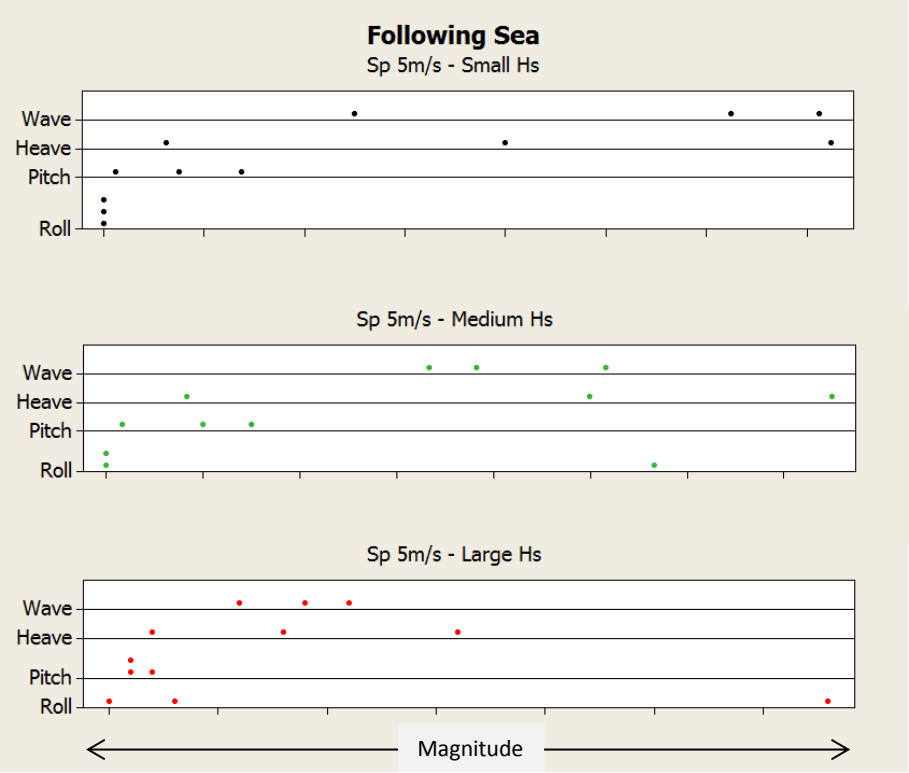

Figure 5.14 Dot plots of peak magnitudes of the wave and motion responses in the following seas with forward speed of 5m/s.

The magnitude of the roll motion has significantly reduced at the higher speed in the following sea as shown in Figure 5.15. In this simulated test, the variations in the heave and the pitch motion magnitudes are not significant in comparison with the similar tests at the lower speed, despite the fact that the encountered wave magnitudes become larger. The peak frequencies of all three motions appeared not to be reliable at the high speed as the ship is riding on the waves. It is clearly shown in Figure 5.15 that detected peaks for all the motions including the incident waves are similar.

The intervals of the dot plots for the wave, the heave and the pitch magnitudes are fairly uniform as depicted in Figure 5.16, and there is no any evidence to indicate the presence of the synchronous rolling to occur.

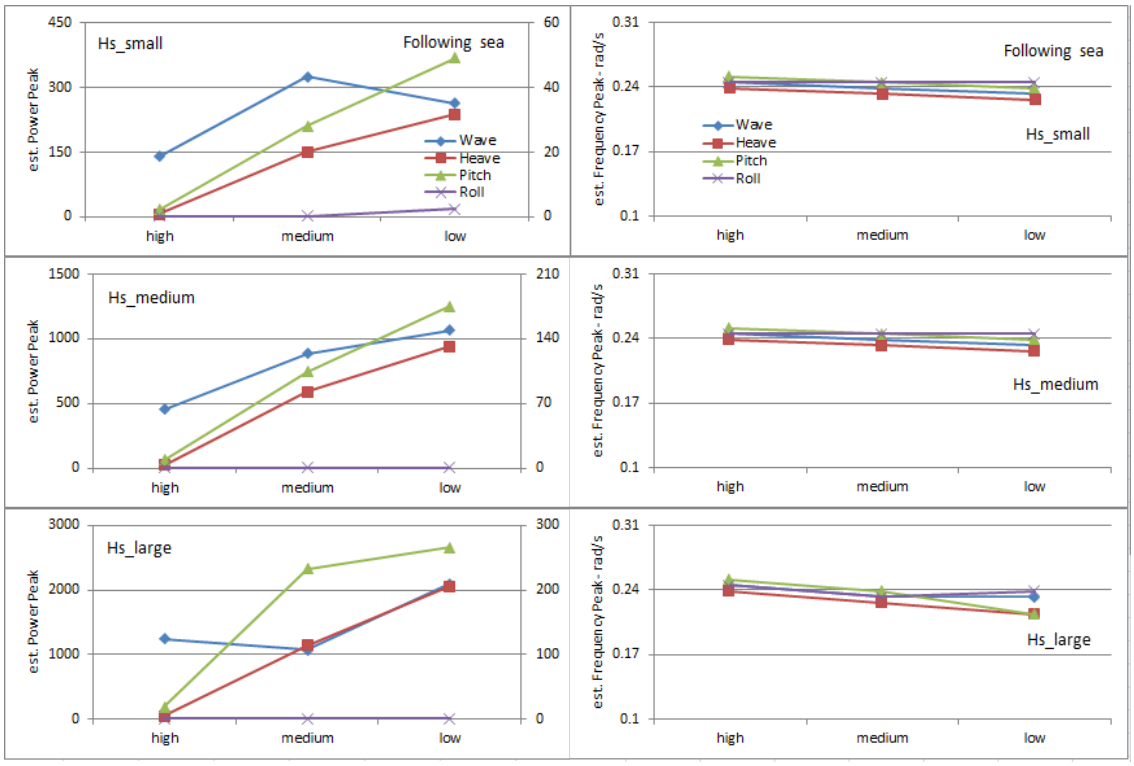

Figure 5.15 Identified Peak magnitudes and peak frequencies of incoming waves and motions responses at forward speed of 10m/s in following seas; tested at different sea conditions and range of Hs.

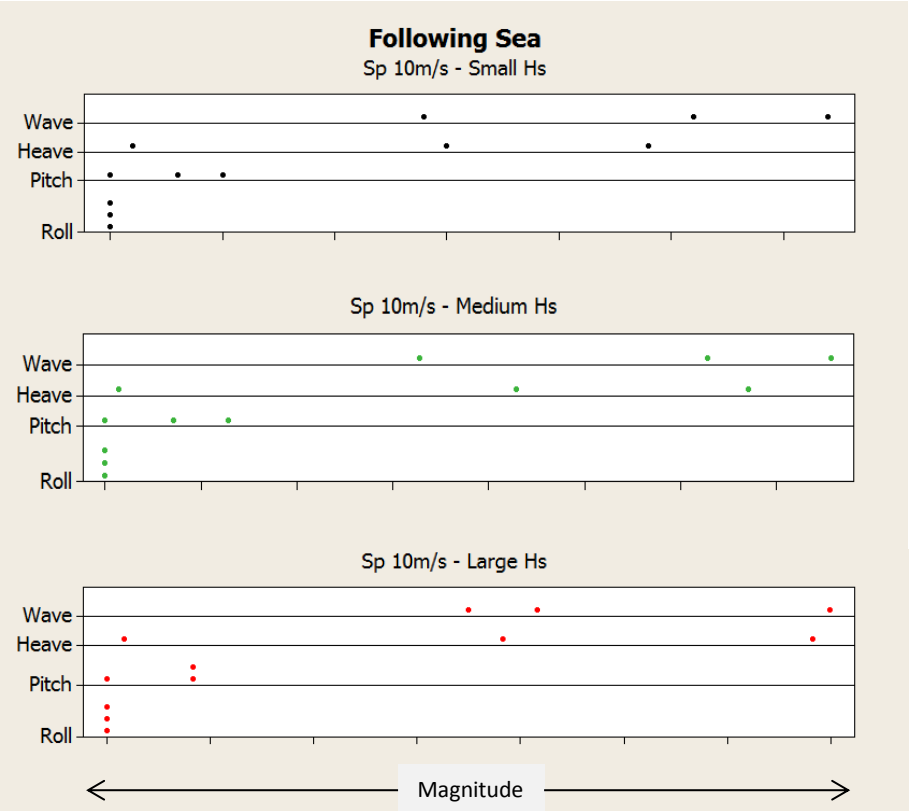

Figure 5.16 Dot plots of peak magnitudes of the wave and motion responses in the following sea with a forward speed of 10m/s.

5.9.2 Quartering Seas

The sensitivity of the roll motion in response to the high-frequency waves is similar to the following sea as shown in Figure 5.17. The associated magnitudes at high frequency are so small that they can practically be ignored. However, through medium and then to low frequency, the roll is oscillating around its natural frequency excessively, therefore the power peaks in Figure 5.17 show a sudden increase in the roll magnitudes. It is clear that the maximum oscillation occurs when the wave's peak frequency approaches the natural roll frequency.

The peak frequencies of both the heave and the pitch track the peak frequencies of the incident wave as depicted in Figure 5.17, yet their corresponding magnitudes behave in a similar manner.

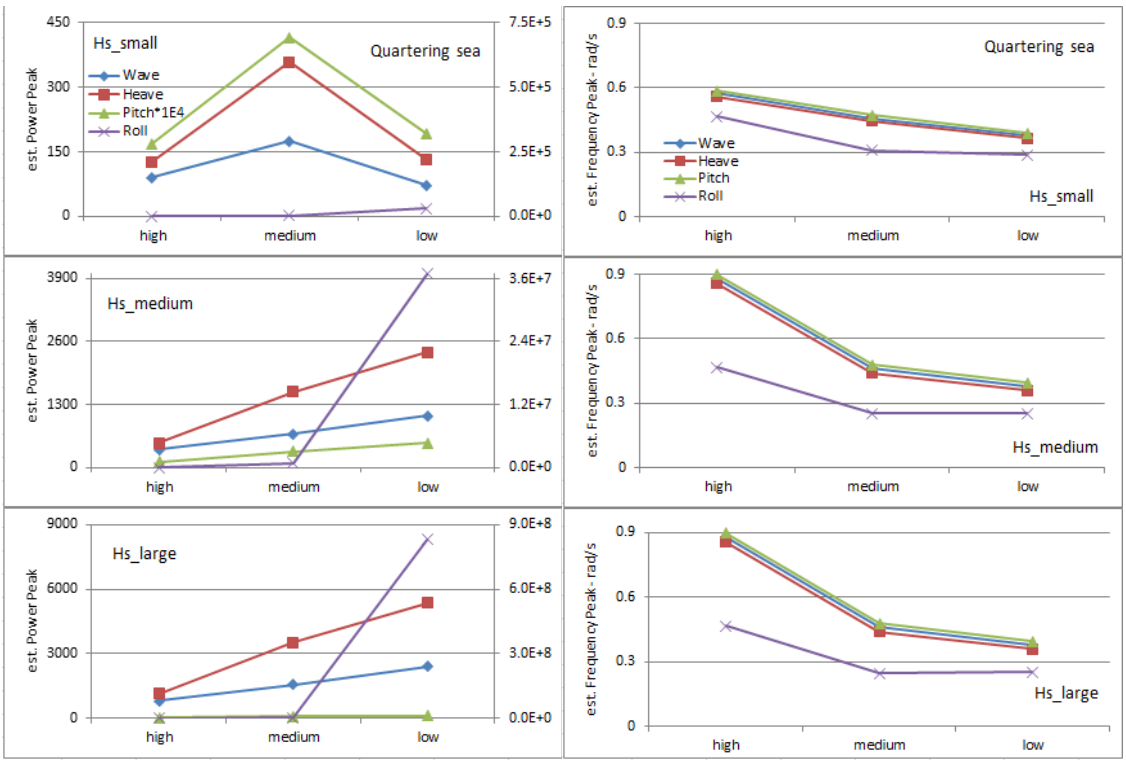

Figure 5.17 Identified Peak magnitudes and peak frequencies of incoming waves and motions responses at zero speed in quartering seas; tested at different sea conditions and range of Hs.

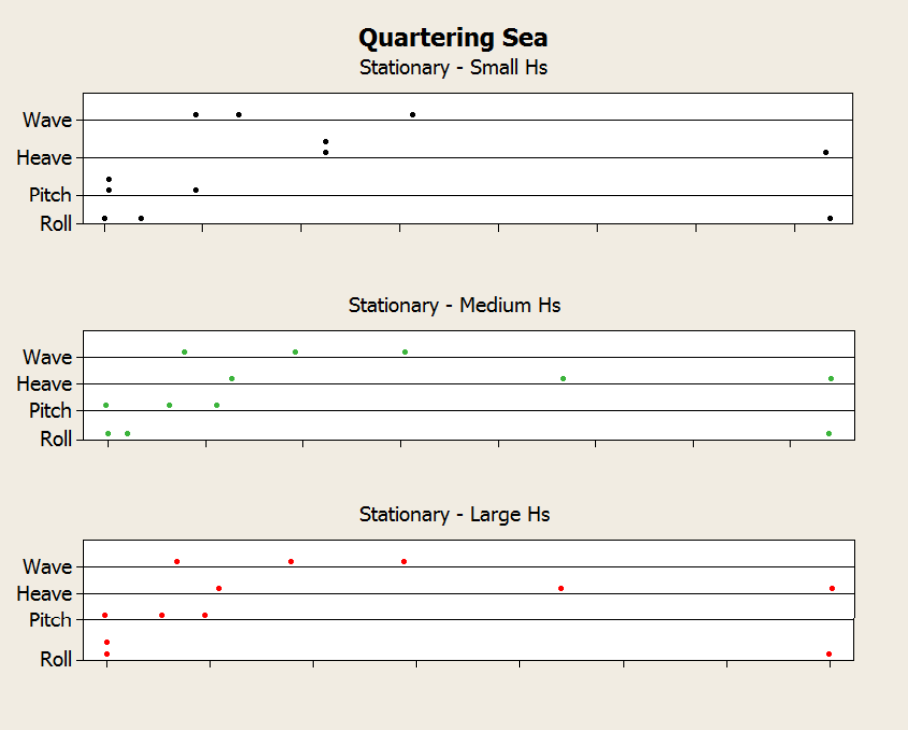

Figure 5.18 Dot plots of peak magnitudes of the wave and motion responses in the quartering seas at stationary condition.

The dot plots of the peak power magnitudes of the first set of tests in this section are shown in Figure 5.18. The intervals between the dots in the terms of each category clearly demonstrate the excessive oscillation of the roll motion between moderate to low frequency waves. What is apparent in Figure 5.18 is the response of the heave and the pitch motions, where their corresponding dot intervals are more consistent with the variation of incident wave dots.

Similar comments apply to the results of the simulations presented in the Figures 5.19 to 5.22. However, the large power peaks of the incident waves at high sea conditions shown in Figure 5.21 are unusual and thus not reliable.

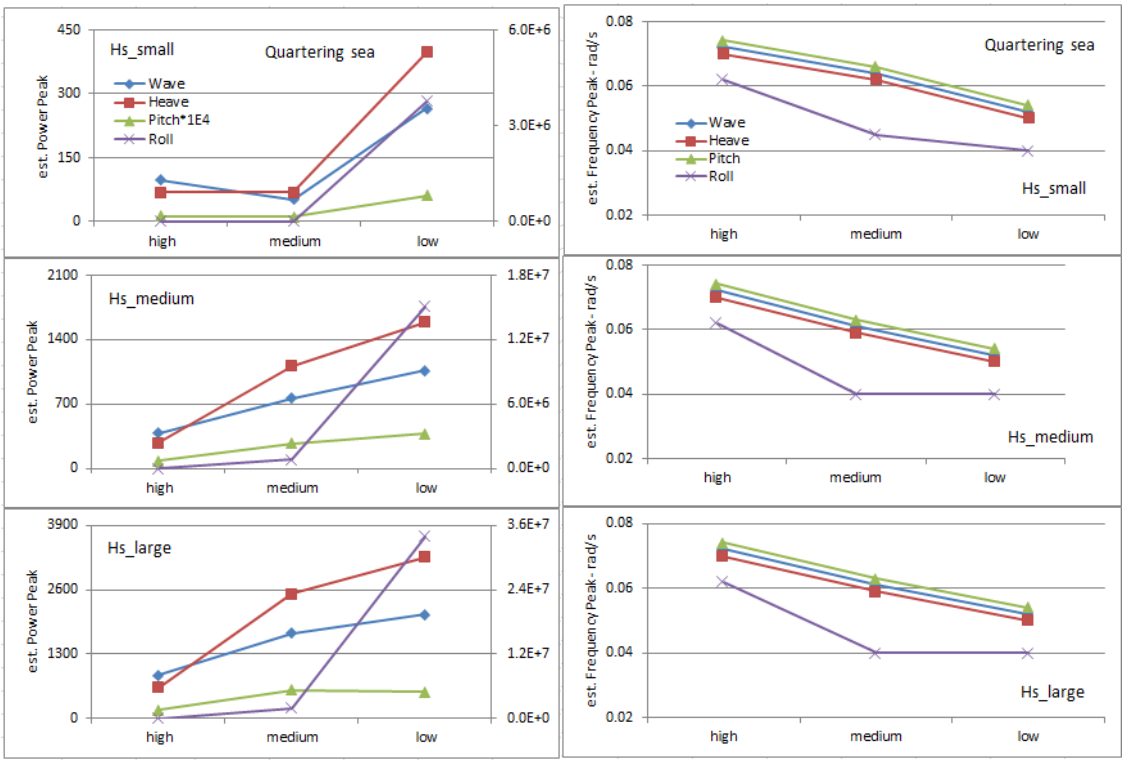

Figure 5.19 Identified Peak magnitudes and peak frequencies of incoming waves and motions responses at forward speed of 5m/s in quartering seas; tested at different sea conditions and range of Hs.

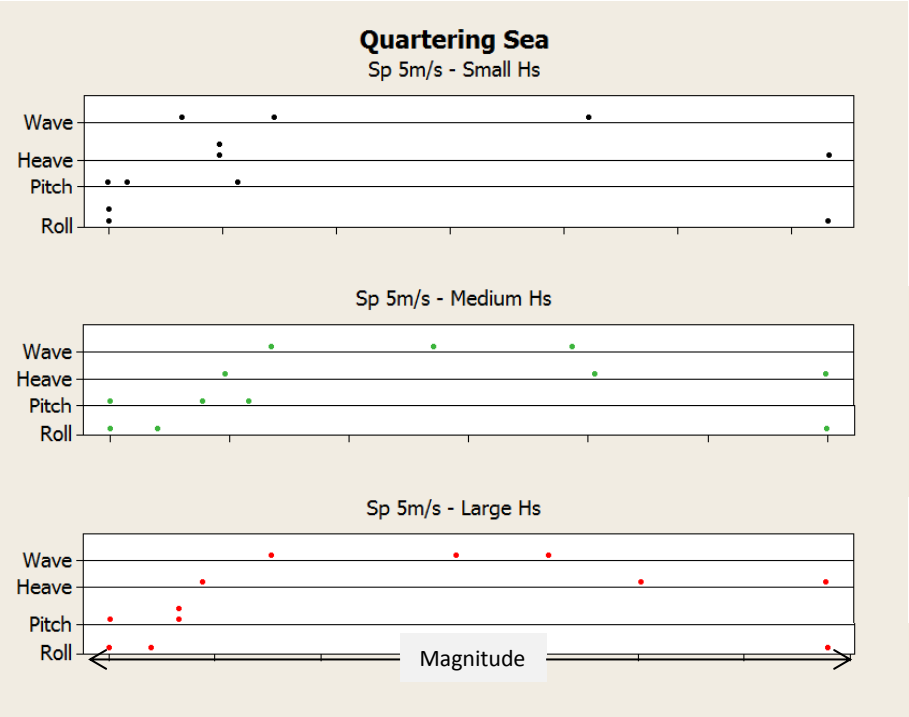

Figure 5.20 Dot plots of peak magnitudes of the wave and motion responses in the quartering seas with a forward speed of 5m/s.

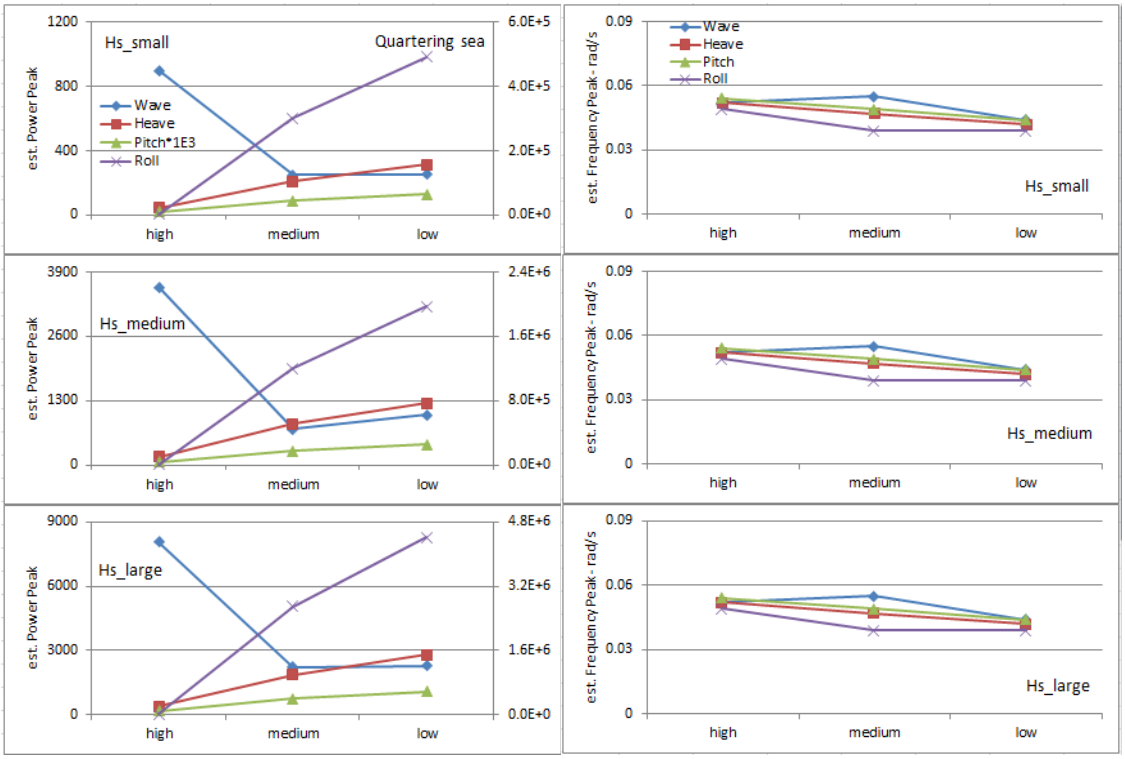

Figure 5.21 Identified Peak magnitudes and peak frequencies of incoming waves and motions responses at a forward speed of 10m/s in quartering seas; tested at different sea conditions and range of Hs.

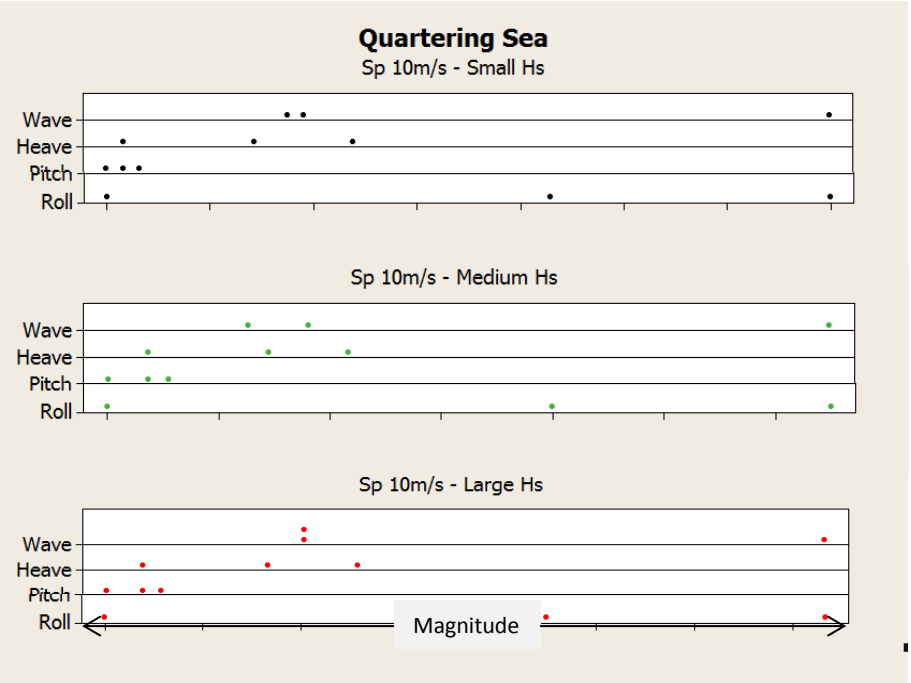

Figure 5.22 Dot plots of peak magnitudes of the wave and motion responses in the quartering sea with a forward speed of 10m/s.

5.9.3 Beam Seas

In the beam sea condition all the motion responses are very much dominated by the roll motion. The peak frequency of the heave motion tracks the incident wave peak frequency in a stationary vessel condition at every Hs values as shown in Figure 5.23. However, the pitch motion responses do not follow the same pattern as of the wave peak frequencies that have been experienced in the following and the quartering seas. The magnitudes of the pitch motions are so low that it makes it impossible for them to be considered effectively for use in further applications. This is a behaviour that is expected for the pitch motion when the ship encounters the waves in a beam sea.

The roll motion maintains its oscillation around its natural frequency except at high frequency waves, where the wave energy is not significant, as depicted in Figure 5.23. The results of the left-hand side of the Figure 5.23 clearly show the sudden increase of power peaks when the sea condition shifts towards the right through medium then to low frequencies.

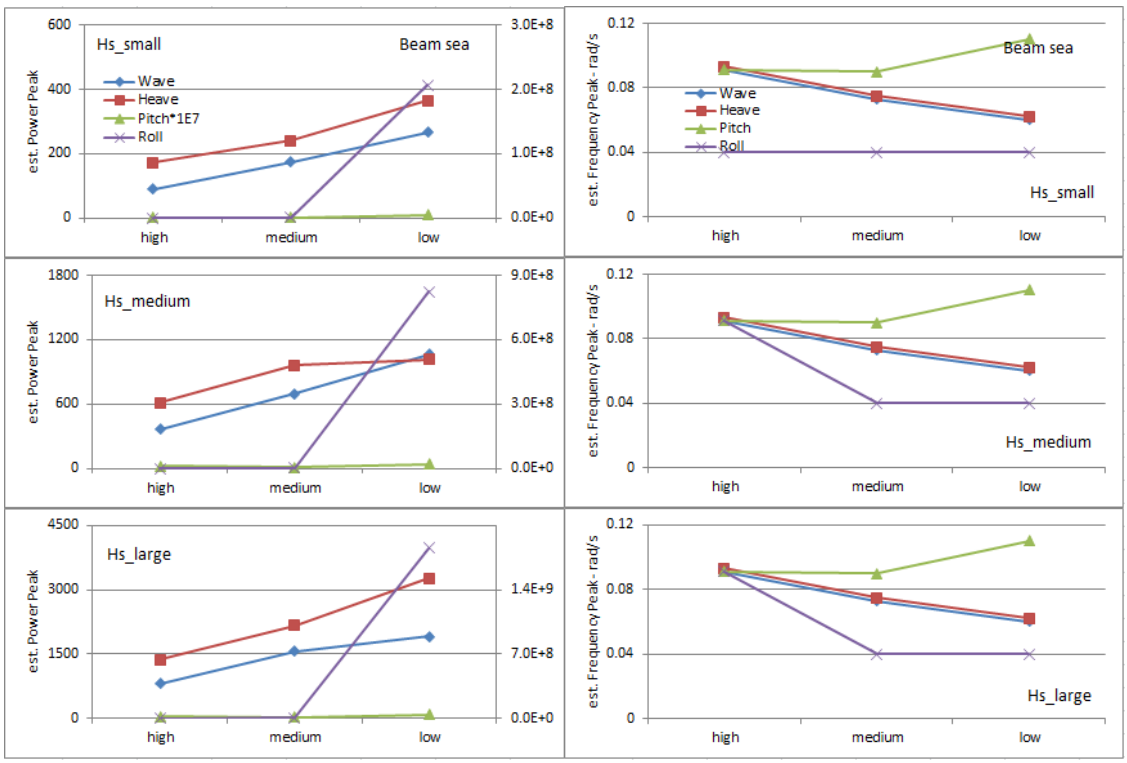

Figure 5.23 Identified Peak magnitudes and peak frequencies of incoming waves and motions responses at zero speed in beam seas; tested at different sea conditions and range of Hs.

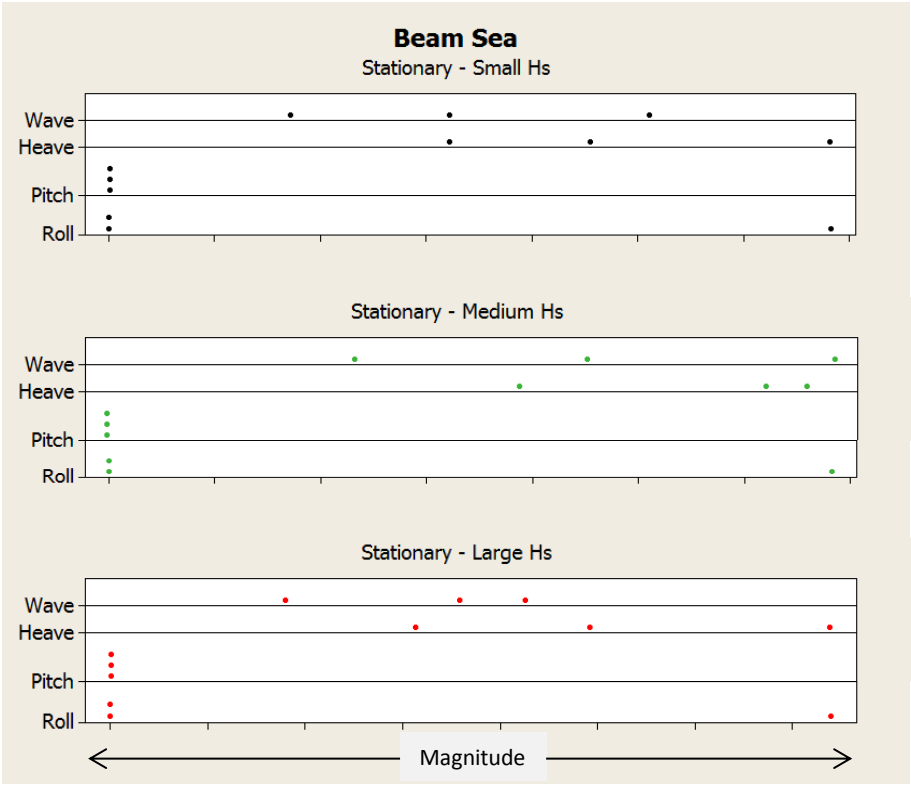

Figure 5.24 Dot plots of peak magnitudes of the wave and motion responses in the beam seas at stationary conditions.

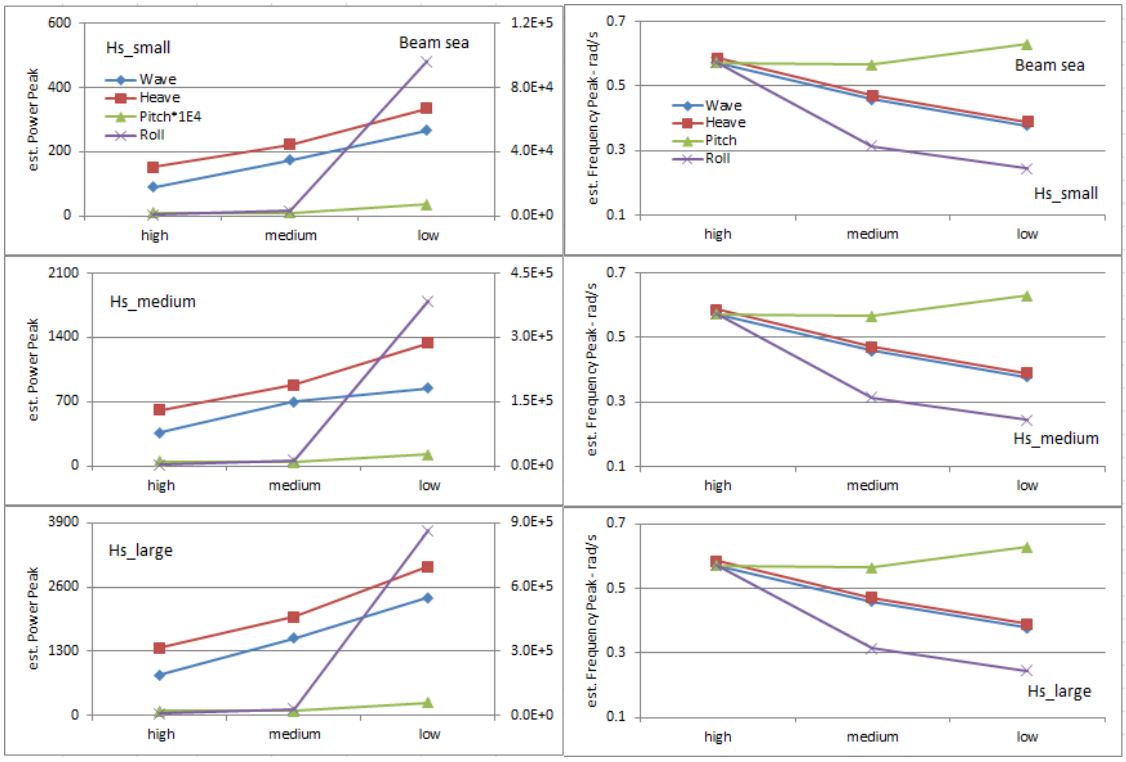

Figure 5.25 Identified peak magnitudes and peak frequencies of incoming waves and motions responses at forward speed of 5m/s in beam seas; tested at different sea conditions and range of Hs.

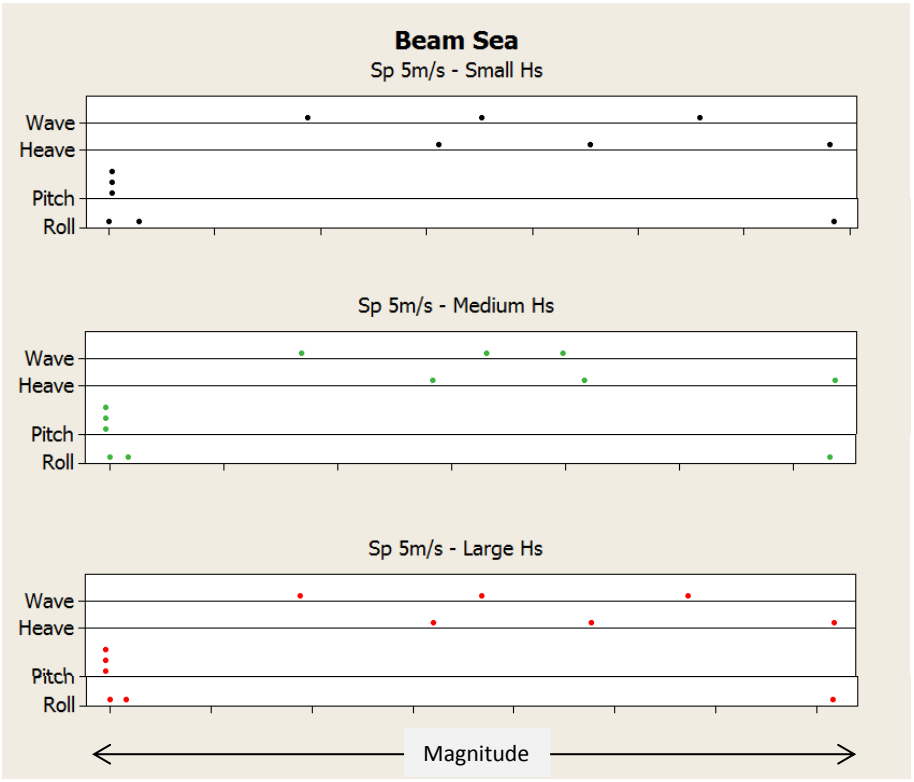

Figure 5.26 Dot plots of peak magnitudes of the wave and motion responses in the beam seas with a forward speed of 5m/s.

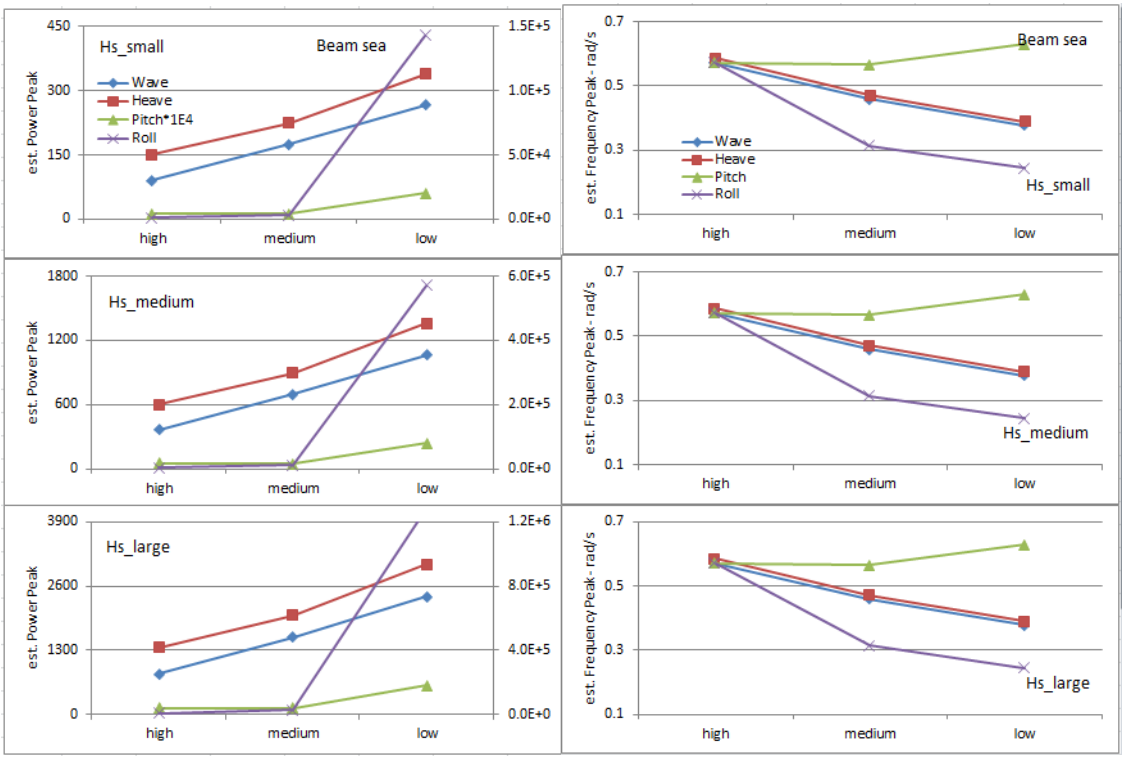

Figure 5.27 Identified peak magnitudes and peak frequencies of incoming waves and motions responses at forward speed of 10m/s in beam seas; tested at different sea conditions and range of Hs.

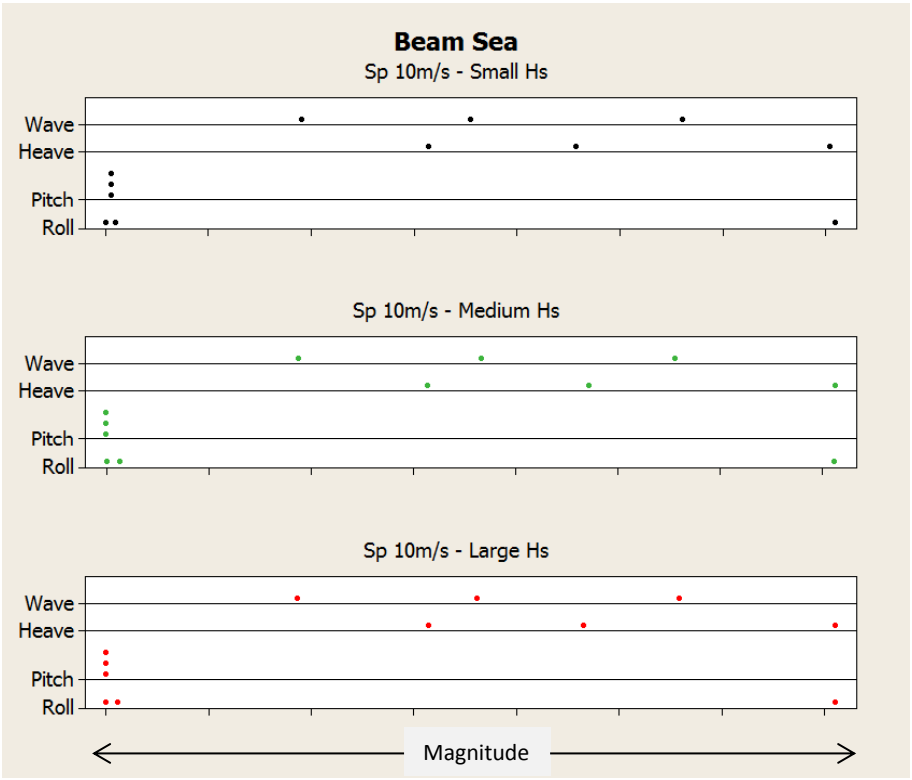

Figure 5.28 Dot plots of peak magnitudes of the wave and motion responses in the beam seas with forward speed of 10m/s.

The intervals between the dot plots of the incident wave and the heave motion are fairly uniform and illustrate that the heave motion tracks the wave, which is depicted in Figure 5.24. The dot intervals of the pitch motion magnitudes reflect pitch contribution as being insignificant at beam sea condition, whereas the dot intervals of the roll motion illustrates the synchronous rolling at medium to low sea conditions at every Hs value.

Similar comments apply to the results of the simulations presented in the Figures 5.25 to 5.28.

5.9.4 Bow Seas

In the bow sea, the oscillations of the roll motions are very consistent around its natural frequency even with high-frequency waves as shown in Figure 5.29. The peak frequencies of both the heave and the pitch motions steadily follow the incident wave peak frequency at a stationary condition and at every Hs value.

The corresponding heave and pitch power peaks shown in Figure 5.29 (left-hand) are also consistent in steadily following the incident wave power peaks in a relatively linear mode. The significant variations in the roll power peaks through medium and then to low sea conditions is an indication of synchronous rolling, when incident wave peak frequency approaches the natural roll frequency of the vessel.

Similar comments apply to the results of the simulations presented in the Figures 5.31 and 5.32. However, the roll motion is less sensitive at high frequency in these diagrams and its magnitude is not significant.

There are seen to be differences in the results depicted in the Figure 5.33 at the higher speed of 10m/s. The roll motion peak frequency appears to mimic the encountered wave peak frequency rather than oscillating at its natural frequency.

It can also be seen through the graphs drawn in this section that magnitudes of both the heave and the pitch motions increase as the Hs value increases at every sea condition. The alteration of speed does not have a significant effect on the detected pattern of the heave and the pitch power peaks. The results obtained from analyses of the roll motion illustrate the large increase of power peaks due to synchronisation, which are magnified by the increase of Hs values. However, the roll motion magnitude declines with the increase of forward speed.

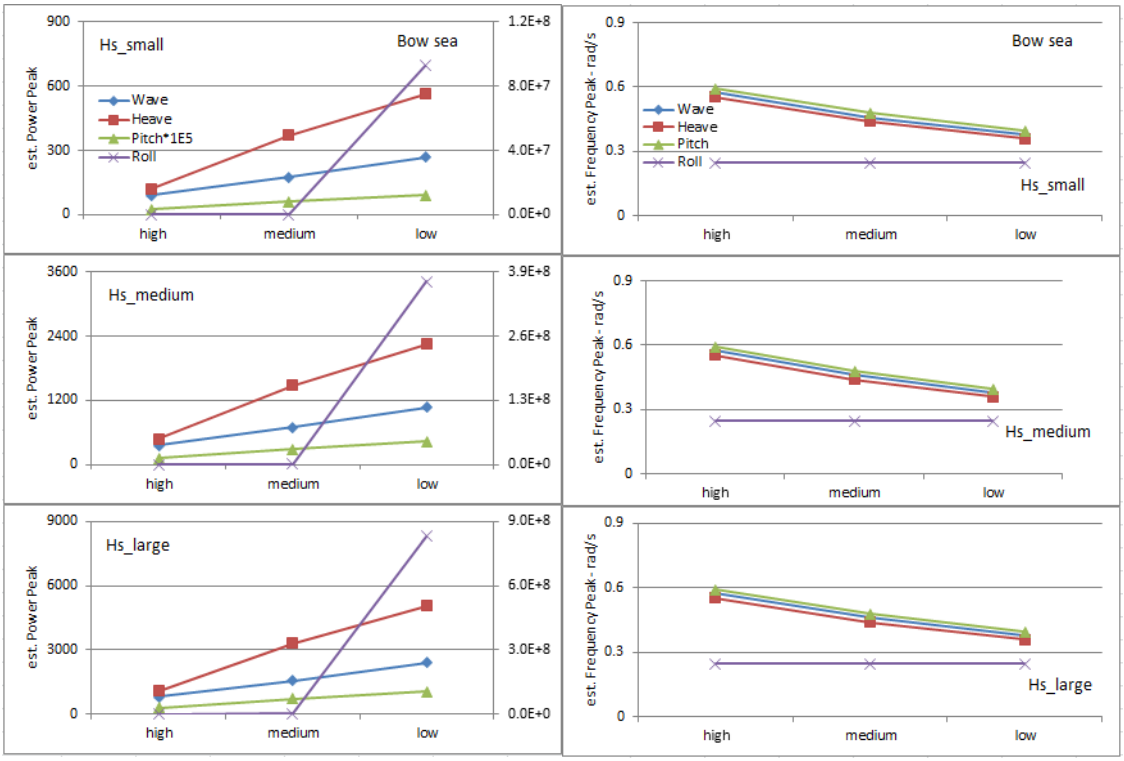

Figure 5.29 Identified peak magnitudes and peak frequencies of incoming waves and motions responses at zero speed in bow seas; tested at different sea conditions and range of Hs.

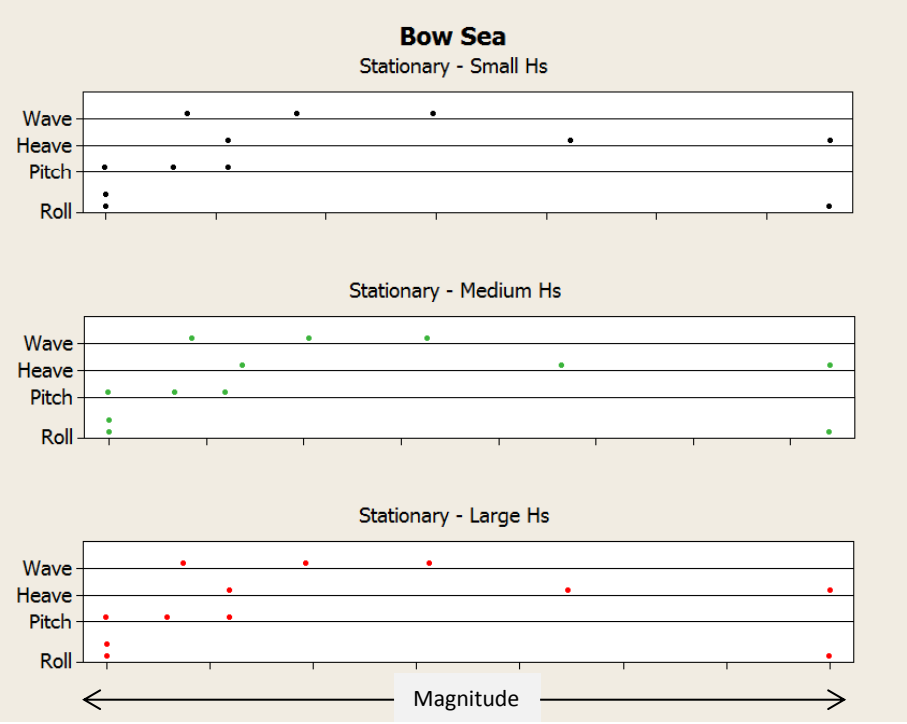

Figure 5.30 Dot plots of peak magnitudes of the wave and motion responses in the bow seas at a stationary condition.

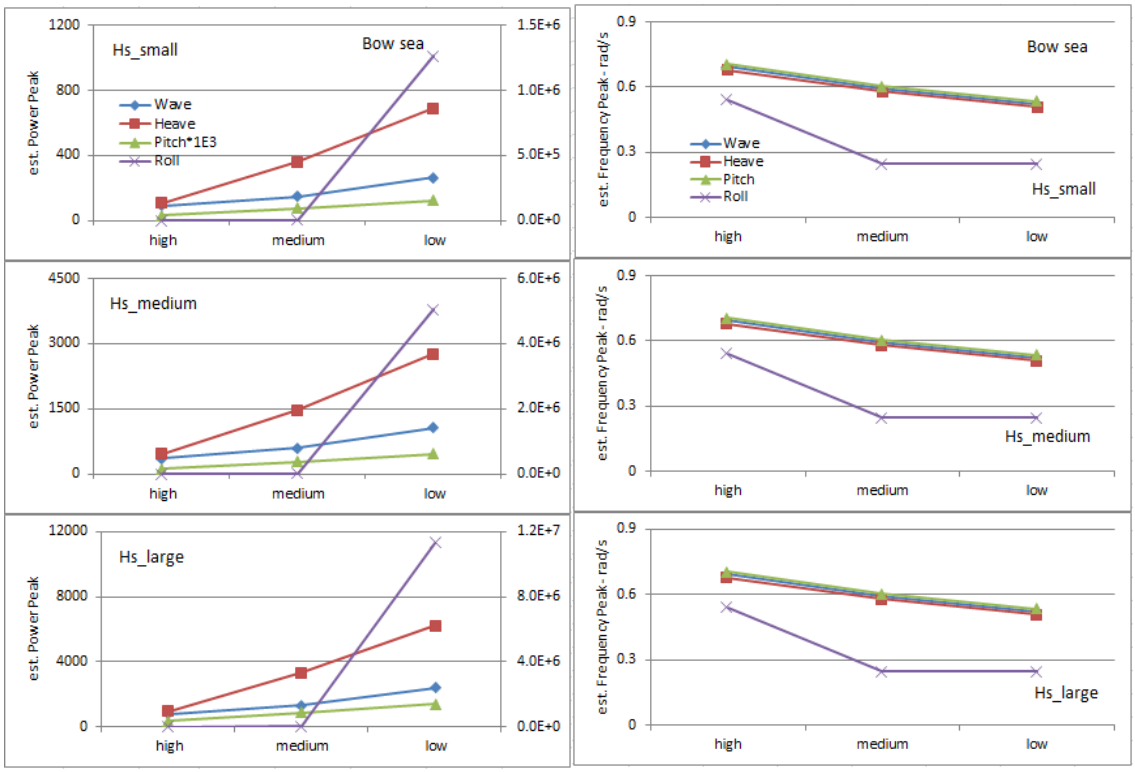

Figure 5.31 Identified peak magnitudes and peak frequencies of incoming waves and motions responses at a forward speed of **5**m/s in bow seas; tested at different sea conditions and range of Hs.

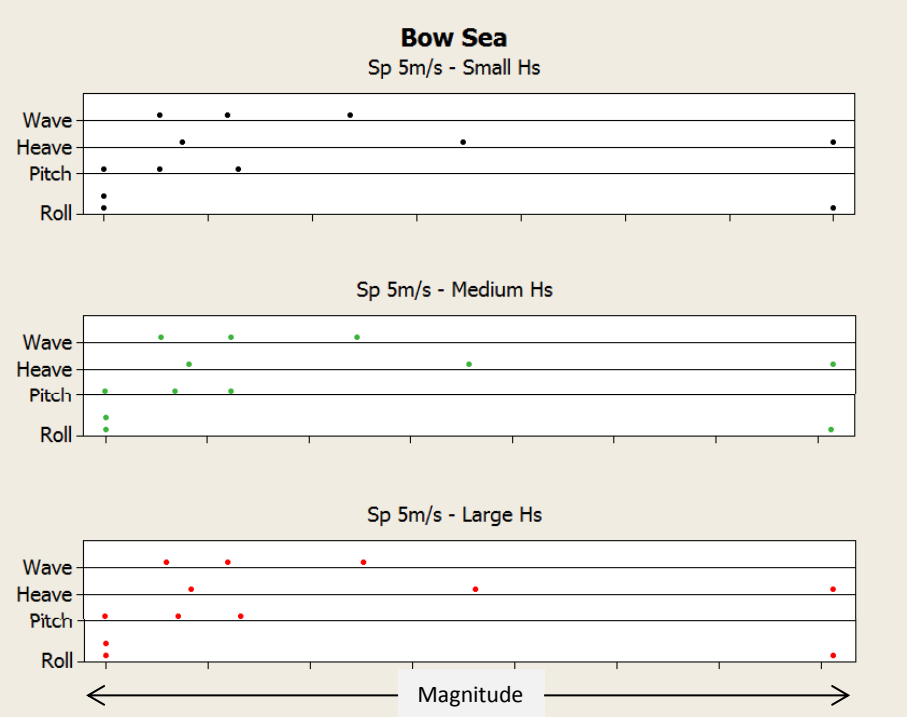

Figure 5.32 Dot plots of peak magnitudes of the wave and motion responses in bow seas with a forward speed of 5m/s

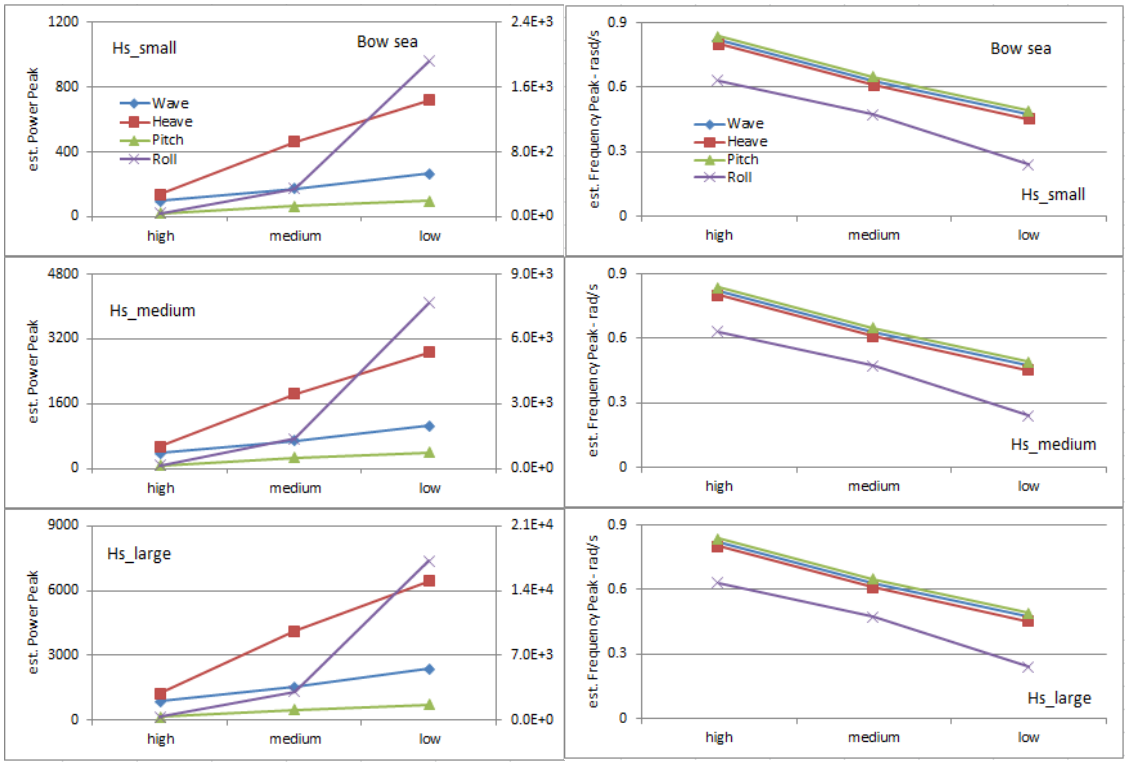

Figure 5.33 Identified peak magnitudes and peak frequencies of incoming waves and motions responses at forward speed of 10m/s in bow seas; tested at different sea conditions and range of Hs.

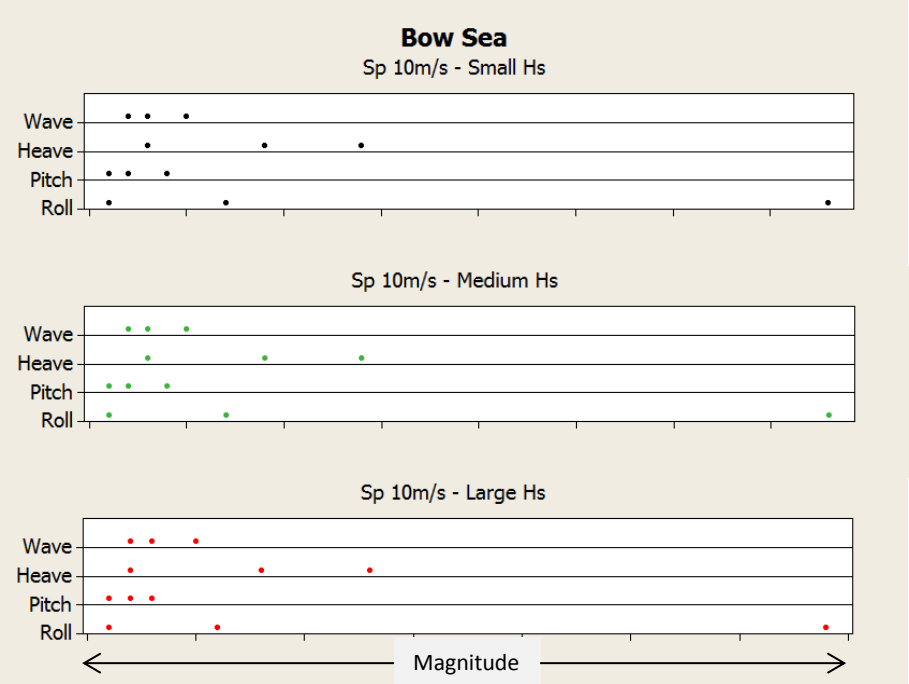

Figure 5.34 Dot plots of peak magnitudes of the wave and motion responses in a bow sea with a forward speed of 10m/s.

The intervals between the dot plots of the incident wave, the heave and the pitch are fairly uniform and support the above arguments that both the heave and the pitch peak frequency track the incident wave peak frequency, as depicted in Figure 5.30. There is seen to be synchronous rolling in the range between medium and low frequencies at every Hs value. The alteration of the forward speed has least effect on the behaviour of the roll motion obtained by simulation tests of bow seas.

5.9.5 Head Seas

The results of the simulation tests obtained from analyses of the motion responses in a head sea have some similarities with other simulations tested at stationary conditions. In Figure 5.35, the peak frequencies of both the heave and the pitch motions track the peak frequencies of the incident wave. The roll motion responses are also reasonably similar to those simulation tests carried out in other heading angles, being less sensitive at high-frequency waves.

The model ship behaves differently when forward speed is applied, where results are shown in Figure 5.37. The peak frequency of the heave and the pitch are in line with the roll motion peak frequency at a higher frequency level, however, the responses of the heave and the pitch motions are being altered to track the encountered wave at a lower frequency level. In the simulation tests at higher speed, the roll response is not distinguishable, and the peak frequencies of all three motions come in line with the encountered wave frequency as shown in Figure 5.39.

The trend in alterations of the wave, the heave and the pitch magnitudes are similar to the bow sea conditions explained in the last section. The roll magnitude becomes smaller and less significant as the forward speed increases.

The intervals of the corresponding dot plots shown in Figures 5.36, 5.38 and 5.40 illustrate quite clearly the linear modes of the wave, the heave and the pitch responses. These figures also show the importance of the effect of encountered waves on the roll motion responses, which are not significant.

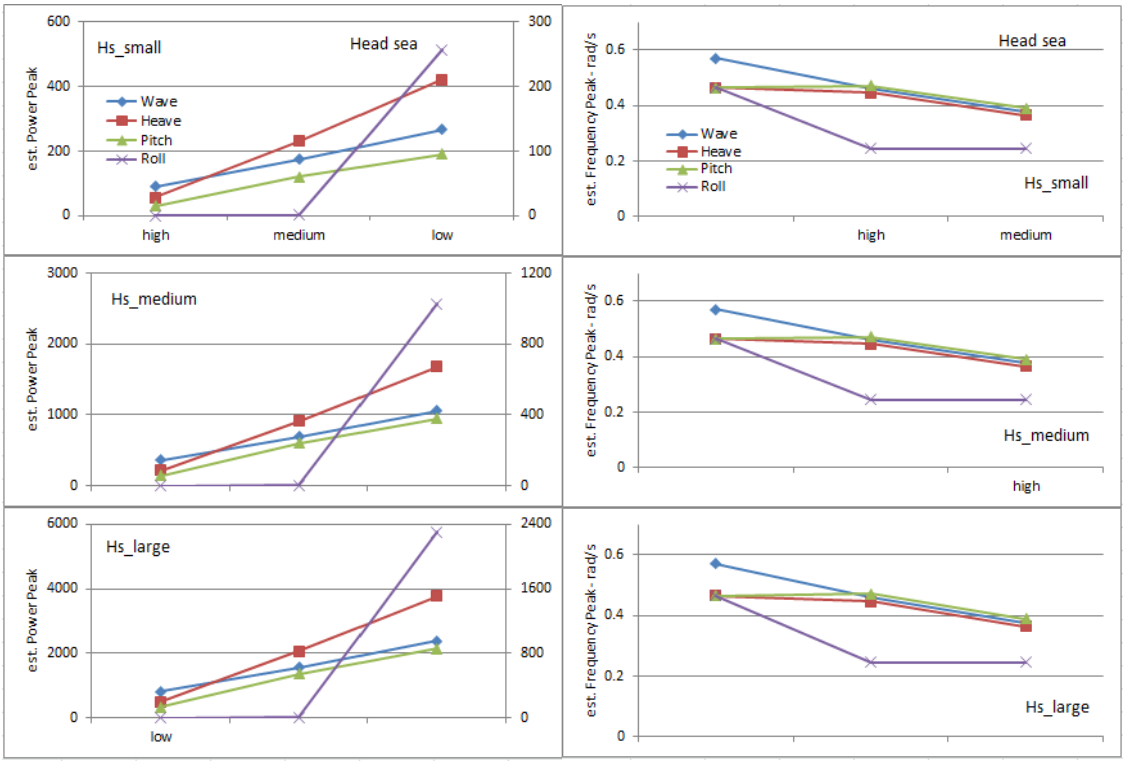

Figure 5.35 Identified peak magnitudes and peak frequencies of incoming waves and motions responses at zero speed in head seas; tested at different sea conditions and range of Hs.

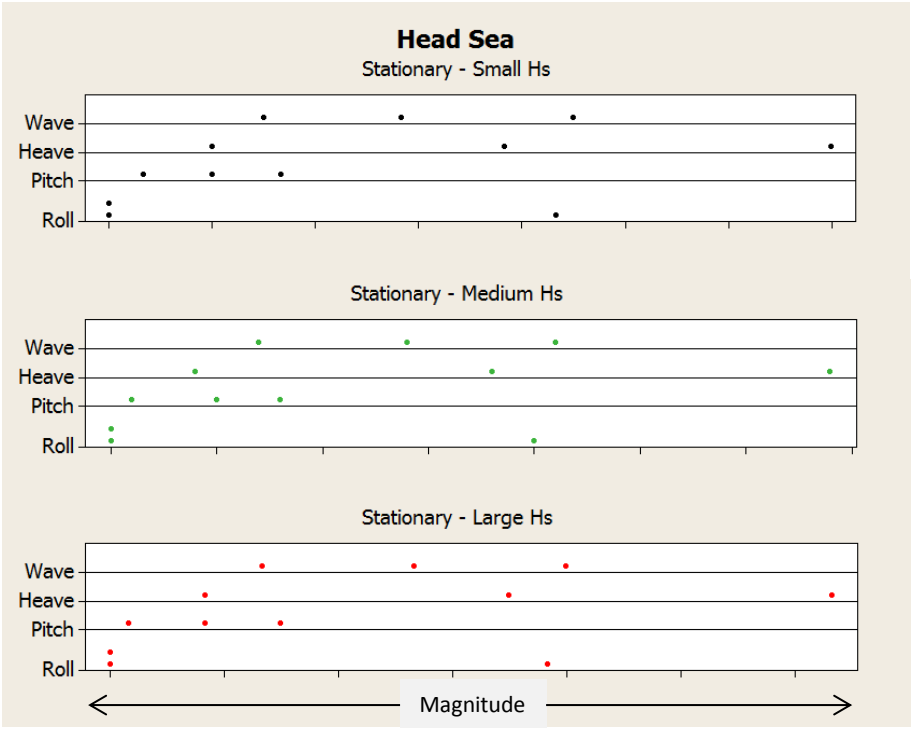

Figure 5.36 Dot plots of peak magnitudes of the wave and motion responses in the head seas at a stationary condition.

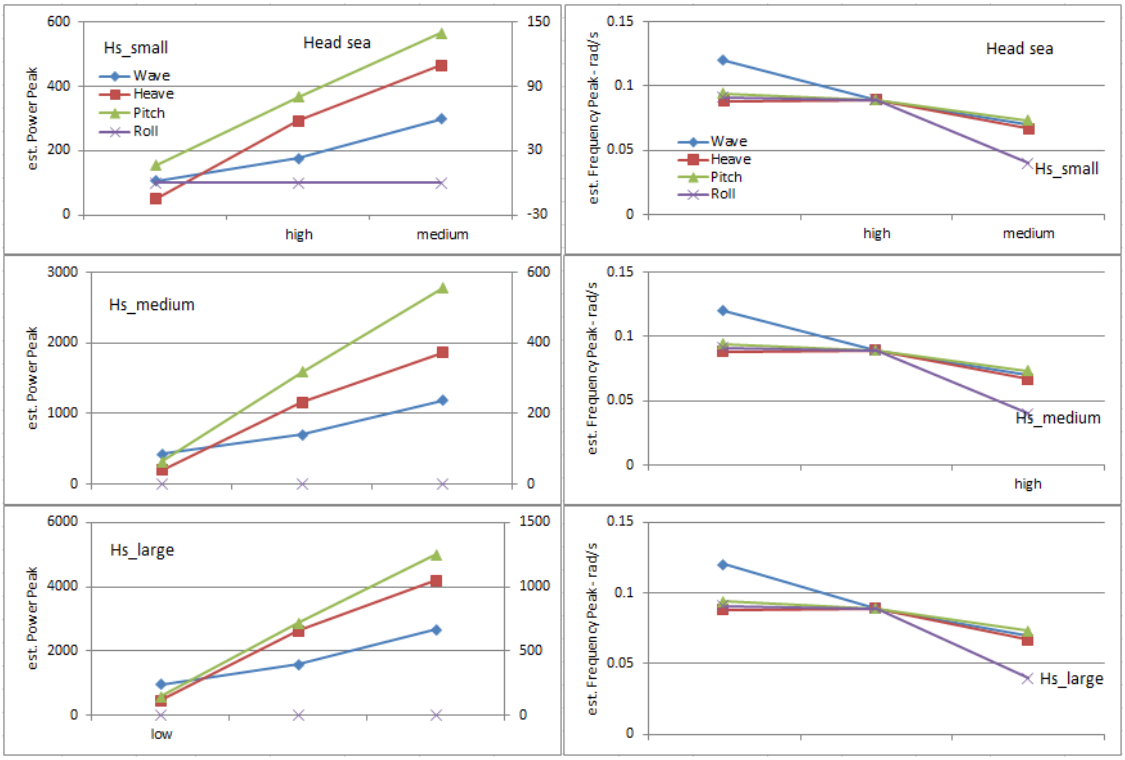

Figure 5.37 Identified peak magnitudes and peak frequencies of incoming waves and motions responses at a forward speed of 5m/s in head seas; tested in different sea conditions and range of Hs.

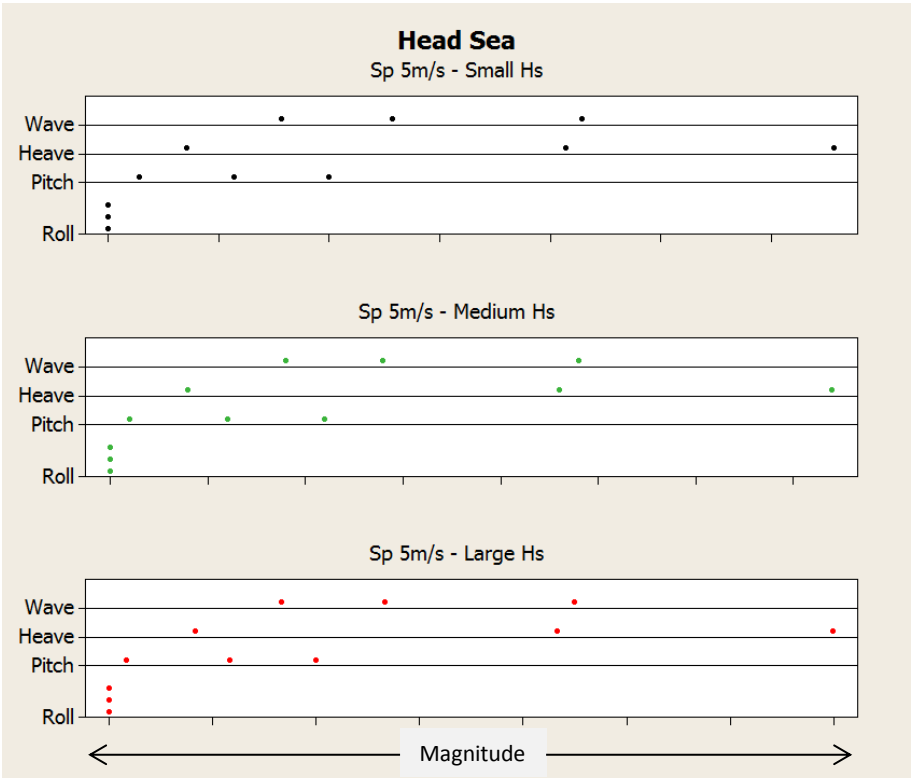

Figure 5.38 Dot plots of peak magnitudes of the wave and motion responses in the head seas with a forward speed of 5m/s.

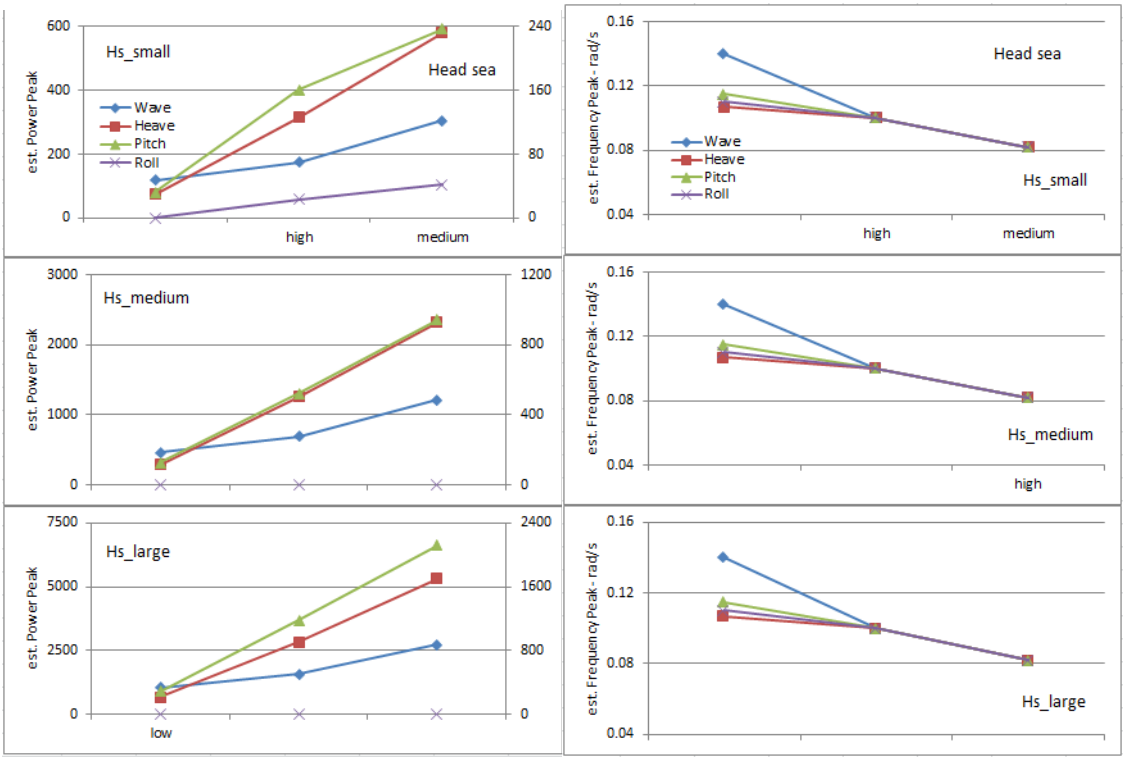

Figure 5.39 Identified peak magnitudes and peak frequencies of incoming waves and motions responses at a forward speed of 10m/s in head seas; tested at different sea conditions and range of Hs.

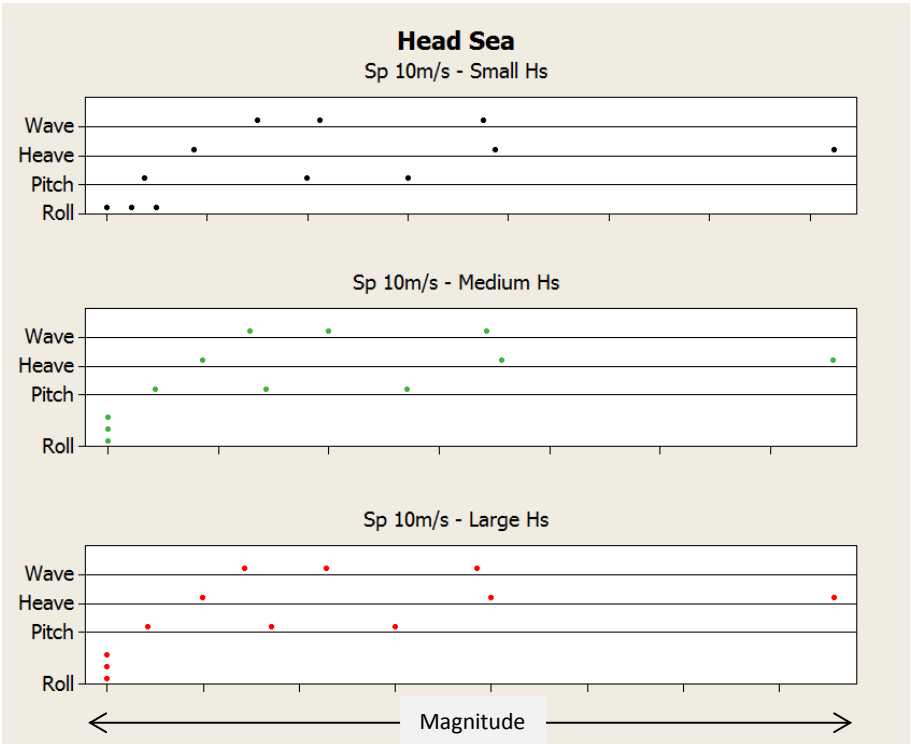

Figure 5.40 Dot plots of peak magnitudes of the wave and motion responses in head seas with a forward speed of 10m/s.

5.10 Summary

The detailed analyses that are presented in this chapter have shown that the motion behaviour of a ship under a progressively-changing sea condition is affected by a number of parameters, including the direction of travel, relative speed, significant wave height, significant wave period and natural rolling period. Some of these parameters have been shown to have a significant influence on the behaviour of the motion responses of the ship. A particularly important finding from the analyses concerns the influence of the peak frequency of the incident wave on the vessel's rolling motion. If these peak frequencies approach the roll natural frequency, then the magnitude of roll drastically increases towards the possibility of synchronous rolling.

The analysis procedures that have been followed in this chapter have also yielded some important insights with relevance to the analyses of the heave and pitch motion responses. Despite only a few simulations results, in the majority of cases they track the incident wave spectrum and present the same frequency pattern.

This approach can lead to the development of a real-time on-board modelling procedure to track the characteristics of a slowly varying sea state. Subsequently, monitoring of the changes could be used to warn in advance of the potentials of dangers that mariners are exposed to in that condition. It can lead to safer ship operations by providing ships' Masters with the necessary information for altering speed and/or heading in rough seas.

The outcome of this chapter has provided a great stimulus to study the ship motion behaviour through model testing in Chapter 6 and development of detection mechanism in Chapter 7.

Chapter 6

Model Testing

6.1 Introduction

Motion responses of a ship are an attractive method of assessing and comparing the performance of ships in a rough sea. Ship motions and the waves encountered are recorded simultaneously and are analysed using spectral analysis techniques. However, the waves are irregular, and without an accurate technique for recording them, the results obtained are unreliable estimates of the sea state. This becomes even more complicated when the ship is underway and the frequency of encounters changes.

There are two methods of predicting ship performance: computer modelling and traditional towing-tank testing with a model of a ship. Computer modelling, discussed in Chapter 5, has its drawbacks however. Fluid flow around a ship's hull is very complex, especially near the stern where the hull's shape changes rapidly, and in many cases the flow in this region is difficult to analyse. This often necessitates an alternative method of determining a ship's performance.

In this chapter, in addition to computer modelling, we will investigate the ship modelling and how full-scale ship performance can be predicted using models in a towing tank. Towing-tank testing of a ship model is the traditional method of understanding the nature of the ship hydrodynamics and the ship's behaviour in waves. Therefore a Roll-on/Roll-off model ship is chosen, having a greater variation of hull at both ends hence larger changes of water-plane area, which would be more susceptible to stability losses. However, in order for model test results and full-scale ship predictions to be useable, two fundamental relationships between the model and ship must be met: geometric and dynamic similarity.

A series of model tests were planned to be conducted in this chapter over the expected range of sea conditions. The main objective of these experiments is to estimate the wave-influential parameters through the motion responses of a hull, which can subsequently be generalised for other types of ship.

Six degrees of freedom motion response tests of a Ro-Ro model have been carried out in irregular waves under intact conditions. A stationary model was tested in different sea states in following, quartering and beam seas. The investigation was limited to the effect of encountered frequency components and associated magnitude of energy of the ship's motion responses. Analyses of heave, pitch and roll motions confirmed the vulnerability of the model to certain frequency ranges, resulting in an adverse effect on the responses, and these were closely related to its natural frequencies.

This chapter demonstrates that some influential parameters of encountered waves can be detected through the monitoring of heave and pitch motions. Because of a strong coupling nature, these motions are in tune with irregular wave patterns, and therefore their responses can be regarded as applicable tools for the detection and estimation of influential wave parameters.

Out of a ship's dynamic responses the roll motion has attracted the attention of many investigators and a number of regulatory bodies. Synchronous rolling and large roll motion are two potential dangers for ship's stability, and can be avoided by taking appropriate action in ample time.

This chapter also shows that peak frequency of an irregular wave (spectrum) and associated magnitude are the two most influential parameters to stimulate the roll motion which can be measured by monitoring the heave and pitch motions.

6.2 Description of the Experimental Set-Up

6.2.1 Wave Maker Technology

Waves in the ocean are stochastic in nature, and the energy distribution associated with it is determined by the spectrum specified in terms of frequency and angle to fit with previously-recorded real data.

To reproduce spectra in a wave basin, it is necessary to use a pseudo random number generator (Rogers, 1997) to mimic the stochastic nature of the sea. An advantage of generating these spectra is repeatability.

The advantage can be taken to generate the rare events that could occur in the sea within the tank at any time. The concern is therefore centred on maintaining a sufficiently representative sea state to test the idea, or to model and repeat them a number of times. Waves are described by defining their frequency domain spectra and converted into time series for output to the wave makers. With the availability of large disk drives and high power computing capability, the signal is converted beforehand, enabling the use of efficient FFT algorithms. The complete time series can then be stored on disc ready for replay at any time.

The spectrum is defined by its equation and the integral of which over a frequency interval gives the variance, which is defined as half the sum of the square of all the amplitudes. It is necessary to integrate this function over the associated frequency range and apply the associated amplitude to it.

The spectrum is characterised by its peak frequency, that is, the point at which the given equation is a maximum.

6.2.2 Newcastle University Towing Tank

Experiments were carried out in the towing tank of Newcastle University (see Figure 6.1). The tank uses Edinburgh Designs Ocean software suite (Rogers, 1997) which provides a complete package for defining, running and processing the results of an experiment in a wave tank.

A range of significant wave heights and peak frequencies were chosen to develop a particular short-term sea state with a Pierson Moskowitz (PM) sea spectrum. This tank is 36 m in length, 4 m wide and has a water depth of 1.2 m. The experiments involved systematic measurements of six degrees of freedom (6DOF) motion responses (Enshaei, 2012b). The stationary model was tested in an intact condition for three different headings in irregular model seas. Comparative observations and recording of restorative motions, heave, pitch and roll were carried out.

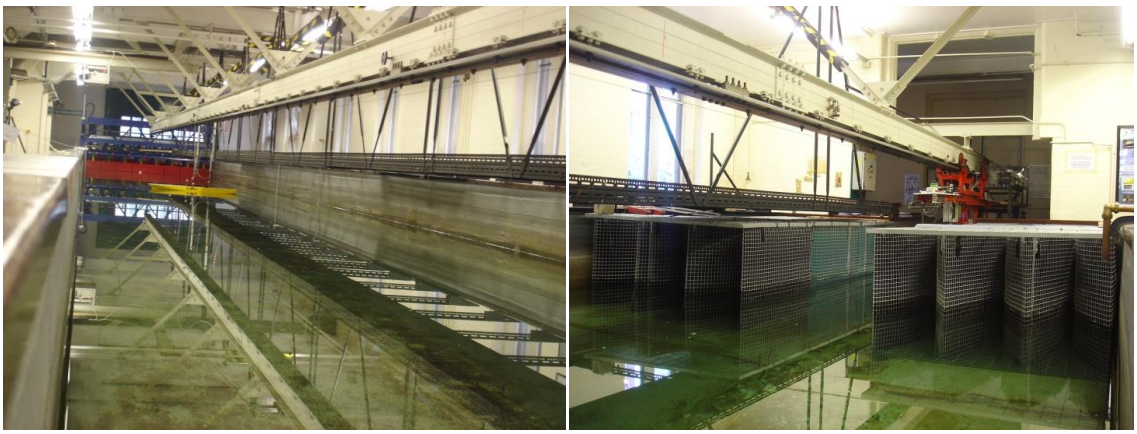

Figure 6.1 Newcastle University towing tank

In the experimental programme, waves were generated by a group of wave makers at one end of the tank and were absorbed by a parabolic beach located at the far end of the tank, which consisted of energy-absorbing sheets.

The wave heights and periods were monitored and recorded using two wave probes and an associated monitor. One was close to the model and the other was located at a distance of 2.9m and closer to the wave maker.

Figure 6.2 The Ro-Ro model in the towing tank with the Qualisys marker in place

The Qualisys Track Manager (QTM) with a ProRelex motion capture camera was used to track the motions of the model under different wave conditions shown in Figure 6.2. The QTM processes the video data directly as shown in the Figure 6.3 and converts it into coordinates.

This system offers a quick way to obtain accurate 6DOF information compared with traditional methods using motion sensors attached to a model. Data output has 6DOF tracking which in every frame locates the position and orientation of one or more rigid bodies in the measurement volume. The data output is available and may be visualised as graphs on the monitor in real time. The Ro-Ro model with attached Qualysis marker in the floating condition is shown in Figure 6.2.

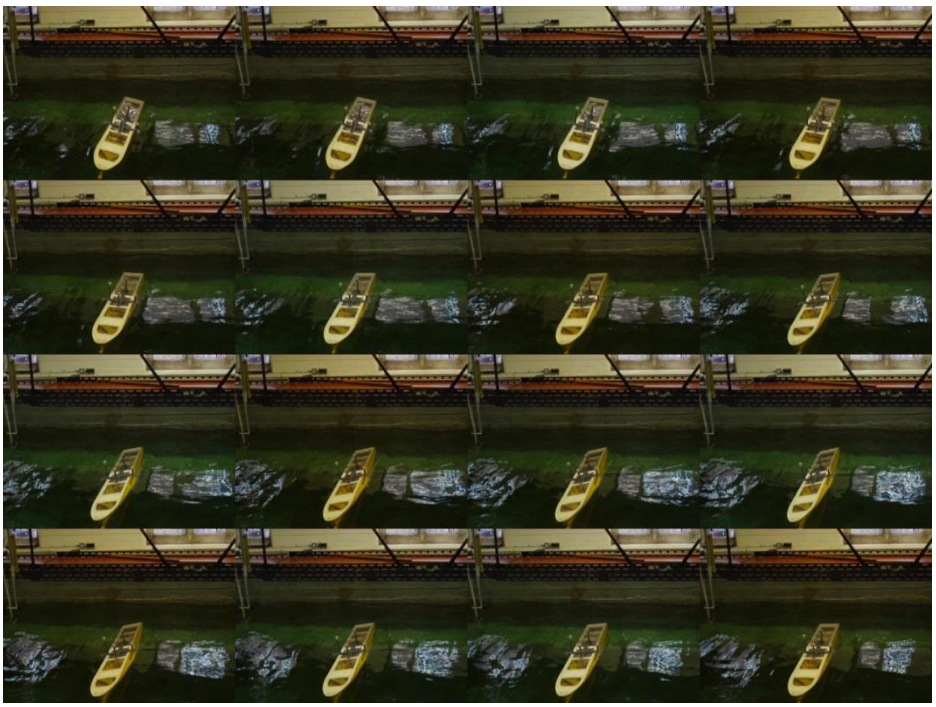

Figure 6.3 Every captured frame is used to convert the motions into respective coordinates

6.3 Construction of Model

The study was carried out using a RO-RO ship for which model test data from previous experiments is available (Emin, 2004). The main particulars of the model together with the prototype are given in Table 6.1.

The model is constructed from fibreglass and is based on the offsets of a prototype Ro-Ro vessel (Arias, 1998b; Arias, 1998a). The ship has a model ratio of 1:125 which is suitable for the size of the towing tank facility.

The justification of the model scale can be summarised as follows:

- The length of the model tested in irregular waves at zero speed was just less than 1.5 m.
- The measuring instrumentation did not affect the behaviour of the model when encountering waves because there was no direct connection.
- The model was not equipped with a bilge keel. However, a lightly-damped model performs large roll resonant behaviour which adds to the nonlinear coupling effect on the heave and pitch motions.

Table 6.1 Main particular of the Ro-Ro ferry and its scaled model

Particulars	Ship	Model (1/125)
Length overall (m)	187	1.496
Length between perpendiculars (m)	173	1.384
Breadth moulded (m)	26	0.208
Depth moulded (m)	15.7	0.126
Design draft (m)	6.5	0.052
Volume (m3)	16391	0.0084
Displacement) (N)	164800	0.08
Block coefficient	0.561	0.561
Prismatic coefficient	0.604	0.604
Midship section coefficient	0.929	0.929
Water plane coefficient	0.794	0.794
Height of metacentre above keel (m)	14.08	0.113
Height of centre of gravity above keel (m)	11.04	0.0897
Metacentric height (m)	2.86	0.0229
Longitudinal position of CoG from aft perpendicular (m)	78.73	0.636
kxx, Roll radius of gyration (m)	-	0.098
kyy, Pitch radius of gyration (m)	45.22	0.353
kzz, Yaw radius of gyration (m)	45.22	0.353

Model kyy and kzz were obtained from the DEXTREMEL report.

6.3.1 Natural Frequencies of the Model

Prior to the motion tests in waves, a set of free decay tests was carried out by manually forcing the model to respective motions. The recorded data were analysed by QTM to determine the average natural frequency shown in table 6.2. The roll decay of the model is presented in Figure 6.4.

However, since heave and pitch stiffness of the model is high, the decay curves had a limited number of oscillation cycles and therefore the results may have a certain degree of uncertainty. Consequently, the heave and pitch natural frequency is quoted from (Emin, 2004).

Table 6.2 Predicted natural frequency of the model

Particulars	Heave	Pitch	Roll
Natural frequency of model [Hz]	1.49	1.71	1.44
[rad/s]	9.4	10.7	9

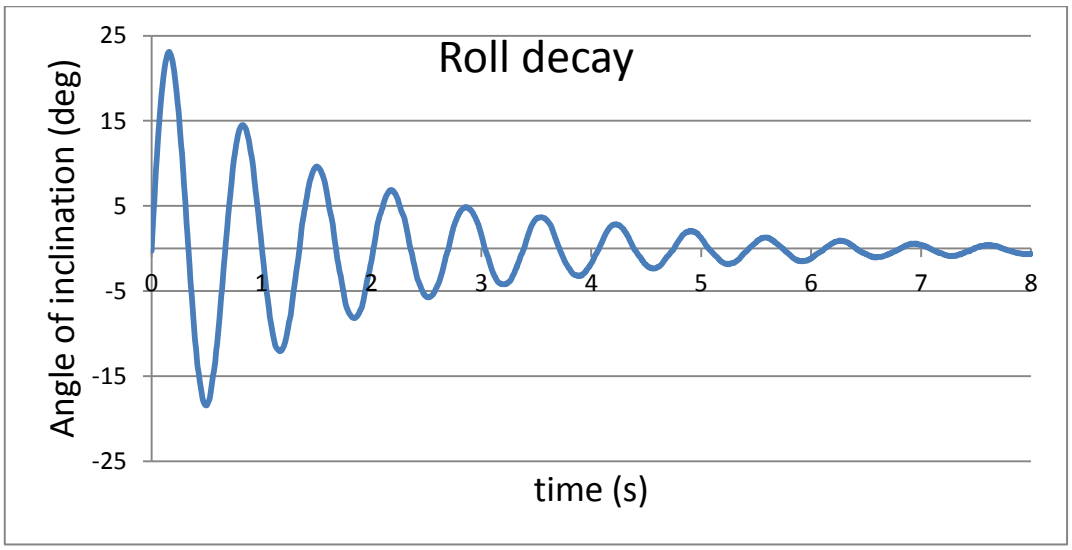

Figure 6.4 The roll motion of the model as a function of time

6.4 Accuracy of Data Recorded

To ensure that the data recorded from the wave probes matched with the desired output spectrum, test data was evaluated in the Wave Analysis for Fatigue and Oceanography (WAFO) environment (WAFO, 2000).

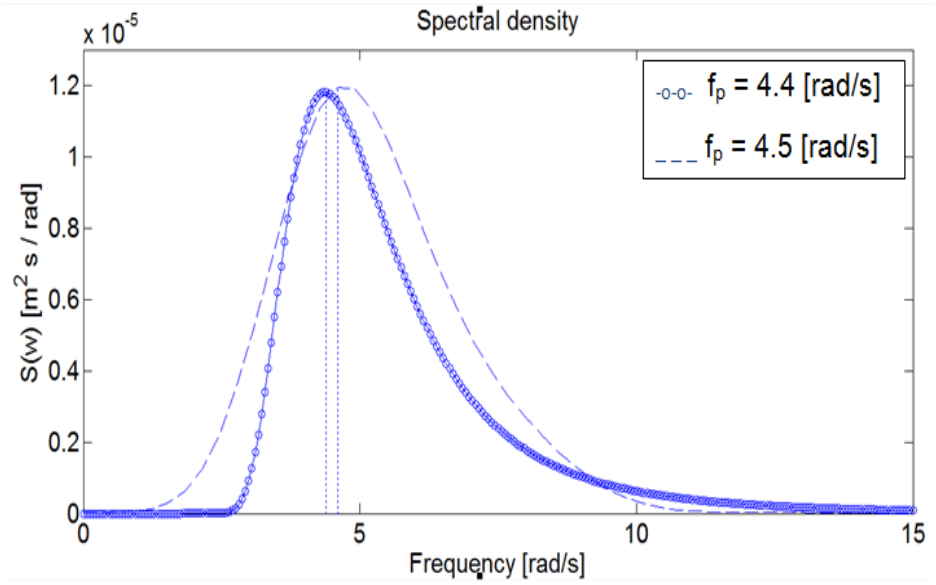

Figure 6.5 Comparison of Pierson Moskowitz sea spectrums developed by discrete time-varying data and WAFO mathematical modelling

In Figure 6.5 the input signal to the wave maker consists of a significant wave height (H_S) of 0.024 m and peak frequency of 4.4 rad/s. The spectrum output characteristic which

was compared against a mathematical model had a H_S of 0.027 m and a peak frequency of 4.5 rad/s.

Although there is a slight discrepancy between the two curves shown in Figure 6.5, it was finally the motion responses that compared against certain characteristics of the generated spectrum. These characteristics are estimated frequency peak and power peak, as depicted in the figures shown in the results of section 6.5.

In order to consider the influence of the nonlinear interactions between encountered, reflected, and radiated waves, the readings of the two wave probes were compared against each other. Although there was a slight difference in the histogram output, the variance and mean remained exactly the same for every test condition.

Prior to the experiments to commence, a matching calibration frame was used for the QTM in order to calibrate the measurement setup for optimum performance. The mass of the bare model was measured and then ballasted with weights to obtain an even keel condition (see Table 6.1).

The model was positioned at a distance of 12 m from the wave makers with two wave probes placed between the model and the wave makers on the centre line of the tank. One probe was placed close to the model and the other at a distance of 2.9 m. Transverse beams were located on the tank walls with studs attached to them in order to fasten mooring lines to the vessel. Mooring lines were connected to the bow and stern at the water level so that essentially the lines remained horizontal. Each line was comprised of a number of low stiffness tension springs connected to a nylon line, and was fastened to the studs.

In this manner the vessel was maintained on the station without preventing freedom of motion for the entire test period. However, the model was subjected to wave forces which resulted in both lateral and longitudinal movement and was arrested by the mooring lines in tension. This inevitably affected the motions to some degree, but was unavoidable without allowing the unmoored vessel to move freely in the tank due to the wave action.

6.5 Test Conditions

The model was tested in a stationary mode in the intact condition. The total number of recorded runs was 27, which consisted of three peak frequencies, with three significant wave heights and three heading angles. The heading angles were 0°, 45° and 90° corresponding to following, quartering and beam seas respectively. Table 6.3 lists the intended spectrum characteristic applied to the wave maker to generate irregular waves.

Table 6.3 Experimental wave conditions

Peak Frequency (rad/s)		Significant wave Height, H_s (m)		Sea state
Model	Ship	Model	Ship	
4.37	0.39	0.024	3	Low
6.42	0.57	0.048	6	Medium
9.92	0.89	0.072	9	High

Each test run lasted for eight minutes to avoid unreliable results and once the model had reached the steady condition then motions were recorded. The wave conditions stated above were selected in order to maximise the possible test runs over a wide range of frequencies. The model was free from green water effects and the mooring lines did not apply excessive force to restrain the motions.

6.6 Presentation of the Recorded Data

The discrete time-varying data of the motion responses and incoming waves were monitored by QTM and two wave probes respectively, and were recorded using LabVIEW software (National Instruments, 2011). Recorded data was analysed using power spectral density (PSD), which describes how the power of a signal or time series is distributed with frequency. The time domain window selected for these analyses was the Hanning type. LabVIEW and MATLAB environments were used for analysing the data obtained and the sampling rate for data acquisition was 100 Hz. The time series recorded had a duration of eight minutes.

In the following figures, heave motion and pitch motion in each column is the response to the corresponding wave in the same column. The y-axis presents the PSD and the unit is measured as $S(\omega)[m^2 s/rad]$ for wave and heave motions, whilst it is $S(\omega)[\deg^2 s/rad]$

for pitch and roll motions. The vertical dash line in every figure is the corresponding natural frequency of the motion. The magnitude vertical scales in each diagram vary for presentation purposes.

6.6.1 Following Sea

In the first row of Figure 6.6 the spectra of the waves are presented for a range of frequencies. The area under the spectrum is decreasing towards a higher frequency which is a clear indication of energy of the wave. The numbers in each frame indicate the setting values for irregular waves as input into the wave maker, which is not necessarily achieved in these figures. The heave response spectrum is shown at every sea condition, which tracks the corresponding wave spectrum as well as portraying the reduction in the energy. The same trend is illustrated for the pitch response spectrum too. Due to coupling effects, the heave and pitch responses are very similar in their patterns and it is of interest to note that peak frequency of both motions are close or nearly close to that of the waves in every sea state.

The high frequency in general has least effect on large ships, where the ratio of ship length to wave length is much greater than one. Therefore, less agreement in patterns of the heave and pitch spectrum with waves at higher frequencies is of less concern for this size of model ship. It is also evident from the magnitude of heave and pitch motions that have been reduced in comparison with the lower frequencies.

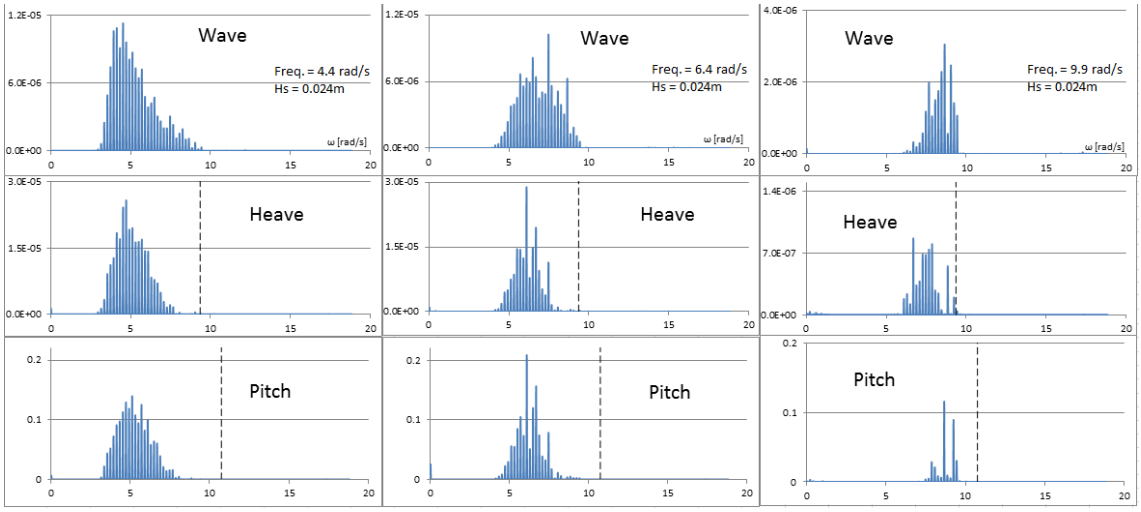

Figure 6.6 Power spectra density in the following sea at three different peak frequencies and identical significant wave heights of 0.024m

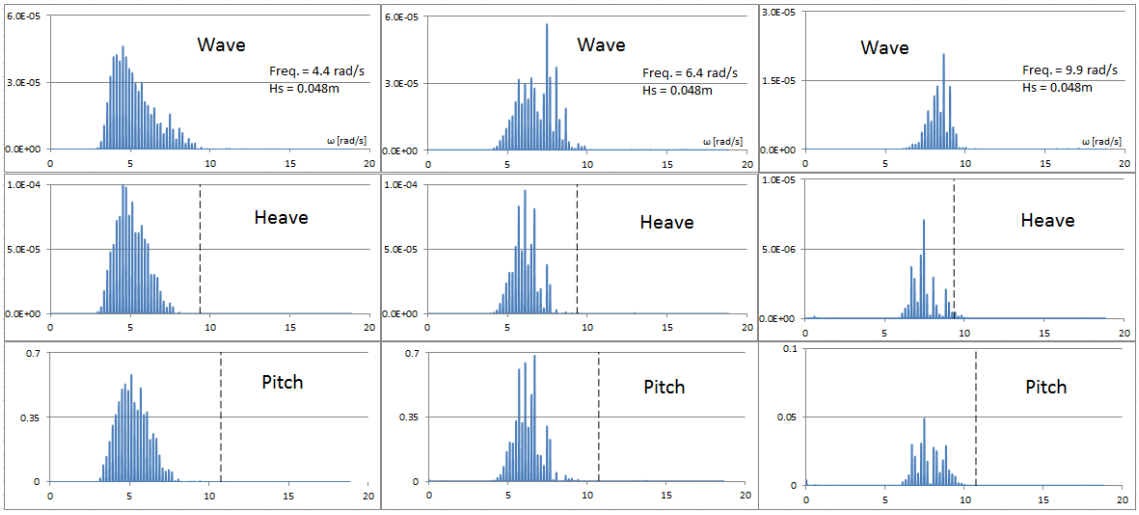

Figure 6.7 Power spectra density in a following sea at three different peak frequencies and identical significant wave heights of 0.048m

The results shown in Figures 6.6 to 6.8 demonstrate that a similar trend has been detected upon analyses of motion responses in various significant wave heights and directions.

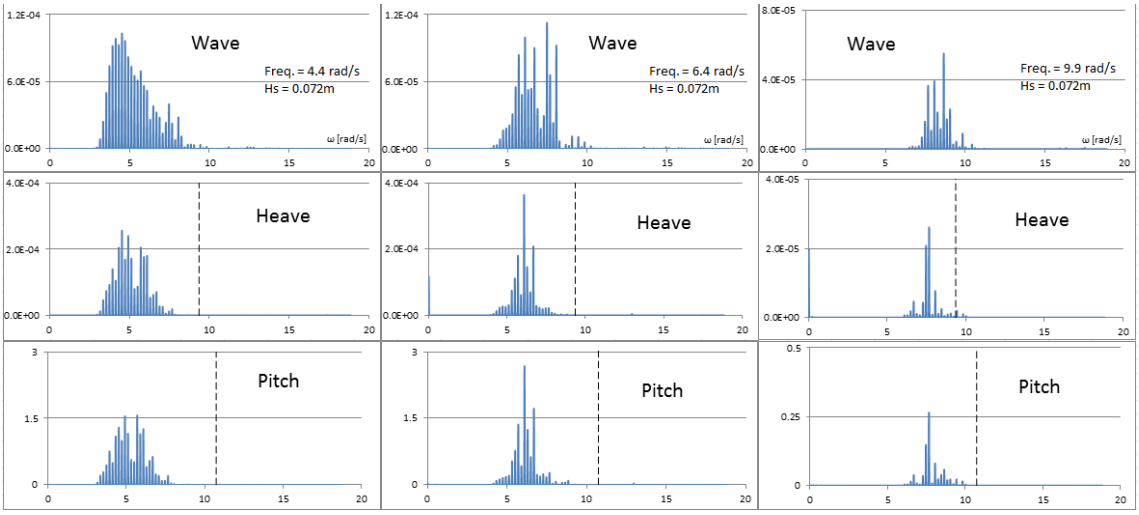

Figure 6.8 Power spectra density in a following sea at three different peak frequencies and identical significant wave heights of 0.072m

6.6.2 Quartering Sea

The series of tests in quartering seas shows the similar results obtained in the following seas. The peak frequency of both heave and pitch motions are close or nearly close to that of the waves at every sea state and have similar patterns.

The patterns of both heave and pitch motions illustrated at higher frequencies are improved in the tracking of the waves in comparison with the following seas.

At a higher value of Hs shown in Figure 6.11, the wave spectrum at the middle frequency appears to be split into two parts. It is interesting to observe that both heave and pitch responses illustrate the similar pattern and detect dual peak frequencies.

The results shown in Figures 6.9 to 6.11 demonstrate that a similar trend has been detected upon analyses of motion responses in various significant wave heights and directions.

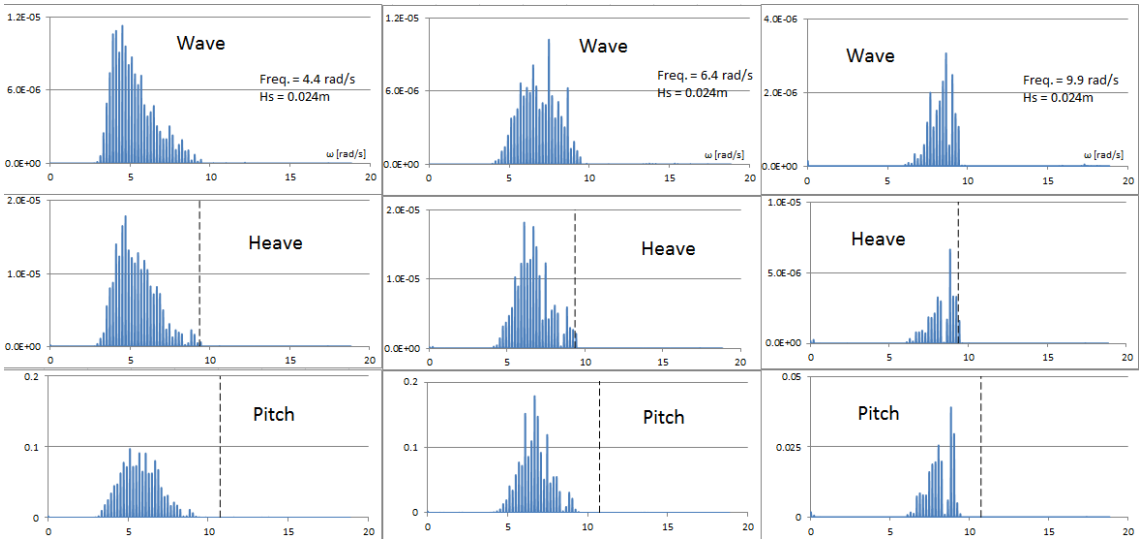

Figure 6.9 Power spectra density in a quartering sea at three different peak frequencies and with identical significant wave heights of 0.024m

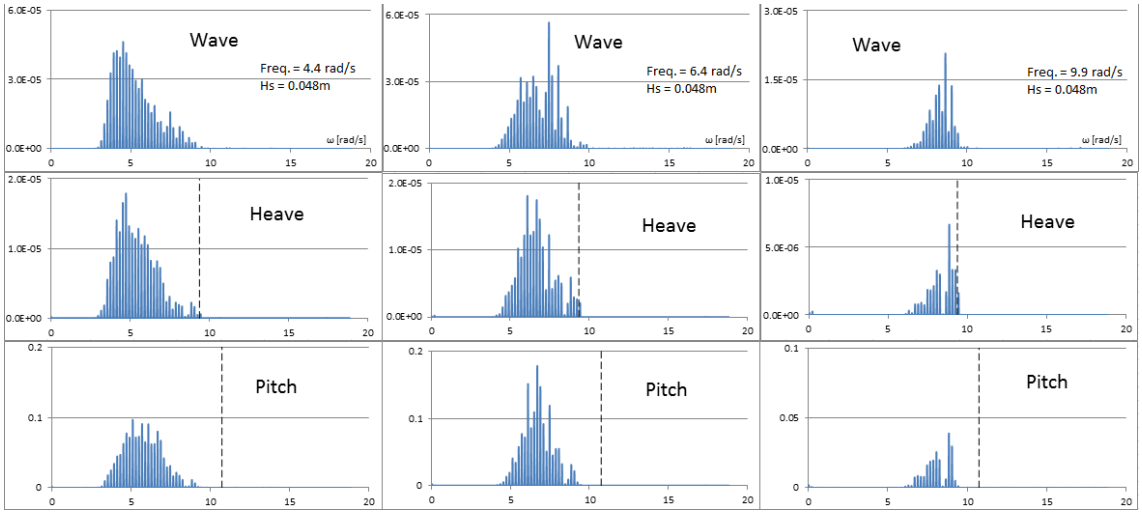

Figure 6.10 Power spectra density in a quartering sea at three different peak frequencies and with identical significant wave heights of 0.048m

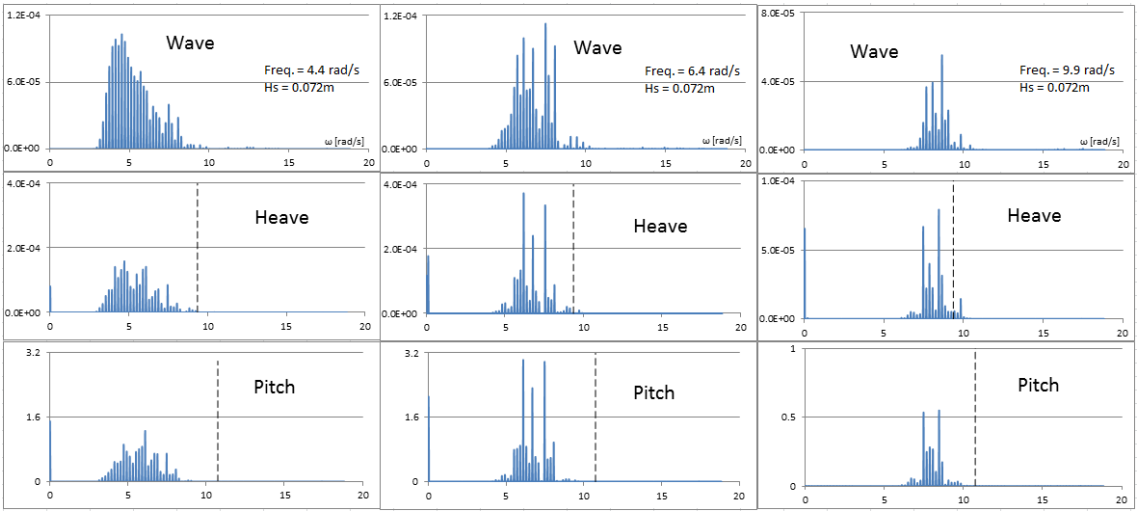

Figure 6.11 Power spectra density in a quartering sea at three different peak frequencies and identical significant wave heights of 0.072m

6.6.3 Beam Sea

At the low peak frequency of the wave spectrum in Figure 6.12 the response of the heave and pitch motions are more random (left column). This condition is expected in a beam sea where the ratio of the breadth of the ship to wave's length is of concern rather than the ship's length.

The tracking of the peak frequency of a wave's spectrum by both heave and pitch motion responses improves as the peak frequency of wave is growing higher. However, the pitch response should not be very reliable in a beam sea in general, and even the magnitude is quite low compared with quartering sea results.

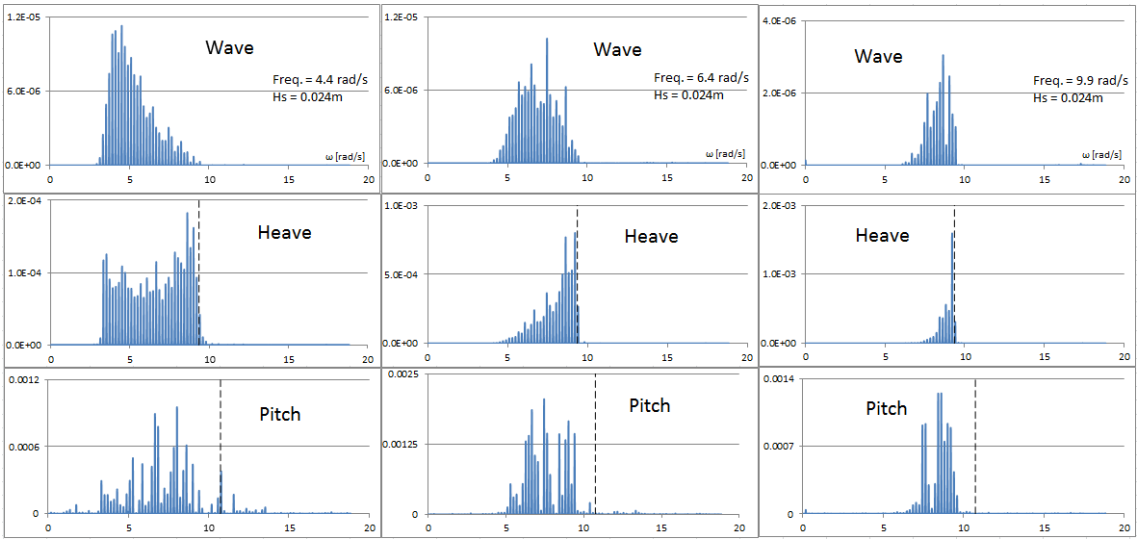

Figure 6.12 Power spectra density in a beam sea at three different peak frequencies and identical significant wave heights of 0.024m

The results shown in Figures 6.12 to 6.14 demonstrate that a similar trend has been detected upon analyses of motion responses in various significant wave heights and directions.

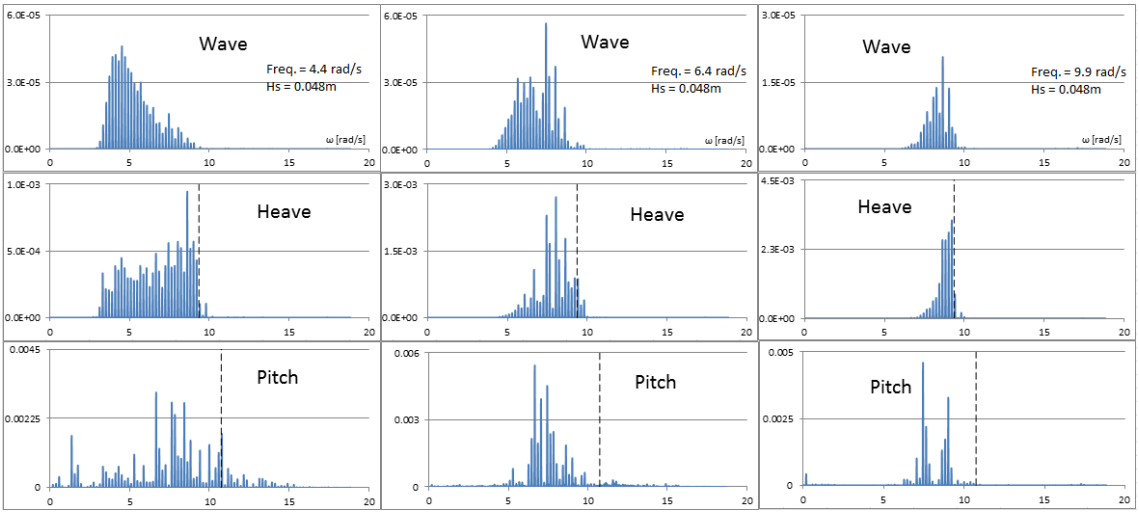

Figure 6.13 Power spectra density in a beam sea at three different peak frequencies and identical significant wave heights of 0.048m

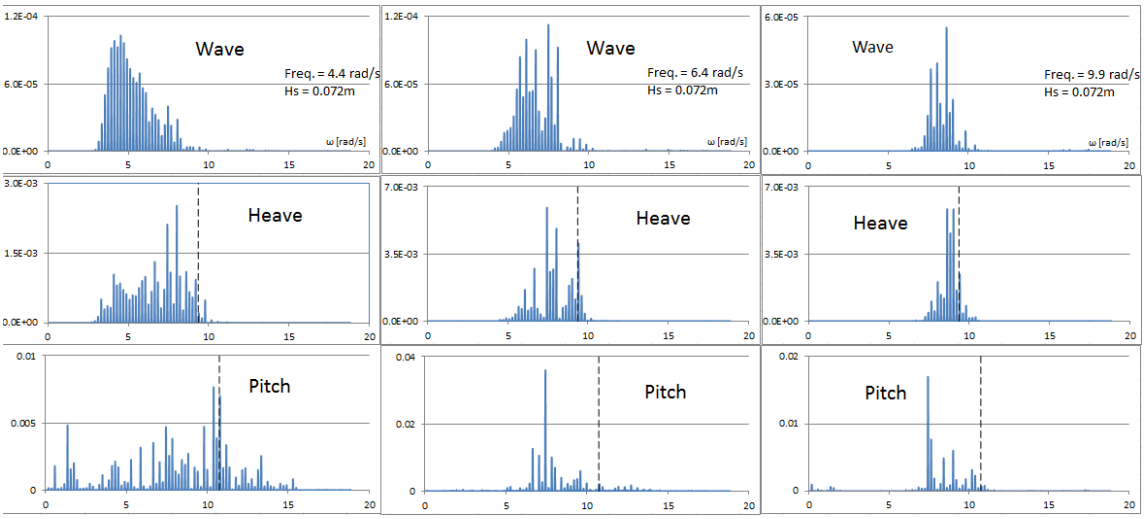

Figure 6.14 Power spectra density in a beam sea at three different peak frequencies and identical significant wave heights of 0.072m

6.6.4 Roll Motion at Different Sea Conditions and Headings

The roll motion spectrum shown in the Figures 6.15 to 6.17 is the response to a particular wave spectrum having specific peak frequency and significant wave heights discussed in section 6.6.3.

The roll motion responses in Figure 6.15, unlike the heave and pitch motions, do not mimic the corresponding wave spectrum. The majority of oscillations are concentrated around the natural roll frequency regardless of the sea conditions. The magnitude of

every test condition is different and it is obvious that when the wave peak frequency is getting close to the natural roll frequency, the magnitude is escalated. The effect of higher significant wave height is also apparent on escalation of the magnitude.

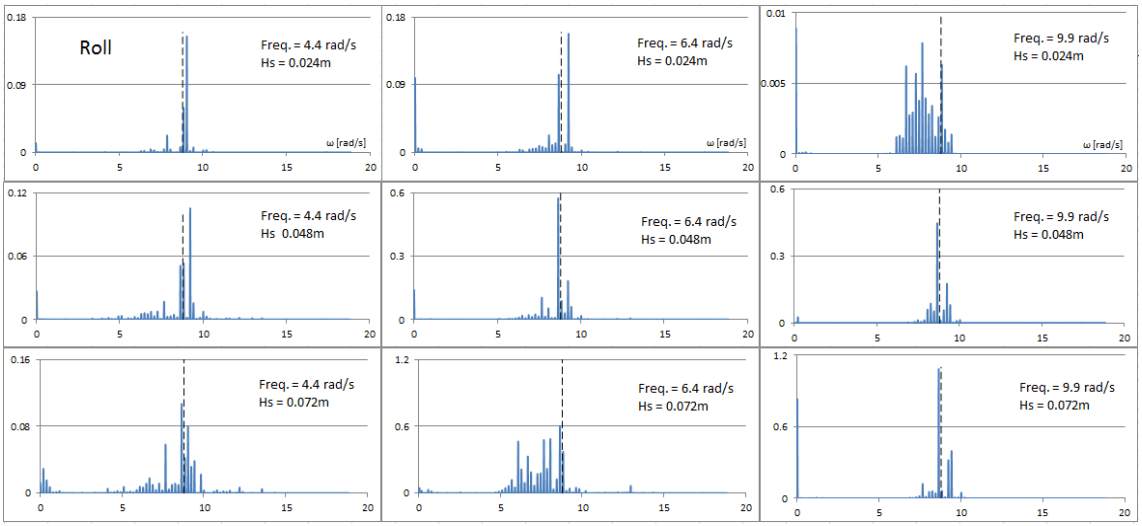

Figure 6.15 Power spectra density in a following sea at three different peak frequencies and three different significant wave heights

The top right frame of Figure 6.15 has least energy with reference to its magnitude scale, and it lies in a fact that roll amplitude was negligible at this particular frequency and Hs. Similar patterns are identified with spectral analysis of roll motions in quartering seas depicted in Figure 6.16. At lower frequencies, the model ship is capable of detecting the responses around the roll natural frequency as well as the frequency range swept over the wave spectrum. However, towards the higher frequencies, detection of the frequencies far-off from the roll natural frequency is damped-out.

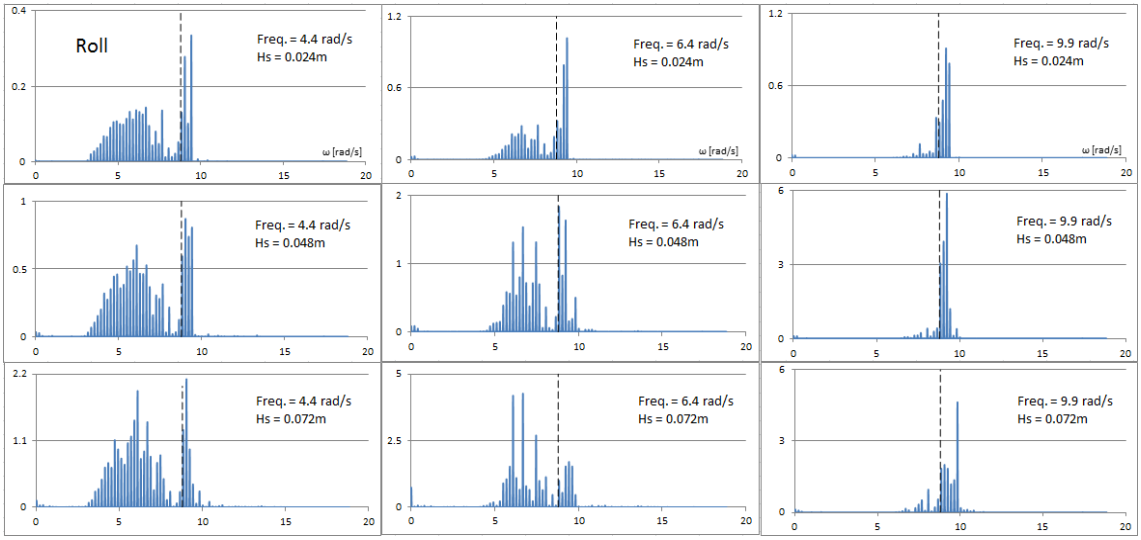

Figure 6.16 Power spectra density in a quartering sea at three different peak frequencies and three different significant wave heights

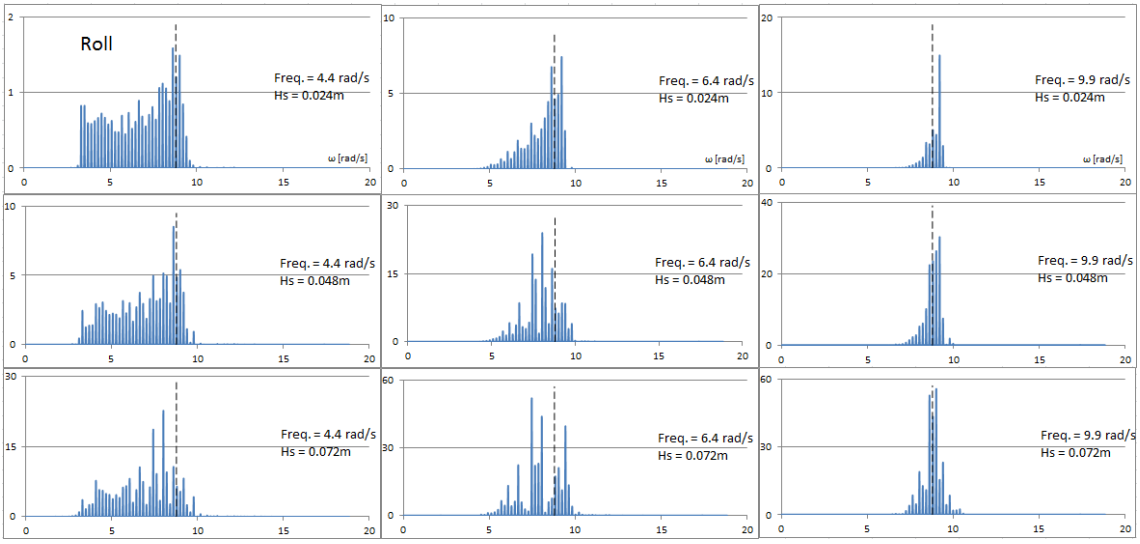

Figure 6.17 Power spectra density in a beam sea at three different peak frequencies and three different significant wave heights

At the lower peak frequency of the wave spectrum the response of the roll motions are more random (left column), as shown in Figure 6.17. These are the similar conditions illustrated in Figure 6.12. These conditions improve as the peak frequency of the wave grows higher and the encountered wave length is much longer with respect to the ship's model breadth.

6.7 Results of the Tests

The figures presented in this section correspond to the motion responses of the ship. The x-axis presents the sea conditions (defined as 'low', 'medium' and 'high' for the three different peak frequencies utilised in generating the wave spectrum) and the y-axis is estimated frequency peak in Hz. The results are presented for the three values of H_S and these are defined as 'small', 'medium' and 'large' in line with the three different frequencies. The magnitude scales vary for presentation purposes.

The estimated frequency peak of the wave and the three motions considered in this experiment are shown in Figure 6.18. Two sets of plots in following and quartering seas are compared against each other to illustrate the similarities of the motion behaviours.

The response of heave and pitch motions are strongly coupled and closely follow the frequency peak of waves in different sea conditions. However, the roll motion maintains the response close to its natural frequency.

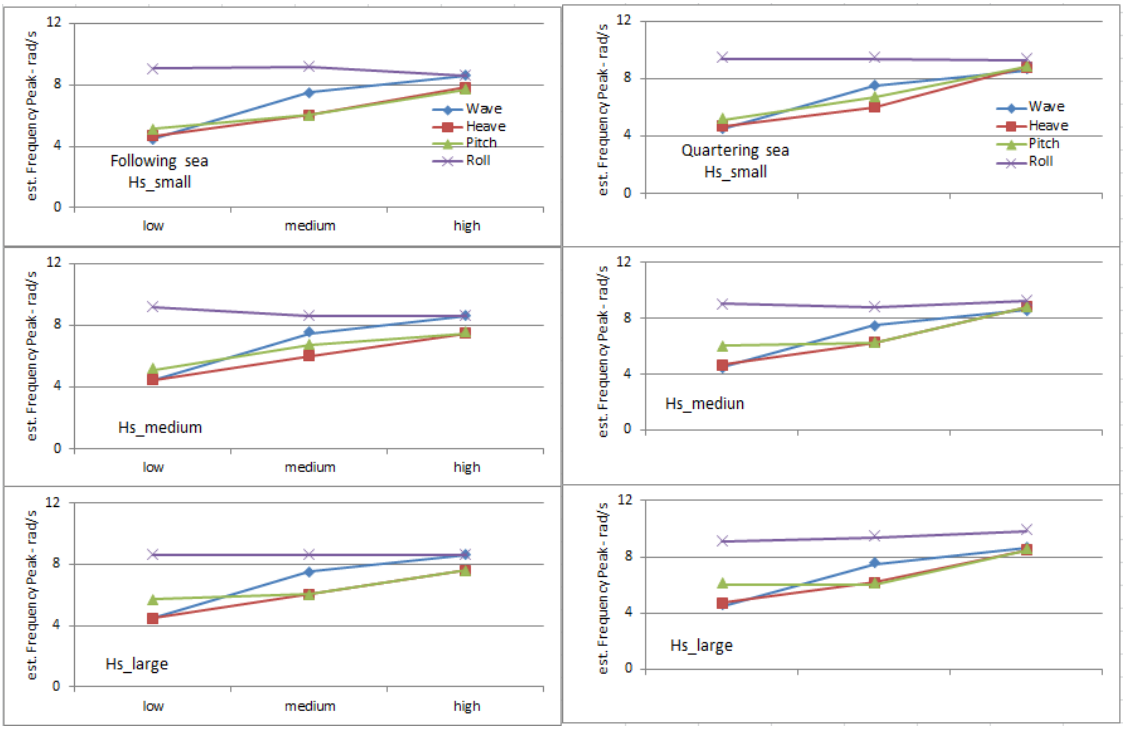

Figure 6.18 Comparison of frequency peaks for each sea condition tested in a following and quartering sea at small, medium and large H_S

A similar trend can be observed in all frames of Figure 6.18 as the value of H_S is increasing. However, the coupling effect of heave and pitch under low sea conditions is not as strong as in high sea conditions and it appears to be less significant at a medium H_S value. The roll response remains pretty constant for every sea condition and H_S values tested.

The results are slightly different in beam seas which are shown in Figure 6.19. The heave motions are not coupled with pitch motions anymore and the frequency peaks follow that of the roll motions. There is not a noticeable trend in the frequency peaks of pitch motions.

In the following discussions, the main emphasis is on the effect of the estimated frequency peak and power peak on the motion responses, as well as any other notable trends observed in the response curves.

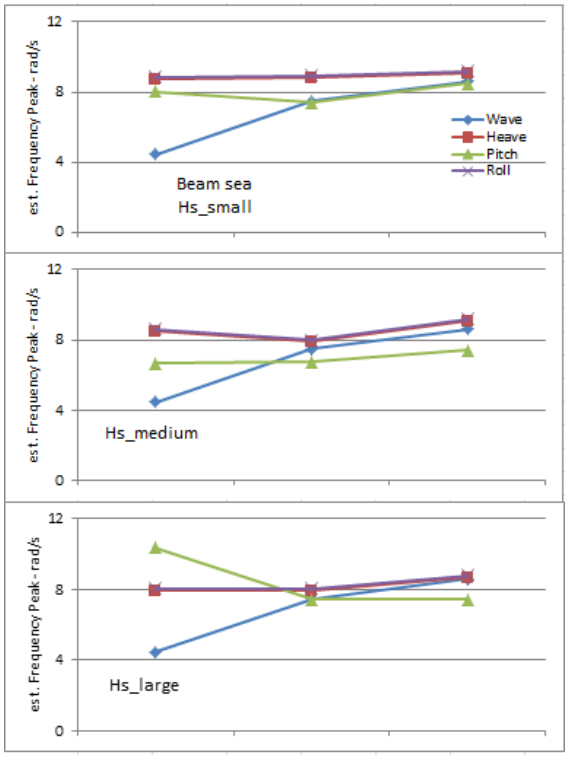

Figure 6.19 The frequency peaks for each sea condition tested in a beam sea at small, medium and large H_S

6.7.1 Motion Responses in a Following Sea

The energy of the irregular wave has a dissimilar effect on each of the ship's motions and the impacts vary in different sea conditions. Figure 6.20 shows the energy of waves generated by the wave maker at Newcastle towing tank over a range of peak frequency and significant wave height. The energy diminishes towards the higher frequency over the X-axis and reduces by smaller significant wave heights.

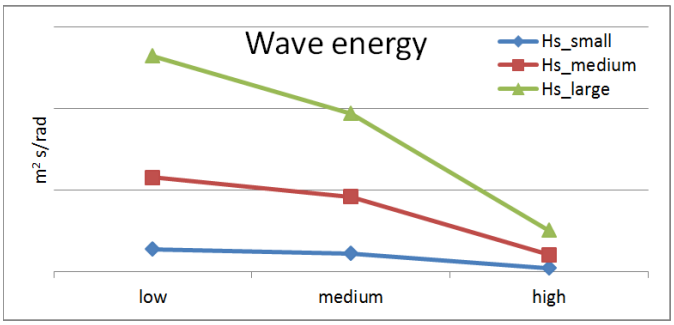

Figure 6.20 Wave energy generated by the wave maker at Newcastle towing tank

The variations in heave and pitch magnitudes shown in Figure 6.21 are in line with changes in wave magnitudes. However, roll magnitude does not display a sharp refraction and follows a steady trend with a slight decrease at high frequencies.

In medium and large Hs the rate of roll motion response increases at the higher sea state, where the range of wave peak frequencies is closer to the natural roll frequency and it reaches its maximum at the large H_S value. It is a clear indication of synchronous rolling. The coupling effects of heave and pitch motions are obvious in all sea conditions and at every H_S value tested. Their magnitudes remain high except at high frequencies.

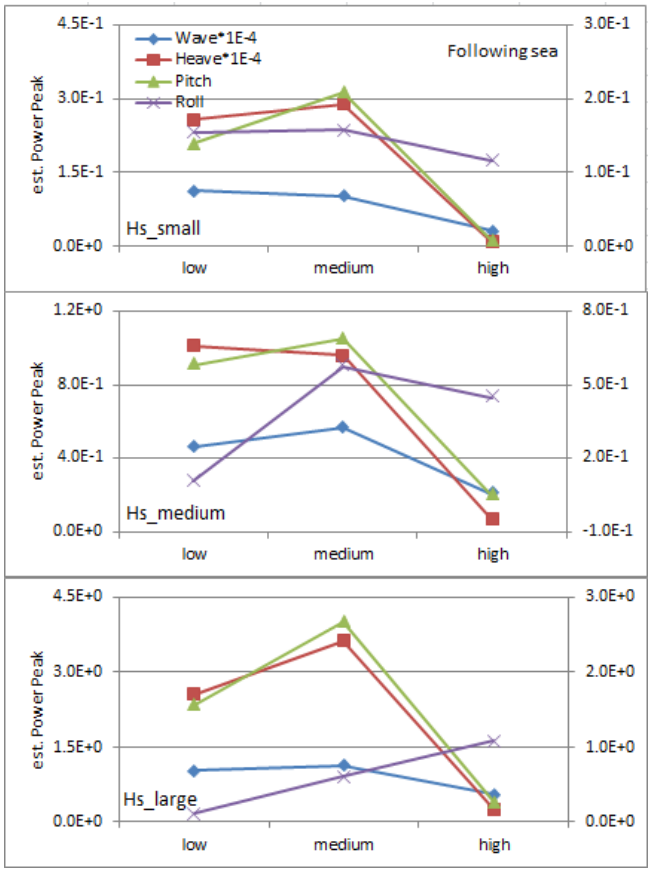

Figure 6.21 Comparison of energy magnitudes for each sea condition tested in a following sea at different H_S

The y-axis presents the PSD and the unit is measured as $[m^2 s/rad]$ for wave and heave motions whilst it is $[\deg^2 s/rad]$ for pitch and roll motions. The second scale on the right is for the roll and pitch motions.

6.7.2 Motion Responses in a Quartering Sea

The results in a quartering sea are interesting because a change of sea direction from stern to quarter has less effect on peak frequencies of motions in comparison with Figure 6.21. The coupling effects of heave and pitch motions are similarly maintained throughout the change in heading angles (see Figure 6.22).

The trend in variation of amplitude is depicted in Figure 6.22 which is complimentary, and corresponds to roll responses in a following sea. The synchronous rolling is more evident around the roll natural frequency. The magnitudes of heave and pitch reach the maximum in the medium sea conditions.

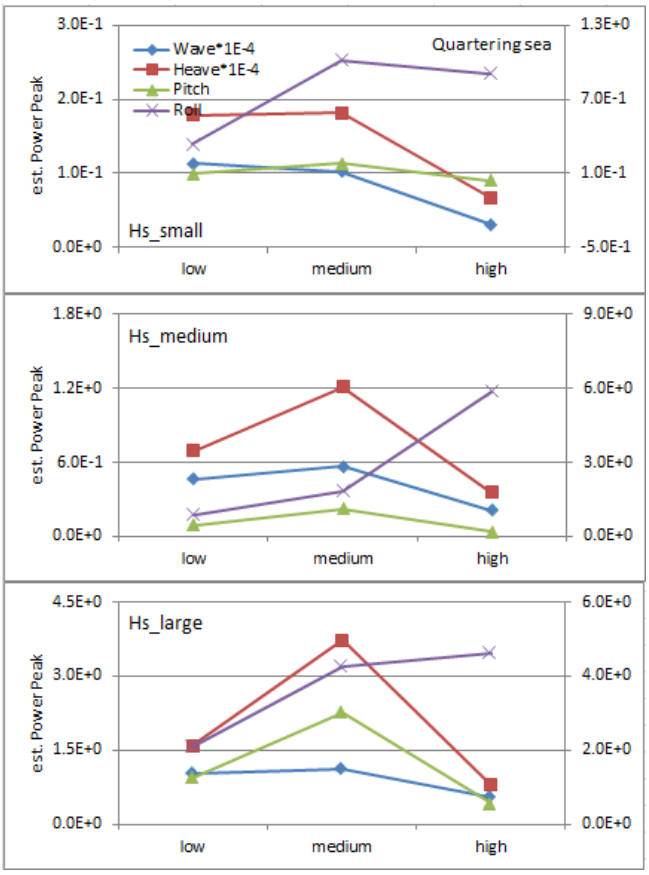

Figure 6.22 Comparison of energy magnitudes for each sea condition tested in a quartering sea at different H_S

6.7.3 Motion Responses in a Beam Sea

In a beam sea there is a strong coupling between roll motions and heave motions at all sea conditions and significant wave heights, therefore the magnitude of the heave response follows from the roll response which is a dominant motion (see Figure 6.23). However, the magnitude of pitch response tracks that of the wave, but is less sensitive at small Hs.

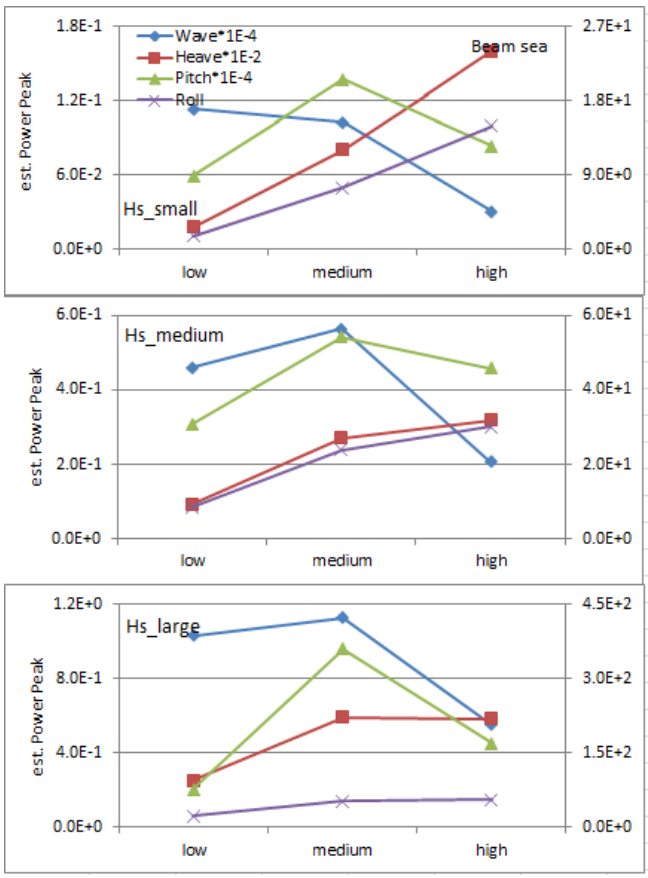

Figure 6.23 Comparison of energy magnitudes for each sea condition tested in a beam sea at different H_S

6.7.4 Roll Response at Different Sea Conditions and Headings

With reference to Figure 6.20, it is apparent that wave energy decreases while frequency increases. Therefore, roll responses should be damped accordingly with the changes of the frequency to higher values. This is a condition observed for the heave and pitch motion responses.

It is of no surprise that roll magnitude escalates around natural frequency and Figure 6.24 confirms the same behaviour under the sea conditions at different headings tested. It is shown that magnitude of roll motion responses are directly related to the ratio of wave peak frequency to natural roll frequency. Therefore, detection of current peak frequency of waves and monitoring the changes could be an index to monitoring the development of critical situations causing larger roll motions.

Figure 6.24 shows the maximum responses that occur close to unity where the wave energy is least. It also confirms that the maximum power peak is obtained in beam seas.

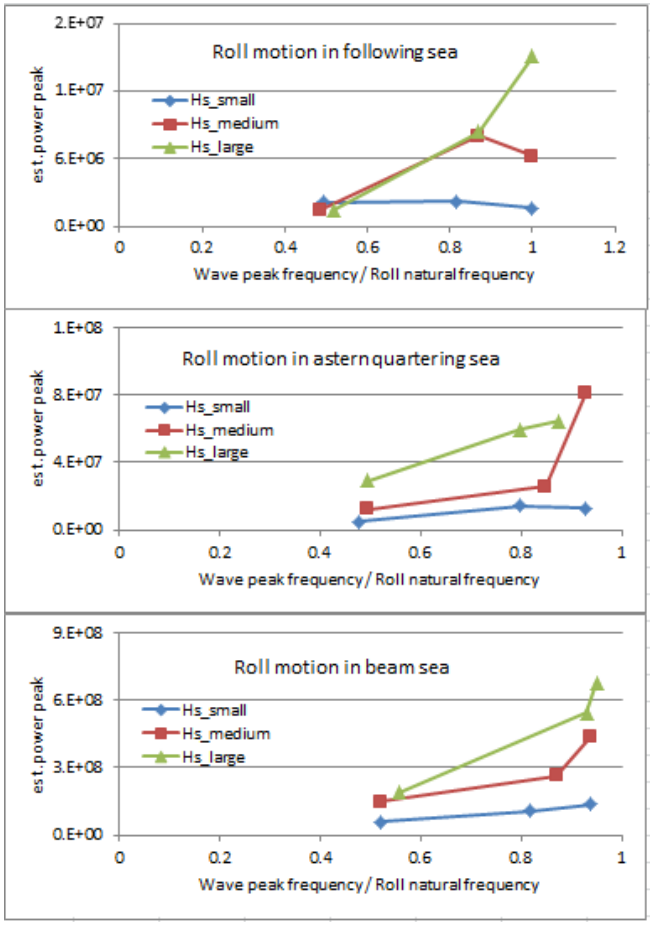

Figure 6.24 Roll responses under different operating conditions

6.8 Summary

An experimental model test approach was carried out for the development of practical tools to monitor the behaviour of dynamic stability in waves.

A Roll-on/Roll-off (Ro-Ro) model ship was chosen because of its vulnerability to greater stability losses which has been of great concern owing to the large car deck spaces. Systematic motion tests have been carried out in the simulated irregular waves having different Hs and different peak frequency at different heading angles. The ship's motions were detected and recorded using Qualisys Track Manager (QTM). The recorded data were analysed by the power spectral technique that presents the distribution of signal energy against frequency. It was observed that the spectrum of the heave and pitch motions follow the wave spectrum pattern, which is due to the strong coupling between the two motions. Therefore, the frequency peaks and power peaks of the waves are followed by these two motions.

Monitoring the behaviour of the motion responses were demonstrated to be a good performance indicator to study development of a critical situation which could cause large roll motions.

It was observed that the roll motion maintains its largest oscillation around the natural frequency in all sea conditions regardless of the heading angles. Roll is magnified when the peak frequency of the wave approaches the natural roll frequency; therefore, keeping these two apart avoids large roll motion. However, the wave peak frequency can be estimated by either heave or pitch spectral analysis.

The results of the tests for a following sea and a quartering sea confirm the applicability of this method in detection of wave peak frequency. However in a beam sea, heave motion turns to be in strong coupling with dominant roll motion.

It was concluded that peak frequency and associated magnitude are two important inherent characteristics of motion responses. Detection of these influential parameters of encountered waves through heave and pitch responses could be utilised to limit a large roll motion at sea.

Chapter 7

Application of Signal Processing Techniques

7.1 Introduction

A ship sailing in adverse weather conditions is likely to encounter various kinds of dangerous phenomena; these may lead to capsizing or severe roll. The vulnerability to dangerous responses, including capsizing and its probability of occurrence in a particular sea state, may differ for each ship (Altes, 1980; IMO, 2007).

Since many years, there has been an increasing interest in the development of the on-board monitoring systems with the view of operational safety (Huss, 1994). A number of studies suggest that the only way to overcome the many difficulties lies in the development of a time-domain simulation of ship motions in a seaway (Francescutto, 1993), including a detailed description of the environment.

This chapter intends to use the knowledge gained in Chapters 5 and 6 in order to develop a tool to compute the energy of a signal as a function of time and frequency. This monitoring tool should be fast in responding and be capable of providing information in ample time for the operator for decision-making, while considering gradual changes of the sea conditions.

Most of the on-board monitoring systems lack an estimate of the weather conditions, and in particular the prediction of the wave spectrum. Therefore, such systems are more effective in simple cases than in intact stability, where complex dynamics and multiple degrees of freedom are involved (Francescutto, 2004).

The concept of a wave-rider buoy may be applied to ships, even when sailing in an arbitrary direction. However a moving ship adds to the complexity of data analysis and should be taken into consideration when the measured ship responses are used for estimation of the wave characteristics.

Ship motions are assumed to follow linear theory in light and moderate sea states, where the relationship between ship motions and waves are modelled by transfer functions. However, the prediction of ship motions in response to wave excitation forces becomes vital in a rough seaway which is nonlinear and cannot be simply achieved.

It is strongly believed that operational safety of the ship can be significantly improved by the monitoring of ship responses (Nielsen, 2005) to detect wave-influential parameters. Through a measured set of ship responses, the potential dangerous events can be predicted on the basis of analysis of the past recorded signals.

A reliable, easily applicable method is essential to alleviate the seaway dangers and should avoid any possibility of manual computation. Operational stability is very complex; however, it is important to understand the links between the sea state and the effective course of a ship. The motion behaviour of ships in an environment characterised by waves and wind varies for different types and scopes, which adds to the complexity of dynamic responses at sea.

Development of such an instrument for evaluating the effect of ship design parameters on ship safety in a seaway has been emphasised in the IMO Intact Stability Code of 2002 where it requires that a range of sea conditions should be taken into account.

7.2 Analysis of Measured Time Series

To date various methods have been developed and introduced to measure sea waves. The techniques commonly used for wave measurement that discussed in Chapter 4 are as follows:

- Sea State Estimated by Observers at Sea
- Satellite Altimeters
- Radar waves
- Accelerometer Mounted on a Meteorological Buoy
- Wave Gauges

Data collected by these methods can be used for weather prediction, however there are certain constraints associated with the above techniques and each of them suffers from one or more deficiencies such as accuracy, availability or delays in obtaining data for the

analysis of time series. Therefore, they will not be necessarily a good choice for development of a real time monitoring system on board the ship.

In 1953 St Denis (St Denis, 1953) suggested that a ship could be treated as a filter with an input, not of electrical signals, but of waves. The ship as a black box receives the waves as an input, which contain a number of different frequencies and components, and generates ship motions as the output as shown in Figure 7.1.

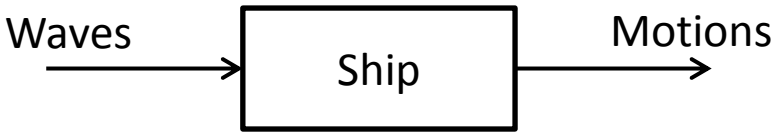

Figure 7.1 The electronic filter analogy

These motions are a response to sea states which can be considered as a combination or superposition of a large number of regular sinusoidal wave components with different frequencies, amplitudes and directions. In the study of motion responses, the spectral analysis can be utilised as a powerful and popular approach that exists for treating complex signals.

The spectral approach indicates which frequencies have significant energy content, and can readily be plotted in a frequency vs. energy density graph. This graph can provide important information either about a wave sample, or about ship motion responses.

The motion responses could be the best representation of the current sea state, and signal processing techniques could be an effective way to detect wave-influential parameters through the analysis of heave and pitch motion responses. These variables are the wave peak frequencies and associated magnitudes which can cause a high roll motion when close or nearly close to the roll natural frequency.

In general, time series are analysed over short periods, from 20 minutes to several hours which are too lengthy for online monitoring. Without a proper technique for recording and analysing the waves experienced by a ship, the results obtained can only be related to potentially unreliable visual estimates of the sea state.

Throughout this chapter the term “peak frequency” will be used to refer to frequency at the peak of the spectrum defined by $dS(\omega)/d(\omega) = 0$.

7.3 Spectral Analysis of Time Varying Signal

A natural seaway can be decomposed into a sum of sinusoidal waves, each having a relatively small steepness, even for a severe sea. Therefore, the spectral approach with a sum of waves constitutes a valid representation for a random sea. It is worth pointing out that seaway spectra are narrow banded (Kobylinski, 2003a), and the total wave energy is concentrated at a narrow frequency range.

In this study the discrete time-varying data of the motion responses and incoming waves were studied through the power spectral analyses. Figure 7.2 illustrates the results from one of the test scenarios presented in Chapter 6 which demonstrates how the power spectral density (PSD) of an irregular wave, heave, pitch and roll motion is distributed over a range of frequencies during an eight-minute period.

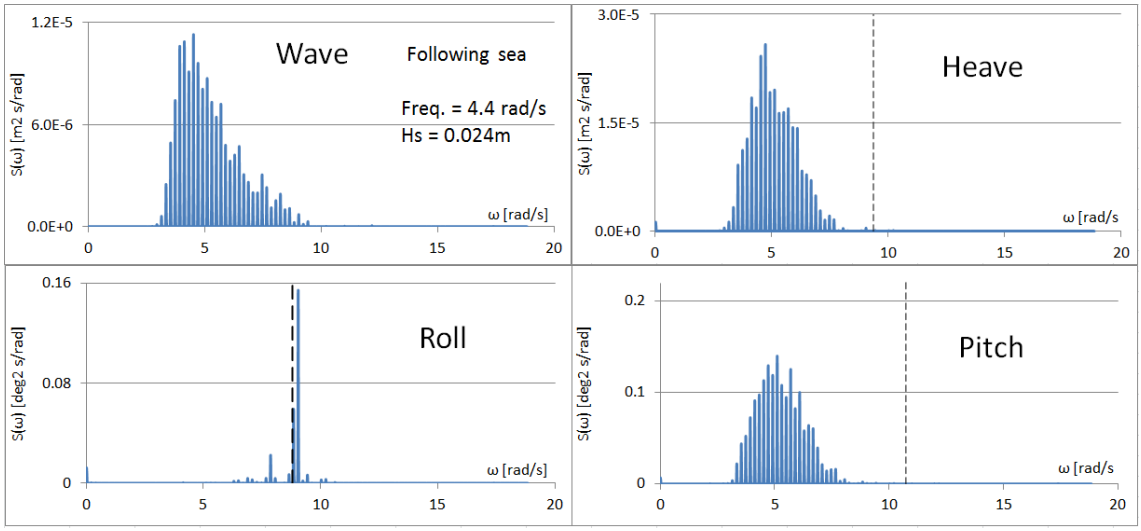

Figure 7.2 Power spectral analysis of the ship's motion responses in an irregular sea. The time series are recorded over an eight-minute period using a model ship in a following sea

The detailed interpretation of Figure 7.2 is given in Chapter 6, however this is not the only single method to analyse this type of discrete time-varying data.

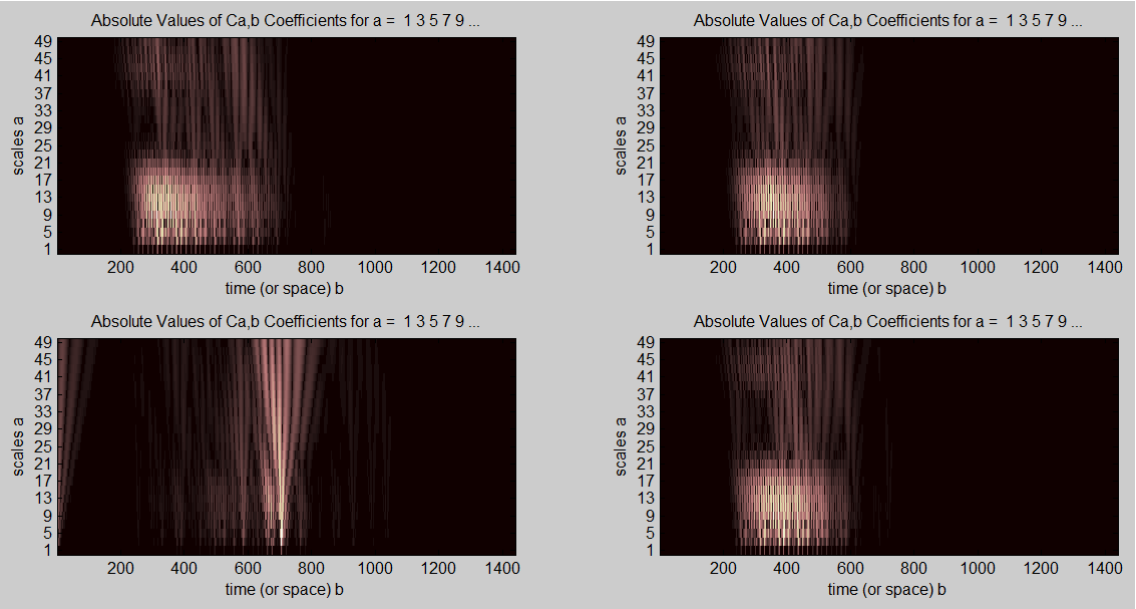

Figure 7.3 Scaleogram analyses of the time series used in Figure 7.2

The wavelet analysis method shown in Figure 7.3 is applied to the same time series shown in Figure 7.2. Wavelet analysis is a technique which is useful in identifying frequencies and calculating power distributions, however the output of this test did not revealed extra information compared with the results obtained from the PSD.

The extent of information provided by these methods might be sufficient to develop a monitoring mechanism, while the energy of a seaway changes gradually and can be considered to be constant for short periods of time. However, the duration of the above analyses may not be sufficiently short to provide ample time for decision-making. Therefore, a fast and reliable method is required for online monitoring of dynamic ship responses.

7.4 Method of Signal Detection

For the purpose of signal analysis and detection of influential wave parameters, Laboratory Virtual Instrument Engineering Workbench (LabVIEW) was utilised, which is a graphical programming language that uses icons instead of lines of text to create programs.

The appearance and operation of LabVIEW programs imitate physical instruments, such as a spectrogram and control knobs. LabVIEW contains a comprehensive set of tools (National Instruments, 2009a) for acquiring, analysing, displaying, and storing data, as well as tools to help the operator troubleshoot the error. LabVIEW is comprised of a user

interface (front panel), using icons and structures to control the front panel objects and the block diagram which contains the codes.

The computer program developed in this section uses the power spectrum to detect the harmonics of a signal and to examine the frequency response of a system when the spectral content does not change over time. Because the power spectrum is usually estimated by the square of the Fourier Transform, the power spectrum is considered a quadratic frequency analysis method.

For signals with a spectral content that changes over time, this method computes the energy of a signal as a function of time and frequency, resulting in a quadratic time-frequency representation of the signal. Because a quadratic time-frequency representation approximately describes the energy density of a signal in the time-frequency domain, the representation is called a “distribution” or a “spectrogram” (National Instruments, 2009b).

A spectrogram is displayed in an intensity graph as a colour map, from which the spectral content of a signal and how the spectral content evolves over time can be determined. Features of the signal, such as mean instantaneous frequency, can be extracted from the spectrogram and this information can be used in signal analysis, detection, estimation and classification. The time-scale information and the frequency-scale information of the time-frequency representation are recorded separately and presented along with spectrogram.

However, the quadratic time-frequency analysis methods are not reversible, and time-domain signals cannot be reconstructed from spectrograms.

There exist several methods for the Time-Frequency Analysis (TFA) and the most popular are as follows:

- Short-Time Fourier Transform (STFT) spectrogram
- Gabor spectrogram
- Adaptive spectrogram
- Wigner-Ville distribution (WVD)
- Choi-Williams distribution (CWD)
- Cone-shaped distribution (CSD)

7.5 STFT Spectrogram

The STFT spectrogram is the normalised, squared magnitude of the coefficients produced by the STFT. This approach has a number of attractive features which have been chosen as a suitable technique for this study. Normalisation makes the STFT spectrogram obey Parseval's energy conservation property (National Instruments, 2009b) that makes the energy in the STFT spectrogram equal the energy in the original time domain signal. Therefore, energy of the ship's motion responses recorded through a time series are preserved. It is also possible to estimate the spectral content of a signal, and how the spectral content evolves over time, by seeing where the energy is concentrated in the STFT spectrogram.

The other advantage of a STFT spectrogram over the alternative quadratic time-frequency analysis method is that it is considered to be simple and fast. This makes it a suitable technique for online monitoring purposes, where simplicity and computation time are two main concerns.

However, a STFT spectrogram may not be as superior as the other methods in providing a fine time-frequency resolution as a result of window effects, but its output would be sufficient for the online monitoring and its application.

This deficiency can be resolved by the reassignment method to improve the time-frequency resolution of the STFT spectrogram artificially. In this method the energy is automatically concentrated toward the centres of gravity of the signal components, with the assumption that the energy of the signal is tightly concentrated. However this improvement can bias the location of spectral peaks, merge distinct spectral components, falsely split compact signal components, or excessively sharpen naturally blurred signal components in the resulting time-frequency representation (National Instruments, 2009b).

7.6 Development of Computer Program

A computer program shown in the Figure 7.4 is developed on the basis of the STFT concept to fulfil the objectives of this study. The STFT is applied in the time-frequency domain and discovers characteristics of time-varying signals that are not obvious in the time domain or in the frequency domain alone.

The software requires the following information as input:

- No. of samples per second, for detection of fine frequency peak and adjacent frequencies
- Window length for detection of fine frequency peak and adjacent frequencies
- Time steps which define the number of rows in frequency abscissa by dividing the number of samples by time steps
- Frequency bins which define the number of bins and directly affect the resolution

The details of the window information and sampling effect on the quality of detection are given in Section 7.7.

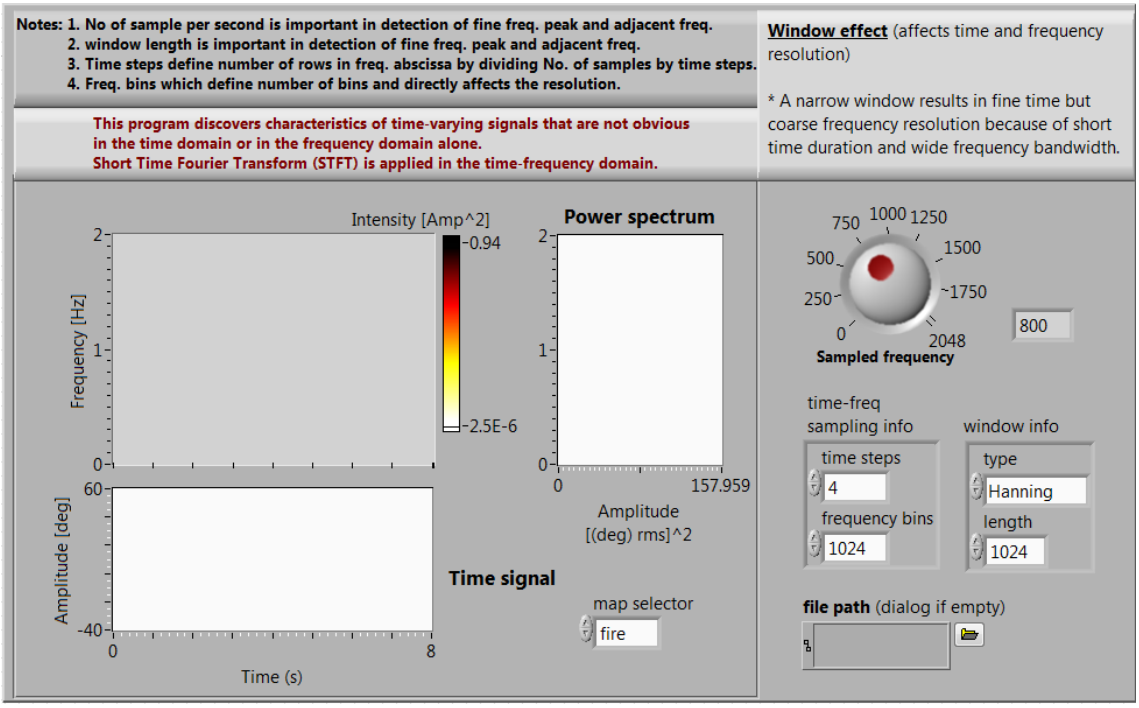

Figure 7.4 Real time monitoring of frequency peaks and associated magnitude of ship motion responses

In Figure 7.4, the top left window is an intensity graph which returns the quadratic time-frequency representation of a signal, and each row corresponds to the instantaneous power spectrum at a certain time. The attached intensity bar illustrates the strength of the signal presented. The lower window depicts the sampled time signal and the right window shows the corresponding frequencies of the sampled signal obtained by FFT.

7.6.1 Detection of Wave Influential Parameters

For online monitoring of a large roll motion, a relatively reliable and fast method is required to predict wave peak frequencies and associated magnitudes. By referring to Figure 7.2 we can realise that a timeframe of eight minutes is rather long, and a ship could have been lost if it is left in a critical situation. However, by the computer program developed in the last section, detection and estimation of peak frequency and associated amplitude can be achieved in less than a minute (Enshaei, 2013). The data utilised in these analyses are the recorded heave, pitch and roll motions in the form of discrete time-varying signals.

A sampled heave power spectrum of a signal analysed for the duration of eight minutes from Chapter 6 is shown in Figure 7.5. A portion of this eight-minute signal is utilised to run the STFT computer program in order to observe the quality of spectrograms in detecting the signal in shorter time. Figure 7.5 compares the spectrograms of three different runs of eight, fourteen and twenty seconds' duration. It is obvious that accuracy of the frequency distribution detected by the power spectrum chart improves as the time sample becomes larger.

Distribution of energy is also refined in spectrograms when the recorded time signal is larger. Detection of the frequency peak is more accurate and sharpens as shown in the lower section of Figure 7.5, having sampled the frequency of 2048.

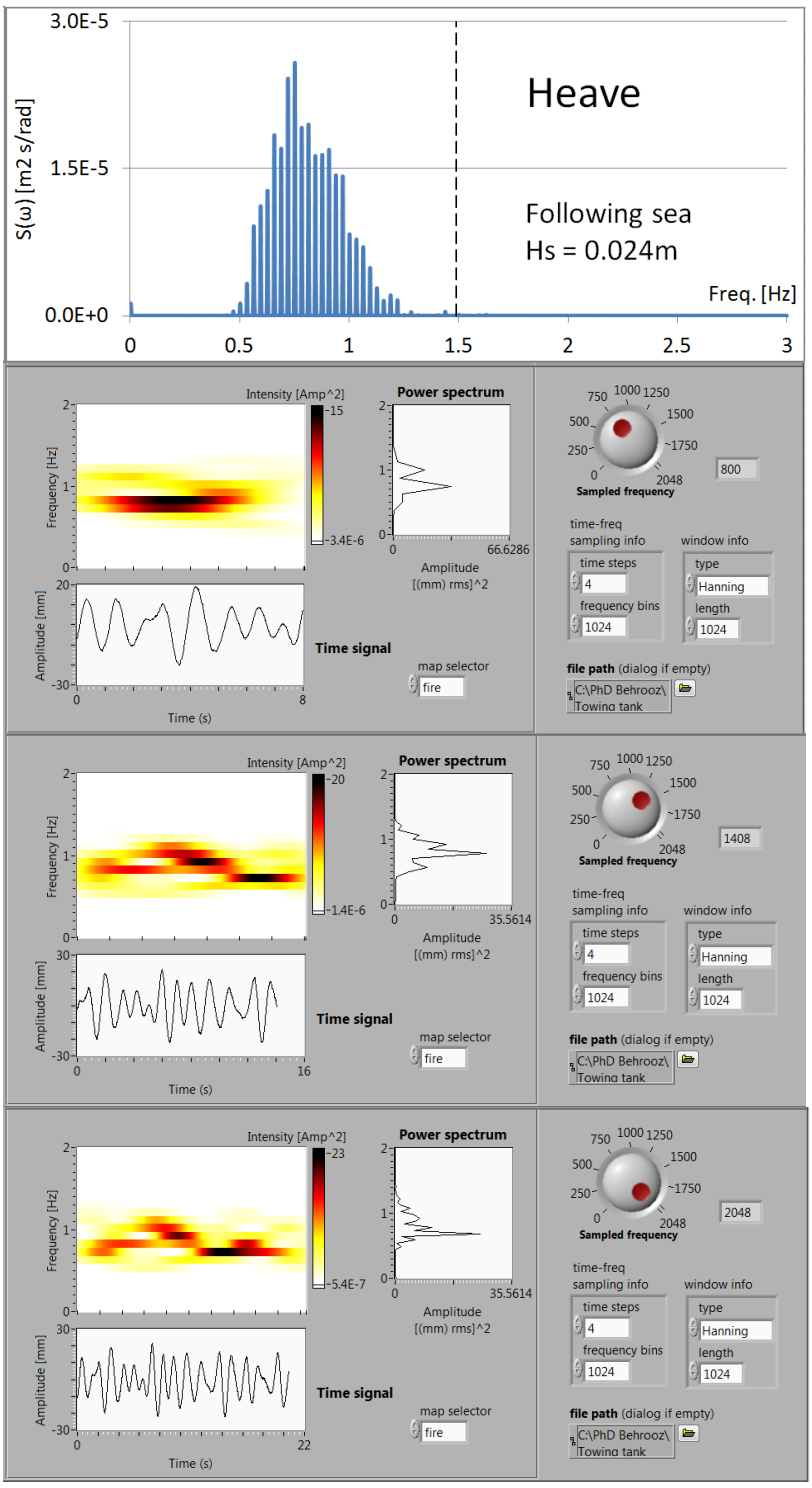

Figure 7.5 Spectrograms of heave motion response in a following sea for three different time durations

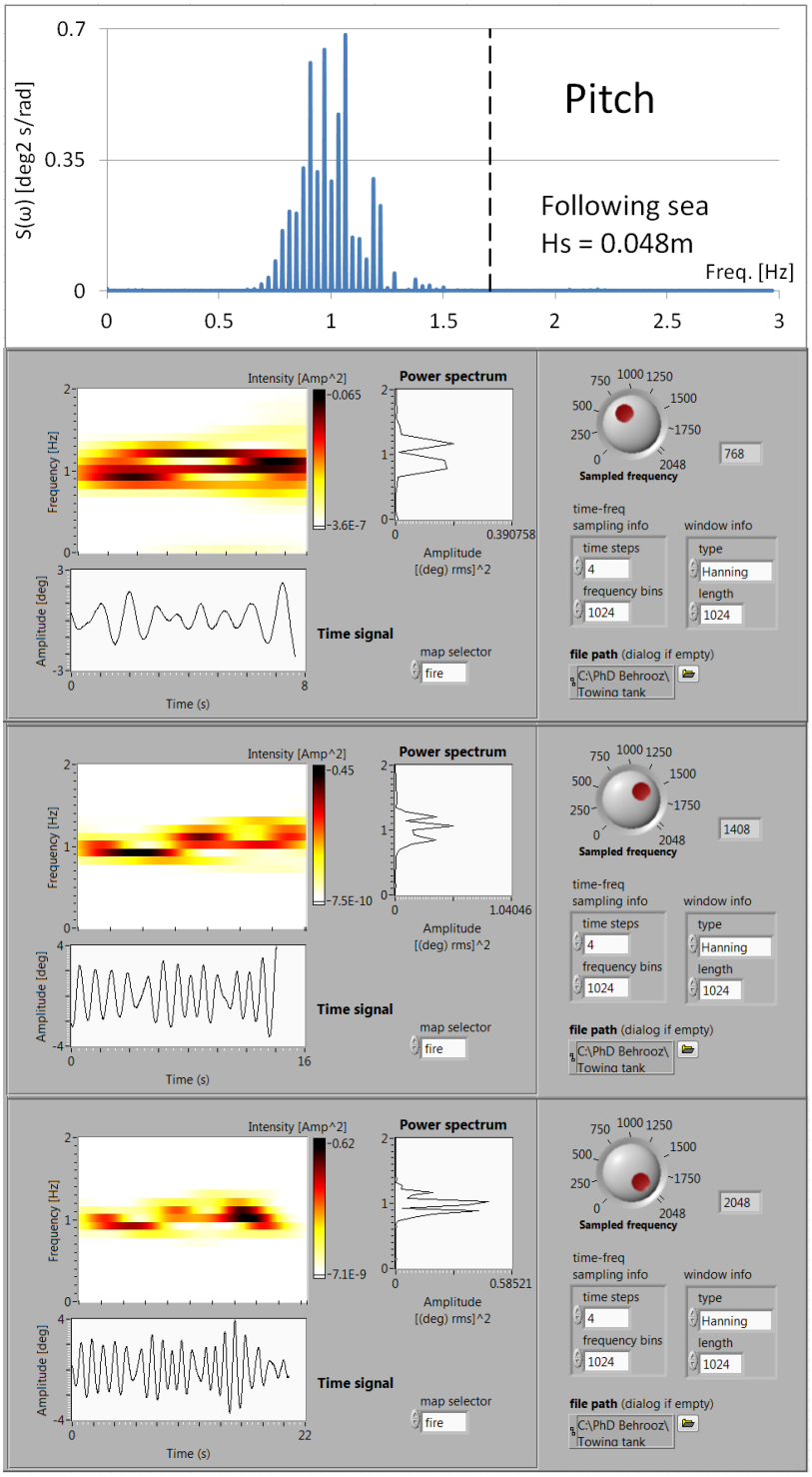

Figure 7.6 Spectrograms of pitch motion response in a following sea for three different time durations

Typical results are obtained in Figure 7.6 for the analysis of pitch motion responses.

The program is capable of detecting two peaks from a recorded signal of less than 8 seconds. It certainly improves by the lower figures when the sampled duration increases to 20 seconds.

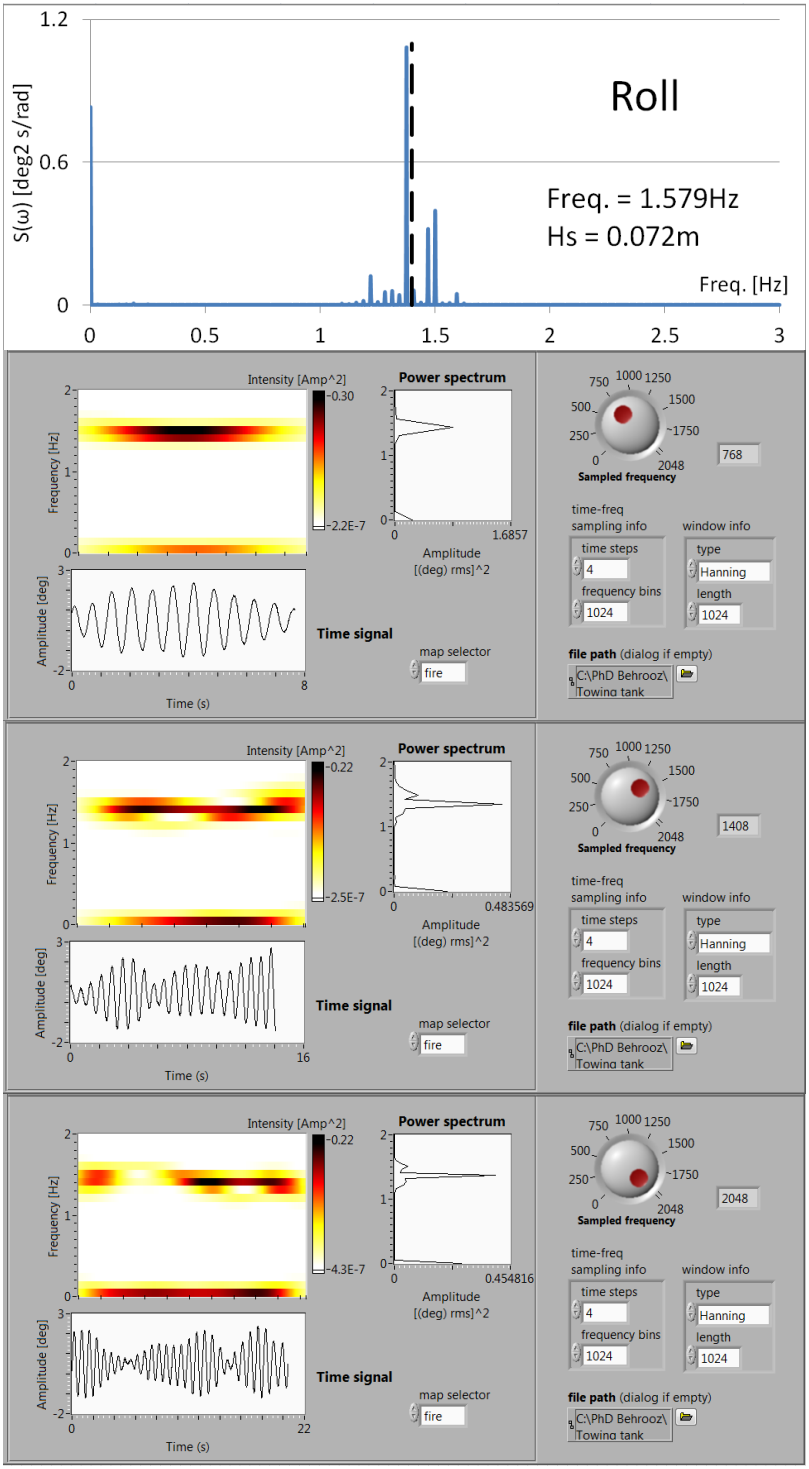

Figure 7.7 Spectrograms of roll motion response in a following sea for three different time durations

Figure 7.7 analyses and detects a sampled roll motion signal. For the means of comparison, all the settings on the right-hand side of the program screen remain unchanged except for the sampled frequency. This signal is also tested in a similar way as the heave and pitch motions depicted in Figures 7.5 and 7.6.

7.6.2 On-Line Monitoring Program

The main objective of detecting the peak frequency of waves through heave and pitch motions is achieved by the computer program developed in this section. This program presents the energy distribution of the ship's motion responses which has been recorded as a signal. It is assumed that signals are received from a motion sensor in the form of discrete time-varying signals. The desired accuracy can be acquired by adjusting the "sampled frequency" knob. Increasing the sampled frequency can improve the resolution of the spectrogram and hence detection of peak frequency. In this program, the options are provided through "sampling info" and "window info" clusters to improve the quality of presentation. The time steps, frequency bins, window type and window length are among those taken into consideration for adjustment.

A test run of this program is shown in Figure 7.8, and the heave and pitch motions are evaluated against a corresponding simulated irregular wave, which was generated in the towing tank. The three rows of the program show the test carried out at different Hs, and the detected peak frequency of heave and pitch motions tracks the wave peak frequency in all cases. The vertical intensity bar alongside each spectrogram indicates the strength of the signal at every moment in time. The magnitudes indicate that the intensity bars are denser as the significant wave height increases.

The proximity of the detected peak frequency to natural roll frequency is an indication of whether a critical situation is developing. It is certainly meaningful for a particular ship, having specific geometry and dynamic characteristics in current loading conditions.

The spectrogram in this program uses the magnitude squared of the elements of the STFT for calculation. In principle, because the FFT returns symmetrical results (the input data are real, in which case the outputs satisfy the symmetry), the spectrogram shows only the left half of the STFT.

Due to the large volume of the results, only one case is shown in Figure 7.8 and the remaining tested conditions are given in Appendix II.

It is to be noted that all the tests, including tests in Figure 7.8, are demonstrated for a sampled duration of 20.5 seconds.

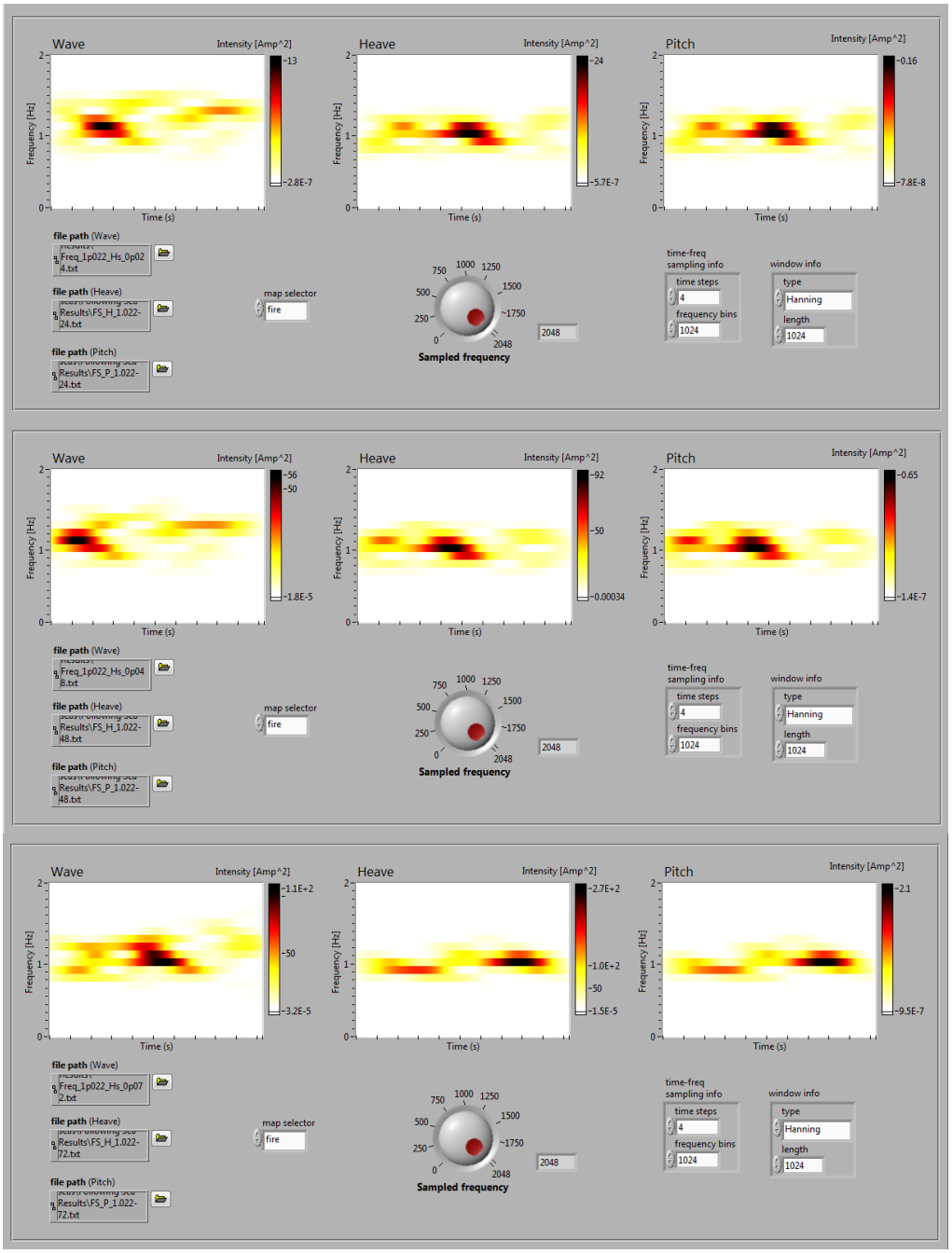

Figure 7.8 Tracking of the wave's peak frequency by heave and pitch motions in a following medium sea with different Hs

7.7 Effect of Window and Sampling on the Quality of Detection

An important feature of a spectrogram is its readability which corresponds to a good concentration of signal components. The type of window and sampling size can influence the visual interpretation, which is necessary for good discrimination between the known patterns. Different types of window are reviewed in Chapter 4 and their effects discussed in the computation of the spectral estimate.

To study the impact of window types, a 20 second sampled signal of pitch motion response has been tested by the on-line monitoring program. The test is conducted with six different window types, and results are shown in Figure 7.9.

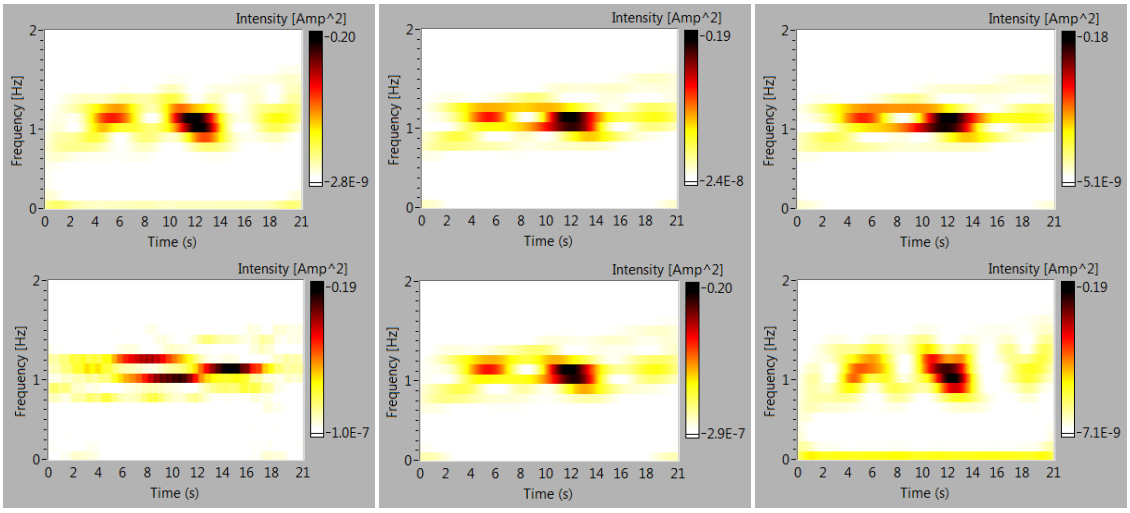

Figure 7.9 Pitch motion in response to an irregular wave, having a peak frequency of 1.022Hz and Hs of 0.024m in a quartering sea.

Concentration of individual components is significant for good resolution in different windows, which directly affects the clarity of display. However, variations in the intensity of detected signals are small and are depicted in the intensity bar of each chart. The type of windows employed in these tests in the row, from top left, are Gaussian, Hanning, Hamming, Rectangle, Blackman-Harris and Flat top. The option is provided in the program for the operator to choose an appropriate window.

Sampling size. The quality of detection is considerably affected by the sample size. Figure 7.10 shows the results of the tests for the same signal utilised in Figure 7.9. The sampled size employed in these tests in the row from top left are 1.3 seconds, 2.5 seconds, 5 seconds, 10 seconds, 15 seconds and 20 seconds. It is apparent that the variation in magnitude is significant and improves as the sample becomes larger. It is worth mentioning that the result can also be influenced by the sampling rate, which is 100Hz in these scenarios.

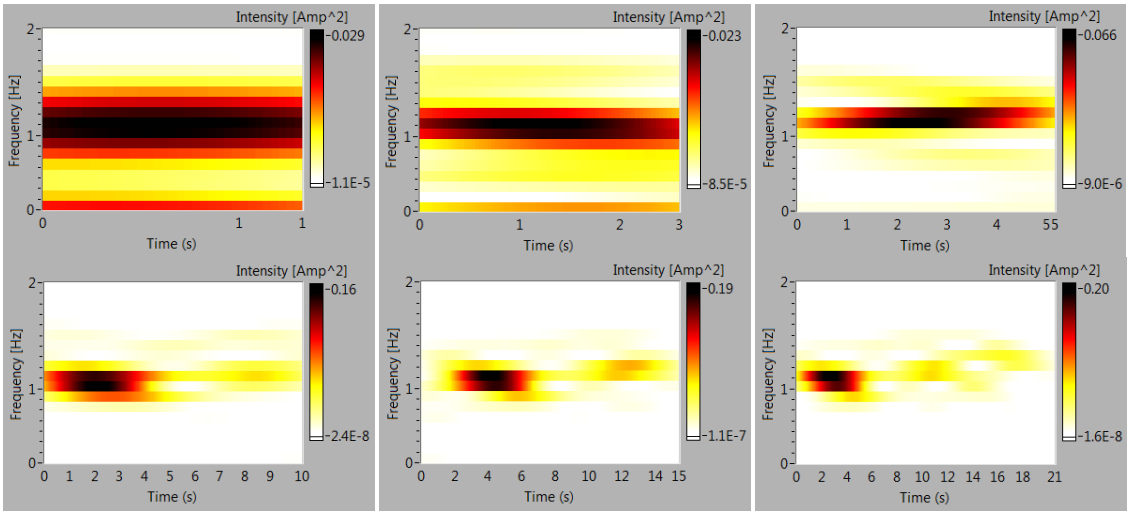

Figure 7.10 Effect of sample size on the quality of detection. The window type used is Hanning.

Window length shapes the time resolution and the frequency resolution of the STFT. A narrow window results in a fine time, but a coarse frequency resolution, because of the short time duration and wide frequency bandwidth. However, a wide window results in a fine frequency but a coarse time resolution. Therefore, the window length should be calibrated for optimum concentration and obviously better resolution. Different window lengths are applied to the energy-density distribution of the signal utilised in Figure 7.9 and the results are shown in Figure 7.11. It is obvious that the frequency becomes coarse once the time duration is shorter. The window length employed in these tests from left is 2.5 seconds, 5 seconds and 10 seconds.

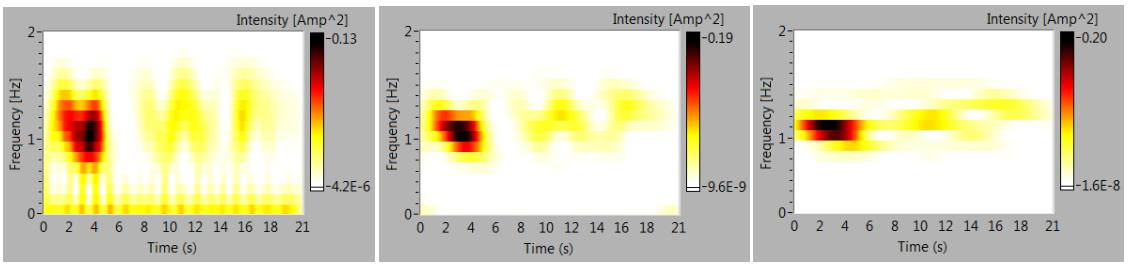

Figure 7.11 Effect of window length on the quality of detection. The window type used is Hanning and sample size is 20 seconds.

The frequency bin specifies the FFT size of the STFT. The frequency bin defines the number of bins, which directly affects the resolution and is described as the ratio of sample size to number of samples. It should be adjusted for optimum concentration and improved resolution. The energy density distribution of a roll motion response is utilised in testing at different frequency bins and is depicted in Figure 7.12. It is apparent that a

higher resolution improves detection of the peak frequency with increased accuracy. The frequency bin employed in these tests from left is 256, 1024 and 2048.

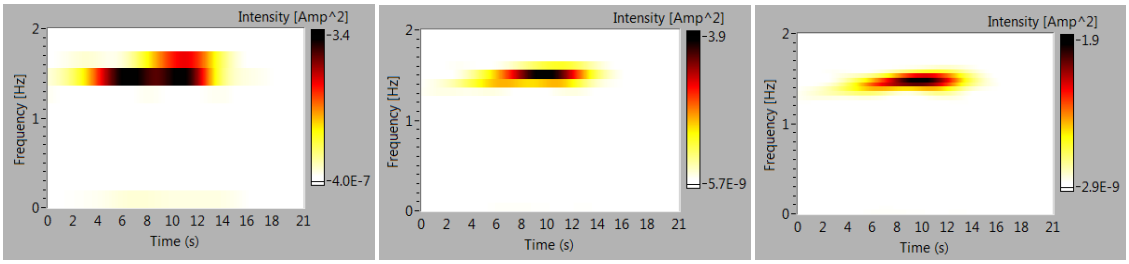

Figure 7.12 Effect of frequency bins on the quality of detection. The window type used is Hanning and window length is 10 seconds.

7.8 Automated control system

Ships' operators are concerned with the understanding and controlling of segments of their environment, often called systems, to provide useful marine products. In this approach, when understanding of the dynamics of the ship increases, the ability to control the system will also increase. One of the present challenges is the modelling and control of modern, complex and integrated systems such as real-time monitoring to be integrated with auto-steering systems.

A control system could be developed based on the fundamental of feedback theory and linear system analysis. Such a system with the theories developed in this thesis is presented in Figure 7.13. It has been designed with the view of using ship motions for the estimation of current sea conditions, and to establish a causality link between the two. It shows an interconnection of components forming a system that will provide a desired system response ($\Delta\omega_0$). Because the desired system response is known, a signal proportional to the error between the desired and the actual response ($\Delta\omega$) is generated. The use of this signal to control the process results in a closed-loop sequence of operations.

The closed-loop sequence of operations depicted in Figure 7.13 consists of measurements, comparison, controller, process and output. This system automatically adjusts the ship's heading by alteration of the course to maintain the desired output and hence to increase the level of ship safety to avoid extreme roll motions from developing. This will maintain the defined difference between roll natural frequency and the estimated wave's peak frequency.

To improve the ship's safety by an automatic system, the introduction of feedback is often necessary (Dorf, 2011). In this case this could have the following advantages:

- Decreased sensitivity of the system to variations in the parameters of the process
- Improved rejection of the disturbances (i.e. wind, wave and current)
- Improved measurement noise attenuation (e.g. machinery noise and vibration)
- Improved reduction of the steady-state error of the system

The control system of Figure 7.13 has two operational functions:

1. Manual operation: The operator can slightly change the ship's heading manually in order to visually observe the changes in $\Delta\omega$ and hence to monitor the proximity of the irregular wave's peak frequencies to the natural roll frequency. This available information is helpful to the navigator in respect of decision-making which provides valuable information in ample time.
2. Automatic operation: The estimated wave's peak frequency through a ship's motion responses is compared with the natural roll frequency to produce an output signal. The closed-loop system uses a measurement of the output signal, and in comparison with the desired output, generates an error signal. This signal is used by the controller to adjust the steering system which acts as an actuator to maintain the desired output $\Delta\omega_0$.

This system uses the characteristics and advantages of introducing feedback where benefits can best be obtained from the single-loop system and then extended to multi-loop systems. Using the notion of a tracking error signal, it will be readily apparent that it is possible to utilize feedback with a controller in the loop to improve the system performance.

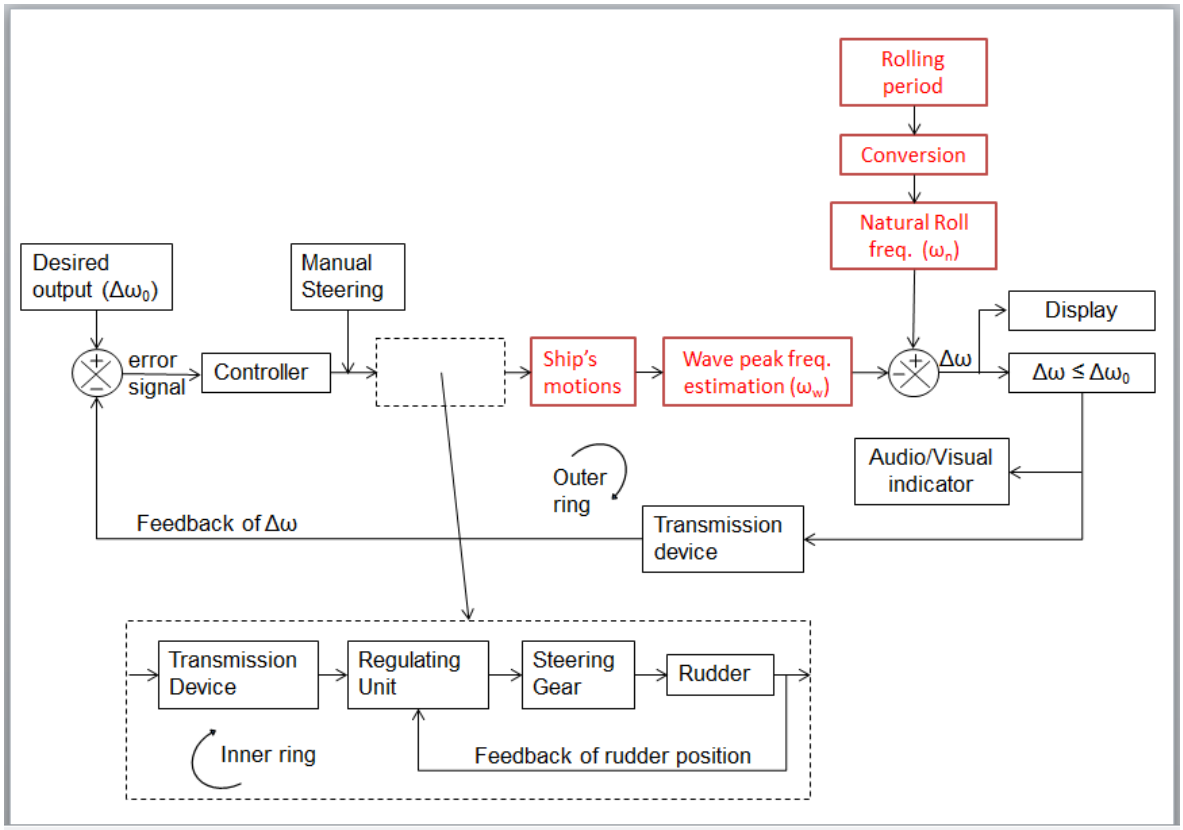

Figure 7.13 Proposed closed loop automatic control system to avoid extreme roll motion

This control system is the synergistic integration of mechanical, electrical and computer systems, leading to a new breed of intelligent products. This feedback control encompasses the aspects of five key elements:

1. Physical systems modelling
2. Sensors and actuators
3. Signals and systems
4. Computers and logic systems
5. Software and data acquisition

7.9 Summary

This chapter has proposed signal processing techniques utilised in analyses of data obtained in Chapter 6. Different methods were discussed and some of their features were explored. The STFT is found to be one of the most practical methods to be employed with a number of attractive features associated with it.

This method has proved to give representative results, which encapsulate the characteristics of the ship's motion responses that lead to the prediction of wave-influential parameters.

The On-Line Monitoring program developed on the bases of the STFT is capable of predicting a wave's peak frequency and associated magnitude. The experiments show the sensitivity of the program in choosing the correct window function and the tuning of the system for the optimum readability.

The on-line monitoring system is integrated into a closed loop feedback to make an automatic control system to improve ship's safety.

Chapter 8

Conclusions and Recommendations

8.1 Compliance of numerical and experimental results against theory

The basic statistical concept, which was discussed in section 3.2.1, suggests that irregularity of the seaway produces a low, wider histogram which can be modelled theoretically by the Rayleigh function. The numerical data utilised for generating the seaway through the SESAM program follows the same theory. The spectrum shown in Figure 8.1 is one of those seaways generated using recorded waves on the basis of the Rayleigh function which has been employed as an irregular wave to induce motions. Therefore, the underlying principle for the entire numerical analysis of the motions of the containership model follows the same mathematical concept as used in the Rayleigh function.

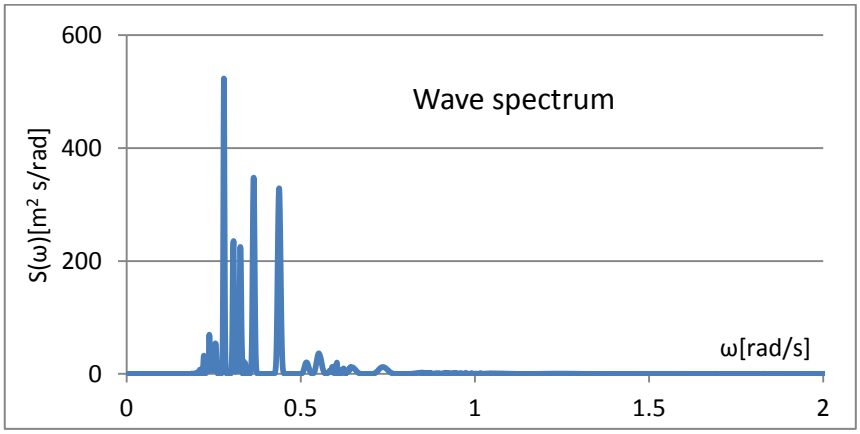

Figure 8.1 Wave spectrum generated by SESAM at stationary with Hs=6m and modal period of 20s

Prior to using the wave spectrums generated by the mechanical wave maker in the towing tank, the recorded wave heights were examined to check in compliance with the

Rayleigh concept; the diagrams are given in figure 3.2. Therefore, the entire experimental analyses to study the motions of the model ship are in line with the theoretical and numerical analysis discussed above.

In the application of the spectral theory it has been realised that ocean waves can be described in terms of a spectrum. The spectrum provides the distribution of wave energy among different wave frequencies on the sea surface. Therefore, spectral analysis can also be effectively used as a suitable tool to study the ship's motion responses.

The Pierson Moskowitz Spectrum (PMS) was used throughout this thesis for the analysis of numerical and experimental data where much useful information can be derived. Prior to employing the PMS for experimental tests, the output characteristic of the spectrum produced by the wave maker was compared against a mathematical model details of which are discussed in section 6.4. Despite a slight difference in appearance, the variance and mean remained the same for every test condition.

In this approach, by analogy, graphs of the square of the amplitude of the ships' motions (e.g. heaving, pitching and rolling) as a function of frequency were generated, on the basis of the influence of the amplitude of a particular wave component. The results of the wave and motion response spectrum are discussed in Chapter 5, 6 and 7 where the following statistical information was taken into consideration:

- Distribution of energy against the range of frequencies
- The energy content at different frequency bands
- The modal frequency at which the maximum energy occurs

The forward speed of the ship had significant effect on the distribution of frequency, and hence the wave energy. It has been pointed out in the literature that in the case of a head sea condition the energy is spread out over a wider band of higher frequencies, while for a following sea the energy tends to be concentrated in narrower bands and at low frequencies. However, the spectral density becomes infinite at the frequency of encounter. Figures 8.2 & 8.3 shows the spectrum encountered by the ship in identical sea conditions, the difference being that in figure 8.2 it is a head sea and in figure 8.3 a following sea. These results are a confirmation of the above theory, which have been used in all the defined scenarios analysed in this Thesis.

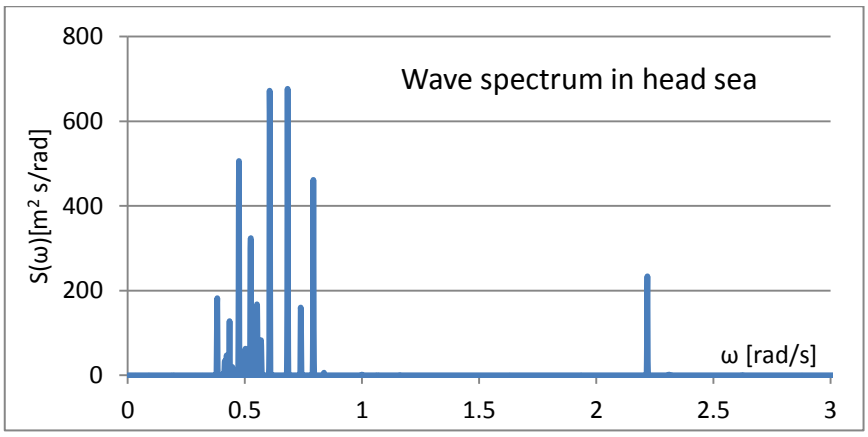

Figure 8.2 Wave spectrum generated by SESAM in a head sea with a speed of 10m/s, Hs=6m and modal period of 15s

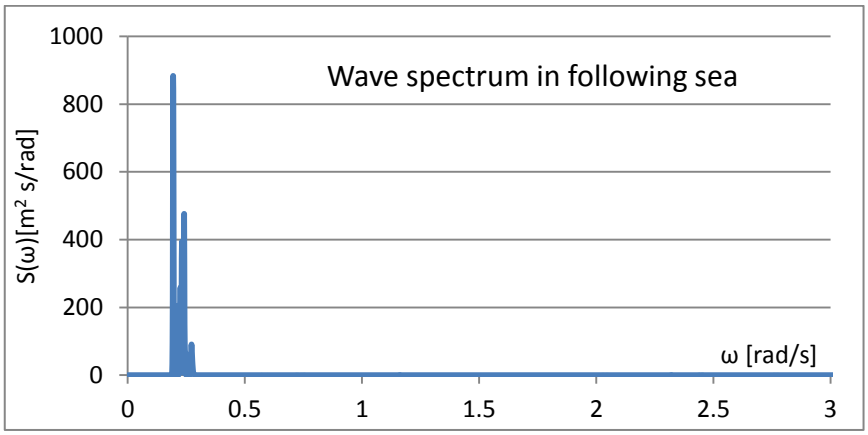

Figure 8.3 Wave spectrum generated by SESAM in a following sea with a speed of 10m/s, Hs=6m and modal period of 15s

In this thesis the detection of a signal from the time average of the recorded ship's motion is based on the Parseval theorem given in section 4.2.2. This theory confirms that spectral analysis by Fourier transformation is energy conserved, and therefore the area under the spectrum represents the average energy of random waves with respect to time.

The energy of the peak frequency utilised in decision-making by an on-line monitoring tool follows the same principle. In such a tool the relation between time and frequency behaviour is graphically presented by the spectrogram discussed in sections 4.4.6, 7.4 and 7.6.2. The spectrogram uses the magnitude squared of the elements of the STFT for calculation. This approach has two attractive features as it is simple and fast and provides suitable technique for online monitoring purposes. It obeys Parseval's energy conservation property in that it makes the energy in the STFT spectrogram equal to the

energy in the original time domain signal. Therefore, the energy of the ship's motion responses, as recorded through a time series, is preserved. Furthermore, it should be noted that increasing the sampled frequency and using a larger time signal improves the resolution.

8.2 Conclusions

This thesis investigates the dynamic behaviour of a ship at sea, focusing on indirectly monitoring the gradual adverse changes of the seaway through a ship's measured wave-induced motions. The research is organised to contribute to the development of real-time operational safety guidance by the IMO in order to avoid dangerous situations at sea.

Firstly, priority was given to several earlier studies with regard to the provision of operational guidance. The concept of each method was explored and the relevance of identified key parameters was discussed. The study highlights the operational applicability of such methods and indicates the trend of generalising them towards a common goal in the form of enhanced IMO guidance. The current IMO guidance has been in place for a number of years but could not achieve its ultimate goal because of several limitations, which have been discussed in detail in this thesis. This has triggered consideration of a new way of looking at a ship's dynamics in order to address the current and latent operational needs.

Secondly, this thesis highlights the need to account for the possibility of alternative theoretical methods in the modelling of environmental conditions, as well as in the modelling of the corresponding motion behaviour of a ship. Through the usage of statistical methods many physical parameters, such as wave heights, were studied. These methods have been integrated into the advanced numerical analysis that has also been employed. A further analysis of a ship's motion response among the waves has shown that linearization can result in a significant improvement in the understanding of the dynamic behaviour of ships at sea. Some of the more influential wave parameters can be explored through the same methodology, including those parameters which have the greatest impact on a ship's motions.

Thirdly, in response to the aims and objectives of this thesis, a novel methodology has been proposed in order to make the operation of a ship safer. This method is able to

demonstrate some of the influential wave parameters through the monitoring of a vessel's heave and pitch motions and is capable of detecting and determining the gradual changes in sea conditions. Knowledge of these changes will provide adequate information for warnings should the ship encounter a potentially dangerous situation.

Fourthly, a series of ship motions' test scenarios were conducted numerically through application of the well-known Boundary Element Methods (BEM). These tests were intended to pursue the objectives of the study and to confirm whether there are any links between the responses of a ship's motions and irregular encountered waves. The results were validated by the results from a series of experimental tests that were carried out on a model ship in a towing tank. The comparison of the results of these two tests provided a good indication of the amount of uncertainty within these methods.

A fundamental assumption in the established determination of the motion responses of ships in an irregular sea is based on linearization, and thus that responses are taken to be linearly proportional to the wave excitation. It has been shown in this research that this assumption is no longer acceptable for the modelling of some of a ship's motions. The findings of the research have an important impact on the applicability of the proposed methodology to indirectly monitor the gradual changes of the seaway, and hence help considerably in avoiding potentially dangerous situations.

Finally, in response to these findings, a signal-processing based computer program has been developed for detection purposes. This program can detect the influential parameters within a ship's motions that have been recorded in the form of a continuous signal in a fraction of a minute. This results in a reliable advisory tool for providing adequate information to the ship's crew in ample time for them to make prudent operational decisions.

In fulfilling the overall aims of this research, the following objectives have been achieved:

1. Current methodologies for operational safety to reduce the risk when encountering heavy weather have been reviewed, with the main focus being on the ship's motions responses.
2. A rigorous nonlinear BEM approach that is suitable for analysing the motion behaviour of ship in diverse sea conditions was chosen, and a series of scheduled tests have been carried out.

3. Validation of the numerically-tested results was carried out through a series of experimental model tests in a towing tank, investigating the effects of the wave's influential parameters on the ship's motions responses.
4. Reviewing methods have been developed that are available for the detection and analysis of signals in the shortest possible time, and which should be both simple to use and reliable in their function.
5. An on-line monitoring tool has been developed which can monitor and analyse the currently-experienced sea conditions, and to provide advisory support to the crew.

Suitable techniques need to be employed whilst at sea in order to shed a light on the detection of a wave's most influential parameters. There are certain parameters which are influenced by the sea conditions, and their detection can reflect the status of the current irregular waves that are being encountered. The monitoring of the gradual changes that are taking place in a seaway, and the consequent impact on the ship's response, provide invaluable information to the master of a ship, prior to his making calculated operational decisions.

It is challenging to measure and then monitor the environmental disturbances while a ship is underway and, as a result, it is difficult to predict their impact on the ship's dynamics both current and future. That situation becomes even more complicated while operating in severe sea conditions.

The evidence from the numerical analyses undertaken in Chapter 3 suggests that the assumption of a Rayleigh probability distribution can reasonably predict the amplitudes of motions even in severe sea conditions. Therefore, statistical analyses are a reasonable way for the prediction of a ship's motion characteristics. However, the significant predictions from these kind of analyses is more useful for design criteria rather than for operational purposes.

The study has made good progress towards developing on understanding of spectral applications in the measurement of motion responses as discussed in Chapter 4. The application of linear superposition in order to model an irregular seaway is discussed for the analysis of ship motion responses, and reviewed in detail. This is a conventional method that is employed, for example, for testing a model in a towing tank, or to develop

a numerical algorithm from which to run a simulation to derive Response Amplitude Operators (RAO), which are transfer functions. There have been several attempts made by researchers to develop on-line monitoring systems through this methodology, yet there are still some weaknesses that need to be addressed before it becomes a practical and reliable system.

The assumption of linearity in this method is the limiting factor in its applicability, and which increases the uncertainty in the ship's motion predictions in severe sea conditions. However, the spectral analyses that have been employed in this method of approach can reveal many aspects of the ship's behaviour, and which have been unrecognised for many years.

In order to perform good estimates of a wave spectrum, the directional wave spectrum has been considered in some studies. This concept is thus utilised in the prediction of the motion responses of a stationary ship on the basis of previous dynamic knowledge. In this method of approach the ship is considered to behave in the same as a wave rider buoy when subjected to waves. The dynamic behaviour is achieved either by model testing, by analytical methods, or by other numerical analyses.

Two alternative methods of parametric and non-parametric assessments are reviewed in Chapter 3 for the estimation of a directional wave spectrum. Although both concepts are a function of frequency however, different approaches are utilised. The case studies demonstrate that the spectrum is smoothly changing in the frequency range as well as allowing for a change in the heading direction. However, a number of important limitations still need to be considered, such as non-linear effects, and variations in ship deadweight loading conditions need to be taken into account. It is to be noted, however, that this method of approach is not very effective at high frequencies, where it would need to be used with caution.

Although many research studies have summarised the application of different approaches for analysing the motion responses in detail, there is still a lack of meaningful information provided in order to describe fully such studies in the context of an irregular sea. Therefore, the reliability of such approaches to predict the motion responses adequately could be questioned.

In response to the various questions that were raised from the review of literature that has been undertaken and summarised above, a novel methodology was introduced in Chapter 4. In order to understand better the dynamic behaviour of a ship, and to identify links between the sea state and the motion responses, two distinct methods of numerical analysis and model testing were proposed. In the initial approach, and in response to the research questions, comprehensive numerical experiments were utilised and undertaken using the boundary element method (BEM). This method was selected as it could provide a set of case study data pertaining to the nature of a ship's motions in response to different sea conditions. In order to ensure that the numerical analyses were comprehensive and the results reliable, a number of simulated scenarios were scheduled. Each simulated test was capable of taking into account the sea conditions, wave angle of attacks, and to allow for the inclusion of forward speeds. It is of prime importance to define wave spectrum parameters accurately, the numbers of panels defining the hull surface, and the integration method for the computation of the both the modelled ship and the modelled sea surface behaviour.

Therefore, Chapter 5 summarises in detail the approach that was used to investigate the particular wave-influential parameters through the ship's motion responses. A rigorous modelling approach was developed that considers the influence of the ship's various geometric properties and loading conditions, and that provides an adequate recognition of the factors which affect the motion responses. The general modelling approach in this environment is running with different ship speeds, and it uses elementary Rankine sources distributed over both the mean wetted surface and the mean water free surface in order to determine the hydrodynamic forces.

In the second method that was discussed in Chapter 4, actual physical scale model testing was suggested as a means to validate the results of the numerical analyses that were obtained in Chapter 5. In line with the numerical analyses, a set of experimental approaches was chosen for a systematic set of motion tests to be performed with a model ship. To avoid any questionable simplifications, and to test the model in similar conditions to an actual natural sea, the experiments were carried out in simulated irregular waves, which were generated in a towing tank. Although the measurements made during these tests recorded the full six degrees of freedom motions, only heave,

pitch and roll motions, together with incident waves, have been analysed. The results are presented in Chapter 6 and there, discussion is focused on the key parameters of frequency peak and power peak of the motion responses.

Determination of the power spectral density was used, as a popular tool, to analyse the heave and pitch motions as well as the corresponding mechanically-generated irregular waves in the towing tank. The most obvious findings that emerged from these analyses are the detected patterns within the ship motions, which were seen to track the corresponding wave spectrum. As a result, the peak frequency of the wave can be estimated by reference to the ship's motion spectrum in conditions where it is difficult to actually measure the waves.

One of the most significant of the findings to emerge from this study is that the roll motion maintains its highest oscillations around the natural roll frequency in all sea conditions, regardless of the heading angles. This fact could be used as a means for measuring parameters in monitoring the gradual changes of a developing sea state, and hence changes of the wave's peak frequency, in order to avoid large roll motions.

This study has given a review of, and the reasons for, the widespread use of signal processing techniques in the detection of frequency peaks and associated magnitudes. Ship motion is a time-varying phenomenon and it can be readily measured by suitable sensors and recorded as discrete continuous time signals. Therefore, signal processing techniques are an acceptable tool to analyse such signals for providing information for operational purposes.

Due to a number of attractive features that are associated with short time Fourier transform (STFT), this method has been proven to provide a good representation of the recorded signals and corresponding analysed results. The STFT method has been confirmed in that it is capable of predicting wave-influential parameters through characterisation of the ship's motion responses. In a series of test runs, STFT proved that the results of analysed motions, which were recorded and presented in Chapter 6, were detected with reasonable accuracy in a fraction of a minute.

This study was completed by adapting a computer program that was developed on the basis of STFT for predicting the currently-encountered wave's peak frequency and its associated magnitude. The program was made simple to use in order to become user-

friendly for less computer-skilled operators, particularly those working in a stressful situation which may exist when a vessel is experiencing rough seas. However, further accurate tuning is required in order to overcome the sensitivity of this method to certain parameters.

Bearing in mind that the main objective of the study was to explore the effects of encountered waves on the responses of the model, the following conclusions were drawn:

1. Continuous monitoring of motion responses has been demonstrated to be a good performance indicator in order to watch for the development of critical situations, and hence a potential adverse reduction in stability.
2. It was concluded that the frequency peak and its associated magnitude are the two most important inherent characteristics of encountered waves, and that their detections could be utilised to limit the potential for large roll motions developing at sea.
3. Heave and pitch motions are strongly coupled and their spectral pattern copies the wave spectral pattern in the majority of cases. Therefore, wave peak frequencies and their associated magnitudes can also be estimated through these motions.
4. To increase the safety of a ship, and in particular to avoid large roll motions from developing, it is essential to keep the natural roll frequency away from the estimated wave's peak frequency.
5. The evidence from this study suggests that STFT is a suitable method for the detection and estimation of a time-varying signal of motion responses. The instantaneous frequency (IF) and magnitudes of heave, pitch and roll motions could be obtained through signal-processing techniques.
6. One of the most significant of the findings that have emerged from this study is that the detection of peak frequencies of wave systems and associated magnitudes of model ship motions can be achieved in less than a minute.

The findings of this study have a number of important implications for future ship operational practices:

1. A modest investment in equipment and training for the ship owner is required.
2. The avoidance of high roll motions can provide the opportunity to expand the operation at sea whilst the ship is making way through the water. An operation such as the processing of commodities is considered to be the latest area of research with the greatest economic implications.
3. Criteria for warnings of developing undesirable events can be initiated on board in real-time, and which raise an alarm when acceptable risk levels are being exceeded.
4. It is important to be able to evaluate the vulnerability of a ship to motion responses by detecting components of encountered frequencies and their corresponding magnitude.
5. It provides a tool for the master to consider and evaluate the effects of alteration of course and speed, which has an immediate and effective impact on encountered frequency.
6. The time history of motion behaviour that is maintained by the program can be implemented in line with IMO guidance as instructed by MSC 707.

8.3 Recommendations for Future Work

The stability status of a ship changes during operations, and the decisions that are taken regarding the maintenance of sufficient stability should not rely solely on the experience of the master. It is important that the master should be made aware of a developing critical and probably stressful situation that could result in the stability condition deteriorating, thereby maximising the time that is still available for him to take corrective action by means of altering the course and/or speed.

Thus, if this debate is to be progressed in order to improve ship safety, a better understanding of different ship hull responses in extreme conditions needs to be developed. More broadly, research is also needed to consider the effect of length, displacement and loading conditions and other dynamic factors, such as the effects of transient green seas and spray, high winds particularly on the beam of the ship, and the movement of liquids in slack tanks with the two different effects of slushing and free surface effects.

References

Akaike, H. (1980) 'Likelihood and Bayes procedure. In Bernado, J.M., Groot, M. H. D., Lindley, D. U. And Smith, A. F. M. (editors), Bayesian statistics, University press, Valencia. ', pp. 143-166.

Altes, R.A. (1980) 'Detection, estimation and classification with spectrograms', *The journal of Acoustical Society of America*, 67(4), pp. 1232-1246.

Arias, C. (1998a) 'Definition of relevant design cases and operation scenarios. DEXTREMEL Report. Report No DTR-2.0-AESA-07.98, Rev. 1'.

Arias, C. (1998b) 'Selection of design cases and operation scenarios. DEXTREMEL Report. Report No DTR-1.0-AESA-03.98, Rev. 2'.

Aschehoug, M. (2003) 'Scientific paper on the sea state estimation methodology', *Technical report, SIREHNA, France*.

Basu, J.K., Bhattacharyya, D., Kim, T. (2010) 'Use of artificial neural network in pattern recognition', *International Journal of Software Engineering and Its Applications*, Vol. 4, No. 2.

Belenky, V., Ottodekat, J. et al (2008) 'Toward Performance-Based Criteria for Intact Stability', *Marine technology*, 45(2), pp. 101-123.

Bhattacharyya, R. (1978) *Dynamics of marine vehicles*.

Boashash, B. (1992) 'Estimating and Interpreting the Instantaneous frequency of a signal-part II. Algorithms and Applications', *PROCEEDINGS OF THE IEEE*, 80(4).

Boashash, B. (2003) 'Time-Frequency signal analysis and processing', *Prentice-Hall, NJ, USA*.

Christopher, C.B., Belenky, V., Bulian, G., Francescutto, A., Spyrou, K., Umeda, N. (2009) 'A review of available methods for application to second level vulnerability criteria. ', *STAB2009*. StPetersburg-Russia. pp. 111-128.

Cleary, W.A. (1975) 'Marine stability criteria', *Workshop on human factors, synopsis by the moderator S.Allen STAB 94: 5th international conferece on stability of ships and ocean vehicles, Melbourne, Florida.*

Cowley, J. (1988) 'Passenger ship legislation', *IME conference*, IMAS'88, London.

Cramer, H., Stefan Kruger, S., Sanslzon, J. (2003) 'Working towards the design of safer ships and pragmatic support for safe operation', *Proceedings of the 8th international conference, STAB2003, Madrid-Spain*, pp. 155-169.

Daubechies, I. (1990) 'The wavelet transform, time-frequency localization and signal analysis', *IEEE Transactions on Information Theory*, 36(5), pp. 961-1005.

De kat, J.O., Thomas, W. L. (1994) 'The use of numerical simulation tools in the derivation of operational guidelines for severe weather conditions. Workshop on manoeuvring and survival in storm seas', *STAB 94: 5th International conference on stability of ships and ocean vehicles, Melbourne-Florida.*

DNV (2007) 'Environmental conditions and environmental loads', (Norway).

DNV (2011) 'Wasim - Wave loads on vessels with forward speed', version 5.1-01(Norway).

Dorf, R.C., Bishop, R.H. (2011) 'Modern Control Systems', Pearson education, twelfth edition.

Emin, K., Atlar, M., Incecik, A. (2004) 'An experimental study of motion behaviour with an intact and damaged Ro-Ro ship model', *Ocean Engineering 31*, pp. 483-512.

Enshaei, H., Birmingham, R. (2012a) 'Monitoring of dynamic stability via ship's motion responses', *Proceedings of 11th International Conference on the Stability of Ships and Ocean Vehicles 23-28 Sept, Athens, Greece*.

Enshaei, H., Birmingham, R. (2013) 'The application of signal processing techniques for real-time monitoring of the dynamic stability of a ship via its motion responses', *Proc IMechE Part M: J Engineering for Maritime Environment*, 227(2), pp. 114-124.

Enshaei, H., Birmingham, R., Mesbahi, E. (2012b) 'Identification of influential parameters in a ship's motion responses: a route to monitoring dynamic stability ', *Trans RINA, (Part A1), Intl J Maritime Eng 154*, pp. 43-51.

Ewans, K.C., Van der Vlugt, T. (1999) 'Estimating bimodal frequency-direction spectra from surface buoy data recorded during tropical cyclones ', *Journal of Offshore Mechanics and Arctic Engineering*, 121, pp. 172-80.

Faltinsen, O.M. (1990) *Sea Loads on Ships and Offshore Structures*. Cambridge University Press.

Fisher, R. (1922) 'On the mathematical foundations of theoretical statistics', *Phil. Transaction, Roy. Soc., series A-222*.

Francescutto, A. (1993) 'Is it Really Impossible to Design Safe Ships?', *RINA Transactions* 135.

Francescutto, A. (2004) 'Intact ship stability: the way ahead', *Marine Technology*, 41(1), pp. 31-37.

Frechot, J., (Belenky), V. (2006) 'Realistic simulation of ocean surface using wave spectra". ', *Laboratoire bordelais de recherche en informatique, Domaine universitaire, 351 cours de la Lib´eration, 33405 Talence CEDEX, France*.

Goda, Y. (2000) *Randum seas and design of maritime structures*.

Grochowalski, S. (1989) 'Investigation into the Physics of Ship Capsizing by Combined Captive and Free Running Model Tests', *Trans. SNAME 97*.

Harris, J.F. (1978) 'On the use of windows for harmonic analysis with the discrete Fourier transform', *Proceedings of the IEEE*, Vol. 66, No. 1.

Hlawatsch, F.a.B.-B., G. F. (1992) 'Linear and quadratic time-frequency signal representations', *IEEE signal processing magazine*, 9(No. 2), pp. 21-67.

Hoffman, D. (1976) 'The impact of seakeeping on ship operations', *Marine Ttechnology*, 13(3), pp. 241-262.

Hogben, N., Cobb, F.C. (1986) 'Parametric modelling of directional wave spectra', *Proceedings of 18th Offshore Technology Conference*.

Hua, J., Palmquist, M. (1994) 'Wave estimation through ship motion measurement', *Technical report, naval architecture, department of vehicle engineering, royal institute of technology*.

Huss, M., Olander, A. (1994) 'Theoretical seakeeping predictions on board ships – A system for operational guidance and real time surveillance', *Royal institute of technology, Stockholm*.

Hutchinson, B.L. (1986) 'Risk and operability analysis in the marine environmrnt ', *Transaction SNAME*, 89, pp. 127-154.

IMO (1995) 'Guidance to the master for avoiding dangerous situations in following and quartering seas ', (MSC/Circ.707).

IMO (2006) 'Review of the intact stability code - Revised intact stability code prepared by intersessional correspondence group', SLF 49/5.

IMO (2007) 'Revised guidance to the master for avoiding dangerous situations in adverse weather and sea conditions', (MSC.1/Circ.1228).

IMO (2007b) 'Revised Guidance to the master for avoiding dangerous situations in adverse weather and sea conditions ', MSC.1/Circ.1228.

Iseki, T.O., K (1999) 'Bayesian estimation of directional wave spectra based on ship motions', *Control engineering practice*, 8, pp. 215-219.

Iseki, T.T., D. (2002) 'Bayesian estimation of directional wave spectra for ship guidance systems', *International journal of Offshore Polar Eng*, 12, pp. 25-30.

Isobe, M., Kondo, K., Horikawa, K. (1984) 'Extension of MLM for estimating directional wave spectrum', *Proceedings of symposium on description and modelling of directional seas*, A-6.

ITTC (1966) 'recommendations of the 11th International towing Tank Conference', *Proceeding of 11th ITTC, Tokyo*.

Journee, J.M.J. (1992) 'Quick Strip Theory calculations in ship design', *PRADS 92 Conf. on Practical design of ships and mobile structures*, Volume I, Newcastle upon tyne, UK.

Kastner, S. (1986) 'Operational stability of ships and safe transport of cargo', *STAB 86, 3rd international conference on stability of ships and ocean vehicles*

pp. 207-215.

Kastner, S., Kobylinski, L.K. (2003) 'Stability and safety of ships - Vol. I: Regulation and Operation, Part 2', *Elsevier ocean engineering book series*, 9.

Kobilinski, L. (2000) 'Stability standards - future outlook', *Proc. of STAB 2000: 7th international conference on stability of ships and ocean vehicles*, 1(Launceston, Tasmania), pp. 52-61.

Kobylinski, K.L., Kastner. S. (2003a) 'Stability and safety of ships Vol I: Regulation and Operation', *Elsevier ocean engineering book series*, 9.

Kobylinski, L.K. (2008) 'Proposed approach to stability requirements based on goal determination and risk analysis', *Maritime university of Szczecin*, 13(85)(33-39).

Kobylinski, L.K., Kastner, S. (2003b) *Stability and safety of ships - Vol. I: Regulation and Operation*. Kidlington, Oxford: Elsevier ocean engineering book series.

Kobylinski, L.K.a.K., S. (2003c) 'Stability and safety of ships - Vol. I: Regulation and Operation', *Elsevier ocean engineering book series*, 9.

Krylov, A.N. (1958) 'Selected papers', *Published by Academy of science of the USSR, Moscow*.

Kuo, C. (2000) 'the impact of human factors on ship stability', *Proc. of STAB 2000: 7th international conference on stability of ships and ocean vehicles*, 1(Launceston, Tasmania), pp. 4-22.

Kuteynikov, M.A., Lipis, V. B. (2000) 'On indices of ships operational seaworthiness ', *Proc. of STAB 2000, 7th International conference on stability of ships and ocean vehicles, Vol. 1, Launceston, Tasmania*, pp. PP. 176-189.

Lloyd, A.R.J.M. (1998) *Seakeeping: Ship behaviour in rough weather*. Gosport, Hampshire, UK.

Longuet-Higgins, M.S. (1952) 'On the statistical distribution of the heights of sea waves', *Journal of marine research*, Vol. 11, No. 3., pp. 245-266.

Longuet Higgins, M., Cartwright, D. And Smith, N. (1963) 'Observations of the directional spectrum of sea waves using the motions of a floating buoy', *Ocean wave spectra*, pp. 111-136.

Mielke, A. (2011) 'Neuronal networks', *Andteas hofer weg 47, D-69121 Heidelberg, Germany*.

Minitab (2012) 'Statistical software version 16.1.0.0'.

MIT, O. (2012) *Energy-Wave spectra*.

Mitsuyasu, H., Hasen, Oslen and Passer (1975) 'Observation of the directional spectrum of ocean waves using a cloverleaf buoy', *Journal of physical oceanography*, 5, pp. 750-760.

MOD (1983) *Admiralty Manual of seamanship*. London: her majesty's stationary office.

Molland, A.F. (2008) *The maritime engineering reference book: A guide to ship design*. Elsevier Science.

Munif, A., Ikeda, A., Fujiwara, T., Katayama, T. (2006) 'Parametric roll resonance of a large passenger ship in dead ship condition in all heading angles', *Proceedings, STAB'06: Ninth International Conference on Stability of Ships and Ocean Vehicles, Rio de Janeiro, Brazil*, 1(81).

National Instruments, C. (2009a) *Getting started with LabVIEW*.

National Instruments, C. (2009b) *Graphical programming for instrumentation*.

National Instruments, C. (2011) *LabVIEW: Graphical programming for instrumentation* (Version 2011) [Computer program].

Nielsen, U.D. (2005) 'Estimation of directional wave spectra from measured ship responses ', *PhD thesis, Section of coastal maritime and structural engineering, department of mechanical engineering, Technical university of Denmark*.

O'Hanlon, J.F., McCauley, M.E. (1974) 'Motion Sickness Incidence as a Function of Vertical Sinusoidal Motion', *Aerospace Medicine, AM-45(4)*, pp. 366-369.

Ochi, M. (1998) 'Ocean waves - The stocastic approach', *Cambridge ocean technology series; 6*.

Ovegard, E., Rosen, A., Palmquist, M.,Huss, M., (2012) 'Operational guidance with respect to pure loss of stability and parametric rolling', *Proceedings of the 11th international conference, STAB2012, Athens-Greece*, pp. 655-667.

Palmquist, M. (1994) 'On the statistical properties of the metacentric height of ships in following deas', *STAB94, Fifth international conference on stability of ships and ocean vehicles*

Papanikolao u, A., Gratsos, G., Boulougouris, E., Eliopoulou, E. (2000) 'Operational measures for avoiding dangerous situations in extreme weather conditions', *Proc. of STAB 2000, 7th International conference on stability of ships and ocean vehicles, Vol. 1, Launceston, Tasmania*, 1, pp. 137-148.

Pascoal, R., Guedes Soares, C., Sørensen. A.J. (2007) 'Ocean Wave Spectral Estimation Using Vessel Wave Frequency Motions', *Journal of Offshore Mechanics and Arctic Engineering*, 129.

Pawlowski, M. (2013) 'Moving ship wave spectrum', *Personal communication*.

Pawłowski, M. (2009) 'Sea spectra revisited ', *Proceedings of the 10th international conference, STAB2009, St.Petersburg-Russia*, pp. 463-472.

Qian, S., Chen, D. (1996a) *Joint time-frequency analysis*. New Jersey, USA.

Qian, S.a.C., D. (1996b) 'Joint time-frequency analysis', *Prentice-Hall, NJ, USA*.

Rahola, J. (1939) 'The judging of the stability of ships and the determination of the minimum amount of stability', *PhD.Thesis, Helsinki*.

Rainey, R.C.T., Thompson, J. M. T., Tam, G. W., Noble, P. G. (1990) 'The transient capsize diagram – a route to soundly based new stability regulations', *Proc. of STAB 90: 4th International conference on stability of ships and ocean vehicles, Naples-Italy*.

Rakhmanin, N.N. (1994) 'Workshop on information to the master', *STAB94, Fifth international conference on stability of ships and ocean vehicles*.

Rodrigues, J.M., Perera, L.P.,Guedes Soares, C. (2012) 'Decision support system for the safe operation of fishing vessels in waves', *Journal of Maritime Engineering and Technology, Taylor & Francis Group, London, 2012, PP153-161*.

Rogers, D., Bolton King, G. (1997) 'Wave generation using Ocean and wave', *Edinburgh Designs Ltd, Version 3.62, Edinburgh, UK.*

SESAM (2010) 'Integrated comprehensive software system for hydrodynamic and structural analysis'.

Shafi, I., Ahmad, J., Ismail Shah, S., Kashif, F.M. (2009) 'Techniques to Obtain Good Resolution and Concentrated Time-Frequency Distributions: A Review', *EURASIP Journal on Advances in Signal Processing*, 2009(Article ID 673539), p. 43.

Shigunov, V. (2009) 'operational guidance for prevention of container loss', *Proceedings of the 10th international conference, STAB2009, St.Petersburg-Russia*, pp. 473-482.

Spyrou, K.J., Thompson, J. M. T. (2000) 'The nonlinear dynamics of ships: A field overview and some recent developments ', *Philosophical Transactions of the Royal Society of London*, (385), pp. 1735-1760.

St Denies, M.P., W. J. (1953) 'On the motions of ships in confused seas', *TSNAME*.

St Denis, M.P., W.J. (1953) 'On the motions of ships in confused seas', *TSNAME*.

Stankovic, L.J.a.S.S. (1995) 'Analysis of instantaneous frequency representation using time-frequency distributions-generalized Wigner distribution', *IEEE Transactions on signal processing*, 43(No. 2), pp. 549-552.

Tannuri, E.A., Sparano, J.V., Simos, A. N., Druz, J.J. (2003) 'Estimating directional wave spectrum based on stationary ship motion measurements', *Applied ocean research*, 25, pp. 243-261.

Ursell, F. (1949a) 'On the heaving motion of a circular in the surface of a fluid', *OJMAM(2)*.

Ursell, F. (1949b) 'On the rolling motion of cylinder in the surface of a fluid', *OJMAM(2)*.

Vassalos, D., Hamamoto, M., Papanikolaou, A., Molyneux, D. (2000) *Contemporary Ideas on Ship Stability*. Elsevier.

Waals, O.J., Aalbers, A.B., Pinkster, J. A. (2002) 'Maximum likelihood method as a means to estimate the directional wave spectrum and the mean wave drift force on a dynamically positioned vessel', *Proceedings of OMAE, Oslo-Norway*.

WAFO (2000) 'A Matlab toolbox for analysis of random waves and loads. ', *Lund Institute of Technology, Centre for mathematical science, version 2.0.02*.

Website1 (2012) *http://en.wikipedia.org/wiki/Window_Function author: http://en.wikipedia.org/wiki/User:Bob_K*

Weinblum, G. (1952) 'Die Künftige Entwicklung des Schiffes im Lichte der Schiffstheorie', *Hansa*, 89, Hamburg.

Bibliography

Atlar, M., Kenevissi, F., Mesbahi, E., Roskilly, A.P. (1997) 'lternative Time Domain Techniques For Multi-Hull Motion Response Prediction', *International Conference FAST97, Australia*, pp. 545-552.

Ayyub, B.M., Kaminskiy, M., Alman, P.R., Engle, A., Campbell, B.L., Thomas, W.L. (2006) 'Assessing the Probability of the Dynamic Capsizing of Vessels', *Journal of Ship Research*, 50, No. 4, pp. 289-310.

Belenky, V.L. (2001) 'Seventh International Conference on the Stability of Ships and Ocean Vehicles (STAB' 2000) - A Review', *Journal of Marine Technology*, 38, No. 1, pp. 1-8.

Breu, D.A., Fossen, T.I. (2011) 'L1 Adaptive and Extremum Seeking Control Applied to Roll Parametric Resonance in Ships', *9th IEEE International Conference on Control and Automation (ICCA), Santiago, Chile, December 19-21, 2011*.

Bruns, T., Lehner, S., Ming Li, X., Hessner, K., Rosenthal, W. (2011) 'Analysis of an Event of "Parametric Rolling" Onboard RV "Polarstern" Based on Shipborne Wave Radar and Satellite Data', *IEEE Journal of Oceanic Engineering*, 36(2).

Bulian, G., Francescutto, A. (2009) 'An assessment methodology for 1st level vulnerability check with respect to parametric rolling', *International Workshop on Dynamic Stability Considerations in Ship Design (DSCSD), 14-15 September 2009, ilawa, Poland*

C., N. (2001) 'References & Bibliographies', *Effective Learning Service 68, University of Bradford, School of Management*.

Dostala, L., Kreuzera, E., Namachchivayab. N. S. (2012) 'Stochastic averaging of roll-pitch and roll-heave motion in random seas', *IUTAM Symposium on Multiscale Problems in Stochastic Mechanics*

Francescutto, A. (2007) 'the intact ship stability code: present status and future developments', *2nd International Conference on Marine Research and Transportation, Naples - Italy*.

Francescutto, A., Papanikolaou, A.D. (2011) 'Buoyancy, stability, and subdivision: from Archimedes to SOLAS 2009 and the way ahead', *Journal of Engineering for the Maritime Environment, Proc. IMechE Vol.225 Part M*.

Fulop S.A., F., K. (2006) 'Algorithms for computing the time-corrected instantaneous frequency (reassigned) spectrogram, with applications', *Journal of Acoustic Society of America* 119(1).

Gourlay, T.P., Lilienthal, T. (2002) 'Dynamic stability of ships in waves', *Proc. Pacific 2002 International Maritime Conference, Sydney, Jan 2002*.

Grochowalski, S. (1989) 'Investigation into the physics of ship capsizing by combined captive and free-running model tests', *The society of Naval Architects and Marine Engineers*.

Hendriks, R.C., Heusdens, R., Jensen, J. Kjems, U. (2009) 'Low Complexity DFT-Domain Noise PSD Tracking Using High-Resolution Periodograms', *EURASIP Journal on Advances in Signal Processing*, 2009, Article ID 925870, 15 pages.

Ibrahim, R.A., Grace, I.M. (2010) 'Modeling of Ship Roll Dynamics and Its Coupling with Heave and Pitch', *Hindawi Publishing Corporation Mathematical Problems in Engineering Volume 2010, Article ID 934714, 32 pages*.

IMO (2004a) 'Human Element Vision, Principles and Goals for the Organization', (Assembly 23/Res.947).

IMO (2004b) 'Safety of Navigation, Transitory non-compliance when conducting ballast water exchange', (MSC 79/10/2, 22 September 2004).

IMO (2005) 'Revision of the Intact Stability Code', (SLF 48/4/5).

IMO (2007a) 'Revision of the Intact Stability Code', (SLF 50/4/2).

IMO (2007b) 'Revision of the Intact Stability Code', (SLF 51/4).

IMO (2008) 'Explanatory Notes to the International Code on Intact Stability, 2008', (MSC.1/Circ.1281).

IMO (2009) 'Revision of the Intact Stability Code', (SLF 49/5).

IMO (2011) 'Development of Second Generation Intact Stability Criteria', (Sub-Committee on Stability and Load Lines and on Fishing Vessels Safety, SLF 54/INF.7).

ITTC (2005) 'Final Report and Recommendations to the 24th ITTC', (Proceedings of the 24th ITTC - Volume II, UK).

Ivce, R., Jurdana, I., Mohovic. D. (2010) 'Parametric Roll Monitoring with an Integrated Ship's System', *52nd International Symposium ELMAR-2010, 15-17 September 2010, Zadar, Croatia*.

J., F. (2006) 'Realistic simulation of ocean surface using wave spectra', *LaBRI- Laboratoire bordelais de recherche en informatique, IN PROC. GRAPP, France*.

Kim, T., Kim, Y. (2011) 'Multi-level approach for parametric roll analysis', *International Journal of Nav Archit Oc Engng*, 2011(3), pp. 53-64.

Kleiman, A., Gottlieb, O. (2009) 'Nonlinear Dynamics and Internal Resonances of a Ship With a Rectangular Cross-Section in Head Seas', *Journal of Offshore Mechanics and Arctic Engineering November 2009*, 131.

Kobyliński, L. (2008) 'Stability and Safety of Ships: Holistic and Risk Approach', *Journal of R&RATA 2008-11*, 1.

Krueger, S. (2005) 'Dynamic Intact Stability Criteria', Technische Universitat Hamburg-Harburg 3rd June 2005.

Kuchler, S., Pregizer, C., Eberharter, J.K., Schneider, K., Sawodny, O. (2011) 'Real-Time Estimation of a Ship's Attitude', *American Control Conference on O'Farrell Street, San Francisco, CA, USA*.

Lilienthal, T., Matsuda, A., Thomas, G. (2007) 'namic stability in following seas: predictive and experimental approaches', *Journal of Marine Science and Technology* 12, pp. 111-118.

Lopez Pena, F., Gonzalez, M.M., Díaz Casas, V., Duro, R.J. (2011) 'Ship Roll Motion Time Series Forecasting Using Neural Networks', *International Conference on Computational Intelligence for Measurement Systems and Applications (CIMSA), 2011 IEEE*.

Maki, A., Akimoto, Y., Nagata, Y., Kobayashi, S., Kobayashi, E., Shiotani, S., Ohsawa, T., Umeda, N. (2011a) 'A new weather-routing system that accounts for ship stability based on a real-coded genetic algorithm', *Journal of Marine Science and Technology*.

Maki, A., Umeda, N., Shiotani, S., Kobayashi, E. (2011b) 'Parametric rolling prediction in irregular seas using combination of deterministic ship dynamics and probabilistic wave theory', *Journal of Marine Science and Technology*.

Meng, T., Juan, G., Feng, G. (2010) 'Research on Balance Control for Ship Roll Stability based on Transferring Liquid Among Water Cabins', *2nd International Conference on Computer Engineering and Technology*, 7.

Neves, M.A.S., Belenky, V.L. (2008) 'A Review of the Ninth International Conference on the Stability of Ships and Ocean Vehicles (STAB 2006)', *Journal of Marine Technology*, 45, No. 3, pp. 147-156.

Nielsen, U.D. (2006) 'Estimations of on-site directional wave spectra from measured ship responses', *Journal of Marine Structures*, 19, pp. 33-69.

Nielsen, U.D., Hansen, P.F., Jensen, J.J. (2009) 'A step towards risk-based decision support for ships - Evaluation of limit states using parallel system analysis', *Journal of Marine Structures*, 22, pp. 209-224.

Nielsen, U.D., Jensen, J.J. (2011) 'A novel approach for navigational guidance of ships using on-board monitoring systems', *Journal of Ocean Engineering*, 38, pp. 444-455.

O'Toole, J.M., Boashash, B. (2011) 'Time-Frequency Detection of Slowly Varying Periodic Signals with Harmonics:Methods and Performance Evaluation', *EURASIP Journal on Advances in Signal Processing*, 2011, Article ID 193797, 16 pages.

Pascoal, R., Soares, C.G. (2008) 'Non-parametric wave spectral estimation using vessel motions', *Journal of Applied Ocean Research*, 30, pp. 46-53.

Perunovic, J.V. (2010) 'Influence of the GZ calculation method on parametric roll prediction', *Journal of Ocean Engineering, 2010.11.002*.

Perunovic, J.V., Jensen , J.J. (2009) 'Parametric roll due to hull instantaneous volumetric changes and speed variations', *Journal of Ocean Engineering*, 36, pp. 891-899

Ribeiro e Silva, S., Fonseca1, N., Pascoal, R., Guedes Soares, C. (2005) 'Motion predictions and sea trials of roll stabilised frigate', *Unit of Marine Technology and Engineering, Technical University of Lisbon*.

Ribeiro e Silva, S., Fonseca, N., Soares, C.G. (2006) 'Performance of a Navy Ship Roll Stabilisation System', *Proceedings of the 9th International Conference on Stability of Ships and Ocean Vehicles (STAB´06)*.

Rojas, L.P., Belenky, V.L. (2003) 'A Review of the Stability of Ship and Ocean Vehicles Conference (STAB'2003)', *Journal of Marine Engineering*, 42(1).

Rojas, L.P., Belenky, V.L. (2005) 'A Review of the 8th International Conference on the Stability of Ship and Ocean Vehicles (STAB 2003)', *Journal of Marine Technology*, 42, No. 1, pp. 21-30.

Salvesen, N., Tuck, E.O., Faltisen, O. (1970) 'Ship motion and sea loads', *The Society of Naval Architects and Marine Engineers, New York, November 12-13, 1970*.

Shafi, I., Ahmad, J., Shah, S.I., Ikram, A.Z., Khan, A.A., Bashir, S., Kashif, F.M. (2010) 'High-Resolution Time-FrequencyMethods' Performance Analysis', *EURASIP Journal on Advances in Signal Processing*, 2010, Article ID 806043, 7 pages.

Shipping, A.B.o. (2008) 'Assessment of Parametric Roll Resonance in the Design of Container Carriers', (Guide for the American Bureau of Shipping Classification, Updated June 2008).

Spyrou, K.J. (2004) 'Non-linear damping coefficients from an asymmetric roll decay time series: an analytical method', *Proc. Instn Mech. Engrs Vol. 218 PartM: J. Engineering for the Maritime Environment*.

Sverdrup, H.U., Munk, W.H. (1947) 'Wind sea swell theory of relations for forecasting', (Technical report, United States Navy Department Hydrographic Office).

Tanaka, N., S. (1995) 'On-line sensing system of dynamic ship's attitude by use of servo-type accelerometers ', *IEEE journal of oceanic engineering*, 20, No. 4.

Themelis, N.I. (2008) 'Probabilistic Assessment of Ship Dynamic Stability in Waves', *Doctoral Thesis, School Of Naval Architecture and Marine Engineering, National Technical University of Athens*.

Ucer, E., Soylemez, M. (2011) 'Stochastic rolling motion of ships in following seas', *Journal of Ocean Engineering, 2011.03.008*.

Umeda, N., Matsuda, A., Hamamoto, M., Suzuki, S. (1999) 'Stability assessment for intact ships in the light of model experiments', *Journal of Marine Science and Technology*, 4, 45-57.

Yılmaza, H., Kukner, A. (1999) 'Evaluation of cross curves of fishing vessels at the preliminary design stage', *Journal of Ocean Engineering*, (26), pp. 979-990.

Yolmaz, H., Guner, M. (2001) 'An Approximate Method for Cross Curves of Cargo Vessels', *Journal of Marine Technology*, 38, No. 2, pp. 92-94.

Zhu, D.X., Katory, M. (1995) '3-D Time Domain Numerical Model for the Prediction of Ship Motions in Random Seas', *International Society of Offshore and Polar Engineers*, 5, No.2.

Appendix – I

Glossary of Terms

Amplitude is the magnitude of the extreme of a sinusoidal quantity with respect to the mean value. The double amplitude is the magnitude of the difference of the extreme.

Broaching is an involuntary and dangerous change in heading produced by a severe following sea.

Coupling is the influence of one mode of motion on another, for instance, coupling between heave and pitch.

Criterion has a Greek origin and literally means "instrument for judgment." In the context of technology regulations, a criterion consists of a value (or values) that represent a measure of the regulated quantity.

Dynamic stability is considered in quasi-static terms when balancing works of heeling and uprighting moments are at the angle of inclination. This corresponds to the dynamic action of the heeling moment (Kobylinski, 2003c).

Effective wave the length of wave is equal to ship length and is unmovable. However, its amplitude is a random process.

Emergence is the relative vertical distance of an oscillating ship above the water surface; opposite to Submergence.

Exciting force is fluctuation of external force that causes motion of a body, for instance as ship when encountering a train of waves.

Exciting moment is fluctuating external moment that caused motion of a body or ship, for example, when encountering a train of regular waves.

Frequency (characteristic) is the number of cycles occurring per unit of time; $f = 1/T$, where T is the period.

Frequency (circular) is the angular velocity in any cyclic motion, or in any periodic motion that may be represented by a cyclic motion. ω is in radians per second, $\omega = 2\pi/T$ where T is the period.

Frequency of encounter (circular) is defined asHere $\omega_e = 2\pi/T_e$ where T_e is the period of encounter.

Frequency of heave, pitch and roll is the frequency of the periodic heaving, pitching and rolling motion of a ship.

Global response is a collective term for rigid body motion, added mass, damping and excitation forces and sectional loads.

Harmonic wave is a wave for which the disturbance at any point in space through which the wave is propagated varies sinusoidally with time. Specifically, if the wave is a plane harmonic wave in the x-direction, the disturbance ζ is given by $\zeta = \zeta_a \sin(\omega_w t - kx)$, where ζ_a is the wave amplitude, $\omega_w = 2\pi/T$ (where T_W is the wave period), and $k = \omega_w / V_w$ (where V_w is the wave velocity).

Heading is a direction assumed by the forward axis or centreline of a body or the bow of a ship in a horizontal plane.

Heaving is the vertical oscillatory motion of a specified point in a vessel, usually the centre of gravity.

LabVIEW is Laboratory Virtual Instrument Engineering Workbench.

Long crested sea is a wave system in which all components advance in the same direction.

Modal frequency is related with the peak period T_p by the expression of $T_p = 2\pi / \omega_m$

Modal period is related with the peak frequency.

Natural period of motion (e.g. T_z) is the time for one complete cycle of the motion resulting when a body is displaced in calm water from its equilibrium position by an external force and then is released.

Operational stability is significantly defined by the ability of the master to load and control the vessel, to observe the characteristics of the ship design and to act in dangerous sea conditions.

Organization means the International Maritime Organization.

performance-based criterion is a measure which could be derived directly by using mathematical and physical modelling of the phenomena (Belenky, 2008).

Period is the length of time for one complete cycle of a periodic quantity or phenomenon, such as the rolling of a ship from port to starboard and back to port.

Period of encounter is the time interval between successive crests of a train of waves passing a fixed point in a ship, at a fixed angle if encounter.

Phase angle is the angle between two vectors representing two harmonically varying quantities having the same frequency.

Pitching is the angular component of the oscillatory motion of a vessel about a transverse axis.

Postresp is a general interactive graphic postprocessor for postprocessing of general responses given as transfer functions in the frequency domain, or postprocessing of time series in the time domain.

Resonance is the dynamic condition of a simple, uncoupled system in which the excitation frequency is equal to the natural frequency. In a coupled system, the dynamic condition is the excitation frequency corresponds to the frequency of maximum response to unit exciting force over a range of frequencies.

Response Amplitude Operator is the square of the ratio of response amplitude to excitation amplitude of a forced harmonic motion applied to a linear system, as a function of frequency.

Restoring force is a force tending to return a body to its equilibrium position when it has been displaced by an external force.

Restoring moment is a moment tending to return a body to its initial condition after it has been displaced by an external moment.

Rolling is the angular component of the oscillatory motion of a ship measured about a longitudinal axis.

Safety is a perceived quality that determines to what extent the management, engineering and operation of a system is free of danger to life, property and the environment (STAB, 90).

Sea direction is defined as:

- **Beam sea**: A condition in which a ship and the waves, or predominant wave components advance at right angles or nearly so.
- **Bow sea**: A condition in which a ship and the waves, or predominant wave components advance at oblique angles. This condition covers the direction between a head sea and a beam sea.
- **Following sea**: A condition in which a ship and the waves, or predominant wave components advance in the same, or nearly the same direction.
- **Head sea**: A condition in which a ship and the waves, or predominant wave components advance in opposite, or nearly opposite direction.
- **Quartering sea**: A condition in which a ship and the waves, or predominant wave components advance at oblique angles. This condition covers the direction between a beam sea and a following sea.

Sea state is the condition of the surface of the seas i.e. calm water, moderate or high waves.

Seaworthy ship is one that is fit for any normal perils of the sea, including the fitness of the vessel itself as well as any equipment on it and the skills and health of its crew. Given the number and type of variables involved, seaworthiness is a relative term that is impossible to be measured or determined in the abstract. The destination, class of ship, place of departure and even the type of cargo are all considerations when determining seaworthiness. It is important to distinguish the difference between a safe ship and a seaworthy ship. In order to be considered seaworthy, the vessel must be suitable for all aspects of its particular voyage. That includes parts of the voyage that happen on the open sea. It also includes the type of sea and weather conditions that the vessel is likely to encounter.

SESAM is DNV life cycle management system delivering strength assessment and operational management from design to operation to decommissioning.

Ship types

- **Bulk carrier** means a ship which is constructed generally with single deck, top-side tanks and hopper side tanks in cargo spaces, and is intended primarily to carry dry cargo in bulk, and includes such types as ore carriers and combination carriers. (SOLAS IX/1.6)

- **Bulk carrier** means a ship which is intended primarily to carry dry cargo in bulk, including such types as ore carriers and combination carriers. (SOLAS XII/1.1)
- **Fishing vessel** is a vessel used for catching fish, whales, seals, walrus or other living resources of the sea. (SOLAS I/2)
- **Fishing vessel** means any vessel used commercially for catching fish, whales, seals, walrus or other living resources of the sea. (SFV 1993 article 2)
- **General cargo ship** is a ship with a multi-deck or single-deck hull designed primarily for the carriage of general cargo. (MEPC.1/Circ.681 Annex)
- **Mobile offshore drilling unit** (MODU) means a vessel capable of engaging in drilling operations for the exploration for or exploitation of resources beneath the sea-bed such as liquid or gaseous hydrocarbons, sulphur or salt. (SOLAS IX/1, MODU Code 2009 para 1.3.40)
- **Nuclear ship** is a ship provided with a nuclear power plant. (SOLAS I/2)
- **Oil tanker** means a ship constructed or adapted primarily to carry oil in bulk in its cargo spaces and includes combination carriers, any "NLS tanker" as defined in Annex II of the present Convention and any gas carrier as defined in regulation 3.20 of chapter II-1 of SOLAS 74 (as amended), when carrying a cargo or part cargo of oil in bulk. (MARPOL Annex I reg. 1.5)
- **Passenger ship** is a ship which carries more than twelve passengers. (SOLAS I/2)

Short crested sea is an irregular wave system in which the components advance in various directions.

Significant wave height $(h_W)_{1/3}$ or characteristic wave height is the arithmetic mean of the heights of the one-third highest waves for a given record at any given time and in a given location at sea.

Spectral density (one dimensional) is a function of frequency whose integral over any interval represents the energy contribution of all the component waves of a random function in that interval: $S_\zeta(\omega)d\omega = \sum_{d\omega} \frac{1}{2}\zeta_{an}^2$ where the subscript n denotes a particular component amplitude.

Spectral density (two dimensional) $(S_{\omega,\mu})$ is a function of frequency and wave direction whose integral over any interval represents the energy contributions of all the component waves of a random function in that interval.

Spectral amplitude is a function of frequency and wave direction whose integral over any interval represents the squared amplitude of a wave at the central frequency having the same energy as all the component waves in that interval.

Stability is the tendency of a ship, when is inclined from the upright position of equilibrium to return back to this position.

Stability is the ability of a ship to float in an upright position and, if inclined under actions of an external cause, to return to the above said position after the external cause has ceased acting (Krylov, 1958).

Stability is a feature which enables the ship to perform, when remaining in determined position, the task she is constructed for (Weinblum, 1952).

Stability as a term in ship stability matters has not the same meaning as in theoretical mechanics. It could be more appropriately represented by "boundedness" of a relevant motion, usually rolling (Francescutto, 2004).

Stability failure

- **Pure loss of stability**: if the stability is reduced for a sufficiently long time, a ship may capsize or attain large roll angle.
- **Parametric roll**: is the gradual amplification of roll amplitude caused by parametric resonance, due to periodic changes of stability in waves.
- **Surf riding and broaching**: broaching is the loss of controllability of a ship in astern seas, which occurs despite maximum steering effort. It can appear as heeling during an uncontrollable, tight turn. It is believed to be intimately connected with the so called surf riding behaviour.
- **Dead ship conditions**: when a ship losses power, it becomes completely uncontrollable. The worst possible scenario is a turn into beam seas, where the ship is then subjected to a resonant roll combines with gusty wind.
- **Total** is defined as complete loss of ship operability or for at least some time due to capsizing.

- **Partial** is defined as an event that includes the occurrence of very large roll angles and/or excessive roll accelerations that will not result in loss of the ship, but that could impair normal operation of the ship and could be dangerous to crew, passengers, cargo, or ship equipment.

Static Stability or simply stability is a concept where the heeling or inclining moment is statically balanced with the uprighting moment corresponding to the angle of inclination from the upright position.

Note: when speaking about stability, **transverse stability** is understood which is inclinations of ship in the transverse plane. Longitudinal stability is of less importance because of rare cases of capsizing over the bow or stern.

Submergence is the relative vertical distance of a part of an oscillating ship below the water surface.

Swell is a wave of generally long period and comparatively regular in shape.

Tuning factor Is the ratio of excitation frequency to natural frequency (or the ration of natural period of a motion to period of encounter). The tuning factor symbol in heave is

$$\Lambda_Z = \frac{\omega_e}{\omega_z}$$

Vulnerability is one of the possible ways to assess stability failure of ships more susceptible to hazards. These criteria would be capable of answering “yes” or “no” in response to the question of whether this particular vessel could be, in principle, vulnerable to a stability-loss phenomenon.

Wasim is an integrated part of the SESAM suite of programs, with interfaces to SESAM Pre and Post processors and the structural analysis module Sestra.

Wasim_Mass computes body mass matrix and sectional mass matrices from a given mass model.

Wasim_Setup sets up and inverts the influence matrix for the radiation/diffraction problem, solves for the basis flow (i.e. the solution in calm water). The computations in Wasim_Setup must only be redone when the panel model is changed on the hull or on the free surface.

Wasim_Solve performs the time domain simulation.

Wave is a disturbance of the surface of a fluid that usually progressed across the surface as the result of circular or other local motions of the fluid components. A standing wave is a special case of a wave that does not advance.

- **Amplitude**: The radius of orbital motion of a surface wave particle, equal to one-half of the wave height.
- **Components**. The infinity of infinitesimal waves of different frequencies and directions that are found by spectral analysis to compose an irregular sea, or the large number of finite waves used to approximate such an irregular sea.
- **Crest**. The position of maximum positive disturbance in a progressive wave, that is, in any wave other than a standing wave.
- **Frequency**. The reciprocal of a wave period = $1/T_w$ (or circular frequency $\omega_w = 2\pi/T_w$.
- **Height**. The vertical distance from wave crest to wave trough, or twice the wave amplitude of a harmonic wave.
- **Instantaneous elevation**. The instantaneous elevation of a point in a wave system above the level of the undisturbed surface.
- **Length**. The horizontal distance between adjacent wave crests in the direction of advance.
- **Period**. The time between the passages of two successive crests in an irregular sea, or between two successive upward crossings of zero in a record.
- **Profile**. The elevation of the surface particles of a wave plotted as a function of space in fixed time.
- **Slope of surface**. The surface slope of a wave profile perpendicular to the crest in space coordinates. The maximum wave slope of a regular harmonic or trochoidal wave is π x steepness ratio.
- **Steepness ratio**. The ration of wave height to length.
- **Train**. A continuous sequence of wave crests and troughs.
- **Trochoidal**. A profile closely approximating that of a regular surface gravity wave in a fluid; it can be geometrically constructed by tracing the path of a point on the radius of a circle as the circle rolls along the underside of a horizontal line.

- **Trough**. A point of minimum value of the disturbance in a progressive wave. Opposite of Wave Crest.

Appendix –II

Simulation Output of Wasim Program

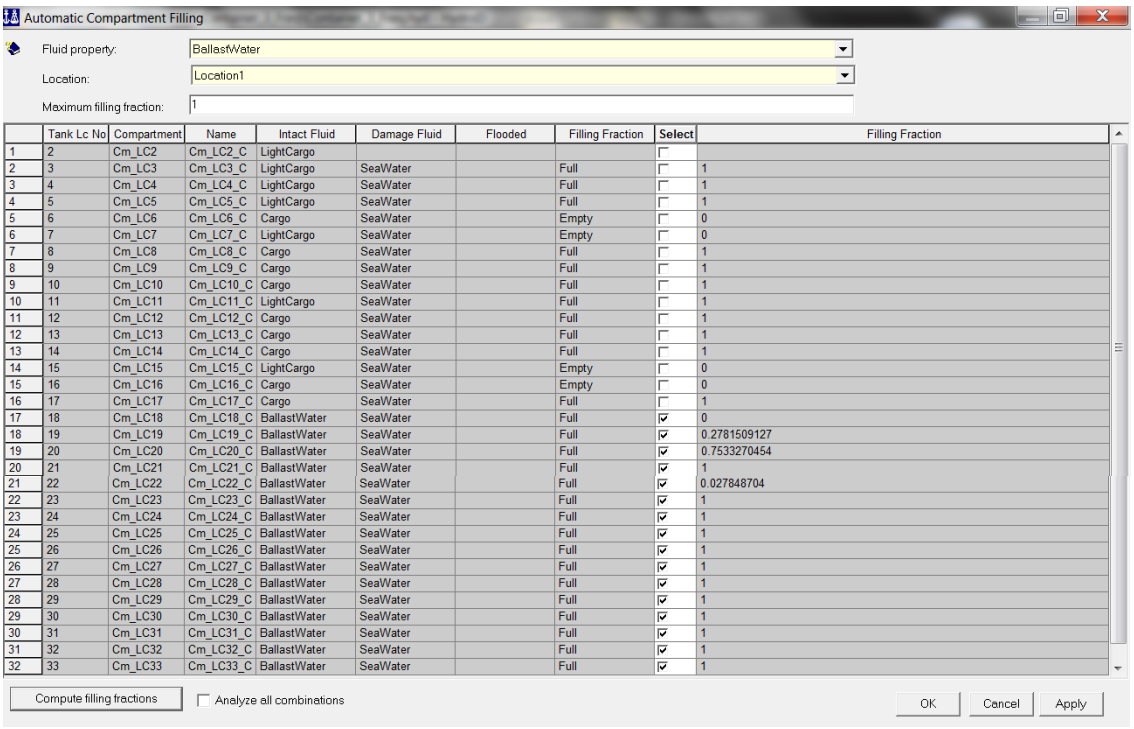

	Tank Lc No	Compartment	Name	Intact Fluid	Damage Fluid	Flooded	Filling Fraction	Select	Filling Fraction
1	2	Cm_LC2	Cm_LC2_C	LightCargo				☐	
2	3	Cm_LC3	Cm_LC3_C	LightCargo	SeaWater		Full	☐	1
3	4	Cm_LC4	Cm_LC4_C	LightCargo	SeaWater		Full	☐	1
4	5	Cm_LC5	Cm_LC5_C	LightCargo	SeaWater		Full	☐	1
5	6	Cm_LC6	Cm_LC6_C	Cargo	SeaWater		Empty	☐	0
6	7	Cm_LC7	Cm_LC7_C	LightCargo	SeaWater		Empty	☐	0
7	8	Cm_LC8	Cm_LC8_C	Cargo	SeaWater		Full	☐	1
8	9	Cm_LC9	Cm_LC9_C	Cargo	SeaWater		Full	☐	1
9	10	Cm_LC10	Cm_LC10_C	Cargo	SeaWater		Full	☐	1
10	11	Cm_LC11	Cm_LC11_C	LightCargo	SeaWater		Full	☐	1
11	12	Cm_LC12	Cm_LC12_C	Cargo	SeaWater		Full	☐	1
12	13	Cm_LC13	Cm_LC13_C	Cargo	SeaWater		Full	☐	1
13	14	Cm_LC14	Cm_LC14_C	Cargo	SeaWater		Full	☐	1
14	15	Cm_LC15	Cm_LC15_C	LightCargo	SeaWater		Empty	☐	0
15	16	Cm_LC16	Cm_LC16_C	Cargo	SeaWater		Empty	☐	0
16	17	Cm_LC17	Cm_LC17_C	Cargo	SeaWater		Full	☐	1
17	18	Cm_LC18	Cm_LC18_C	BallastWater	SeaWater		Full	☑	0
18	19	Cm_LC19	Cm_LC19_C	BallastWater	SeaWater		Full	☑	0.2781509127
19	20	Cm_LC20	Cm_LC20_C	BallastWater	SeaWater		Full	☑	0.7533270454
20	21	Cm_LC21	Cm_LC21_C	BallastWater	SeaWater		Full	☑	1
21	22	Cm_LC22	Cm_LC22_C	BallastWater	SeaWater		Full	☑	0.027848704
22	23	Cm_LC23	Cm_LC23_C	BallastWater	SeaWater		Full	☑	1
23	24	Cm_LC24	Cm_LC24_C	BallastWater	SeaWater		Full	☑	1
24	25	Cm_LC25	Cm_LC25_C	BallastWater	SeaWater		Full	☑	1
25	26	Cm_LC26	Cm_LC26_C	BallastWater	SeaWater		Full	☑	1
26	27	Cm_LC27	Cm_LC27_C	BallastWater	SeaWater		Full	☑	1
27	28	Cm_LC28	Cm_LC28_C	BallastWater	SeaWater		Full	☑	1
28	29	Cm_LC29	Cm_LC29_C	BallastWater	SeaWater		Full	☑	1
29	30	Cm_LC30	Cm_LC30_C	BallastWater	SeaWater		Full	☑	1
30	31	Cm_LC31	Cm_LC31_C	BallastWater	SeaWater		Full	☑	1
31	32	Cm_LC32	Cm_LC32_C	BallastWater	SeaWater		Full	☑	1
32	33	Cm_LC33	Cm_LC33_C	BallastWater	SeaWater		Full	☑	1

Appendix II-1 Loading status with distribution in the compartments

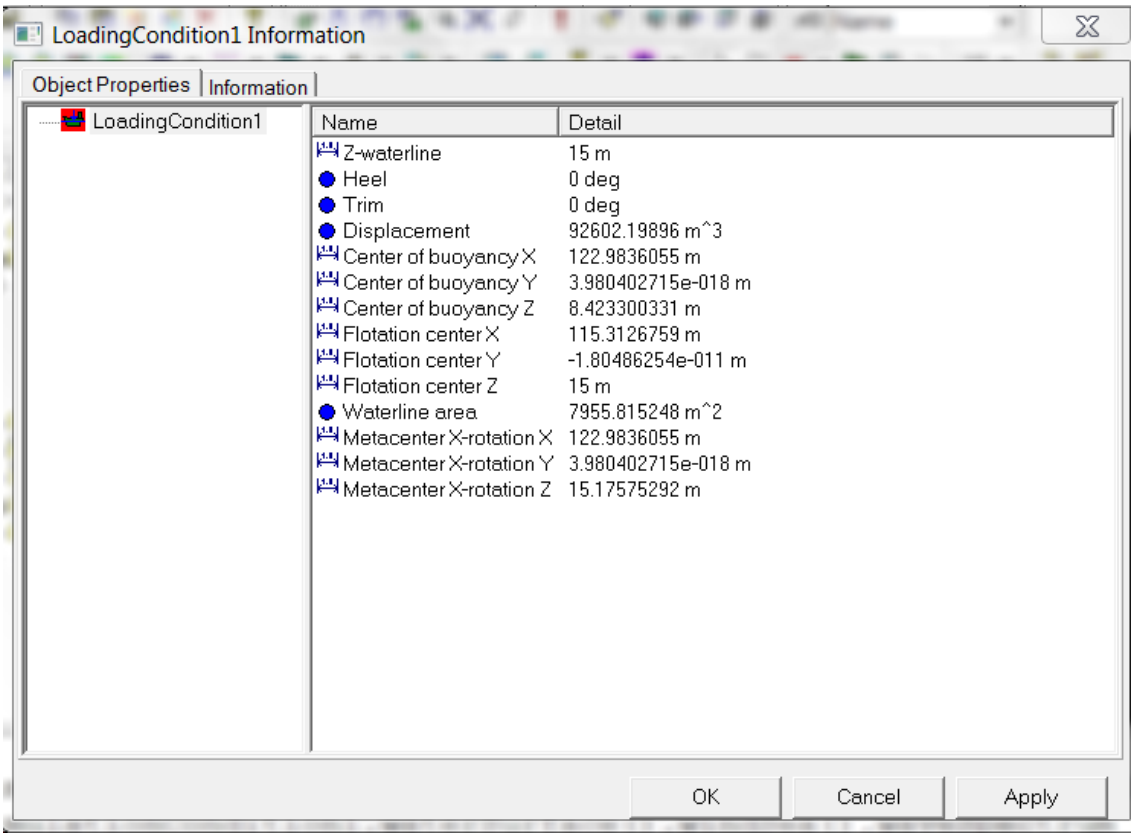

Appendix II-2 Particulars Loading condition from Wasim program

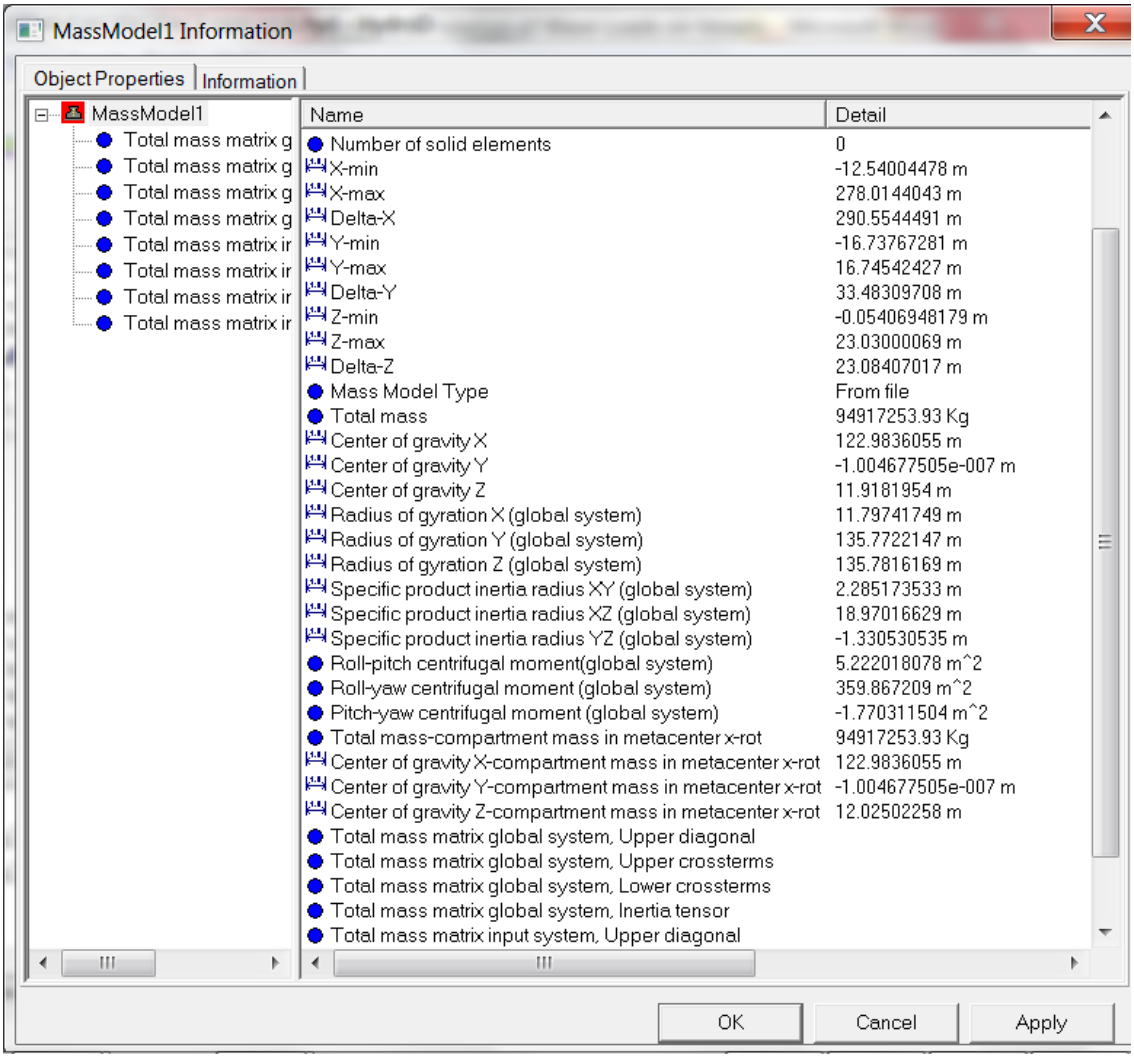

Appendix II-3 Particulars of the Mass model from Wasim program

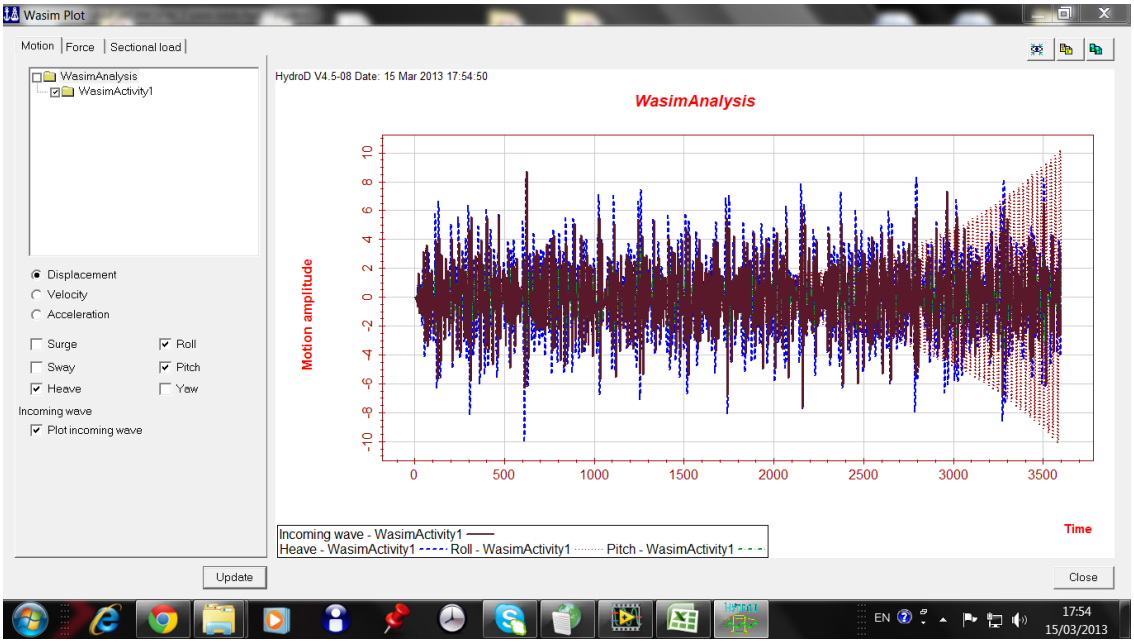

Appendix II-4 Time series of incident wave and motion responses in Following sea, zero speed, Hs of 9m and period of 20sec.

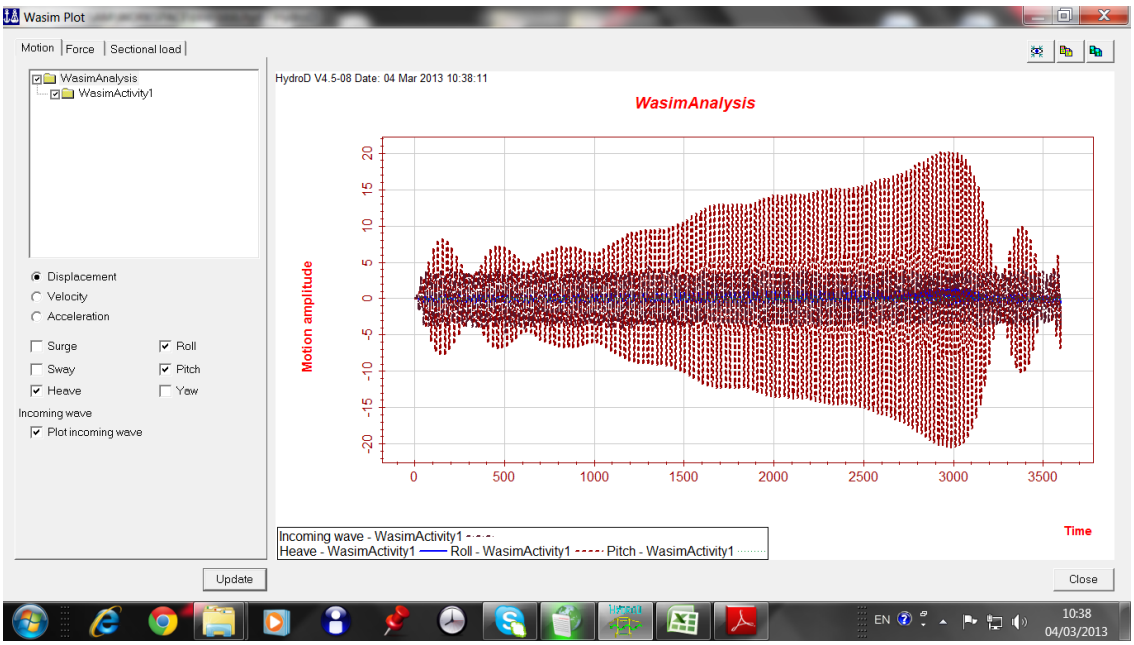

Appendix II-5 Time series of incident wave and motion responses in Quartering sea, speedof 10m/s , Hs of 9m and period of 7sec.

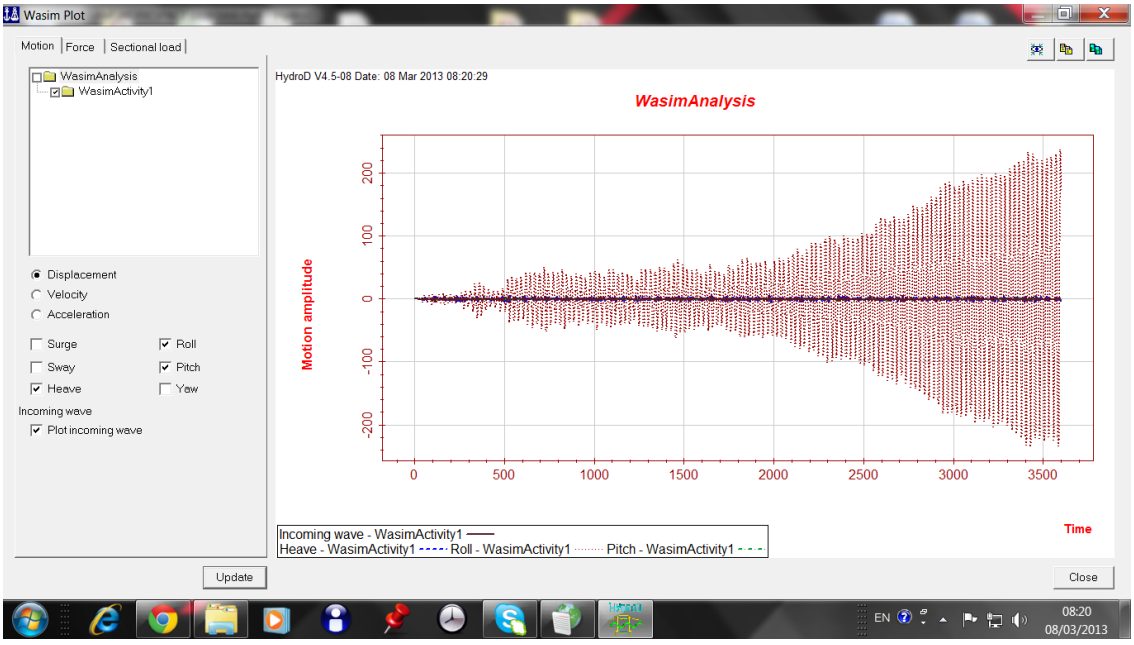

Appendix II-6 Time series of incident wave and motion responses in Beam sea, speed of 5m/s , Hs of 6m and period of 20sec.

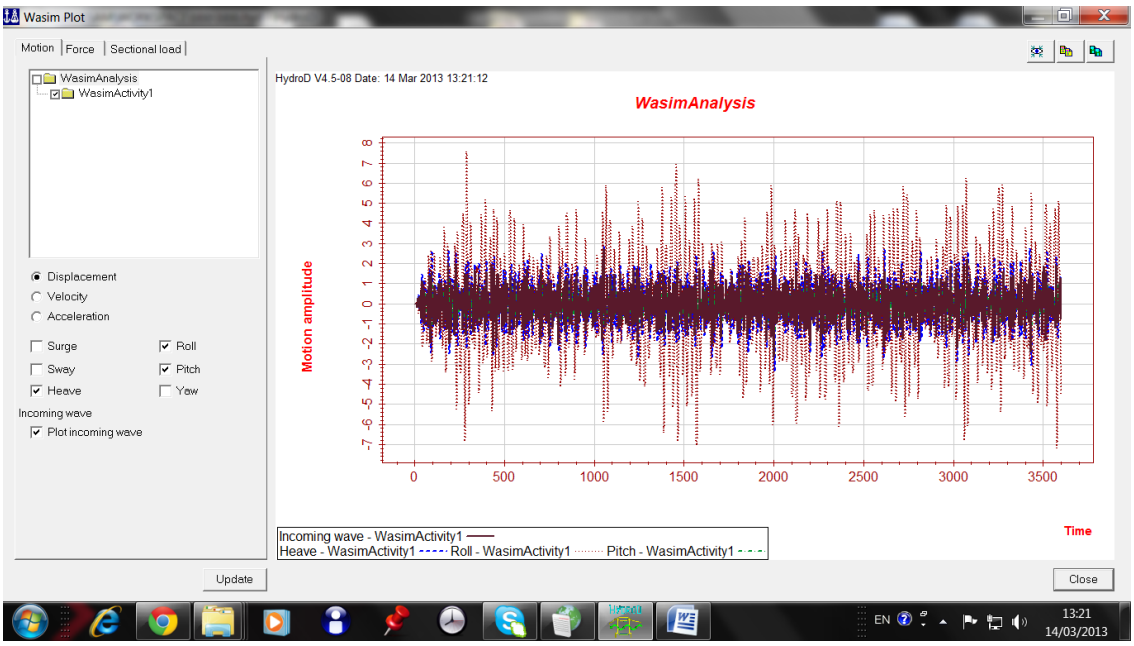

Appendix II-7 Time series of incident wave and motion responses in bow sea, speed of 10m/s , Hs of 3m and period of 20sec.

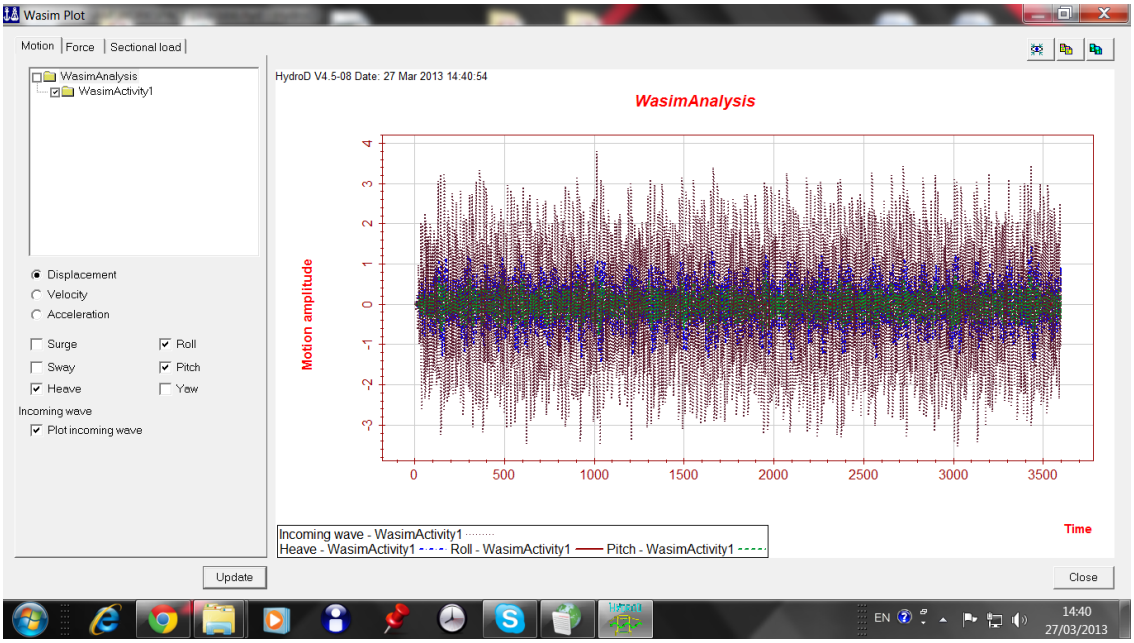

Appendix II-8 Time series of incident wave and motion responses in bow sea, zero speed of, Hs of 6m and period of 10sec.

Appendix –III

Spectrogram Results of Chapter 7

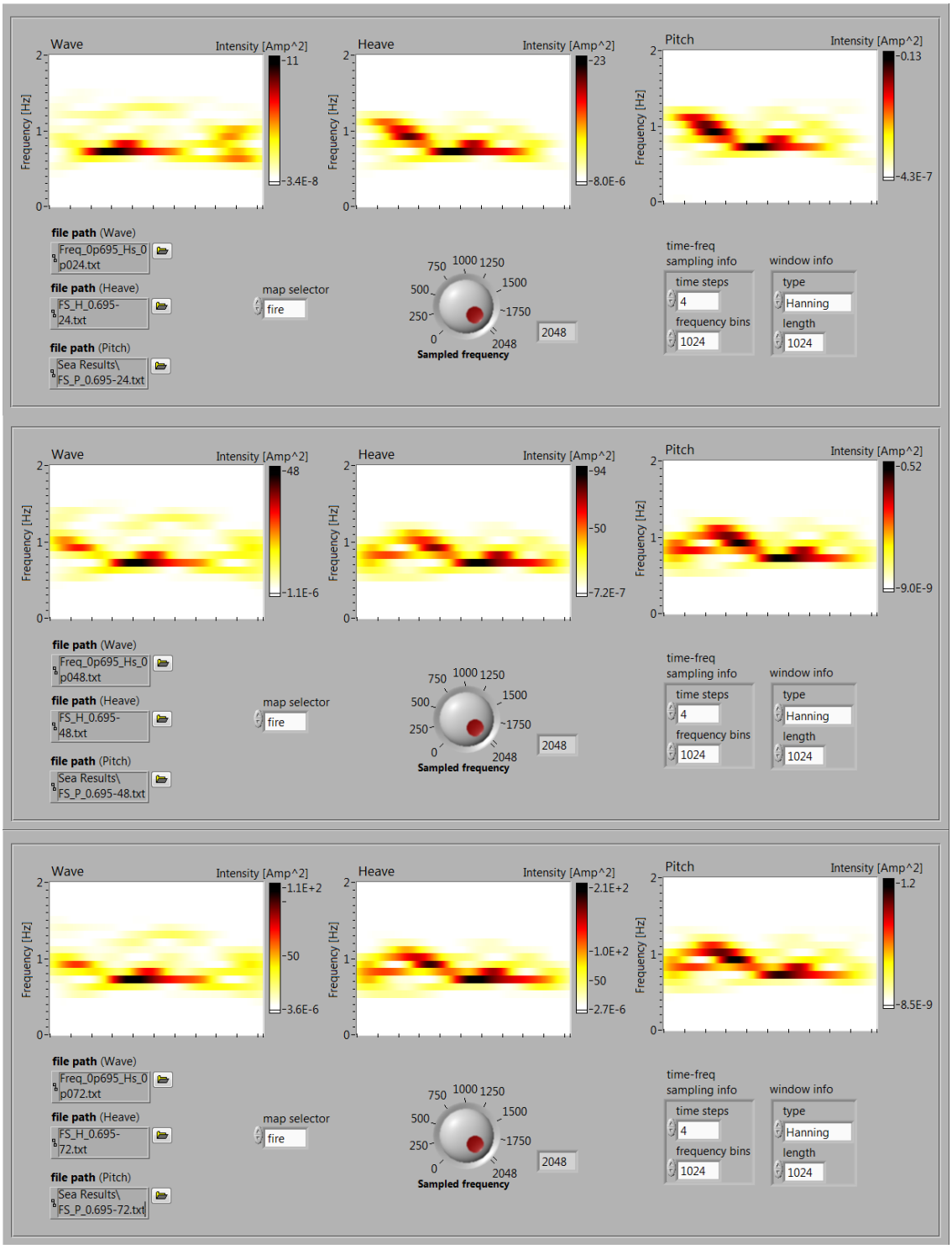

Appendix III-1 Tracking of the frequency peak of the wave by heave and pitch motions in the following low sea state at different Hs

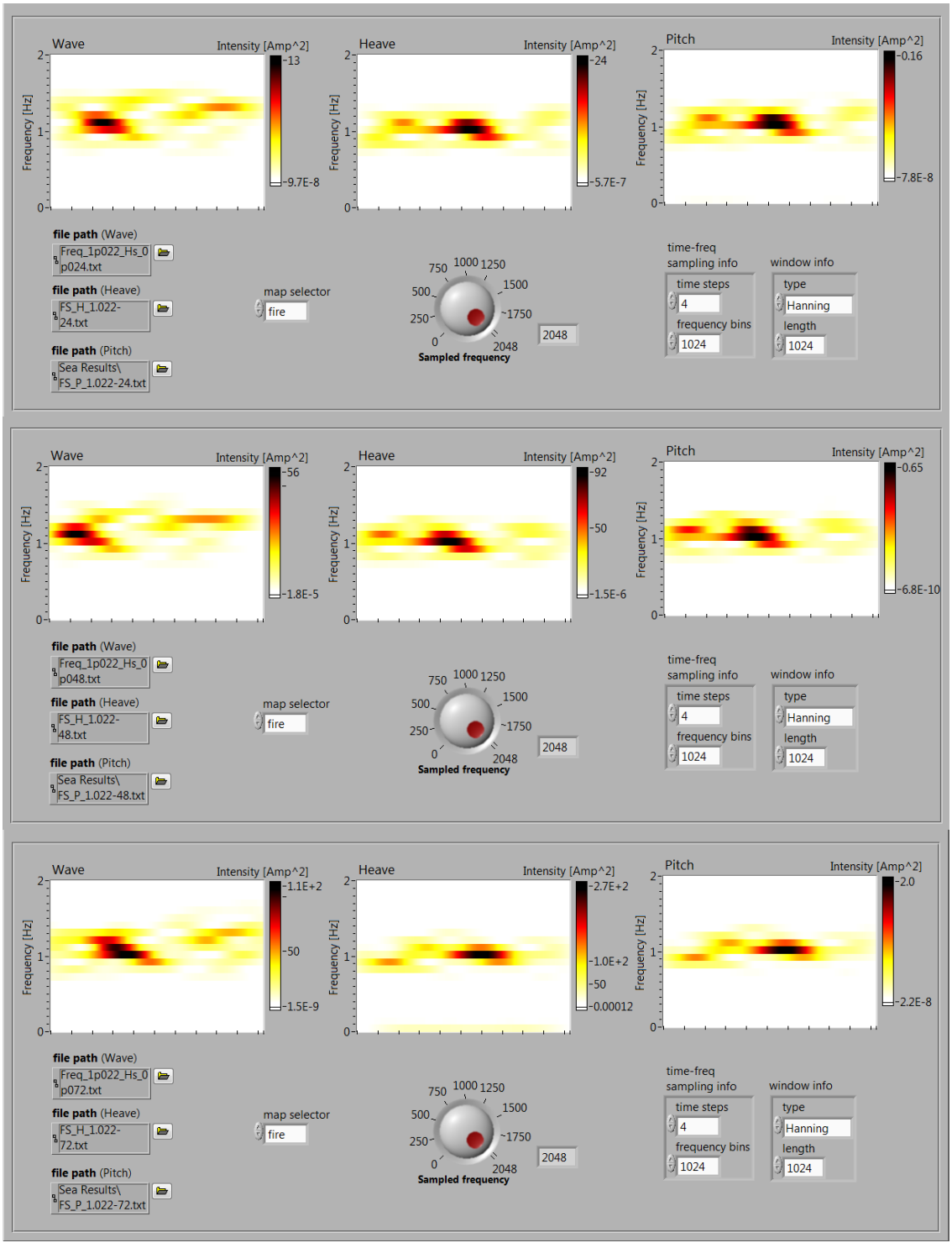

Appendix III-2 Frequency peak tracking of wave by heave and pitch motions in the following medium sea with different Hs

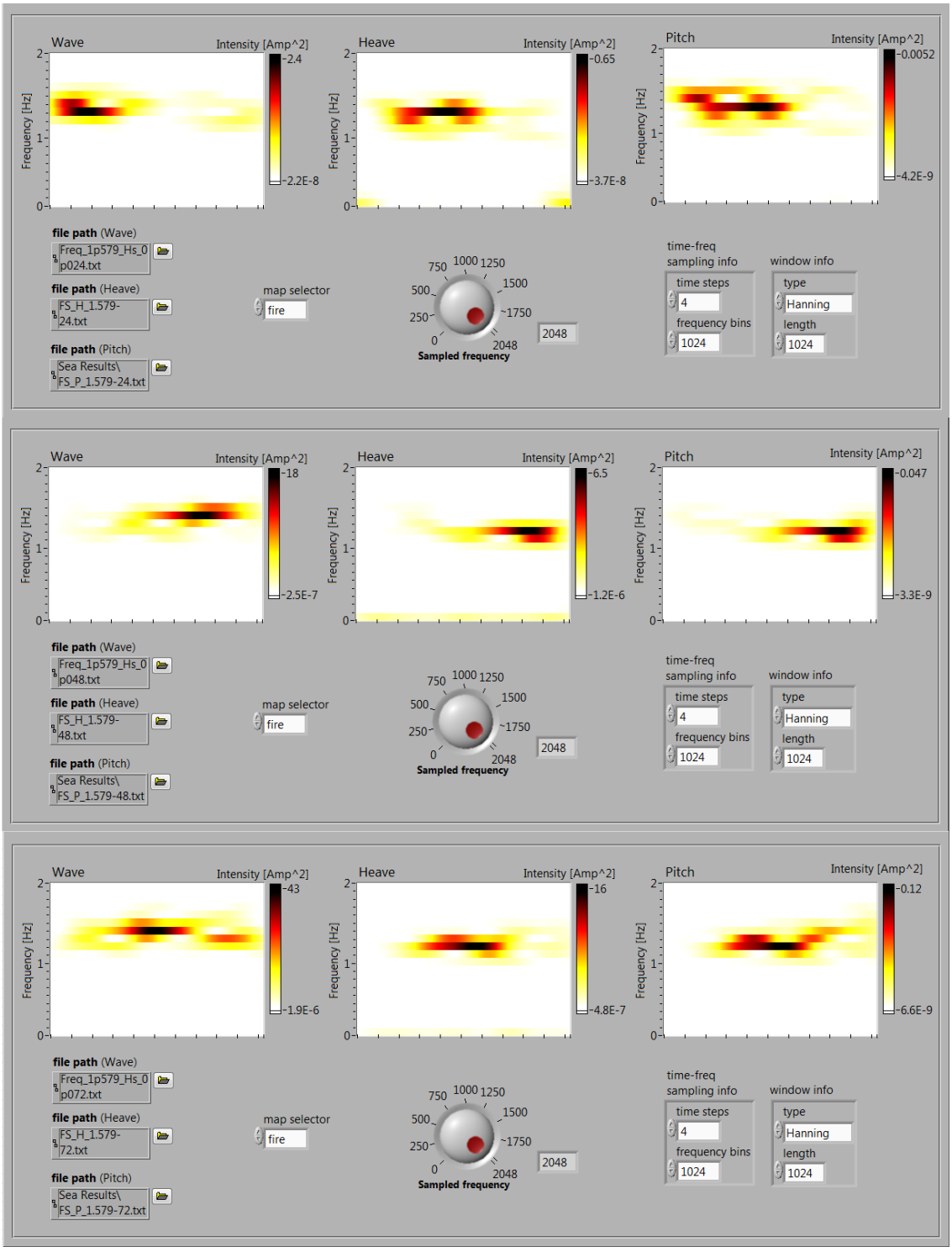

Appendix III-3 frequency peak tracking of wave by heave and pitch motions in the following high sea with different Hs

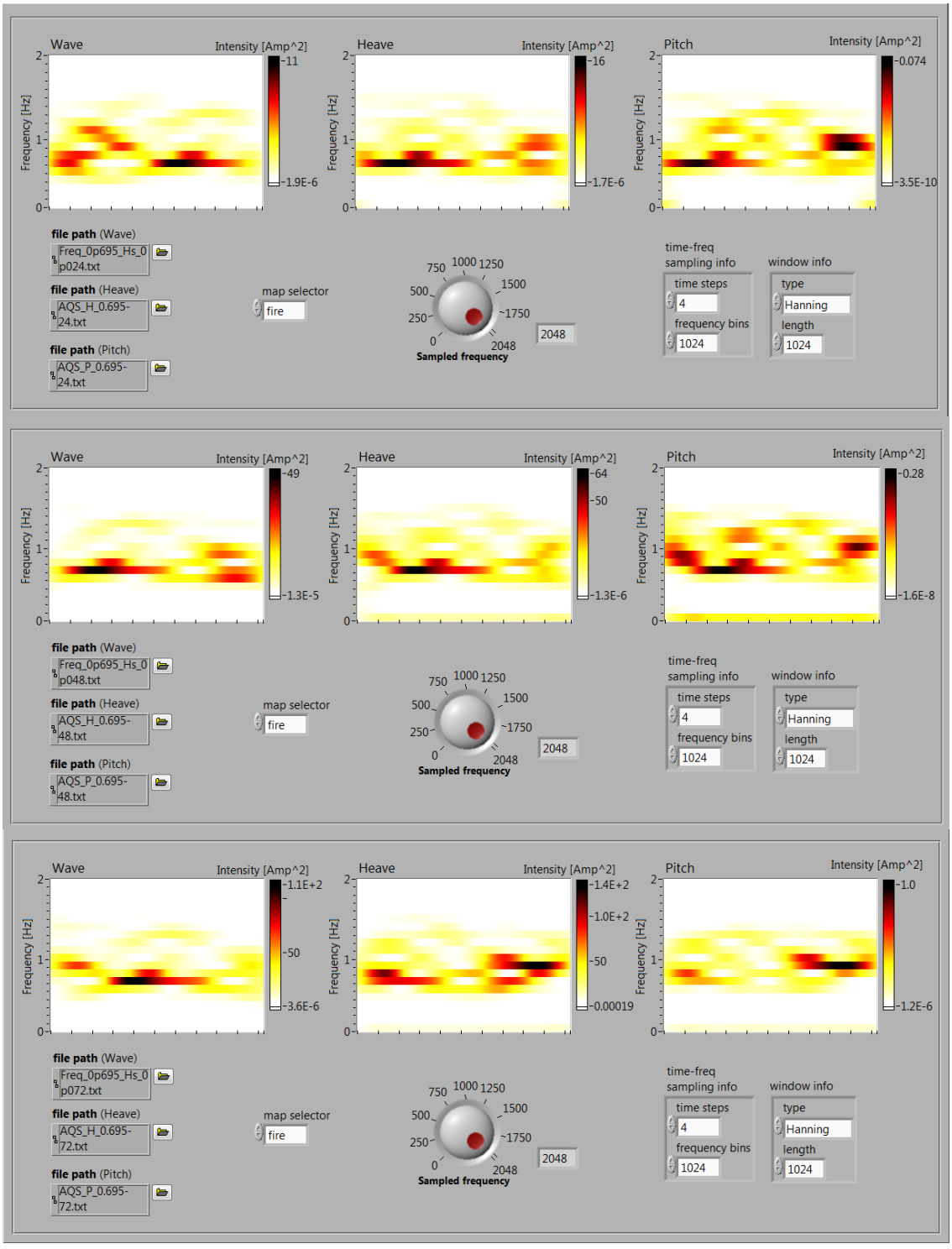

Appendix III-4 Frequency peak tracking of wave by heave and pitch motions in the quartering low sea with different Hs

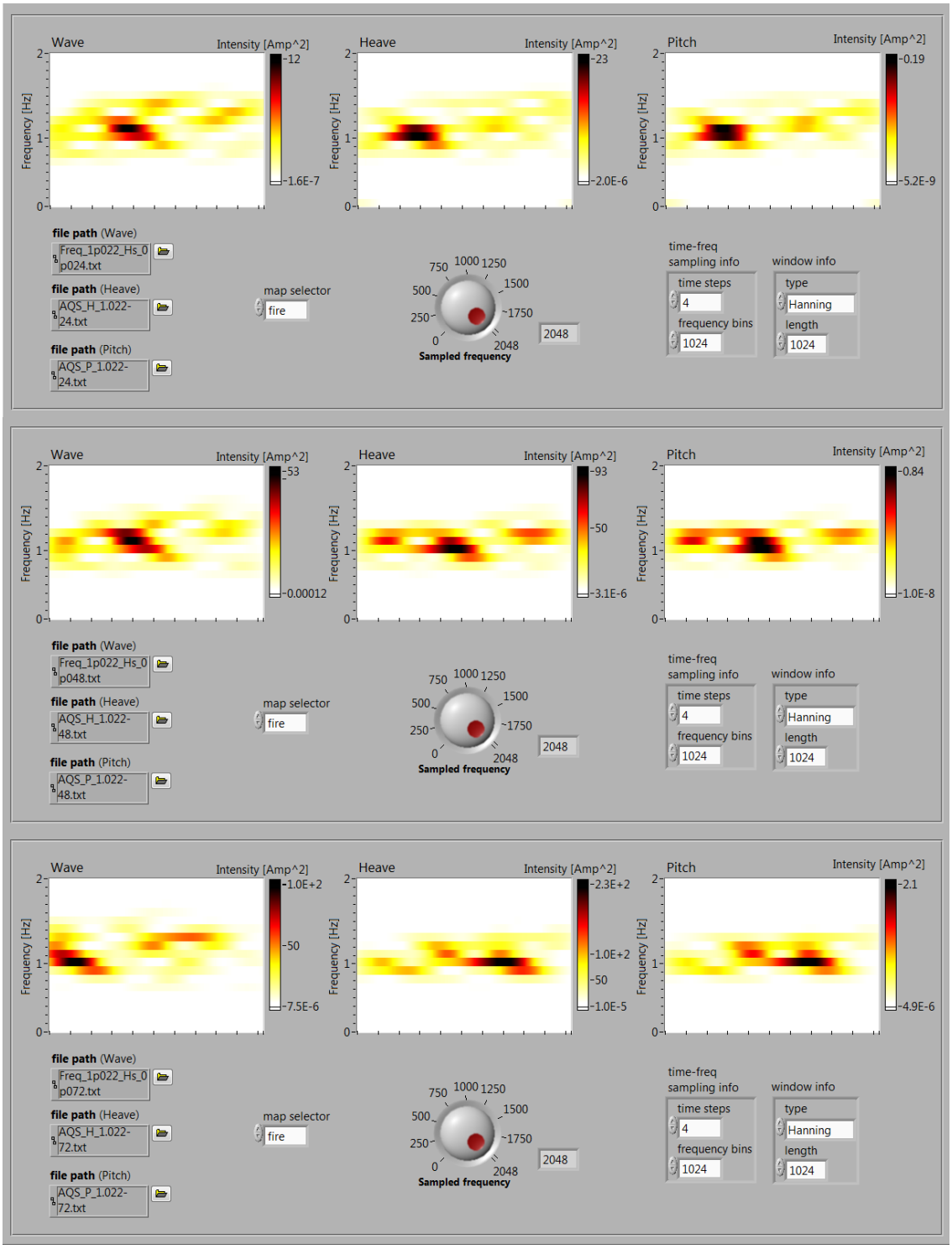

Appendix III-5 Frequency peak tracking of wave by heave and pitch motions in the quartering medium sea with different Hs

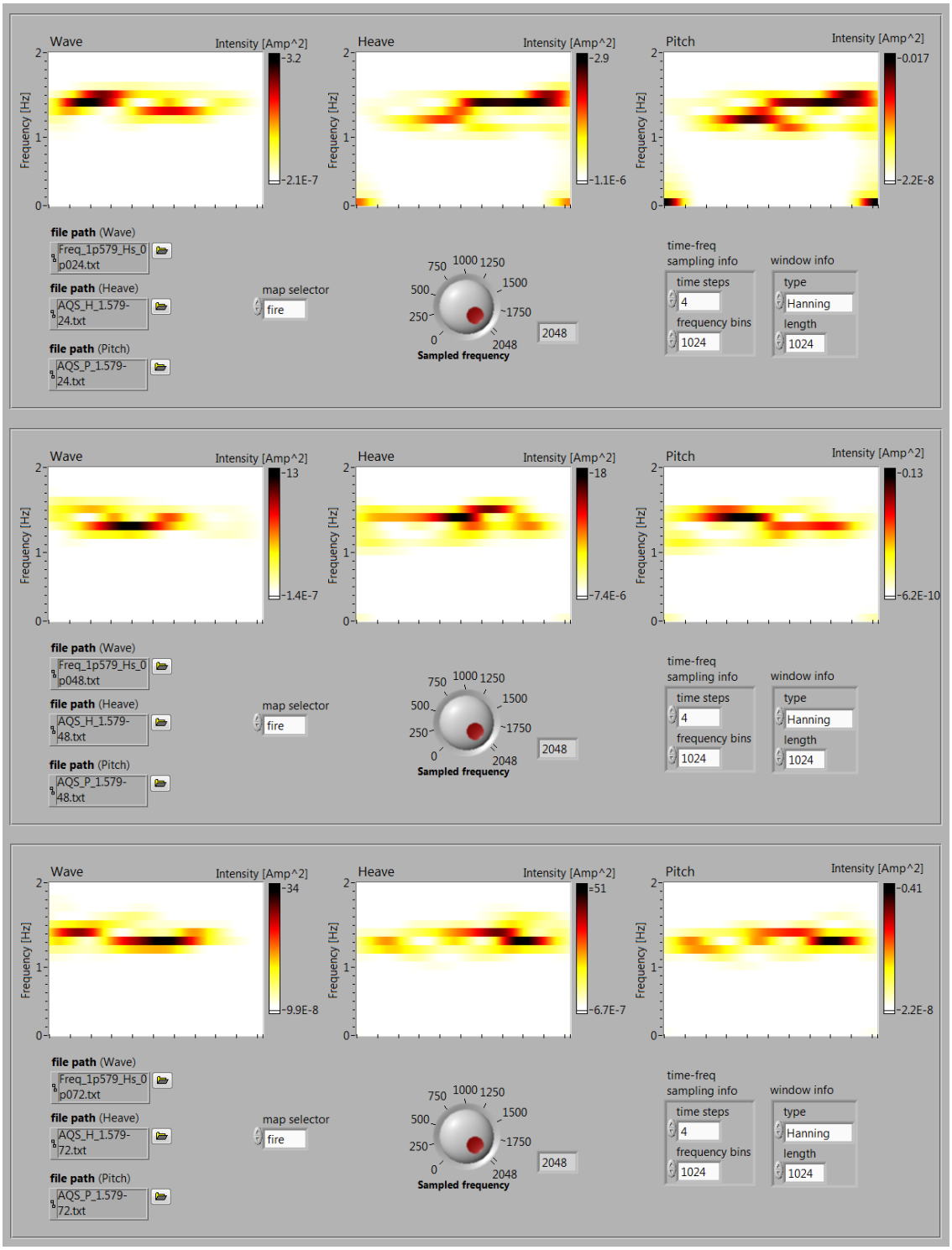

Appendix III-6 Frequency peak tracking of wave by heave and pitch motions in the quartering high sea with different Hs

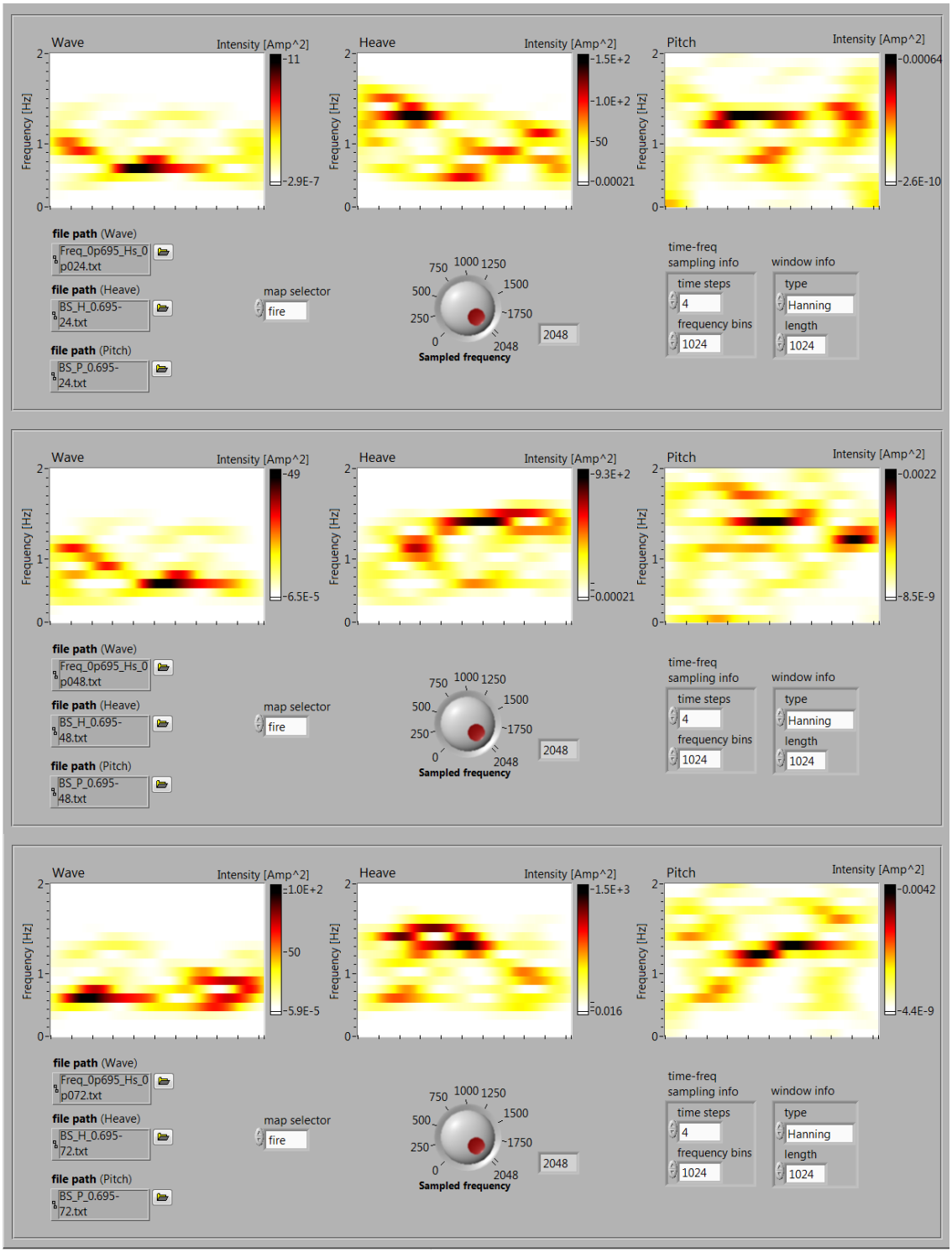

Appendix III-7 Frequency peak tracking of wave by heave and pitch motions in the beam low sea with different Hs

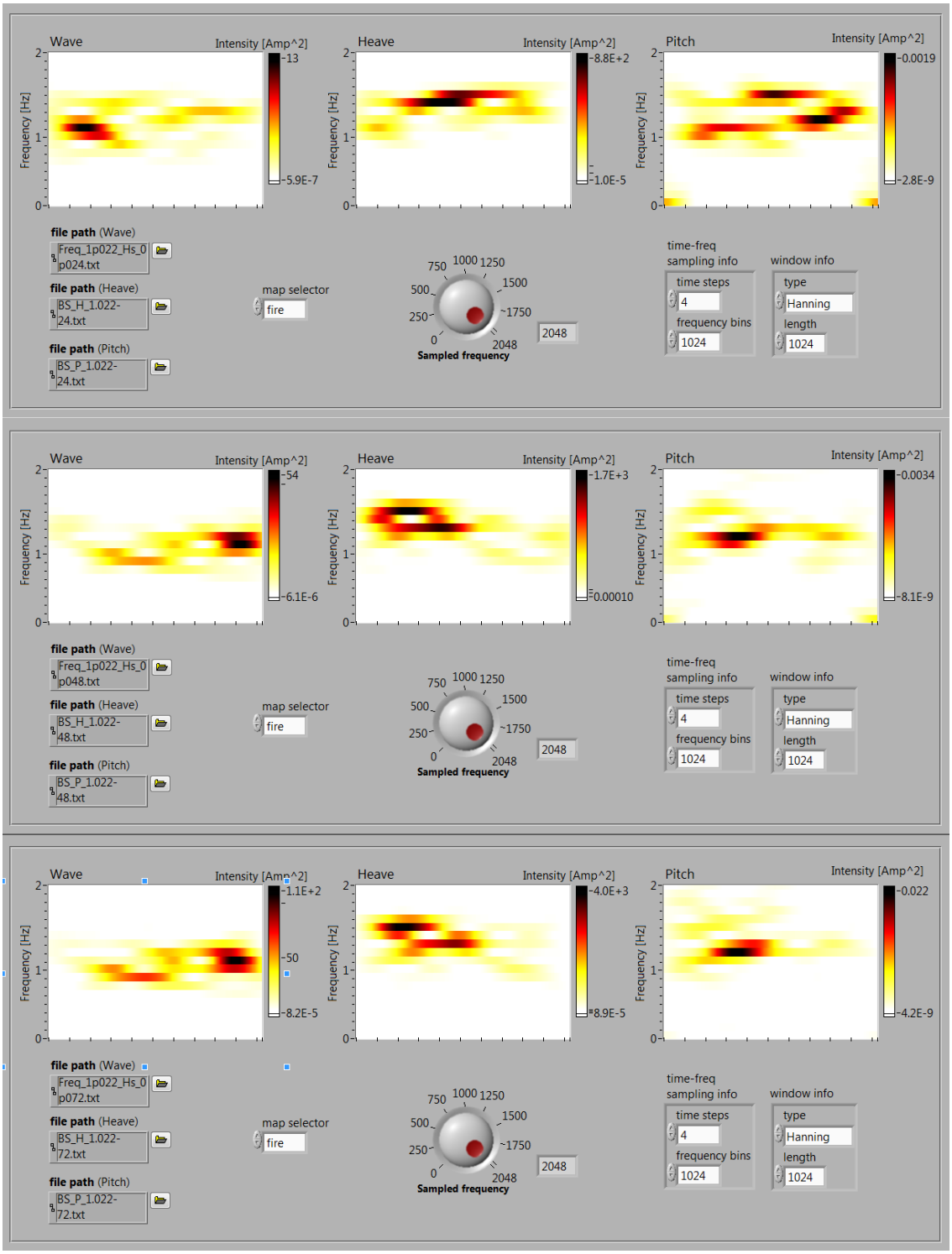

Appendix III-8 Frequency peak tracking of wave by heave and pitch motions in the beam medium sea with different Hs

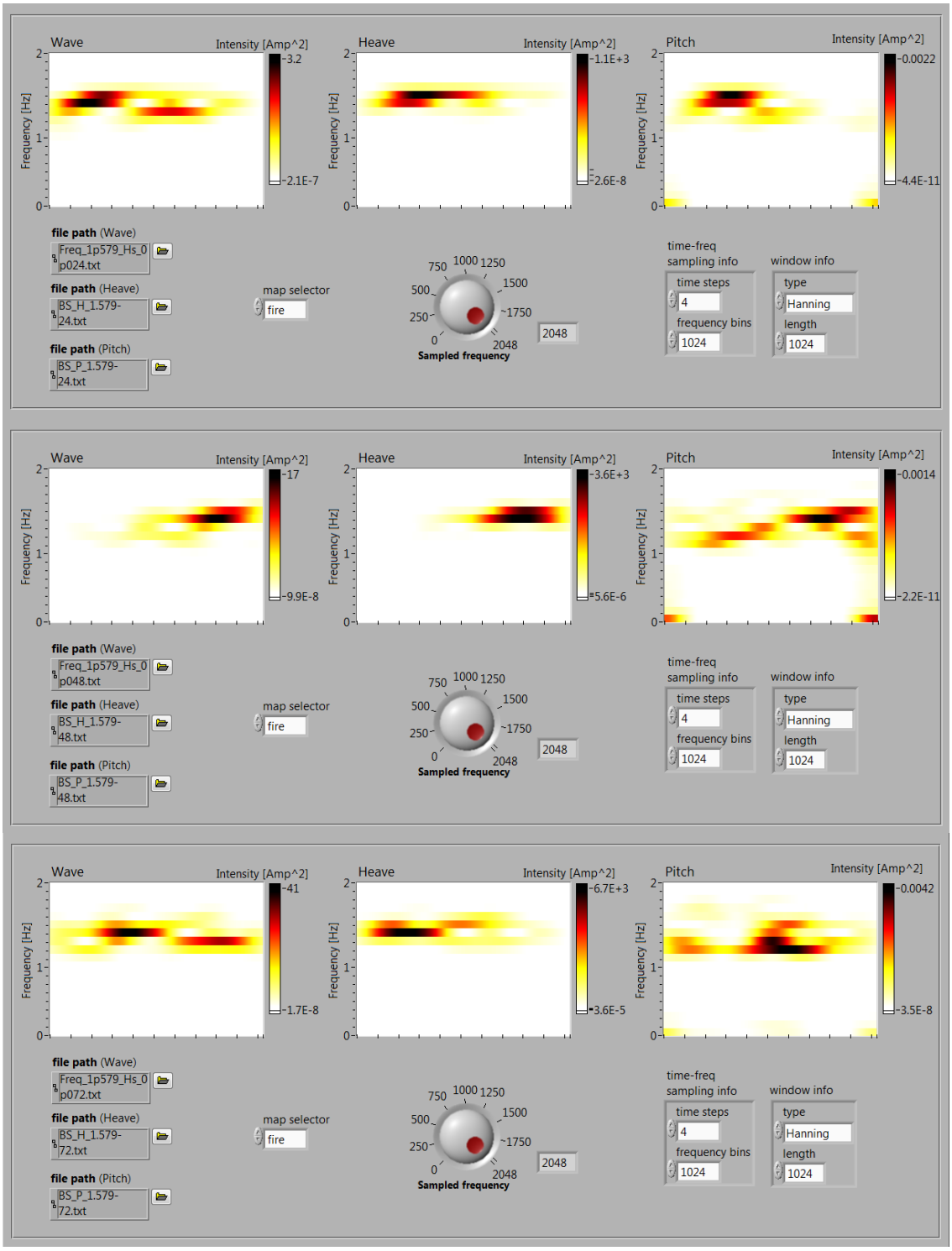

Appendix III-9 Frequency peak tracking of wave by heave and pitch motions in the beam high sea with different Hs